CZECH TECHNICAL UNIVERSITY IN PRAGUE
Faculty of Mechanical Engineering

Process Control Design for Time Delay Systems from Similarity Point of View

Habilitation Thesis

JAROMÍR FIŠER

Department of Instrumentation and Control Engineering

2019

Acknowledgement

The research presented in the habilitation thesis has been supported by the Ministry of Education of the Czech Republic and the Technology Agency of the Czech Republic under Project TE01020197 (Centre for Applied Cybernetics 3) and also in part by ESIF, EU Operational Programme Research, Development and Education, and by the Center of Advanced Aerospace Technology, Faculty of Mechanical Engineering, Czech Technical University in Prague, under Project CZ.02.1.01/0.0/0.0/16_019/0000826.

Also I would like to thank prof. Pavel Zítek for his support of my research in the field of time delay systems. Finally, I would like to appreciate the cooperation with Prof. Tomáš Vyhlídal and Dr. Goran Simeunović in the framework of both the Centre for Applied Cybernetics 3 and Center of Advanced Aerospace Technology, Czech Technical University in Prague.

Last but not least, I have to thank my family.

Annotation

The habilitation thesis presents author's research results in the areas of process control design for time delay systems and in the similarity theory application in this design. The motivation and objectives of the habilitation thesis are presented in Chapter 1. The thesis is motivated by open problem - applicability of dominant pole placement method to the PID controller tuning for higher-order plants with delay. In Chapter 2 the time delay systems in control and estimation are surveyed and at the beginning of Chapter 3 the dimensional analysis application to control design is surveyed, too. In Chapter 4 the generalized dominant three-pole placement as the design method is presented together with resulting PID controller setting common for a set of dynamically similar plants with delay. The same design method is applied in Chapter 4 to the PID controller tuning for a set of integrating plants with delay. At the end of Chapter 3 the third- and fourth-order plants are investigated as samples of higher-order plants with delay. This thesis as the study on applicability of the dominant three-pole placement method to the PID controller tuning for higher-order plants with delay reveals that the PID controller is still tunable for the admissible third- and fourth-order plants while in case of the inadmissible third- and fourth-order plants the PID controller is not already tunable by this method as concluded in Chapter 4. This revelation is mainly enabled by the dimensional analysis application thoroughly in Chapter 3 which gives the control engineering design the capability of its versatility in the area of reasonably constrained (i.e. admissible) similarity numbers. The reasonable constraints are due to dynamic relevance and practical controllability of the considered higher-order systems with delay. Conclusions to Chapter 3 summarize that the constrained similarity numbers are *oscillability*, *retardedness*, *dampeningness* and *stiffness*, in particular. Conclusions to Chapter 4 sum up that once the retardedness number is not negligible the PID controller provides admissible control solution to the plants of maximum order – four, including the integrating plants up to the fourth-order. Moreover the admissible third and fourth-order plants with delay allow assigning the natural frequency number greater than the ultimate frequency number without the loss of three-pole dominance while the inadmissible third and fourth-order plants do not. In fact the inadmissible fifth-order PID control loops with delay show that one is already behind the capability of the PID controller, independently of tuning method applied, to cope with higher-order dynamics because the control loop responses are with extreme overshoot and take overlong. In Chapter 5 the thesis as a whole is concluded that the generalized dominant three-pole placement technique provides the delayed fourth- and fifth-order PID control loop response with low overshoot in contrast to well-known PID tuning method based on ideal-relay feedback test.

Anotace

Předkládaná habilitační práce sestává z pěti kapitol. V první kapitole jsou stanoveny cíle habilitační práce, které jsou motivovány neřešeným problémem ve výzkumu systémů se zpožděními – použitelností metody předepsání dominantních pólů k nastavení PID regulátoru pro systémy se zpožděním vyššího řádu než druhého. V následující druhé kapitole je proto provedena podrobná rešerše výsledků výzkumu v oblasti návrhu řízení a odhadu systémů se zpožděními. Kapitola třetí se zabývá aplikací dimenzionální analýzy a dosahuje se v ní prvního cíle stanoveného v habilitační práci, tj. bezrozměrného popisu regulačního obvodu se zpožděním pro systémy řádu vyššího než druhého. Nedílnou součástí třetí kapitoly je dimenzionální analýza regulovaných systémů se zpožděním a tedy i zavedení podobnostních čísel charakterizujících dynamiku těchto systémů. Úvod k dimenzionální analýze včetně rešerše k využití teorie podobnosti v návrhu řídicích systémů předchází aplikaci dimenzionální analýzy ve třetí kapitole. Ve čtvrté kapitole je nalezeno nastavení PID regulátoru metodou předepsání dominantních pólů bezrozměrnému regulačnímu obvodu se zpožděním. Nejdříve je toto nastavení odvozeno pro zpožděné regulované systémy třetího řádu a následně též pro systémy řádu čtvrtého. Výsledná nastavení PID regulátoru jsou shora ohraničena v důsledku omezení kladených na systémy vyššího řádu se zpožděním, jakými jsou dynamická relevantnost a praktická řiditelnost systému se zpožděním. Právě tato omezení se promítnou do podobnostních čísel, respektive jejich rozsahů uvažovaných při návrhu PID regulátoru. Těmito podobnostními čísly jsou především *kmitavost*, *zpožděnost*, *tlumivost* a *tuhost* systému vyššího řádu se zpožděním. Omezená nastavení PID regulátoru prostřednictvím předepsání dominantních pólů jsou taktéž získána pro astatické systémy vyššího řádu se zpožděním a astatismem prvního stupně. Metoda předepsání dominantních pólů dovoluje předepsat vlastní frekvenci regulačnímu obvodu větší než je kritická frekvence, aniž by předepisovaná trojice pólů ztratila její dominantní polohu v nekonečném spektru pólů regulačního obvodu. Závěr ke čtvrté kapitole zhodnocuje výsledky v ladění PID regulátoru pro systémy třetího a čtvrtého řádu se zpožděním. Jakmile je zpožděnost regulovaného systému nezanedbatelná, poté prakticky řiditelným systémem se zpožděním PID regulátorem je systém maximálně řádu čtvrtého a to včetně astatického systému se zpožděním. Tato řiditelnost systému je posuzována vzhledem k podobnostním číslům příslušně omezeným. Tedy zpožděné regulační obvody čtvrtého a pátého řádu charakterizované podobnostními čísly mimo přijatelný rozsah se ukazují jako neschopné dostatečně regulovat a kompenzovat dynamiku systému vyššího řádu. V případě pátého řádu regulačního obvodu tato neschopnost nastane bez ohledu na použitou metodu naladění PID regulátoru, tj. selhává samotné řízení PID regulátorem. V těchto regulačních obvodech vznikají velké překmity odezev regulačního obvodu a neúměrně se prodlužuje doba regulace. Nakonec v páté kapitole je shrnuta habilitační práce jako celek s výčtem dosažených výsledků pokrývajících cíle stanovené v první kapitole. Nejvýznamnější z výsledků je dán skutečností, že metoda předepsání dominantních pólů nastavuje parametry PID regulátoru takové, že ve zpožděném regulačním obvodu čtvrtého a pátého řádu je výrazně snížen překmit regulační odezvy na poruchu. Totéž snížení je široce rozšířenou metodou nastavení PID regulátoru, známou jako metoda ideálního relé ve zpětné vazbě, v regulačním obvodu nedosažitelné.

Contents

1. Introduction to the habilitation thesis

The habilitation thesis presents author's research results in the area of process control design for time delay systems and in the similarity theory application in this design. The presented design methods are aimed at generalized PID controller setting. The delayed PID control loop optimization according to various criteria is carried out on the framework of dimensionless models obtained by means of the dimensional analysis. As a result an optimum PID control loop with delay is achieved in dimensionless time and frequency variables. Also the limits to PID tuning for higher-order plants with delay are found out and subsequently recommendations for the dominant three-pole placement are given.

Motivation and objectives

The habilitation thesis is aimed at the field of time delay systems by open problem on dominant pole placement applicability to PID controller tuning for higher-order plants with delay constrained in parameters to unknown intervals. To cope with this issue the following objectives are stated:

- To extend the already published, [123, 126], system dynamics descriptions as dimensionless time delay models to higher-order plants with delay. This is achieved by applying the dimensional analysis to time delay system descriptions as presented in Chapter 3.
- To enlarge the already published, [124], pole dominance criterion for higher-order control loops of retarded type. The pole dominance checking is extended to dimensionless control loop description as presented in Chapter 4.
- To extend the dominant pole placement method for PID tuning applicable to all dynamically similar plants of higher-order than two. The extension of this method is based on the dominant three-pole placement already published in [126] for the second-order plants with delay. This extension is presented in Chapter 4.

In the first objective the system model is transformed to the dimensionless model describing all dynamically similar plants following up the research in [123], [126]. Evident advantage of the dimensional analysis is reducing the number of dimensionless parameters necessary to describe the system dynamics. In the habilitation thesis this reduction originates in introducing similarity numbers as presented in Chapter 3. As regards the second objective the pole dominance checking presented in Chapter 4 is based on an extension of argument increment rule from [124] allowing a successful controller design and tuning for higher-order systems with delay. For the second-order systems with delay this rule application has been presented in [123] and [126]. In the third objective the dominant three-pole placement technique is introduced in order to tune the PID for controlling the plant with the natural frequency higher than the ultimate frequency, extending the results of [123] and [126] to the higher-order systems with delay. Thus for the second-order systems with delay the dominant three-pole placement has been already introduced in [123] and [126].

In the habilitation thesis the dominant pole placement is considered as a preferred technique to adjust the PID controller, beside IAE optimization, [30], and magnitude optimum method, [32]. Hence beside the dimensional analysis application to system dynamics reduction also the advancements in the dominant pole placement are the key research achievements presented in the habilitation thesis. As a result of combining this reduction with these advancements the

PID tuning rules applicable to all dynamically similar plants of higher order than two are developed.

The rest of the habilitation thesis is organized as follows. A survey of time delay systems in control and estimation is presented in Chapter 2. In Chapter 3 the delayed control loop description from the similarity point of view is developed for plants with delay, of orders up to four. The process control design from the similarity point of view and advancements in the dominant pole placement achieved are presented in Chapter 4. Finally, in Chapter 5 the habilitation thesis is concluded.

Author's publications cited in the habilitation thesis are specified in Author's list of publications with citations in WoS/MathSci/Scopus.

2. Time delay systems in control and estimation

The chapter overviews the key and recent advancements in the field of time delay systems with an emphasis on the control and observer synthesis.

Time delay system represents a process with latencies and hereditary properties when in case of existing steady-state the process steady-state is reached after rendering transient response [25], [114]. Time delay systems are frequently identified in industry, e.g. mass or heat transport processes, but also chemical processes or processes in biotechnology. An example of biotechnological process is a process of cell population growth described by Volterra delayed equation containing distributed delays [28]. Time delay modelling is of two kinds leading to either finite- or infinite- dimensional model. The former is in fact originally infinite-dimensional model of time delay system which is described by means of commensurate time delays. Such time delay systems are referred to as *n*-D systems [79]. There is a lot of applications of these models to control analysis and synthesis, see at least the key works [15], [67], [94] and references therein. The infinite-dimensional model of time delay system is then composed of incommensurate and rationally independent time delays, see [37]. Thus the time delay system is constituted by general delays which are the parts of mathematical model defined by functional differential equations [43]. One of the earliest works dedicated to control analysis and synthesis is that in [72]. Particularly distributed time delays belong among the general time delays that can be successfully approximated by equally distributed or stepwise lumped delays [116]. These delay approximations have found applications in the field of vibration suppression, for instance [57], [96]. To make the control analysis possible and the control synthesis admissible for time delay systems with continuously distributed delays an anisochronic model was developed [113]. This model is advantageous due to preserving the linearity of model relations hence an integral transform application to both the control analysis and synthesis is obvious [130]. In addition despite distributed delays presence the anisochronic model can be parameterized in the way to apply this model to controller parameterization [128, 129].

Analogously to the delay-free systems the state feedback synthesis for the time delay systems necessitates the system state controllability, [72]. The time delay system is controllable if it is spectrally controllable [116]. Once the system states are delayed there is infinite spectrum of eigenvalues and no eigenvalue of the system matrix of dynamics is uncontrollable if the condition of spectral controllability is satisfied [40]. The case of spectrally uncontrollable system is known but no systematic control synthesis is provided yet. As in the delay-free system representing a finite-dimensional system also an infinite-dimensional system fed back by output controller originates in a feedback system with the characteristic function split into two chains of factors where one of them is composed of immovable spectrum of original system [106]. Once the infinite-dimensional system is related with time delay system both the coefficient state feedback and observer gain matrix can be assessed separately [63], [109]. The approaches to observer and controller design for time delay systems are outlined in [109]. Partial or full delay cancellations in the feedback system are achieved by functional state feedback [116]. Some applications of the functional state feedback are presented in [73], [92]. In [92] a delay cancellation arisen by the so-called delay decoupling while in [73] the functional state feedback is called non-rational state feedback. Advanced method of exact delay cancellation is recognized Finite Spectrum Assignment (FSA) [54]. This method is based on algebraic control synthesis that is extended to more complex systems with delays

[101]. Originally the problem of the FSA was formulated for systems with general delays by [59]. For a class of retarded systems the FSA property is enforced when the time delay system is described by a set of retarded quasi-polynomials [131] and in case of [128] the system is described by meromorphic functions. Previous algebraic control syntheses are preconditioned by the spectral observability of retarded systems [115], [129].

In a prevailing amount of control schemes dealing with time delay compensation the Smith predictor is applied [74], [80]. Originally Smith predictor was introduced by Smith [81] and was intended for systems with input transport delay and with either non-oscillatory or sufficiently damped oscillatory responses. Observer-based Smith predictor scheme for predictive control was applied to unstable systems [36]. Next considerably modified Smith predictor is applicable to delay compensation of unstable systems [26]. Later on unstable systems with delay are handled by generalized PID regulators in the framework of Smith-like scheme [35]. The input delay of unstable systems has been compensated by combining the Smith predictor with Model Predictive Control (MPC) method of controller design [112]. Predictive control applied to various industrial processes is surveyed in [47]. The Smith predictor application has been extended to anisochronic systems by [116]. Major applications of anisochronic models to control or observer design originated from heat and mass transfer control problems. In case of the anisochronic model formulated in state space the state vector is augmented by purely integrating state variable to track robustly the reference variable [130]. Already by [4] the Smith predictor extension to integrating plants with delay has been made.

A required feature of the Smith predictor scheme is also the invariance under acting the disturbances [49], [66]. Measurable disturbance invariance cannot be achieved because of the control input delay being longer than the disturbance input delay. In case of multivariable control at least a disturbance quasi-invariance is reachable [85]. A methodology for invariant and autonomous control of multivariable systems with delays has been worked out by Bošek [12]. A well-known deficiency of the Smith predictor is poor robustness, for instance [69], hence the insensitivity to usually immeasurable disturbances is enhanced by a feedback filter, i.e. invariant feedback [44]. The invariant feedback is able to compensate limited parameter variance of process however it does not prevent from robustness loss due to incorporating the state observer into the Smith predictor scheme in case of unavailable state variables. In case of multivariable control the solution complexity to system delay compensation applying the Smith predictor grows with the number of tracked reference variables [1], [70]. Smith predictor scheme has been also applied to obtaining Finite Spectrum Assignment (FSA), see [47] and references therein.

Other compensation schemes for time delay systems derived from Smith predictor scheme are the double controller scheme [90] and the two-degree-of-freedom Smith predictor [110]. The latter is a combination of Smith predictor and controller adapting control action by an error between the plant and its model. While the former is only with single feedback controller adapting the control action and the latter one is feedforward controller cancelling plant nominal dynamics. An advantage of the double controller scheme consists in both delay cancellation and robustness capabilities. In [29] the double controller scheme has been modified for anisochronic systems. Later on, the scheme in [110] is generalized by [38]. Analogously to separation principle of state feedback control and estimation also the synthesis of classical Smith predictor scheme and controller with non-parametric adaptation can be mutually separated. As mentioned above due to impossible feedforward disturbance

cancellation in classical Smith predictor scheme the feedback disturbance compensation is proposed instead [61].

Popular control scheme for time delay systems is Internal Model Control (IMC) [68]. In [108] the IMC algorithm composed of multiple time delays minimizes the output variance. As well-known the IMC is robust hence an anisochronic IMC has been designed [127]. Next the anisochronic IMC is extended by an antiwind-up compensation scheme in [117]. Another controller design for time delay systems based on the IMC is reached by algebraic control synthesis leading to Youla parameterization of the controller [39]. In case the parameterization evaluates all the stabilizing controllers that are at the same time the anisochronic controllers the Youla-like affine parameterization is obtained for retarded systems [128, 129], [130]. There are also other applications of the Youla parameterization to the controller synthesis, for instance [60], [76].

As soon as a delay appears in the control loop the number of system poles is infinite and due to the limited number of controller parameters only a limited number of these poles can be placed to desired positions. This disadvantage of time delay systems can be overcome by the aforementioned control and estimation algorithms, [36], [54], [108], [115, 116], [118], [127-130]. Those algorithms provide somehow the FSA property. The computational aspect of infinite number of process spectrum poles is deeply studied and solved in [13], [97], and next the pole assignability problem due to the system infinite spectrum of poles is solved in [63-65]. Solution to this problem originates from continuous pole placement working in root loci manner, [63], which is other technique than the FSA approach. In fact the dominant pole placement results instead of the FSA. To avoid the high sensitivity of the roots with respect to the adjusted parameter a continuation based approach to the root loci is used [41]. In [75] and [105] the dominant pole placement technique is supplemented by the root locus technique to tune the PID controller. There are many works dealing with the dominant pole placement where assigning complex conjugate pair of poles is supplemented with guaranteeing the gain or phase margin, at least a few of them are given [88], [104], [120]. In [27] a generalization of linear-quadratic (LQ) optimal control is achieved for linear time delay systems and in [93] this generalization gives rise to dominant pole placement. Subsequently the generalized LQ optimal control is applied to PID controller design in [83]. Work [2] is adjudged to be original in developing a dominant root locus that is later applied to observer based controller design for time delay systems [31]. However, equivalently in principle to [2] the dominant root locus was introduced earlier by Åström and Wittenmark in 1980, [5], who called this as dominant pole-zero placement for discrete system transfer function. Later on different terminology is used when system dominant poles are investigated as leading poles, [52]. Already very early Cohen and Coon in 1953, [22], proposed PID tuning rule leading to pole placement with specific relative damping and natural frequency. Once the PID controller tuning is aimed then placing just three poles corresponding to three parameters of PID this aim is met as reported in [24], [55], [78], [83]. Extensive study on PID control for time delay plants is given by [82] and enlarged survey of PI(D) tuning rules suitable for plants with delay can be found in [71]. Strikingly from historical perspective up to now the PID controllers still play key role in industrial applications because over 80 percent of all control loops are governed by the PID in practice [10]. Regarding the dominance guarantee of placed poles it can be achieved by using the generalization of the Hermite–Biehler theorem [58], [102, 103]. In other words the poles placed have to become the rightmost poles in the system spectrum which are separated from the rest of the infinite spectrum [20]. Alternatively to the dominant pole placement approach the parameter stabilizing set of the PID controller is mapped for admissible plants with delay

[46], [99]. In [122] the dominant pole placement is modified to varying time delay of the process. In case of multi-loop control systems the dominant pole placement is made in [111].

With regard to recent progress in the control and estimation of time delay systems the author's research is focused on a generalization of time delay system description to obtain universally valid controller setting rules. The dominant pole placement is chosen for the controller setting. This method is extended to dimensionless form for the third and higher-order control loops with a delay.

3. Dimensional analysis and its application to dimensionless control loop description

3.1 Introduction

Problems from various areas of physics can be modelled by means of models based on physical similarity providing a more general insight into the considered problems of physics. In experimental investigations the dimensional analysis is applied to replacing the prototype by its scale model [56], [87]. The prototype and model are physically similar where the latter represents smaller or cheaper version of the former. This application can be found in airplane and ship building, or vehicle design, but also in mechanical vibration analysis [9], [84], building construction, river barrage construction, chemical engineering [132] etc. From the technical viewpoint the local or boundary conditions of a physical model lead to dimensional analysis application to physical modelling that is restricted only to these conditions [50], [133]. Lord Rayleigh in his works, [77], [86], used the dimensional analysis for the first time. But he preferred the term "principle of similitude", [77], to "dimensional analysis". In fact the principle of similitude yields the same results as those brought by the so-called Buckingham theorem, [18], but that theorem is mathematically more convenient to apply. Another work on the dimensional analysis relying on the Buckingham theorem was published by Bridgman [16]. The dimensional analysis is historically rooted in the field of the fluid mechanics. For instance, in the case of Navier-Stokes equations for incompressible flow, applying appropriate scaling factor for the length and velocity the Navier-Stokes equations become dimensionless. Thus the flow length, velocity and pressure are changed to dimensionless variables and only one dimensionless parameter, well-known as Reynolds number, is introduced. Then the Reynolds number only is needed to investigate the flow instead of original dimensional parameters, namely fluid density and kinematic viscosity. Analogously utilizing the dimensional analysis for the Boussinesq equation this equation is moved to dimensionless equation providing Rayleigh and Prandtl numbers, and after a finalization the Nusselt number is determined, for more details see [11].

In the dimensional analysis application the following initial consideration is accepted. From the basic dimensional SI units, namely *time*, *mass*, *length*, *current*, *temperature* one can be restricted only to *time* in the dimensional analysis application to process dynamics investigation. The reason why this restriction is acceptable is the fact that the process variables can be considered as quotients resulting from the ratios to the reference (maximum) values of the physical variables. Typically, for instance, the process input can be expressed as percentage of the control instrument's range, thus as dimensionless variable. Then a result of the dimensional analysis application is a purely mathematical model of dimensionless variables and parameters. Regular assumption of the dimensional analysis application is that all the dimensional variables involved into the analysis are relevant variables to describe the problem by the pure mathematical model. To avoid the incomplete equations or dimensionally non-homogeneous functions the listing of the parameters is to consist of all decisive parameters necessary for describing the related problem [18]. To obtain the mathematical model composed of only dimensionless variables and parameters the Buckingham theorem is applied. In the control design or controller tuning the application of dimensional analysis mediates not only the above mentioned prototype-model relation but in fact the whole set of *dimensionally* similar control loop models [6]. For instance the scale model can save space, material and energy. As soon as the original problem of physics is reduced in the dimensions

to *time* only the *dynamically* similar systems are developed instead of the dimensionally similar systems. The largest pitfall of dynamic similarity modelling is the fact there is no universal method for testing the dynamics meaning of the developed dimensionless model. Frequently experiences or expertise in the considered problem are required to compose dynamically true dimensionless model. In principle the dimensional homogeneity is assumed by the Buckingham theorem and this homogeneity facilitates the dimensionless description of the considered problem with a lower number of dimensionless parameters than the original ones. The practical effect is that a substantially lower number of experiments is sufficient to investigate the problem. Moreover in constituting the dimensionless model there are so many scaling factors as many original parameters. However, only the favourably selected scaling factor can bring the dimensionless model describing universally the dynamic nature of the problem. Notice a contradictory statement can be found in [6]. On one hand Callender tuning method, [19], of the PID controller is considered as dimensionally *inhomogeneous* in [6] and on the other hand Ziegler-Nichols method is correctly claimed, [6], that it is dimensionally *homogeneous*. Naturally both the Callender tuning method and the Ziegler-Nichols method must satisfy the homogeneity condition hence the statement above is erroneous in [6]. Of course there are optimization techniques which are inhomogeneous, for instance the gradient based method in [30] and polynomial optimization method, [17]. However in the dimensional analysis the resulting controller gains are searched for the Buckingham theorem application and it does not matter according to which procedure these gains are computed.

Frequently the Buckingham theorem is applied to obtain the dimensionless model of linearized version of original problem [6]. Due to main research results achieved very early there are only a few attempts to describe the linearized problem using the dimensional analysis within the last two decades [7], [14], [21], [42]. In [42] the dimensional analysis is utilized for obtaining linear vehicle bicycle model based on dimensionless ratios of vehicle parameters. In [21] the dimensional analysis is applied to stress-strain relations where the so-called relaxation time is a delay used for dimensionless plant derivation. Concerning the dimensional analysis application to the control engineering there are several works, [7, 8], [14], [89]. In the field of the control engineering the dimensional analysis approach to the control loop design is an advanced method how to design a generic controller which is valid for a set of dynamically similar processes [6]. There are also studies [20], [23], [51] and [53] where the dimensional analysis approach to the control loop design for time delay systems is somewhat intuitively applied.

Until 2013 there was no consistent and generalized survey how to apply the dimensional analysis approach to the control loop design for time delay systems. For the first time this survey is presented in [123] where the generalized PID control loop is designed for time delay systems. Later on the IAE optimum PID controller is tuned up, see [30], for the developed dimensionless plant model from [123]. Next the dimensionless PID control loop optimization, which is based on the magnitude optimum method extended to processes with delay, is performed in [32]. The optimization in [32] differs from the optimization in [23] since it is generalized to both the oscillatory and aperiodic plants. Subsequently the IAE optimization of the dimensionless parameterization of assigned poles to the delayed PID control loop is carried out in [125]. To the end in [126] the research results from [123] are significantly extended towards the disturbance rejection optimization achieved by the natural frequency option greater than the ultimate one with sufficiently high damping. Moreover the resulting dimensionless model is improved by introducing more suitable similarity numbers in [126] than those in [123]. Even robust control design in space of the similarity numbers from [126]

is carried out in [34] and with the help of the same similarity numbers a neutral PID control loop is investigated in [33].

3.2 Dimensionless description of PID control loop with delay

The goal of this section is to apply dimensional analysis to construct the dimensionless PID control loop model of (n+1)-th order in general. Consider the plant variables as quotients resulting from the ratios to the reference (maximum) values of the physical variables, i.e. the input and output variables, u and y, are dimensionless, and assume either *stable* time delay plant or time delay plant without *steady-state* characteristics as follows

$$\frac{d^n y(t)}{dt^n} + a_{n-1}\frac{d^{n-1} y(t)}{dt^{n-1}} + a_{n-2}\frac{d^{n-2} y(t)}{dt^{n-2}} + ... + a_2\frac{d^2 y(t)}{dt^2} + a_1\frac{dy(t)}{dt} + a_0 y(t) = b_0 u(t-\tau), \tag{3.1}$$

where $a_i > 0, i = 1, 2, ..., n-1$, and $a_0 \geq 0, b_0 \neq 0, n \geq 2$. The time delay plant without *steady-state* characteristics is referred to as *integrating* plant with delay while the stable time delay plant is called as *proportional* plant with delay. After performing Laplace transform (L-transform) of (3.1) under zero initial conditions

$$\left(s^n + \sum_{i=0}^{n-1} a_i s^i\right) Y(s) = b_0 U(s)\exp(-s\tau) \tag{3.2}$$

the plant transfer function is obtained

$$G(s) = \frac{Y(s)}{U(s)} = \frac{B(s)}{A(s)}, \tag{3.3}$$

where

$$A(s) = s^n + \sum_{i=0}^{n-1} a_i s^i,\ B(s) = b_0 \exp(-s\tau). \tag{3.4}$$

For the purpose of the controller tuning the transfer function (3.3) describing the stable plant is expressed as follows

$$G(s) = \frac{K}{\tilde{A}(s)}\exp(-s\tau) \tag{3.5}$$

where

$$\tilde{A}(s) = \frac{A(s)}{a_0} = 1 + \sum_{i=1}^{n} \tilde{a}_i s^i,\ \tilde{a}_i = \frac{a_i}{a_0}, i = 1, 2, ..., n-1,\ \tilde{a}_n = \frac{1}{a_0},\ K = \frac{b_0}{a_0}, a_0 \neq 0. \tag{3.6}$$

As the controller the ideal PID controller is considered

$$\frac{du(t)}{dt} = r_P\frac{de(t)}{dt} + r_D\frac{d^2 e(t)}{dt^2} + r_I e(t) \tag{3.7}$$

where $e = w - y$, w is the reference variable and y is the output of plant (3.1).

Linking the plant (3.1) with controller (3.7) in the closed loop the PID control loop with delay is obtained. Applying the dimensional analysis to this loop the dimensionless PID control loop of (n+1)-th order is built. Hence the well-known Buckingham Π theorem [6] is applied to transforming the PID control loop with delay into the dimensionless form simplifying and making this description of the loop much more universal when describing the relation of the controller specific setting with corresponding set of dynamically similar plants.

3.2.1 Dimensional analysis application: Option I

To start the dimensional analysis, automatically, all the already dimensionless parameters or quantities of the PID control loop with delay can be excluded from dimensional investigation. Such a parameter is proportional loop gain, $Kr_P = \rho_P$, which is already dimensionless with respect to the dimensionless y and u. Thus the dimensional consideration for the PID control loop with delay concerns the following quantities

$$\omega\left[\mathrm{s}^{-1}\right], Kr_D\left[\mathrm{s}\right], Kr_I\left[\mathrm{s}^{-1}\right], a_{n-1}\left[\mathrm{s}^{-1}\right], a_{n-2}\left[\mathrm{s}^{-2}\right], \ldots, a_1\left[\mathrm{s}^{-(n-1)}\right], a_0\left[\mathrm{s}^{-n}\right], t\left[\mathrm{s}\right], \tau\left[\mathrm{s}\right] \tag{3.8}$$

where the angular frequency ω is considered with regard to specification of systems poles. The dimensions of all the quantities in (3.8) are powers of time only and the so-called dimensionless arguments constitute the following products of their powers

$$\Pi_i = \omega^{\varepsilon_1}\left(Kr_D\right)^{\varepsilon_2}\left(Kr_I\right)^{\varepsilon_3}, \left(a_{n-1}\right)^{\varepsilon_4}\left(a_{n-2}\right)^{\varepsilon_5}\cdots a_1^{\varepsilon_{n+2}} a_0^{\varepsilon_{n+3}} t^{\varepsilon_{n+4}} \tau^{\varepsilon_{n+5}}, \quad i = 1,2,\ldots,n+3,n+4 \tag{3.9}$$

where the exponents $\varepsilon_1, \varepsilon_2, \ldots, \varepsilon_{n+4}, \varepsilon_{n+5}$ play a key role in constructing the similarity numbers. The arguments in (3.9) are not ordered randomly but primarily the order of the arguments expresses their significance for the PID control loop description. Thus the most important parameter for the control loop design is the natural frequency while the delay, τ, is chosen scaling factor. Following the Buckingham Π theorem the dimensional matrix [6] is due to only one essential dimension considered, i.e. time, one row matrix

$$\mathbf{D} = \begin{bmatrix} -1 & 1 & -1 & -1 & -2 & \cdots & -(n-1) & -n & 1 & 1 \end{bmatrix} \tag{3.10}$$

Then the dimensionless arguments are solved by applying the augmented matrix equation

$$\begin{bmatrix} \mathbf{I}_{n+4} & \mathbf{0}_{(n+4)\times 1} \\ \mathbf{D}_1 & D_2 \end{bmatrix} \begin{bmatrix} \varepsilon_1 \\ \varepsilon_2 \\ \vdots \\ \varepsilon_{n+4} \\ \varepsilon_{n+5} \end{bmatrix} = \begin{bmatrix} \varepsilon_1 \\ \varepsilon_2 \\ \vdots \\ \varepsilon_{n+4} \\ 0 \end{bmatrix} \tag{3.11}$$

where $\begin{bmatrix} \mathbf{D}_1 & D_2 \end{bmatrix} = \mathbf{D}, D_2 = 1$. From (3.11) only one non-trivial solution results in linear equation as follows

$$-\varepsilon_1 + \varepsilon_2 - \varepsilon_3 - \varepsilon_4 - 2\varepsilon_5 \cdots - (n-1)\varepsilon_{n+2} - n\varepsilon_{n+3} + \varepsilon_{n+4} + \varepsilon_{n+5} = 0 \tag{3.12}$$

Simply (3.12) can be solved in the manner that one of the exponents, except the last exponent, is fixed to one and remaining $n+3$ exponents are zero-filled. The last exponent belongs to the scaling factor hence it cannot be the subject to the solution to (3.12). Thus in iterative manner $n+4$ solutions to (3.12) are obtained when gradually one of $n+4$ exponents is fixed to one and the rest of exponents, except the last one, are set zero. After substituting these $n+4$ solutions into (3.9) the dimensionless parameters $\Pi_i, i=1,2,...,n+3,n+4,$ are derived. The order, *n*, cannot be arbitrarily high due to the limited capability of the PID controller to change the plant dynamics and to the involved relations for similarity numbers. For the exponents in (3.9) the following conditions result

1. $\varepsilon_1=1, \varepsilon_2=\varepsilon_3=\varepsilon_4=\varepsilon_5\cdots=\varepsilon_{n+2}=\varepsilon_{n+3}=\varepsilon_{n+4}=0 \rightarrow \varepsilon_{n+5}=1 \rightarrow \Pi_1=\omega\tau$
2. $\varepsilon_2=1, \varepsilon_1=\varepsilon_3=\varepsilon_4=\varepsilon_5\cdots=\varepsilon_{n+2}=\varepsilon_{n+3}=\varepsilon_{n+4}=0 \rightarrow \varepsilon_{n+5}=-1 \rightarrow \Pi_2=\frac{Kr_D}{\tau}$
3. $\varepsilon_3=1, \varepsilon_1=\varepsilon_2=\varepsilon_4=\varepsilon_5\cdots=\varepsilon_{n+2}=\varepsilon_{n+3}=\varepsilon_{n+4}=0 \rightarrow \varepsilon_{n+5}=1 \rightarrow \Pi_3=Kr_I\tau$
4. $\varepsilon_4=1, \varepsilon_1=\varepsilon_2=\varepsilon_3=\varepsilon_5\cdots=\varepsilon_{n+2}=\varepsilon_{n+3}=\varepsilon_{n+4}=0 \rightarrow \varepsilon_{n+5}=1 \rightarrow \Pi_4=a_{n-1}\tau$
5. $\varepsilon_5=1, \varepsilon_1=\varepsilon_2=\varepsilon_3=\varepsilon_4\cdots=\varepsilon_{n+2}=\varepsilon_{n+3}=\varepsilon_{n+4}=0 \rightarrow \varepsilon_{n+5}=2 \rightarrow \Pi_5=a_{n-2}\tau^2$

⋮

n+2. $\varepsilon_{n+2}=1, \varepsilon_1=\varepsilon_2=\varepsilon_3=\varepsilon_4=\varepsilon_5\cdots=\varepsilon_{n+3}=\varepsilon_{n+4}=0 \rightarrow \varepsilon_{n+5}=n-1 \rightarrow \Pi_{n+2}=a_1\tau^{n-1}$

n+3. $\varepsilon_{n+3}=1, \varepsilon_1=\varepsilon_2=\varepsilon_3=\varepsilon_4=\varepsilon_5\cdots=\varepsilon_{n+2}=\varepsilon_{n+4}=0 \rightarrow \varepsilon_{n+5}=n \rightarrow \Pi_{n+3}=a_0\tau^n$

n+4. $\varepsilon_{n+4}=1, \varepsilon_1=\varepsilon_2=\varepsilon_3=\varepsilon_4=\varepsilon_5\cdots=\varepsilon_{n+2}=\varepsilon_{n+3}=0 \rightarrow \varepsilon_{n+5}=-1 \rightarrow \Pi_{n+4}=\frac{t}{\tau}$

Evidently Π_1 and Π_{n+4} are dimensionless frequency and time variables, respectively, at which the control loop model is expressed. Π_2 and Π_3 are dimensionless derivative and integration loop gains, respectively. While $\Pi_4, \Pi_5, \ldots, \Pi_{n+2}, \Pi_{n+3}$ are plant dimensionless parameters. If for modelling purposes $\omega\tau=\phi$ and $t/\tau=\bar{t}$ the plant model (3.1) with $a_0>0$, $a_0=b_0$ is transformed by the dimensional analysis to the dimensionless form

$$\frac{d^n y(\bar{t})}{d\bar{t}^n}+\Pi_4\frac{d^{n-1}y(\bar{t})}{d\bar{t}^{n-1}}+\Pi_5\frac{d^{n-2}y(\bar{t})}{d\bar{t}^{n-2}}+...+\Pi_{n+1}\frac{d^2y(\bar{t})}{d\bar{t}^2}+\Pi_{n+2}\frac{dy(\bar{t})}{d\bar{t}}+\Pi_{n+3}y(\bar{t})=\Pi_{n+3}u(\bar{t}-1), \tag{3.13}$$

where $\Pi_4, \Pi_5, \ldots, \Pi_{n+2}, \Pi_{n+3}$ are the plant similarity numbers. Due to the delay selected as the scaling factor instead of the delay is $\tau/\tau=1$. Because of $a_0=b_0$ the dimensionless plant model (3.13) is developed with unit steady-state gain, i.e. $K=1$. However, in case of non-unit *K* the arguments Π_2, Π_3 are straightforwardly applied to the PID control tuning in dimensionless control loop with delay. Indeed in the control loop arrangement not only the proportional gain is merged with the plant steady state gain, i.e. $\rho_P=Kr_P$, but also the derivative and integration gains are transformed to dimensionless loop gains $Kr_D/\tau=\rho_D$ and $Kr_I\tau=\rho_I$, respectively.

Integrating plant. Once the controlled plant (3.1) is considered with $a_0 = 0$ and $b_0 = 0$ the integrating plant takes place. Then the argument Π_{n+3} disappears. Instead of Π_{n+3} other similarity number is introduced

$$\Pi^I_{n+3} = b_0 \tau^n . \tag{3.14}$$

Thus the dimensionless integrating plant model results in the form

$$\frac{d^n y(\bar{t})}{d\bar{t}^n} + \Pi_4 \frac{d^{n-1} y(\bar{t})}{d\bar{t}^{n-1}} + \Pi_5 \frac{d^{n-2} y(\bar{t})}{d\bar{t}^{n-2}} + ... + \Pi_{n+1} \frac{d^2 y(\bar{t})}{d\bar{t}^2} + \Pi_{n+2} \frac{dy(\bar{t})}{d\bar{t}} = \Pi^I_{n+3} u(\bar{t} - 1), \tag{3.15}$$

that is analogously to (3.13) in the number of parameters reduced by one delay parameter. Though the delay parameter is excluded from the dimensionless arguments the delay phenomenon itself is otherwise present in the dimensionless plant model (3.13) and (3.15) as fixed-value pure delay.

Remark 1. Rightly, the higher the order of (3.13) the greater is the number of Π_i arguments. At the same time this number results less than the number of those parameters describing original plant (3.1). Despite the reduction of plant parameters, the order, *n*, cannot be arbitrarily high due to the aforementioned constraint on *n* restricted up to four. Additionally the plant (3.1) is considered stable. The order of the plant higher than four brings about the control loop dynamics of higher order than fifth which is scarcely changeable into desired behavior by only three loop gains setting.

Due to the limited order *n* only the following cases of plants with delay are considered: $n = 1$, $n = 2$, $n = 3$ and $n = 4$. Also the integrating plants of corresponding order are included.

Case 1. The dimensionless model of the first-order plant with delay, $n = 1$, is described by the following dimensionless parameters

$$\Pi_{n+3} = \Pi_4 = a_0 \tau , \ \Pi_{n+4} = \Pi_5 = \bar{t} \tag{3.16}$$

including the dimensionless frequency variable, i.e. $\Pi_1 = \omega\tau$. Be aware that Π_3 and Π_{n+2} are not two different dimensionless parameters but the same similarity number, the integration loop gain. Π_{n+2} for $n = 1$ does not take place in the model for the first-order plant with delay. The dimensionless parameters derived in (3.16) need not be final similarity numbers of the dimensionless model of the first-order plant with delay. When the reciprocal value of Π_4 is evaluated the new similarity number is introduced

$$\Psi = \frac{1}{\Pi_4} = \frac{1}{a_0 \tau} . \tag{3.17}$$

This number expresses lagging properties of the first-order plant with delay. Different similarity number from Ψ is attained when Π_4 and Π_{n+3} are got together as follows

$$\Xi = \frac{\Pi_4}{\Pi_{n+3}} = \frac{\Pi_4}{\Pi_4} = 1. \tag{3.18}$$

This number, however, degenerates to 1 in case of $n = 1$. The model (3.13) results for $n = 1$ with respect to (3.16) as follows

$$\frac{dy(\bar{t})}{d\bar{t}} + \Pi_4 y(\bar{t}) = \Pi_4 u(\bar{t} - 1) \tag{3.19}$$

and equivalently using number (3.17)

$$\Psi \frac{dy(\bar{t})}{d\bar{t}} + y(\bar{t}) = u(\bar{t} - 1). \tag{3.20}$$

Integrating plant. The integrating plant of the first-order is characterized by the following similarity number

$$\Pi^I_{n+3} = \Pi^I_4 = b_0 \tau \tag{3.21}$$

which is due to (3.14). Dimensionless integrating plant model (3.15) originates for $n = 1$ in

$$\frac{dy(\bar{t})}{d\bar{t}} = \Pi^I_4 u(\bar{t} - 1) \tag{3.22}$$

where no Ψ is defined.

Case 2. The dimensionless model of the second-order plant with delay of type (3.1) has been already developed for the case of $n = 2$, [123]. Here the sets of dynamically similar second-order plants either aperiodic or oscillatory are achieved. The similarity numbers are specified as follows

$$\Pi_4 = a_1 \tau\ ,\ \Pi_5 = a_0 \tau^2\ ,\ \Pi_6 = \bar{t} \tag{3.23}$$

which can be next finalized into the following similarity numbers

$$\Lambda = \frac{\Pi_5}{\Pi_4^{\,2}} = \frac{a_0 \tau^2}{\left(a_1 \tau\right)^2} = \frac{a_0}{a_1^{\,2}} \tag{3.24}$$

and

$$\Theta = \Pi_4 = a_1 \tau. \tag{3.25}$$

Number (3.24) is called the *swingability* number while (3.25) is referred to as *laggardness* number. When the ratio of Π_{n+2} and Π_{n+3} is carried out the analogous similarity number to (3.17) is derived as follows

$$\Psi = \frac{\Pi_{n+2}}{\Pi_{n+3}} = \frac{\Pi_4}{\Pi_5} = \frac{a_1}{a_0\tau} \tag{3.26}$$

which is identical to another similarity number obtained as the ratio

$$\Xi = \frac{\Pi_4}{\Pi_{n+3}} = \frac{\Pi_4}{\Pi_5} = \frac{a_1}{a_0\tau}. \tag{3.27}$$

The dimensionless model of the second-order plant with delay results from (3.13)

$$\frac{d^2y(\bar{t})}{d\bar{t}^2} + \Pi_4\frac{dy(\bar{t})}{d\bar{t}} + \Pi_5 y(\bar{t}) = \Pi_5 u(\bar{t}-1) \tag{3.28}$$

and with respect to final similarity numbers (3.24) and (3.25)

$$\frac{d^2y(\bar{t})}{d\bar{t}^2} + \Theta\frac{dy(\bar{t})}{d\bar{t}} + \Lambda\Theta^2 y(\bar{t}) = \Lambda\Theta^2 u(\bar{t}-1). \tag{3.29}$$

Model (3.29) in contrary to (3.28) permits evaluate both the swingability and laggardness of the plant. Naturally similarity numbers Ψ and Ξ given by (3.26) and (3.27), respectively, are *redundant* for the case of $n=2$.

Integrating plant. In case of integrating plant of the second-order the similarity number as follows

$$\Pi^I_{n+3} = \Pi^I_5 = b_0\tau^2 \tag{3.30}$$

takes over a role of Π_5 and instead of (3.24) it results

$$\Lambda_I = \frac{\Pi^I_5}{\Pi_4^{\,2}} = \frac{b_0\tau^2}{\left(a_1\tau\right)^2} = \frac{b_0}{a_1^{\,2}}. \tag{3.31}$$

Λ_I is no more the *swingability* number. The dimensionless model of the integrating plant of the second-order is obtained

$$\frac{d^2y(\bar{t})}{d\bar{t}^2} + \Pi_4\frac{dy(\bar{t})}{d\bar{t}} = \Pi^I_5 u(\bar{t}-1) \tag{3.32}$$

that is equivalently expressed in more convenient form

$$\frac{d^2y(\bar{t})}{d\bar{t}^2} + \Theta\frac{dy(\bar{t})}{d\bar{t}} = \Lambda_I\Theta^2 u(\bar{t}-1). \tag{3.33}$$

All the similarity numbers specified are summarized in Tab. 1 below.

Case 3. The dimensionless model of the third-order plant with delay, $n=3$, is described by the following dimensionless parameters

$$\Pi_4 = a_2\tau\,,\ \Pi_5 = a_1\tau^2\,,\ \Pi_6 = a_0\tau^3\,,\ \Pi_7 = \bar{t} \tag{3.34}$$

including the dimensionless frequency variable $\Pi_1 = \omega\tau$. Both Π_4 and Π_5 describe dynamic properties of plant of type (3.1) and when these two numbers are fused as follows

$$\Lambda = \frac{\Pi_5}{\Pi_4{}^2} = \frac{a_1\tau^2}{\left(a_2\tau\right)^2} = \frac{a_1}{\left(a_2\right)^2} \tag{3.35}$$

different similarity number, Λ, from both Π_4 and Π_5 is derived. This time the number Λ is plant *oscillability* number. Next when Π_{n+2} and Π_{n+3} are got into ratio for $n=3$ another similarity number is derived

$$\Psi = \frac{\Pi_{n+2}}{\Pi_{n+3}} = \frac{\Pi_5}{\Pi_6} = \frac{a_1\tau^2}{a_0\tau^3} = \frac{a_1}{a_0\tau}\,. \tag{3.36}$$

Another fusion of dimensionless parameters is made as follows

$$\Xi = \frac{\Pi_4}{\Pi_{n+3}} = \frac{\Pi_4}{\Pi_6} = \frac{a_2\tau}{a_0\tau^3} = \frac{a_2}{a_0\tau^2}\,. \tag{3.37}$$

Both Ψ and Ξ are auxiliary similarity numbers. In the fusions (3.35) through (3.7) Π_4 represents the similarity number as follows

$$\Theta = \Pi_4 = a_2\tau\,. \tag{3.38}$$

This number analogously to (3.25) is called *laggardness* number. Next $\Pi_{n+3}\left(\Pi_6\right)$ itself constitutes plant characteristics expressing dimensionless coefficient of zero derivative of differential equation (3.13)

$$\Phi = \Pi_{n+3} = \Pi_6 = a_0\tau^3\,. \tag{3.39}$$

In other words number (3.39) is the absolute term in characteristic polynomial of (3.13). Utilizing the similarity numbers (3.34) the plant dimensionless form (3.13) is expressed for $n=3$

$$\frac{d^3y(\bar{t})}{d\bar{t}^3} + \Pi_4\frac{d^2y(\bar{t})}{d\bar{t}^2} + \Pi_5\frac{dy(\bar{t})}{d\bar{t}} + \Pi_6 y(\bar{t}) = \Pi_6 u(\bar{t}-1) \tag{3.40}$$

In summary applying the final similarity numbers, Λ,Ψ,Ξ, together with originally derived $\Theta\left(\Pi_4\right)$ and $\Phi\left(\Pi_6\right)$ the form (3.40) is equivalently rewritten

$$\frac{d^3y(\bar{t})}{d\bar{t}^3}+\sqrt{\frac{\Psi\Phi}{\Lambda}}\frac{d^2y(\bar{t})}{d\bar{t}^2}+\Psi\Phi\frac{dy(\bar{t})}{d\bar{t}}+\Phi y(\bar{t})=\Phi u(\bar{t}-1). \tag{3.41}$$

Compared to (3.1) both (3.40) and (3.41) reduce the number of plant parameters by one. However there is a square root in (3.41) hence to remove it the following equivalent similarity numbers are introduced

$$\Pi_4=\frac{\Psi}{\Lambda\Xi},\ \Pi_5=\frac{\Psi^2}{\Lambda\Xi^2},\ \Pi_6=\frac{\Psi}{\Lambda\Xi^2}. \tag{3.42}$$

(3.40) is transformed as follows

$$\frac{d^3y(\bar{t})}{d\bar{t}^3}+\frac{\Psi}{\Lambda\Xi}\frac{d^2y(\bar{t})}{d\bar{t}^2}+\frac{\Psi^2}{\Lambda\Xi^2}\frac{dy(\bar{t})}{d\bar{t}}+\frac{\Psi}{\Lambda\Xi^2}y(\bar{t})=\frac{\Psi}{\Lambda\Xi^2}u(\bar{t}-1) \tag{3.43}$$

that is from the dynamic similarity point of view in the final form. To make decision which of the forms is most suitable for the control synthesis neither (3.40) nor (3.41) are appropriate deputies of plant of type (3.1) hence (3.43) should be utilized for the controller tuning with respect to variable Λ, Ψ and Ξ.

Integrating plant. The similarity number (3.14) for $n=3$ is specified as follows

$$\Phi_I=\Pi^I_{n+3}=\Pi^I_6=b_0\tau^3 \tag{3.44}$$

to build the third-order integrating plant model with delay. The number Φ_I is simply the dimensionless coefficient of zero input derivative of differential equation (3.15). On contrary to (3.31) no number Λ_I exist and (3.35) is applied instead. In other words in (3.35) there is not the term a_0. The model (3.40) is overwritten as follows

$$\frac{d^3y(\bar{t})}{d\bar{t}^3}+\Pi_4\frac{d^2y(\bar{t})}{d\bar{t}^2}+\Pi_5\frac{dy(\bar{t})}{d\bar{t}}=\Pi^I_6u(\bar{t}-1). \tag{3.45}$$

where the role of Π_6 from (3.40) takes over Π^I_6 originating from (3.44). Together with (3.35), (3.38) and (3.44) the dimensionless form (3.45) is finalized as follows

$$\frac{d^3y(\bar{t})}{d\bar{t}^3}+\Theta\frac{d^2y(\bar{t})}{d\bar{t}^2}+\Lambda\Theta^2\frac{dy(\bar{t})}{d\bar{t}}=\Phi_Iu(\bar{t}-1). \tag{3.46}$$

Beside Φ_I the third-order integrating plant model with delay is described by the oscillability and laggardness numbers, i.e. Λ and Θ, respectively. Notice the similarity numbers, Ψ and Ξ, are not defined with respect to $a_0=0$.

Case 4. The dimensionless model of the fourth-order plant with delay, $n=4$, is described by the following dimensionless parameters

$$\Pi_4=a_3\tau,\ \Pi_5=a_2\tau^2,\ \Pi_6=a_1\tau^3,\ \Pi_7=a_0\tau^4,\ \Pi_8=\bar{t} \tag{3.47}$$

including the dimensionless frequency variable $\Pi_1 = \omega\tau$. Again from the ratio of Π_4 and Π_5 it results

$$\Lambda = \frac{\Pi_5}{\Pi_4^{\,2}} = \frac{a_2\tau^2}{(a_3\tau)^2} = \frac{a_2}{(a_3)^2}. \tag{3.48}$$

When Π_{n+2} and Π_{n+3} are in the ratio for $n=4$ the similarity number analogously to (3.36) is derived

$$\Psi = \frac{\Pi_{n+2}}{\Pi_{n+3}} = \frac{\Pi_6}{\Pi_7} = \frac{a_1\tau^3}{a_0\tau^4} = \frac{a_1}{a_0\tau}. \tag{3.49}$$

Differently the number (3.37) is given as

$$\Xi = \frac{\Pi_4}{\Pi_{n+3}} = \frac{\Pi_4}{\Pi_7} = \frac{a_3\tau}{a_0\tau^4} = \frac{a_3}{a_0\tau^3}. \tag{3.50}$$

Again Π_4 represents the laggardness number as follows

$$\Theta = \Pi_4 = a_3\tau \tag{3.51}$$

and the absolute term in characteristic polynomial results analogously to (3.38)

$$\Phi = \Pi_{n+3} = \Pi_7 = a_0\tau^4. \tag{3.52}$$

Based on the similarity numbers (3.47) the plant dimensionless form (3.13) is expressed for $n=4$

$$\frac{d^4y(\bar{t})}{d\bar{t}^4} + \Pi_4\frac{d^3y(\bar{t})}{d\bar{t}^3} + \Pi_5\frac{d^2y(\bar{t})}{d\bar{t}^2} + \Pi_6\frac{dy(\bar{t})}{d\bar{t}} + \Pi_7 y(\bar{t}) = \Pi_7 u(\bar{t}-1). \tag{3.53}$$

Once the following arguments are expressed using (3.48) through (3.52) as follows

$$\Pi_4 = \Xi\Phi,\ \Pi_5 = \Xi^2\Phi^2\Lambda,\ \Pi_6 = \Phi\Psi \tag{3.54}$$

the dimensionless model of the fourth-order plant with delay is equivalently expressed

$$\frac{d^4y(\bar{t})}{d\bar{t}^4} + \Xi\Phi\frac{d^3y(\bar{t})}{d\bar{t}^3} + \Lambda\Xi^2\Phi^2\frac{d^2y(\bar{t})}{d\bar{t}^2} + \Psi\Phi\frac{dy(\bar{t})}{d\bar{t}} + \Phi y(\bar{t}) = \Phi u(\bar{t}-1). \tag{3.55}$$

Since in (3.55) Λ, Ψ, Ξ and Φ are involved this model provides enough generalized description of plant of type (3.1) for $n=4$.

Integrating plant. To obtain the integrating plants of the fourth-order the similarity number (3.14) for $n=4$ is specified as follows

$$\Phi_I = \Pi_{n+3}^I = \Pi_7^I = b_0\tau^4 \tag{3.56}$$

(3.55) is the dimensionless coefficient of zero input derivative of differential equation (3.15) in case of $n=4$ and (3.15) changes into the form

$$\frac{d^4y(\bar{t})}{d\bar{t}^4} + \Pi_4\frac{d^3y(\bar{t})}{d\bar{t}^3} + \Pi_5\frac{d^2y(\bar{t})}{d\bar{t}^2} + \Pi_6\frac{dy(\bar{t})}{d\bar{t}} = \Pi_7^I u(\bar{t}-1)\,. \tag{3.57}$$

(3.57) can be rewritten in the more convenient form from the dynamic similarity point of view

$$\frac{d^4y(\bar{t})}{d\bar{t}^4} + \Theta\frac{d^3y(\bar{t})}{d\bar{t}^3} + \Lambda\Theta^2\frac{d^2y(\bar{t})}{d\bar{t}^2} + \Pi_6\frac{dy(\bar{t})}{d\bar{t}} = \Phi_I u(\bar{t}-1)\,. \tag{3.58}$$

where the role of $\Phi(\Pi_7)$ from (3.55) takes over $\Phi_I\left(\Pi_7^I\right)$ originating from (3.56). Be aware $\Pi_6 = \Phi\Psi$ cannot be substituted into (3.58) because Ψ together with Ξ are not defined for the integrating plants in general.

Remark 2. The final similarity numbers provide much better insight into dynamic properties of plants of type (3.1). Simultaneously it can be concluded that the plant (3.1) is reduced in its number of parameters by one parameter, i.e. delay length τ, which resulted in the fixed value by the application of dimensional analysis. Though the delay parameter is excluded from the dimensionless parameters the delay phenomenon itself is otherwise present in the dimensionless plant models (3.13) and (3.15) as unit pure delay.

Let the notation introduced by the dimensional analysis application be summarized in the following table, Tab. 1.

Tab. 1 Similarity numbers derived from Π_i arguments

Order	Similarity number	Definition	Description
1 – 4	$\Pi_1 = \phi$	$\phi = \omega\tau$	frequency angle
	$\Pi_2 = \rho_D$	$\rho_D = Kr_D/\tau$	dimensionless derivative loop gain
	$\Pi_3 = \rho_I$	$\rho_I = Kr_I\tau$	dimensionless integration loop gain
2 – 4	$\Pi_4 = \Theta$	$\Theta = a_{n-1}\tau$	plant *laggardness* number
1 – 4	$\Pi_{n+3} = \Phi$	$\Phi = a_0\tau^n$	absolute term in characteristic polynomial of (3.13) or coefficient of zero input derivative in (3.15)
	$\Pi_{n+3}^I = \Phi_I$	$\Phi_I = b_0\tau^n$	
	$\Pi_{n+4} = \bar{t}$	$\bar{t} = t/\tau$	dimensionless time
$n=1$	$\frac{1}{\Pi_4} = \frac{1}{\Phi} = \Psi$	$\Psi = \frac{1}{a_0\tau}$	plant *laggardness* number
	$\frac{\Pi_4}{\Pi_{n+3}} = \frac{\Pi_4}{\Pi_4} = \Xi$	$\Xi = 1$	relation (3.18)
$n=2$	$\frac{\Pi_5}{\Pi_4^2} = \Lambda$	$\Lambda = \frac{a_0}{a_1^2}$	plant *swingability* number

	$\dfrac{\Pi_{n+2}}{\Pi_{n+3}}=\Psi=\dfrac{\Pi_4}{\Pi_{n+3}}=\Xi$	$\Psi=\Xi=\dfrac{a_{n-1}}{a_0\tau^{n-1}}$	redundancy
	$\Pi_4=\Theta$	$\Theta=a_1\tau$	plant *laggardness* number
	$\dfrac{\Pi_5^I}{\Pi_4^2}=\Lambda_I$	$\Lambda_I=\dfrac{b_0}{a_1^2}$	integrating plant similarity number (3.31)
$n=3$	$\dfrac{\Pi_5}{\Pi_4^2}=\Lambda$	$\Lambda=\dfrac{a_1}{(a_2)^2}$	plant *oscillability* number
	$\dfrac{\Pi_5}{\Pi_6}=\Psi$	$\Psi=\dfrac{a_1}{a_0\tau}$	auxiliary similarity numbers
	$\dfrac{\Pi_4}{\Pi_6}=\Xi$	$\Xi=\dfrac{a_2}{a_0\tau^2}$	
	$\Pi_4=\dfrac{\Psi}{\Lambda\Xi}$	$\Theta=\dfrac{\Psi}{\Lambda\Xi}=a_2\tau$	plant laggardness number, see (3.38)
	$\Pi_5=\dfrac{\Psi^2}{\Lambda\Xi^2}$	$\Theta=\Pi_5\dfrac{\Xi}{\Psi}=a_2\tau$	
	$\Pi_6=\dfrac{\Psi}{\Lambda\Xi^2}$	$\Theta=\Pi_6\Xi=a_2\tau$	
$n=4$	$\dfrac{\Pi_5}{\Pi_4^2}=\Lambda$	$\Lambda=\dfrac{a_2}{(a_3)^2}$	plant *oscillability* number
	$\dfrac{\Pi_6}{\Pi_7}=\Psi$	$\Psi=\dfrac{a_1}{a_0\tau}$	auxiliary similarity numbers
	$\dfrac{\Pi_4}{\Pi_7}=\Xi$	$\Xi=\dfrac{a_3}{a_0\tau^3}$	
	$\Pi_4=\Xi\Phi$	$\Theta=\Xi\Phi=a_3\tau$	plant laggardness number, see (3.51)
	$\Pi_5=\Xi^2\Phi^2\Lambda$	$\Theta=\sqrt{\Pi_5/\Lambda}=a_3\tau$	
	$\Pi_6=\Phi\Psi$	$\Theta=\Pi_6\dfrac{\Xi}{\Psi}=a_3\tau$	

For the purpose of plant pole spectrum investigation the corresponding characteristic polynomial is specified for the plant cases, namely $n=2$, $n=3$ and $n=4$. As regards the *Case 1*, $n=1$, the first-order plant with delay is not considered for PID control synthesis because the dominant pole placement technique is generalized in Chapter 4 for the control loop systems of retarded type. To investigate the pole spectrum the dimensionless Laplace transform of corresponding plant models is made. Simultaneously with $\bar{t}=t/\tau$ and conformly with $\phi=\omega\tau$ the following dimensionless complex variable of Laplace transform results

$$\bar{s}=s\tau. \tag{3.59}$$

Case 2 (*Characteristic polynomial*). The dimensionless Laplace transform of (3.29) under zero initial conditions results in

$$\left[\bar{s}^2 + \Theta\bar{s} + \Lambda\Theta^2\right] Y(\bar{s}) = \Lambda\Theta^2 \exp(-\bar{s}) U(\bar{s}) \tag{3.60}$$

from where

$$\bar{s}^2 + \Theta\bar{s} + \Lambda\Theta^2 = M\left(\bar{s}\right) \tag{3.61}$$

is the characteristic polynomial. The second-order plant transfer function results in

$$G(\bar{s}) = \frac{Y(\bar{s})}{U(\bar{s})} = \frac{\Lambda\Theta^2}{\bar{s}^2 + \Theta\bar{s} + \Lambda\Theta^2} \exp(-\bar{s}) \tag{3.62}$$

where the steady-state gain is $K = 1$. For the integrating plant (3.33) the transfer function results

$$G(\bar{s}) = \frac{Y(\bar{s})}{U(\bar{s})} = \frac{\Lambda_I\Theta^2}{\bar{s}\left(\bar{s} + \Theta\right)} \exp(-\bar{s}) \tag{3.63}$$

where the denominator is the characteristic polynomial

$$M\left(\bar{s}\right) = \bar{s}\left(\bar{s} + \Theta\right). \tag{3.64}$$

Case 3 (*Characteristic polynomial*). The dimensionless Laplace transform of (3.43) under zero initial conditions is given as

$$\left[\bar{s}^3 + \frac{\Psi}{\Lambda\Xi}\bar{s}^2 + \frac{\Psi^2}{\Lambda\Xi^2}\bar{s} + \frac{\Psi}{\Lambda\Xi^2}\right] Y(\bar{s}) = \frac{\Psi}{\Lambda\Xi^2} \exp(-\bar{s}) U(\bar{s}) \tag{3.65}$$

and from the left-hand side of (3.65) the following characteristic polynomial originates as follows

$$M(\bar{s}) = \bar{s}^3 + \frac{\Psi}{\Lambda\Xi}\bar{s}^2 + \frac{\Psi^2}{\Lambda\Xi^2}\bar{s} + \frac{\Psi}{\Lambda\Xi^2}. \tag{3.66}$$

From variety of the similarity numbers the polynomial (3.66) can be equivalently expressed as follows

$$M(\bar{s}) = \bar{s}^3 + \Theta\bar{s}^2 + \Lambda\Theta^2\bar{s} + \Phi. \tag{3.67}$$

The third-order plant transfer function results in

$$G(\bar{s}) = \frac{Y(\bar{s})}{U(\bar{s})} = \frac{\dfrac{\Psi}{\Lambda\Xi^2}}{\bar{s}^3 + \dfrac{\Psi}{\Lambda\Xi}\bar{s}^2 + \dfrac{\Psi^2}{\Lambda\Xi^2}\bar{s} + \dfrac{\Psi}{\Lambda\Xi^2}} \exp(-\bar{s}) \tag{3.68}$$

or equivalently

$$G(\bar{s}) = \frac{Y(\bar{s})}{U(\bar{s})} = \frac{\Phi}{\bar{s}^3 + \Theta\bar{s}^2 + \Lambda\Theta^2\bar{s} + \Phi} \exp(-\bar{s}) \tag{3.69}$$

where again the unit steady-state gain appears. For the integrating plant (3.46) the transfer function results

$$G(\bar{s}) = \frac{Y(\bar{s})}{U(\bar{s})} = \frac{\Phi_I}{\bar{s}^3 + \Theta\bar{s}^2 + \Lambda\Theta^2\bar{s}} \exp(-\bar{s}) . \tag{3.70}$$

and its denominator is the characteristic polynomial

$$M(\bar{s}) = \bar{s}\left(\bar{s}^2 + \Theta\bar{s} + \Lambda\Theta^2\right). \tag{3.71}$$

Case 4 (*Characteristic polynomial*). The dimensionless Laplace transform of (3.55) under zero initial conditions is obtained as follows

$$\left[\bar{s}^4 + \Xi\Phi\bar{s}^3 + \Lambda\Xi^2\Phi^2\bar{s}^2 + \Psi\Phi\bar{s} + \Phi\right] Y(\bar{s}) = \Phi \exp(-\bar{s}) U(\bar{s}) . \tag{3.72}$$

On the left-hand side the characteristic polynomial appears as follows

$$M(\bar{s}) = \bar{s}^4 + \Xi\Phi\bar{s}^3 + \Lambda\Xi^2\Phi^2\bar{s}^2 + \Psi\Phi\bar{s} + \Phi . \tag{3.73}$$

From available similarity numbers the polynomial (3.73) can be equivalently expressed as follows

$$M(\bar{s}) = \bar{s}^4 + \Theta\bar{s}^3 + \Lambda\Theta^2\bar{s}^2 + \Psi\Phi\bar{s} + \Phi . \tag{3.74}$$

The fourth-order plant transfer function originates in

$$G(\bar{s}) = \frac{Y(\bar{s})}{U(\bar{s})} = \frac{\Phi}{\bar{s}^4 + \Xi\Phi\bar{s}^3 + \Lambda\Xi^2\Phi^2\bar{s}^2 + \Psi\Phi\bar{s} + \Phi} \exp(-\bar{s}) \tag{3.75}$$

or equivalently in

$$G(\bar{s}) = \frac{Y(\bar{s})}{U(\bar{s})} = \frac{\Phi}{\bar{s}^4 + \Theta\bar{s}^3 + \Lambda\Theta^2\bar{s}^2 + \Psi\Phi\bar{s} + \Phi} \exp(-\bar{s}) . \tag{3.76}$$

Both (3.75) and (3.76) are with the unit steady-state gain. For the integrating plant (3.46) the transfer function results as

$$G(\bar{s}) = \frac{Y(\bar{s})}{U(\bar{s})} = \frac{\Phi_I}{\bar{s}^4 + \Theta\bar{s}^3 + \Lambda\Theta^2\bar{s}^2 + \Pi_6\bar{s}} \exp(-\bar{s}) \tag{3.77}$$

and its denominator is the characteristic polynomial as follows

$$M(\bar{s}) = \bar{s}\left(\bar{s}^3 + \Theta\bar{s}^2 + \Lambda\Theta^2\bar{s} + \Pi_6\right). \tag{3.78}$$

Number Π_6 is used in (3.77) and (3.78) as it is because other similarity numbers do not enable to exchange it in case of the integrating plants.

Subsequently the dimensionless PID control loop models with delay are obtained for considered plant cases to tune the PID controller by means of the dominant pole placement. Also to test resulting PID setting on disturbance rejection performance corresponding transfer function is computed with the notation in Tab. 1. Add disturbance variable *z* to the control input *u* on the right-hand side of (3.1) and link the PID controller (3.7) to the plant (3.1) with acting disturbance *z* on the plant input in the place of the control variable *u*. Resulting closed loop is described by the following retarded differential equation

$$\begin{aligned}&\frac{d^{n+1}y(t)}{dt^{n+1}}+a_{n-1}\frac{d^{n}y(t)}{dt^{n}}+a_{n-2}\frac{d^{n-1}y(t)}{dt^{n-1}}+\ldots\\&+a_2\frac{d^3y(t)}{dt^3}+b_0r_D\frac{d^2y(t-\tau)}{dt^2}+a_1\frac{d^2y(t)}{dt^2}+b_0r_P\frac{dy(t-\tau)}{dt}+a_0\frac{dy(t)}{dt}+b_0r_Iy(t-\tau)=\\&b_0r_Iw(t-\tau)+b_0r_P\frac{dw(t-\tau)}{dt}+b_0r_D\frac{d^2w(t-\tau)}{dt^2}+b_0\frac{dz(t-\tau)}{dt}\end{aligned}\qquad(3.79)$$

By virtue of the dimensional analysis the dimensionless parameters $\Pi_i, i=1,2,\ldots,n+3,n+4,$ are derived. The dimensionless PID control loop model is then described by retarded differential equation

$$\begin{aligned}&\frac{d^{n+1}y(\bar{t})}{d\bar{t}^{n+1}}+\Pi_4\frac{d^{n}y(\bar{t})}{d\bar{t}^{n}}+\Pi_5\frac{d^{n-1}y(\bar{t})}{d\bar{t}^{n-1}}+\ldots+\Pi_{n+1}\frac{d^3y(\bar{t})}{d\bar{t}^3}+\\&\Pi_{n+3}\rho_D\frac{d^2y(\bar{t}-1)}{d\bar{t}^2}+\Pi_{n+2}\frac{d^2y(\bar{t})}{d\bar{t}^2}+\Pi_{n+3}\rho_P\frac{dy(\bar{t}-1)}{dt}+\Pi_{n+3}\frac{dy(\bar{t})}{d\bar{t}}+\Pi_{n+3}\rho_Iy(\bar{t}-1)=\\&=\Pi_{n+3}\rho_Iw(\bar{t}-1)+\Pi_{n+3}\rho_P\frac{dw(\bar{t}-1)}{d\bar{t}}+\Pi_{n+3}\rho_D\frac{d^2w(\bar{t}-1)}{d\bar{t}^2}+\Pi_{n+3}\frac{dz(\bar{t}-1)}{d\bar{t}}\end{aligned}\qquad(3.80)$$

Although (3.80) is obtained under assumptions $K=1$, i.e. $a_0=b_0$, this equation covers also unconstrained case in parameter values, except $a_0=0$. The control loop models for integrating plants are supplied to considered plant cases as supplements. Providing the dimensionless Laplace transform of (3.80) under zero initial conditions

$$\begin{aligned}&\left[\bar{s}^{n+1}+\Pi_4\bar{s}^{n}+\Pi_5\bar{s}^{n-1}+\ldots+\Pi_{n+1}\bar{s}^3+\right.\\&\left.\left(\Pi_{n+2}+\Pi_{n+3}\rho_De^{-\bar{s}}\right)\bar{s}^2+\Pi_{n+3}\left(1+\rho_Pe^{-\bar{s}}\right)\bar{s}+\Pi_{n+3}\rho_Ie^{-\bar{s}}\right]Y(\bar{s})=\\&=\Pi_{n+3}\left[\rho_I+\rho_P\bar{s}+\rho_D\bar{s}^2\right]e^{-\bar{s}}W(\bar{s})+\Pi_{n+3}e^{-\bar{s}}\bar{s}Z(\bar{s})\end{aligned}\qquad(3.81)$$

both reference and disturbance transfer functions are calculated

$$\frac{Y(\bar{s})}{W(\bar{s})}=$$

$$= \frac{\Pi_{n+3}\left(\rho_I + \rho_P \bar{s} + \rho_D \bar{s}^2\right) e^{-\bar{s}}}{\bar{s}^{n+1} + \Pi_4 \bar{s}^n + \Pi_5 \bar{s}^{n-1} + \ldots + \Pi_{n+1}\bar{s}^3 + \left(\Pi_{n+2} + \Pi_{n+3}\rho_D e^{-\bar{s}}\right)\bar{s}^2 + \Pi_{n+3}\left(1 + \rho_P e^{-\bar{s}}\right)\bar{s} + \Pi_{n+3}\rho_I e^{-\bar{s}}} \tag{3.82}$$

and

$$\frac{Y(\bar{s})}{Z(\bar{s})} =$$

$$= \frac{\Pi_{n+3}\bar{s}e^{-\bar{s}}}{\bar{s}^{n+1} + \Pi_4 \bar{s}^n + \Pi_5 \bar{s}^{n-1} + \ldots + \Pi_{n+1}\bar{s}^3 + \left(\Pi_{n+2} + \Pi_{n+3}\rho_D e^{-\bar{s}}\right)\bar{s}^2 + \Pi_{n+3}\left(1 + \rho_P e^{-\bar{s}}\right)\bar{s} + \Pi_{n+3}\rho_I e^{-\bar{s}}} \tag{3.83}$$

Both as (3.82) as (3.83) contain the characteristic quasi-polynomial of the delayed control loop model

$$Q(\bar{s}) =$$

$$= \bar{s}^{n+1} + \Pi_4 \bar{s}^n + \Pi_5 \bar{s}^{n-1} + \ldots + \Pi_{n+1}\bar{s}^3 + \left(\Pi_{n+2} + \Pi_{n+3}\rho_D e^{-\bar{s}}\right)\bar{s}^2 + \Pi_{n+3}\left(1 + \rho_P e^{-\bar{s}}\right)\bar{s} + \Pi_{n+3}\rho_I e^{-\bar{s}} \tag{3.84}$$

which can be next modified after substituting (3.84) into the characteristic equation $Q(\bar{s}) = 0$ as follows

$$\begin{aligned} &\left[\bar{s}^{n+1} + \Pi_4 \bar{s}^n + \Pi_5 \bar{s}^{n-1} + \ldots + \Pi_{n+1}\bar{s}^3 + \Pi_{n+2}\bar{s}^2 + \Pi_{n+3}\bar{s}\right] e^{\bar{s}} + \\ &\Pi_{n+3}\left[\rho_P \bar{s} + \rho_I + \rho_D \bar{s}^2\right] = M(\bar{s}) = 0. \end{aligned} \tag{3.85}$$

Characteristic roots of $Q(\bar{s}) = 0$ and $M(\bar{s}) = 0$ are the same and additionally (3.85) is more appropriate for the computation of control loop spectrum. Reference and disturbance transfer functions for integrating plants (3.15) are attained analogously to (3.82) and (3.83) as follows

$$\frac{Y(\bar{s})}{W(\bar{s})} =$$

$$= \frac{\Pi^I_{n+3}\left(\rho_I + \rho_P \bar{s} + \rho_D \bar{s}^2\right) e^{-\bar{s}}}{\bar{s}^{n+1} + \Pi_4 \bar{s}^n + \Pi_5 \bar{s}^{n-1} + \ldots + \Pi_{n+1}\bar{s}^3 + \left(\Pi_{n+2} + \Pi^I_{n+3}\rho_D e^{-\bar{s}}\right)\bar{s}^2 + \Pi^I_{n+3}\rho_P e^{-\bar{s}}\bar{s} + \Pi^I_{n+3}\rho_I e^{-\bar{s}}} \tag{3.86}$$

and

$$\frac{Y(\bar{s})}{Z(\bar{s})} =$$

$$= \frac{\Pi^I_{n+3}\bar{s}e^{-\bar{s}}}{\bar{s}^{n+1} + \Pi_4 \bar{s}^n + \Pi_5 \bar{s}^{n-1} + \ldots + \Pi_{n+1}\bar{s}^3 + \left(\Pi_{n+2} + \Pi^I_{n+3}\rho_D e^{-\bar{s}}\right)\bar{s}^2 + \Pi^I_{n+3}\rho_P e^{-\bar{s}}\bar{s} + \Pi^I_{n+3}\rho_I e^{-\bar{s}}} \tag{3.87}$$

respectively. The characteristic quasi-polynomial differs from (3.84) instead of Π_{n+3} number Π^I_{n+3} is introduced by (3.14). Then analogously to (3.85) the modified characteristic equation results

$$M(\overline{s}) = \\ = \left[\overline{s}^{n+1} + \Pi_4 \overline{s}^n + \Pi_5 \overline{s}^{n-1} + ... + \Pi_{n+1}\overline{s}^3 + \Pi_{n+2}\overline{s}^2\right] e^{\overline{s}} + \Pi^I_{n+3}\left[\rho_P \overline{s} + \rho_I + \rho_D \overline{s}^2\right] = 0. \tag{3.88}$$

Case 2 (*Control loop*). The dimensionless PID control loop with delay has been already developed for the case of $n = 2$ [123]. Here the sets of dynamically similar second-order plants either aperiodic or oscillatory are controlled by the PID of which settings correspond to those sets. The PID controller settings are evaluated versus derived similarity numbers that are achieved in (3.24), (3.25) and (3.31). As regards the reference and disturbance transfer functions for both proportional and integrating plants they are achieved from (3.82), (3.83) and (3.86), (3.87) by substituting 2 for *n*

$$\frac{Y(\overline{s})}{W(\overline{s})} = \frac{\Lambda\Theta^2\left(\rho_I + \rho_P\overline{s} + \rho_D\overline{s}^2\right)e^{-\overline{s}}}{\overline{s}^3 + \Theta\left(1 + \Lambda\Theta\rho_D e^{-\overline{s}}\right)\overline{s}^2 + \Lambda\Theta^2\left(1 + \rho_P e^{-\overline{s}}\right)\overline{s} + \Lambda\Theta^2\rho_I e^{-\overline{s}}}, \tag{3.89}$$

$$\frac{Y(\overline{s})}{Z(\overline{s})} = \frac{\Lambda\Theta^2\overline{s}e^{-\overline{s}}}{\overline{s}^3 + \Theta\left(1 + \Lambda\Theta\rho_D e^{-\overline{s}}\right)\overline{s}^2 + \Lambda\Theta^2\left(1 + \rho_P e^{-\overline{s}}\right)\overline{s} + \Lambda\Theta^2\rho_I e^{-\overline{s}}} \tag{3.90}$$

and

$$\frac{Y(\overline{s})}{W(\overline{s})} = \frac{\Lambda_I\Theta^2\left(\rho_I + \rho_P\overline{s} + \rho_D\overline{s}^2\right)e^{-\overline{s}}}{\overline{s}^3 + \Theta\left(1 + \Lambda_I\Theta\rho_D e^{-\overline{s}}\right)\overline{s}^2 + \Lambda_I\Theta^2\rho_P e^{-\overline{s}}\overline{s} + \Lambda_I\Theta^2\rho_I e^{-\overline{s}}}, \tag{3.91}$$

$$\frac{Y(\overline{s})}{Z(\overline{s})} = \frac{\Lambda_I\Theta^2\overline{s}e^{-\overline{s}}}{\overline{s}^3 + \Theta\left(1 + \Lambda_I\Theta\rho_D e^{-\overline{s}}\right)\overline{s}^2 + \Lambda_I\Theta^2\rho_P e^{-\overline{s}}\overline{s} + \Lambda_I\Theta^2\rho_I e^{-\overline{s}}}, \tag{3.92}$$

respectively. Notice $\Theta = \Pi_4$, $\Lambda\Theta^2 = \Pi_5$ and $\Lambda_I\Theta^2 = \Pi^I_5$ while Π_1, Π_2, Π_3 do not belong to the plant similarity numbers. Lastly the characteristic quasi-polynomial of both delayed PID control loop models results from (3.89) and (3.91)

$$Q(\overline{s}) = \overline{s}^3 + \Theta\left(1 + \Lambda\Theta\rho_D e^{-\overline{s}}\right)\overline{s}^2 + \Lambda\Theta^2\left(1 + \rho_P e^{-\overline{s}}\right)\overline{s} + \Lambda\Theta^2\rho_I e^{-\overline{s}}, \tag{3.93}$$

$$Q(\overline{s}) = \overline{s}^3 + \Theta\left(1 + \Lambda_I\Theta\rho_D e^{-\overline{s}}\right)\overline{s}^2 + \Lambda_I\Theta^2\rho_P e^{-\overline{s}}\overline{s} + \Lambda_I\Theta^2\rho_I e^{-\overline{s}}, \tag{3.94}$$

and analogously to their modification according to (3.85) and (3.88) into the characteristic equation one gets

$$\left[\overline{s}^3 + \Theta\overline{s}^2 + \Lambda\Theta^2\overline{s}\right]e^{\overline{s}} + \Lambda\Theta^2\left[\rho_P\overline{s} + \rho_I + \rho_D\overline{s}^2\right] = M(\overline{s}) = 0 \tag{3.95}$$

and

$$\left[\overline{s}^3+\Theta\overline{s}^2\right]e^{\overline{s}}+\Lambda_I\Theta^2\left[\rho_P\overline{s}+\rho_I+\rho_D\overline{s}^2\right]=M\left(\overline{s}\right)=0, \tag{3.96}$$

respectively. Both characteristic equations have been subsequently applied to dominant-three pole placement in order to tune control loop gains.

Case 3 (*Control loop*). The dimensionless PID control loop model with delay is found for the sets of dynamically similar third-order plants, aperiodic or oscillatory, characterized by similarity numbers (3.35), (3.38), (3.39) and (3.44). Corresponding reference and disturbance transfer functions are attained from (3.82), (3.83) and (3.86), (3.87) by substituting 3 for *n*

$$\frac{Y\left(\overline{s}\right)}{W\left(\overline{s}\right)}=\frac{\Phi\left(\rho_I+\rho_P\overline{s}+\rho_D\overline{s}^2\right)e^{-\overline{s}}}{\overline{s}^4+\Theta\overline{s}^3+\left(\Lambda\Theta^2+\Phi\rho_De^{-\overline{s}}\right)\overline{s}^2+\Phi\left(1+\rho_Pe^{-\overline{s}}\right)\overline{s}+\Phi\rho_Ie^{-\overline{s}}}, \tag{3.97}$$

$$\frac{Y\left(\overline{s}\right)}{Z\left(\overline{s}\right)}=\frac{\Phi\overline{s}e^{-\overline{s}}}{\overline{s}^4+\Theta\overline{s}^3+\left(\Lambda\Theta^2+\Phi\rho_De^{-\overline{s}}\right)\overline{s}^2+\Phi\left(1+\rho_Pe^{-\overline{s}}\right)\overline{s}+\Phi\rho_Ie^{-\overline{s}}} \tag{3.98}$$

and

$$\frac{Y\left(\overline{s}\right)}{W\left(\overline{s}\right)}=\frac{\Phi_I\left(\rho_I+\rho_P\overline{s}+\rho_D\overline{s}^2\right)e^{-\overline{s}}}{\overline{s}^4+\Theta\overline{s}^3+\left(\Lambda\Theta^2+\Phi_I\rho_De^{-\overline{s}}\right)\overline{s}^2+\Phi_I\rho_Pe^{-\overline{s}}\overline{s}+\Phi_I\rho_Ie^{-\overline{s}}}, \tag{3.99}$$

$$\frac{Y\left(\overline{s}\right)}{Z\left(\overline{s}\right)}=\frac{\Phi_I\overline{s}e^{-\overline{s}}}{\overline{s}^4+\Theta\overline{s}^3+\left(\Lambda\Theta^2+\Phi_I\rho_De^{-\overline{s}}\right)\overline{s}^2+\Phi_I\rho_Pe^{-\overline{s}}\overline{s}+\Phi_I\rho_Ie^{-\overline{s}}}, \tag{3.100}$$

respectively. Notice $\Theta=\Pi_4$, $\Lambda\Theta^2=\Pi_5$, $\Phi=\Pi_6$ and $\Phi_I=\Pi_6^I$. Finally the characteristic quasi-polynomial of both delayed PID control loop models results from (3.97) and (3.99) as follows

$$Q\left(\overline{s}\right)=\overline{s}^4+\Theta\overline{s}^3+\left(\Lambda\Theta^2+\Phi\rho_De^{-\overline{s}}\right)\overline{s}^2+\Phi\left(1+\rho_Pe^{-\overline{s}}\right)\overline{s}+\Phi\rho_Ie^{-\overline{s}}, \tag{3.101}$$

$$Q\left(\overline{s}\right)=\overline{s}^4+\Theta\overline{s}^3+\left(\Lambda\Theta^2+\Phi_I\rho_De^{-\overline{s}}\right)\overline{s}^2+\Phi_I\rho_Pe^{-\overline{s}}\overline{s}+\Phi_I\rho_Ie^{-\overline{s}}. \tag{3.102}$$

With respect to (3.85) and (3.88) the corresponding characteristic equations are achieved

$$\left[\overline{s}^4+\Theta\overline{s}^3+\Lambda\Theta^2\overline{s}^2+\Phi\overline{s}\right]e^{\overline{s}}+\Phi\left[\rho_P\overline{s}+\rho_I+\rho_D\overline{s}^2\right]=M\left(\overline{s}\right)=0 \tag{3.103}$$

and

$$\left[\overline{s}^4+\Theta\overline{s}^3+\Lambda\Theta^2\overline{s}^2\right]e^{\overline{s}}+\Phi_I\left[\rho_P\overline{s}+\rho_I+\rho_D\overline{s}^2\right]=M\left(\overline{s}\right)=0, \tag{3.104}$$

respectively.

Case 4 (*Control loop*). The dimensionless PID control loop model with delay is got for the sets of dynamically similar fourth-order plants with delay characterized by similarity numbers (3.48), (3.51), (3.52) and (3.56). Corresponding reference and disturbance transfer functions are attained from (3.82), (3.83) and (3.86), (3.87) by substituting 4 for *n*

$$\frac{Y(\overline{s})}{W(\overline{s})}=\frac{\Phi\left(\rho_I+\rho_P\overline{s}+\rho_D\overline{s}^2\right)e^{-\overline{s}}}{\overline{s}^5+\Theta\overline{s}^4+\Lambda\Theta^2\overline{s}^3+\Phi\left(\Psi+\rho_De^{-\overline{s}}\right)\overline{s}^2+\Phi\left(1+\rho_Pe^{-\overline{s}}\right)\overline{s}+\Phi\rho_Ie^{-\overline{s}}}, \tag{3.105}$$

$$\frac{Y(\overline{s})}{Z(\overline{s})}=\frac{\Phi\overline{s}e^{-\overline{s}}}{\overline{s}^5+\Theta\overline{s}^4+\Lambda\Theta^2\overline{s}^3+\Phi\left(\Psi+\rho_De^{-\overline{s}}\right)\overline{s}^2+\Phi\left(1+\rho_Pe^{-\overline{s}}\right)\overline{s}+\Phi\rho_Ie^{-\overline{s}}} \tag{3.106}$$

and

$$\frac{Y(\overline{s})}{W(\overline{s})}=\frac{\Phi_I\left(\rho_I+\rho_P\overline{s}+\rho_D\overline{s}^2\right)e^{-\overline{s}}}{\overline{s}^5+\Theta\overline{s}^4+\Lambda\Theta^2\overline{s}^3+\left(\Pi_6+\Phi_I\rho_De^{-\overline{s}}\right)\overline{s}^2+\Phi_I\rho_Pe^{-\overline{s}}\overline{s}+\Phi_I\rho_Ie^{-\overline{s}}}, \tag{3.107}$$

$$\frac{Y(\overline{s})}{Z(\overline{s})}=\frac{\Phi_I\overline{s}e^{-\overline{s}}}{\overline{s}^5+\Theta\overline{s}^4+\Lambda\Theta^2\overline{s}^3+\left(\Pi_6+\Phi_I\rho_De^{-\overline{s}}\right)\overline{s}^2+\Phi_I\rho_Pe^{-\overline{s}}\overline{s}+\Phi_I\rho_Ie^{-\overline{s}}}, \tag{3.108}$$

respectively. Notice $\Theta=\Pi_4$, $\Lambda\Theta^2=\Pi_5$, $\Phi\Psi=\Pi_6$, $\Phi=\Pi_7$ and $\Phi_I=\Pi_7^I$. Be aware $\Phi\Psi=\Pi_6$ is not applicable for the fourth-order integrating plants with delay. Next the characteristic quasi-polynomial of both delayed PID control loop models is identified with the denominator of (3.105) and (3.107) as follows

$$Q(\overline{s})=\overline{s}^5+\Theta\overline{s}^4+\Lambda\Theta^2\overline{s}^3+\Phi\left(\Psi+\rho_De^{-\overline{s}}\right)\overline{s}^2+\Phi\left(1+\rho_Pe^{-\overline{s}}\right)\overline{s}+\Phi\rho_Ie^{-\overline{s}}, \tag{3.109}$$

and

$$Q(\overline{s})=\overline{s}^5+\Theta\overline{s}^4+\Lambda\Theta^2\overline{s}^3+\left(\Pi_6+\Phi_I\rho_De^{-\overline{s}}\right)\overline{s}^2+\Phi_I\rho_Pe^{-\overline{s}}\overline{s}+\Phi_I\rho_Ie^{-\overline{s}}, \tag{3.110}$$

respectively. Applying (3.85) and (3.88) to (3.101) and (3.102), respectively, the corresponding characteristic equations are achieved as follows

$$\left[\overline{s}^5+\Theta\overline{s}^4+\Lambda\Theta^2\overline{s}^3+\Phi\Psi\overline{s}^2+\Phi\overline{s}\right]e^{\overline{s}}+\Phi\left[\rho_P\overline{s}+\rho_I+\rho_D\overline{s}^2\right]=M(\overline{s})=0, \tag{3.111}$$

$$\left[\overline{s}^5+\Theta\overline{s}^4+\Lambda\Theta^2\overline{s}^3+\Pi_6\overline{s}^2\right]e^{\overline{s}}+\Phi_I\left[\rho_P\overline{s}+\rho_I+\rho_D\overline{s}^2\right]=M(\overline{s})=0. \tag{3.112}$$

3.2.2 Dimensional analysis application: Option II

To remedy the disadvantage of dimensionless forms (3.13) and (3.15) of plant model (3.1) consisting in the fixed delay parameter equal to one the appropriate reformulation of both model (3.1) and dimensional analysis procedure is made in the sequel. In contrast to (3.1) the following time delay plant model is identified

$$\tilde{a}_n \frac{d^n y(t)}{dt^n} + \tilde{a}_{n-1} \frac{d^{n-1} y(t)}{dt^{n-1}} + \tilde{a}_{n-2} \frac{d^{n-2} y(t)}{dt^{n-2}} + ... + \tilde{a}_2 \frac{d^2 y(t)}{dt^2} + \tilde{a}_1 \frac{dy(t)}{dt} + y(t) = Ku(t-\tau), \qquad (3.113)$$

of which transfer function results in (3.5). However the model (3.113) covers proportional plants only, i.e. $a_0 \neq 0$, hence the plant model (3.113) is completely reformulated as follows

$$c_n \frac{d^n y(t)}{dt^n} + c_{n-1} \frac{d^{n-1} y(t)}{dt^{n-1}} + c_{n-2} \frac{d^{n-2} y(t)}{dt^{n-2}} + ... + c_2 \frac{d^2 y(t)}{dt^2} + c_1 \frac{dy(t)}{dt} + y(t) = Ku(t-\tau), \qquad (3.114)$$

with transfer function

$$G(s) = \frac{K}{A(s)} \exp(-s\tau) \qquad (3.115)$$

where

$$A(s) = 1 + \sum_{i=1}^{n} c_i s^i,\ c_i > 0, i = 1, 2, ..., n, K \neq 0, n \geq 2\ . \qquad (3.116)$$

Again the plant model (3.114) is stable because the plant model (3.1) is assumed stable too. In case of the integrating plants the unit from $A(s)$ in (3.116) disappears and model (3.114) is modified to the form

$$c_n \frac{d^n y(t)}{dt^n} + c_{n-1} \frac{d^{n-1} y(t)}{dt^{n-1}} + c_{n-2} \frac{d^{n-2} y(t)}{dt^{n-2}} + ... + c_2 \frac{d^2 y(t)}{dt^2} + c_1 \frac{dy(t)}{dt} = Ku(t-\tau)\,. \qquad (3.117)$$

Also for the case of plant models (3.114) and (3.117) the dimensionless description of PID control loop is obtained by means of the dimensional analysis. Analogously to (3.8) the following quantities of this control loop are considered for the dimensional analysis

$$\omega\left[\mathrm{s}^{-1}\right], t\left[\mathrm{s}\right], Kr_D\left[\mathrm{s}\right], Kr_I\left[\mathrm{s}^{-1}\right], \tau\left[\mathrm{s}\right], c_{n-1}\left[\mathrm{s}^{n-1}\right], c_{n-2}\left[\mathrm{s}^{n-2}\right], \ldots, c_2\left[\mathrm{s}^2\right], c_1\left[\mathrm{s}\right], c_n\left[\mathrm{s}^n\right]. \qquad (3.118)$$

Let be stressed that as in (3.8) product $Kr_P = \rho_P$ is not considered again and the order of the quantities in (3.118) again obeys their significance for dimensionless control loop description. The most significant parameter for the control loop remains its natural frequency while for forming a scaling factor the coefficient c_n is used instead of the delay, τ, see (3.8). This choice of the independent parameter removes the aforementioned disadvantage of the dimensional analysis procedure presented in section Option I. Continuing the dimensional

analysis procedure the dimensionless parameters searched are arguments of the following products

$$\pi_i = \omega^{\varepsilon_1} t^{\varepsilon_2} \left(Kr_D\right)^{\varepsilon_3} \left(Kr_I\right)^{\varepsilon_4}, \tau^{\varepsilon_5}, \left(c_{n-1}\right)^{\varepsilon_6} \left(c_{n-2}\right)^{\varepsilon_7} \cdots c_2^{\varepsilon_{n+3}} c_1^{\varepsilon_{n+4}}, c_n^{\varepsilon_{n+5}}, \quad i = 1,2,...,n+3,n+4 \quad (3.119)$$

Now analogously to (3.10) the one row dimensional matrix is obtained

$$\mathbf{D} = \begin{bmatrix} -1 & 1 & 1 & -1 & 1 & n-1 & n-2 & \cdots & 2 & 1 & n \end{bmatrix} \quad (3.120)$$

The similarity numbers given by (3.119) originate from the augmented matrix equation given by (3.11) from where

$$\mathbf{D}_1 = \begin{bmatrix} -1 & 1 & 1 & -1 & 1 & n-1 & n-2 & \cdots & 2 & 1 \end{bmatrix},\ D_2 = n. \quad (3.121)$$

So that it results a linear equation as follows

$$-\varepsilon_1 + \varepsilon_2 + \varepsilon_3 - \varepsilon_4 + \varepsilon_5 + \left(n-1\right)\varepsilon_6 + \left(n-2\right)\varepsilon_7 \cdots + 2\varepsilon_{n+3} + \varepsilon_{n+4} + n\varepsilon_{n+5} = 0 \quad (3.122)$$

Again be aware the order, *n*, cannot be arbitrarily high due to the limited capability of the PID controller to change the plant dynamics and to the involved relations for similarity numbers. In analogous way to the exponents in (3.9) iteratively $n+4$ solutions to (3.122) are obtained and after their insertions into (3.119) the dimensionless parameters describing the delayed PID control loop models are derived as follows

1. $\varepsilon_1 = 1, \varepsilon_{2,3,4,5,6,7} \cdots = \varepsilon_{n+2} = \varepsilon_{n+3} = \varepsilon_{n+4} = 0 \rightarrow \varepsilon_{n+5} = n^{-1} \rightarrow \pi_1 = \omega\sqrt[n]{c_n}$
2. $\varepsilon_2 = 1, \varepsilon_{1,3,4,5,6,7} \cdots = \varepsilon_{n+2} = \varepsilon_{n+3} = \varepsilon_{n+4} = 0 \rightarrow \varepsilon_{n+5} = -n^{-1} \rightarrow \pi_2 = \dfrac{t}{\sqrt[n]{c_n}}$
3. $\varepsilon_3 = 1, \varepsilon_{1,2,4,5,6,7} \cdots = \varepsilon_{n+2} = \varepsilon_{n+3} = \varepsilon_{n+4} = 0 \rightarrow \varepsilon_{n+5} = -n^{-1} \rightarrow \pi_3 = \dfrac{Kr_D}{\sqrt[n]{c_n}}$
4. $\varepsilon_4 = 1, \varepsilon_{1,2,3,5,6,7} \cdots = \varepsilon_{n+2} = \varepsilon_{n+3} = \varepsilon_{n+4} = 0 \rightarrow \varepsilon_{n+5} = n^{-1} \rightarrow \pi_4 = Kr_I\sqrt[n]{c_n}$
5. $\varepsilon_5 = 1, \varepsilon_{1,2,3,4,6,7} \cdots = \varepsilon_{n+2} = \varepsilon_{n+3} = \varepsilon_{n+4} = 0 \rightarrow \varepsilon_{n+5} = -n^{-1} \rightarrow \pi_5 = \dfrac{\tau}{\sqrt[n]{c_n}}$
6. $\varepsilon_6 = 1, \varepsilon_{1,2,3,4,5,7} \cdots = \varepsilon_{n+2} = \varepsilon_{n+3} = \varepsilon_{n+4} = 0 \rightarrow \varepsilon_{n+5} = -\dfrac{n-1}{n} \rightarrow \pi_6 = \dfrac{c_{n-1}}{\sqrt[n]{\left(c_n\right)^{n-1}}}$
7. $\varepsilon_7 = 1, \varepsilon_{1,2,3,4,5,6} \cdots = \varepsilon_{n+2} = \varepsilon_{n+3} = \varepsilon_{n+4} = 0 \rightarrow \varepsilon_{n+5} = -\dfrac{n-2}{n} \rightarrow \pi_7 = \dfrac{c_{n-2}}{\sqrt[n]{\left(c_n\right)^{n-2}}}$

$\vdots$

n+3. $\varepsilon_{n+3} = 1, \varepsilon_{1,2,3,4,5,6,7} \cdots = \varepsilon_{n+2} = \varepsilon_{n+4} = 0 \rightarrow \varepsilon_{n+5} = -2n^{-1} \rightarrow \pi_{n+3} = \dfrac{c_2}{\sqrt[n]{c_n^{\,2}}}$

n+4. $\varepsilon_{n+4} = 1, \varepsilon_{1,2,3,4,5,6,7} \cdots = \varepsilon_{n+2} = \varepsilon_{n+3} = 0 \rightarrow \varepsilon_{n+5} = -n^{-1} \rightarrow \pi_{n+4} = \dfrac{c_1}{\sqrt[n]{c_n}}$

Here π_1 and π_2 are dimensionless frequency and time variables, respectively, at which the control loop models are expressed. Another meaning of π_1 is dimensionless natural frequency (or natural frequency angle) with the following notation $\pi_1 = \nu$. π_3 and π_4 are the derivative and integration loop gains, respectively, which are defined with non-zero steady-state gain, $K \neq 0$. Thus $\pi_3 = \rho_D$ and $\pi_4 = \rho_I$. As regards π_5 it is dimensionless time delay which is not fixed to one as in case of the dimensionless models described by (3.13). Naturally the higher π_5 the more delayed are the control loop responses. Regarding $\pi_6, \pi_7, \ldots, \pi_{n+3}, \pi_{n+4}$ they are plant dimensionless parameters. Thus using $\pi_2 = \bar{t} = t \big/ \sqrt[n]{c_n}$ the plant model (3.114) is transformed to the dimensionless form

$$\frac{d^n y(\bar{t})}{d\bar{t}^n} + \pi_6 \frac{d^{n-1} y(\bar{t})}{d\bar{t}^{n-1}} + \pi_7 \frac{d^{n-2} y(\bar{t})}{d\bar{t}^{n-2}} + \ldots + \pi_{n+3} \frac{d^2 y(\bar{t})}{d\bar{t}^2} + \pi_{n+4} \frac{dy(\bar{t})}{d\bar{t}} + y(\bar{t}) = Ku(\bar{t} - \pi_5), \quad (3.123)$$

which resulted analogously to (3.13) in the delayed model of order *n* restricted up to four. Model (3.123) provides reducing the number of plant parameters by one in comparison with original model identified as (3.114). Of course a particular selection of the similarity numbers has to be made for achieving this reduction for considered cases of plants below. The reduced and independent parameter from (3.114) is c_n used to form the scaling factor $\sqrt[n]{c_n}$.

Integrating plant. What is changed in the dimensional analysis in case the plant is the integrating plant (3.117)? As soon as $n > 2$ in (3.117) all the results of the dimensional analysis beginning with (3.118) through (3.122) are applicable to plant (3.117) controlled by (3.7) without any change. The dimensionless form of model (3.117) is obtained by omitting the term $y(\bar{t})$ in (3.123) as follows

$$\frac{d^n y(\bar{t})}{d\bar{t}^n} + \pi_6 \frac{d^{n-1} y(\bar{t})}{d\bar{t}^{n-1}} + \pi_7 \frac{d^{n-2} y(\bar{t})}{d\bar{t}^{n-2}} + \ldots + \pi_{n+3} \frac{d^2 y(\bar{t})}{d\bar{t}^2} + \pi_{n+4} \frac{dy(\bar{t})}{d\bar{t}} = Ku(\bar{t} - \pi_5). \quad (3.124)$$

Some alterations in deriving the similarity numbers take place depending on the plant order, *n*. In describing the integrating plant dynamics both *oscillability* and *stiffness* participate. Generally the *stiff* behaviour of servomechanisms was observed very early, [45], and this behaviour is modelled as a ratio of short and long impulse response time constant.

Remark 3. In practice the order of (3.123) cannot be arbitrary due to the PID control application, see Remark 1. Since the PID controller applicability is further limited up to $n = 4$ the following assumptions on the plant (3.114) parameters are required. When $n = 3$

$$c_3 < c_1 c_2 \quad (3.125)$$

and when $n = 4$

$$c_2 c_3 > c_1 c_4, \; c_3 \left(c_1 c_2 - c_3 \right) > c_1^2 c_4. \quad (3.126)$$

Both (3.125) and (3.126) originate from Hurwitz criterion application and their fulfilment guarantees the plant stability. In this case the dimensionless form (3.123) is also stable.

Due to the limited order n only the following cases of plants (3.114) with delay are considered: $n=1$, $n=2$, $n=3$ and $n=4$. Also the integrating plants (3.117) of corresponding order are included.

Case 1. The dimensionless model of the first-order plant with delay, $n=1$, is described by the following dimensionless parameters

$$\pi_1 = \omega c_1,\ \pi_2 = \frac{t}{c_1},\ \pi_5 = \frac{\tau}{c_1}. \tag{3.127}$$

Be aware that from all the similarity numbers belonging to the plant parameters only π_{n+4} for $n=1$ exists

$$\pi_{n+4} = \frac{c_1}{\sqrt[n]{c_n}} = 1 \tag{3.128}$$

and gives the trivial solution. In fact instead of π_{n+4} for $n=1$ the similarity number π_5 describes plant *retardedness*, i.e. retarded property, and is denoted as follows

$$\pi_5 = \vartheta. \tag{3.129}$$

In other words (3.129) indicates how far is the plant *delayed* or *retarded*. Be aware that also $\pi_6 = 1$ analogously to (3.128). The model (3.123) results for $n=1$ with respect to (3.127) and (3.129) as follows

$$\frac{dy(\bar{t})}{d\bar{t}} + y(\bar{t}) = Ku(\bar{t} - \vartheta) \tag{3.130}$$

Integrating plant. The integrating plant of the first-order is simply obtained by omitting the term $y(\bar{t})$ in (3.130) as follows

$$\frac{dy(\bar{t})}{d\bar{t}} = Ku(\bar{t} - \vartheta) \tag{3.131}$$

where *K* is no more in the role of the steady-state gain.

Case 2. The dimensional analysis has been presented for plants of type (3.114) and (3.117) when $n=2$ in [126]. For the case of aperiodic or oscillatory second-order plants with delay the dimensional analysis leads to deriving the following similarity number

$$\pi_1 = \omega\sqrt{c_2},\ \pi_2 = \frac{t}{\sqrt{c_2}} = \bar{t},\ \pi_5 = \frac{\tau}{\sqrt{c_2}},\ \pi_6 = \frac{c_1}{\sqrt{c_2}}. \tag{3.132}$$

Using (3.132) final similarity numbers are given as follows

$$\lambda = \frac{1}{\pi_6} = \frac{\sqrt{c_2}}{c_1} \tag{3.133}$$

and

$$\vartheta = \pi_5 = \frac{\tau}{\sqrt{c_2}}. \tag{3.134}$$

λ is called the *swingability* number while ϑ is the so-called *laggardness* number [126]. The swingability number can be obtained from two different similarity numbers introduced as

$$\lambda = \frac{\pi_{n+3}}{\pi_{n+4}} = \frac{c_2}{c_1}\frac{1}{\sqrt[n]{c_n}} \tag{3.135}$$

and

$$\theta = \frac{\pi_7}{\pi_6} = \frac{c_{n-2}}{c_{n-1}}\sqrt[n]{c_n} \tag{3.136}$$

when substituting $n = 2$ into both (3.135) and (3.136). In (3.136) it results $c_0 = 1$. For $n = 2$ λ and θ are the same and there is the redundancy. Next redundancy emerges between the following similarity numbers

$$\mu = \pi_6 = \frac{c_1}{\sqrt{c_2}} = \lambda^{-1} \tag{3.137}$$

and

$$\sigma = \pi_{n+3}\pi_{n+4} = \frac{c_1 c_2}{\sqrt[n]{c_n^{\,3}}} = \frac{c_1}{\sqrt{c_2}} \equiv \mu \tag{3.138}$$

that result the same for $n = 2$. In addition both μ and σ are reciprocal to λ. With respect to the definition of both π_{n+3} and π_7 one can write for $n = 2$

$$\pi_7 = \theta\pi_6 = \theta\mu = 1,\ \pi_{n+3} = 1. \tag{3.139}$$

Let be remarked there is a collision between π_5 and π_{n+3} for $n = 2$. While π_5 is ϑ the number, π_{n+3}, is other plant similarity number that disappears as apparent from (3.139). In fact this collision is resolved by introducing another similarity number

$$\psi = \frac{\pi_5}{\pi_6} = \frac{\tau}{c_{n-1}}\sqrt[n]{c_n^{n-2}} \tag{3.140}$$

which for $n=2$ results in $\pi_5/\pi_6=\tau/c_1$ where $\pi_6=\psi^{-1}\vartheta=\lambda^{-1}=c_1/\sqrt{c_2}$. Then, however, (3.140) is very similar to already introduced similarity number $\pi_5=\vartheta$ hence (3.140) is the *redundant* similarity number, too. Due to aforementioned redundancies among the similarity numbers the plant stability is guaranteed if $\mu>0$ in case of $n=2$. The dimensionless model (3.123) for $n=2$ results with respect to (3.137)

$$\frac{d^2y(\bar{t})}{d\bar{t}^2}+\lambda^{-1}\frac{dy(\bar{t})}{d\bar{t}}+y(\bar{t})=Ku(\bar{t}-\vartheta) \tag{3.141}$$

which confirms the dimensionless model for both aperiodic and oscillatory plants in [126].

Integrating plant. The integrating plant of the second-order is formally obtained by omitting the term $y(\bar{t})$ in (3.141) as follows

$$\frac{d^2y(\bar{t})}{d\bar{t}^2}+\lambda_I^{-1}\frac{dy(\bar{t})}{d\bar{t}}=Ku(\bar{t}-\vartheta) \tag{3.142}$$

where λ_I is in the same form as (3.135) and it is no more *swingability* number. This number is called *inertiality* number, [126].

Case 3. The dimensionless model (3.123) of the third-order plant with delay, $n=3$, is described by the following dimensionless parameters

$$\pi_1=\omega\sqrt[3]{c_3},\ \pi_2=\frac{t}{\sqrt[3]{c_3}}=\bar{t},\ \pi_5=\frac{\tau}{\sqrt[3]{c_3}},\ \pi_6=\frac{c_2}{\sqrt[3]{(c_3)^2}},\ \pi_7=\frac{c_1}{\sqrt[3]{c_3}}. \tag{3.143}$$

Based on (3.143) final similarity numbers are obtained with respect to (3.135) and (3.136) as follows

$$\lambda=\frac{\pi_{n+3}}{\pi_{n+4}}=\frac{c_2}{c_1}\frac{1}{\sqrt[n]{c_n}}=\frac{\pi_6}{\pi_7}=\frac{c_2}{c_1}\frac{1}{\sqrt[3]{c_3}}, \tag{3.144}$$

and

$$\theta=\frac{\pi_7}{\pi_6}=\frac{c_{n-2}}{c_{n-1}}\sqrt[n]{c_n}=\frac{c_1}{c_2}\sqrt[3]{c_3}=\lambda^{-1} \tag{3.145}$$

respectively. Apparently from (3.145) for $n=3$ between (3.144) and (3.145) there is the *redundancy* $\theta=\lambda^{-1}$. Hence one of θ, λ is omitted in describing the dynamically similar plants (3.123) when $n=3$. The number, λ, is the *oscillability* number and expresses a tendency to oscillate. Next similarity numbers are simply due to (3.134) and (3.137) as follows

$$\vartheta=\pi_5=\frac{\tau}{\sqrt[3]{c_3}} \tag{3.146}$$

and

$$\mu = \pi_6 = \frac{c_2}{\sqrt[3]{(c_3)^2}}, \tag{3.147}$$

respectively. The similarity number (3.140) for $n = 3$ results in

$$\psi = \frac{\pi_5}{\pi_6} = \frac{\tau}{c_2}\sqrt[3]{c_3} \tag{3.148}$$

and using (3.146) the number μ is expressed as follows

$$\pi_6 = \psi^{-1}\vartheta = \mu. \tag{3.149}$$

The number, ψ, according to (3.148) is in the role of a supplementary similarity number. Significant similarity number from the stability point of view is according to (3.138)

$$\sigma = \pi_6\pi_7 = \frac{c_1c_2}{c_3}. \tag{3.150}$$

The stability condition (3.125) for $n = 3$ is equivalent to the following condition

$$\sigma > 1. \tag{3.151}$$

Opposite to (3.139) π_{n+3} for $n = 3$ does not disappear and results with respect to (3.144) and (3.150) as follows

$$\pi_{n+3}^2 = \pi_6^2 = \lambda\sigma \equiv \mu^2 \tag{3.152}$$

In building the dimensionless forms of plant (3.114) the relation (3.152) can be also reformulated as follows

$$\lambda^{-1}\mu = \sqrt{\lambda^{-1}\sigma}. \tag{3.153}$$

The dimensionless model (3.123) for $n = 3$ results with respect to (3.143)

$$\frac{d^3y(\bar{t})}{d\bar{t}^3} + \pi_6\frac{d^2y(\bar{t})}{d\bar{t}^2} + \pi_7\frac{dy(\bar{t})}{d\bar{t}} + y(\bar{t}) = Ku(\bar{t} - \pi_5). \tag{3.154}$$

Applying more convenient similarity numbers from dynamics description the form (3.154) is equivalently expressed as

$$\frac{d^3y(\bar{t})}{d\bar{t}^3} + \mu\frac{d^2y(\bar{t})}{d\bar{t}^2} + \lambda^{-1}\mu\frac{dy(\bar{t})}{d\bar{t}} + y(\bar{t}) = Ku(\bar{t} - \vartheta) \tag{3.155}$$

by which the square root on the right-hand side of (3.153) is avoided. On contrary to model form (3.40) the third-order dimensionless model for plants of type (3.114) results more appropriate for the purpose of control loop optimization because the form (3.154) can originate in either (3.155) or such a form where θ is present but λ is missing. Both θ and λ cannot be involved in order to keep the parameter number reduction and to avoid the parameter redundancy (3.145). The number, λ, declines for more oscillatory plants, see Chapter 3.3.

Integrating plant. The integrating plant of the third-order is got by omitting the term $y(\bar{t})$ in (3.154) as follows

$$\frac{d^3y(\bar{t})}{d\bar{t}^3}+\pi_6\frac{d^2y(\bar{t})}{d\bar{t}^2}+\pi_7\frac{dy(\bar{t})}{d\bar{t}}=Ku(\bar{t}-\pi_5)\,. \tag{3.156}$$

In contrast to (3.142) some alterations in deriving the final similarity numbers take place so that (3. 144) defines reciprocal value of the following similarity number

$$\lambda_I=\left(\lambda^{-1}\right)=\frac{\pi_{n+4}}{\pi_{n+3}}=\frac{c_1}{c_2}\sqrt[n]{c_n}=\frac{\pi_7}{\pi_6}=\frac{c_1}{c_2}\sqrt[3]{c_3} \tag{3.157}$$

and (3.145) defines formally the same number

$$\theta_I=\left(\theta\right)=\frac{\pi_7}{\pi_6}=\frac{c_{n-2}}{c_{n-1}}\sqrt[n]{c_n}=\frac{c_1}{c_2}\sqrt[3]{c_3}\,, \tag{3.158}$$

but denoted differently, i.e. θ_I is instead of θ. One can see for $n=3$ the identity between (3.157) and (3.158), $\lambda_I=\theta_I$. In applications number (3.158) is modified in such a way to be θ_I expressed as a function of this ratio which is afterwards used for the evaluation of the integrating plant *stiffness*, see Chapter 3.3. In view of (3.138) and (3.157) one can express π_7 as

$$\pi_{n+4}^2=\pi_7^2=\lambda_I\sigma \tag{3.159}$$

and from (3.139) with respect to (3.158) results

$$\pi_7=\theta_I\mu\,. \tag{3.160}$$

Again for the dimensionless plant description is more suitable to apply (3.160) than the square root resulting from (3.159)

$$\pi_7=\sqrt{\lambda_I\sigma}\,. \tag{3.161}$$

The dimensionless form (3.156) is equivalently exchanged by

$$\frac{d^3y(\bar{t})}{d\bar{t}^3}+\mu\frac{d^2y(\bar{t})}{d\bar{t}^2}+\lambda_I\mu\frac{dy(\bar{t})}{d\bar{t}}=Ku(\bar{t}-\vartheta) \tag{3.162}$$

because $\lambda_I = \theta_I$ and $\mu = \theta_I^{-1}\pi_7$.

Case 4. The dimensionless model (3.123) of the fourth-order plant with delay, $n = 4$, is described by the following dimensionless parameters

$$\pi_1 = \omega\sqrt[4]{c_4}\,,\ \pi_2 = \frac{t}{\sqrt[4]{c_4}} = \bar{t}\,,\ \pi_5 = \frac{\tau}{\sqrt[4]{c_4}}\,,\ \pi_6 = \frac{c_3}{\sqrt[4]{(c_4)^3}}\,,\ \pi_7 = \frac{c_2}{\sqrt{c_4}}\,,\ \pi_8 = \frac{c_1}{\sqrt[4]{c_4}}\,. \tag{3.163}$$

Utilizing the similarity numbers (3.163) the final ones are as follows

$$\lambda = \frac{\pi_7}{\pi_8} = \frac{c_2}{c_1}\frac{1}{\sqrt[4]{c_4}}\,, \tag{3.164}$$

$$\theta = \frac{\pi_7}{\pi_6} = \frac{c_2}{c_3}\sqrt[4]{c_4}\,, \tag{3.165}$$

$$\vartheta = \pi_5 = \frac{\tau}{\sqrt[4]{c_4}}\,, \tag{3.166}$$

$$\mu = \pi_6 = \frac{c_3}{\sqrt[4]{(c_4)^3}}\,, \tag{3.167}$$

$$\psi = \frac{\pi_5}{\pi_6} = \frac{\tau}{c_3}\sqrt{c_4}\,. \tag{3.168}$$

Both λ and θ are the *oscillability* numbers and ϑ is the *retardedness* number. μ and ψ play the role of supplementary similarity numbers. In case of $n = 4$ number (3.138) results in

$$\sigma = \pi_{n+3}\pi_{n+4} = \frac{c_1 c_2}{\sqrt[n]{c_n{}^3}} = \pi_7\pi_8 = \frac{c_1 c_2}{\sqrt[4]{c_4{}^3}}\,. \tag{3.169}$$

By means of the final similarity numbers the numbers π_6, π_7 and π_8 in (3.163) are expressed

$$\pi_6 = \psi^{-1}\vartheta = \mu\,,\ \pi_7 = \sqrt{\lambda\sigma} = \theta\mu\,,\ \pi_8 = \sqrt{\lambda^{-1}\sigma} = \lambda^{-1}\theta\mu\,. \tag{3.170}$$

Be aware the number (3.152) is not the power of μ in case of $n = 4$ but

$$\pi_{n+3}^2 = \pi_7^2 = \lambda\sigma \neq \mu^2\,. \tag{3.171}$$

The dimensionless plant model of the fourth-order is obtained from (3.123) for $n = 4$

$$\frac{d^4 y(\bar{t})}{d\bar{t}^4} + \pi_6\frac{d^3 y(\bar{t})}{d\bar{t}^3} + \pi_7\frac{d^2 y(\bar{t})}{d\bar{t}^2} + \pi_8\frac{dy(\bar{t})}{d\bar{t}} + y(\bar{t}) = Ku(\bar{t} - \pi_5) \tag{3.172}$$

and using (3.170) this model is modified to

$$\frac{d^4y(\bar{t})}{d\bar{t}^4}+\mu\frac{d^3y(\bar{t})}{d\bar{t}^3}+\sqrt{\lambda\sigma}\frac{d^2y(\bar{t})}{d\bar{t}^2}+\sqrt{\lambda^{-1}\sigma}\frac{dy(\bar{t})}{d\bar{t}}+y(\bar{t})=Ku(\bar{t}-\vartheta)\,. \tag{3.173}$$

Both (3.172) and (3.173) guarantee the original plant parameter reduction by one. Also another universal plant model beside both (3.172) and (3.173) is formulated

$$\frac{d^4y(\bar{t})}{d\bar{t}^4}+\theta^{-1}\sqrt{\lambda\sigma}\frac{d^3y(\bar{t})}{d\bar{t}^3}+\sqrt{\lambda\sigma}\frac{d^2y(\bar{t})}{d\bar{t}^2}+\sqrt{\lambda^{-1}\sigma}\frac{dy(\bar{t})}{d\bar{t}}+y(\bar{t})=Ku(\bar{t}-\vartheta) \tag{3.174}$$

since $\mu=\theta^{-1}\sqrt{\lambda\sigma}$. Analogously to the stability condition (3.151) in case of $n=3$, the following condition

$$\sigma=\frac{c_1c_2}{\sqrt[4]{c_4{}^3}}>1 \tag{3.175}$$

is a necessary condition of the plant stability. Condition (3.175) is proved from the conditions (3.126) and Stodola stability criterion. One gets the requirement, $c_1c_2-c_3>0$, and expressing this requirement by means of the similarity numbers the following relation is obtained for the model (3.174)

$$\sqrt{\lambda^{-1}\sigma}\cdot\sqrt{\lambda\sigma}-\theta^{-1}\sqrt{\lambda\sigma}>0\,. \tag{3.176}$$

Because $\sqrt{\lambda^{-1}\sigma}\cdot\sqrt{\lambda\sigma}=\sigma$ and $\theta^{-1}\sqrt{\lambda}<1$ one rewrites (3.176) as follows

$$\sigma>\sqrt{\sigma}\,. \tag{3.177}$$

Relation (3.177) is satisfied only when condition (3.175) is satisfied too. The reason why $\theta^{-1}\sqrt{\lambda}<1$ originates from the reasonable constraints to λ,θ shown in Chapter 3.3 where λ,θ are close to one another and result greater than 1. Thus the necessary condition of the stability (3.175) is proved for all the dynamically similar plants of fourth-order. This condition is different from the Stodola criterion, in fact condition (3.175) supplements the Stodola criterion. Since number σ given by both (3.150) and (3.169) somehow reflects the stability property this is called plant *dampeningness* number. To express the dimensionless model of the fourth-order plant with delay as simple as possible and to avoid any square root from the dimensionless model formulation the relations in (3.170) free of any square root are applied to model (3.172) as follows

$$\frac{d^4y(\bar{t})}{d\bar{t}^4}+\mu\frac{d^3y(\bar{t})}{d\bar{t}^3}+\theta\mu\frac{d^2y(\bar{t})}{d\bar{t}^2}+\lambda^{-1}\theta\mu\frac{dy(\bar{t})}{d\bar{t}}+y(\bar{t})=Ku(\bar{t}-\vartheta) \tag{3.178}$$

where both θ and λ are involved as in (3.174). Due to the parameter reduction four similarity numbers, namely λ, θ, σ and μ, cannot be applied to forming the dimensionless plant model. One of them has to be eliminated. As regards the numbers, λ and θ, they rise for the more oscillatory plants, see Chapter 3.3.

Integrating plant. The integrating plant of the fourth-order is attained by omitting the term $y(\bar{t})$ in (3.172) as follows

$$\frac{d^4y(\bar{t})}{d\bar{t}^4}+\pi_6\frac{d^3y(\bar{t})}{d\bar{t}^3}+\pi_7\frac{d^2y(\bar{t})}{d\bar{t}^2}+\pi_8\frac{dy(\bar{t})}{d\bar{t}}=Ku(\bar{t}-\pi_5) \tag{3.179}$$

Analogously to (3.157) and (3.158) the similarity numbers result

$$\lambda_I=\left(\lambda^{-1}\right)=\frac{\pi_{n+4}}{\pi_{n+3}}=\frac{c_1}{c_2}\sqrt[n]{c_n}=\frac{\pi_8}{\pi_7}=\frac{c_1}{c_2}\sqrt[4]{c_4} \tag{3.180}$$

and

$$\theta_I=\left(\theta\right)=\frac{\pi_7}{\pi_6}=\frac{c_{n-2}}{c_{n-1}}\sqrt[n]{c_n}=\frac{c_2}{c_3}\sqrt[4]{c_4} \tag{3.181}$$

which are again the reciprocal value of (3.164) and number (3.165), respectively. For integrating plants the number σ given by (3.169) is of negligible importance analogously to (3.159) as follows

$$\pi_{n+4}^2=\pi_8^2=\lambda_I\sigma \tag{3.182}$$

because the plant stability is not the case. In addition π_8 is expressed differently from (3.182) to avoid the square root in the dimensionless model (3.179). Using relations (3.170) adapted to the fourth-order integrating plant with delay

$$\pi_6=\mu,\ \pi_7=\theta_I\mu,\ \pi_8=\lambda_I\pi_7 \tag{3.183}$$

the form (3.179) is changed to

$$\frac{d^4y(\bar{t})}{d\bar{t}^4}+\lambda_I^{-1}\theta_I^{-1}\pi_8\frac{d^3y(\bar{t})}{d\bar{t}^3}+\lambda_I^{-1}\pi_8\frac{d^2y(\bar{t})}{d\bar{t}^2}+\pi_8\frac{dy(\bar{t})}{d\bar{t}}=Ku(\bar{t}-\vartheta)\,. \tag{3.184}$$

From the dynamic similarity point of view the model (3.184) receives the final form

$$\frac{d^4y(\bar{t})}{d\bar{t}^4}+\mu\frac{d^3y(\bar{t})}{d\bar{t}^3}+\theta_I\mu\frac{d^2y(\bar{t})}{d\bar{t}^2}+\lambda_I\theta_I\mu\frac{dy(\bar{t})}{d\bar{t}}=Ku(\bar{t}-\vartheta) \tag{3.185}$$

where λ_I and θ_I are two different similarity numbers. The former is the plant *oscillability* number while the latter is the plant *stiffness* number. Both (3.184) and (3.185) are with the least possible number of dimensionless parameters involving both λ_I and θ_I.

Tab. 2 Similarity numbers derived from π_i arguments

Order	Similarity number	Definition	Description
$1-4$	$\pi_1 = \nu$	$\nu = \omega \sqrt[n]{c_n}$	dimensionless frequency
	$\pi_2 = \bar{t}$	$\bar{t} = t \big/ \sqrt[n]{c_n}$	dimensionless time
	$\pi_3 = \rho_D$	$\rho_D = Kr_D \big/ \sqrt[n]{c_n}$	dimensionless derivative loop gain
	$\pi_4 = \rho_I$	$\rho_I = Kr_I \sqrt[n]{c_n}$	dimensionless integration loop gain
	$\pi_5 = \vartheta$	$\vartheta = \tau \big/ \sqrt[n]{c_n}$	plant *retardedness* number
$2-4$	$\pi_6 = \mu$	$\mu = c_{n-1} \big/ \sqrt[n]{(c_n)^{n-1}}$	supplementary number
$1-4$	$\pi_1 \pi_5 = \phi$	$\phi = \nu \vartheta$	natural frequency angle
$2-4$		$\mu = \psi^{-1} \vartheta$	redundancy
$n=2$		$\mu = \lambda^{-1} = c_1 \big/ \sqrt{c_2}$	redundancy
		$\lambda \equiv \theta$	
		$\Psi = \dfrac{\tau}{c_1}$	relation (3.140), resemblance to ϑ
$n=3$	$\dfrac{\pi_6}{\pi_7} = \lambda$	$\lambda = \dfrac{c_2}{c_1} \dfrac{1}{\sqrt[3]{c_3}}$	plant *oscillability* number
		$\lambda = \theta^{-1}$	redundancy
	$\dfrac{\pi_5}{\pi_6} = \psi$	$\psi = \dfrac{\tau}{c_2} \sqrt[3]{c_3}$	supplementary number according to (3.140)
	$\pi_6^2 = \lambda \sigma$	$\mu^2 = \lambda \sigma$	relation (3.152)
	$\pi_6 \pi_7 = \sigma$	$\sigma = \dfrac{c_1 c_2}{c_3} > 1$	stability condition (3.125), plant *dampeningness*
$n=4$	$\dfrac{\pi_7}{\pi_8} = \lambda$	$\lambda = \dfrac{c_2}{c_1} \dfrac{1}{\sqrt[4]{c_4}}$	plant *oscillability* numbers
	$\dfrac{\pi_7}{\pi_6} = \theta$	$\theta = \dfrac{c_2}{c_3} \sqrt[4]{c_4}$	
	$\dfrac{\pi_5}{\pi_6} = \psi$	$\psi = \dfrac{\tau}{c_3} \sqrt{c_4}$	supplementary number according to (3.140)
		$\lambda^{-1} \theta = \dfrac{c_1}{c_3} \sqrt{c_4}$	When this ratio is 1 then all the plant poles are complex and given with common factor $\xi > 0$, see Chapter 3.3.
	$\pi_7 = \sqrt{\lambda \sigma}$	$\mu = \theta^{-1} \sqrt{\lambda \sigma}$	application of (3.171)
	$\pi_7 \pi_8 = \sigma$	$\sigma = \dfrac{c_1 c_2}{\sqrt[4]{c_4^{\,3}}} > 1$	necessary condition of stability (3.175), plant *dampeningness*
$n=3$	$\dfrac{\pi_7}{\pi_6} = \lambda_I = \theta_I$	$\lambda_I = \dfrac{c_1}{c_2} \sqrt[3]{c_3}$	integrating plant *oscillability*, redundancy
		$\lambda_I = \theta_I$	

		$\frac{\lambda_I}{\mu}=\frac{c_1c_3}{c_2^2}<\frac{1}{4}$	integrating plant *stiffness* number
$n=4$	$\frac{\pi_8}{\pi_7}=\lambda_I$	$\lambda_I=\frac{c_1}{c_2}\sqrt[4]{c_4}$	integrating plant *oscillability* number
	$\frac{\pi_7}{\pi_6}=\theta_I$	$\theta_I=\frac{c_2}{c_3}\sqrt[4]{c_4}$	integrating plant *stiffness* number
		$\theta_I=\frac{\sigma_I+2}{1+2\sigma_I}\neq 1$	*stiffness* number for $\xi=\nu_n=1$ where σ_I is dimensionless spectral abscissa, see (3.310)
	$\pi_8=\sqrt{\lambda_I\sigma}$	$\lambda_I\sigma=\frac{c_1^2}{\sqrt{c_4}}$	application of (3.182)
	$\frac{\pi_8}{\pi_6}=\lambda_I\theta_I$	$\lambda_I\theta_I\mu=\pi_8$	application of (3.183)

For the purpose of plant pole spectrum investigation the corresponding characteristic polynomial is specified for the plant cases, namely $n=2$, $n=3$ and $n=4$. As regards the Case 1, $n=1$, the first-order plant with delay is not considered for PID control synthesis because the dominant pole placement technique is generalized in Chapter 4 for control loop systems of retarded type. To investigate the pole spectrum the dimensionless Laplace transform of corresponding plant models is made. Simultaneously with $\bar{t}=t/\sqrt[n]{c_n}$ and conformly with $\nu=\omega\sqrt[n]{c_n}$ the following dimensionless complex variable of Laplace transform results

$$\bar{s}=s\sqrt[n]{c_n}\,. \tag{3.186}$$

Case 2 (*Characteristic polynomial*). The dimensionless Laplace transform of (3.141) under zero initial conditions results in

$$\left[\bar{s}^2+\lambda^{-1}\bar{s}+1\right]Y(\bar{s})=K\exp(-\vartheta\bar{s})U(\bar{s}) \tag{3.187}$$

from where

$$\bar{s}^2+\lambda^{-1}\bar{s}+1=M\left(\bar{s}\right) \tag{3.188}$$

is the characteristic polynomial. The second-order plant transfer function results in

$$G(\bar{s})=\frac{Y(\bar{s})}{U(\bar{s})}=\frac{K}{\bar{s}^2+\lambda^{-1}\bar{s}+1}\exp(-\vartheta\bar{s}) \tag{3.189}$$

For the integrating plant (3.142) the transfer function results

$$G(\bar{s})=\frac{Y(\bar{s})}{U(\bar{s})}=\frac{K}{\bar{s}\left(\bar{s}+\lambda_I^{-1}\right)}\exp(-\vartheta\bar{s}) \tag{3.190}$$

where the denominator is the characteristic polynomial

$$M\left(\bar{s}\right)=\bar{s}\left(\bar{s}+\lambda_I^{-1}\right). \tag{3.191}$$

Case 3 (*Characteristic polynomial*). The dimensionless Laplace transform of (3.155) under zero initial conditions is given as

$$\left[\bar{s}^3+\mu\bar{s}^2+\lambda^{-1}\mu\bar{s}+1\right]Y(\bar{s})=K\exp(-\vartheta\bar{s})U(\bar{s}) \tag{3.192}$$

and from the left-hand side of (3.192) the following characteristic polynomial originates as follows

$$M\left(\bar{s}\right)=\bar{s}^3+\mu\bar{s}^2+\lambda^{-1}\mu\bar{s}+1 \tag{3.193}$$

The third-order plant transfer function results in

$$G(\bar{s})=\frac{Y(\bar{s})}{U(\bar{s})}=\frac{K}{\bar{s}^3+\mu\bar{s}^2+\lambda^{-1}\mu\bar{s}+1}\exp(-\vartheta\bar{s}) \tag{3.194}$$

For the integrating plants (3.162) the transfer function results

$$G(\bar{s})=\frac{Y(\bar{s})}{U(\bar{s})}=\frac{K}{\bar{s}^3+\mu\bar{s}^2+\lambda_1\mu\bar{s}}\exp(-\vartheta\bar{s}) \tag{3.195}$$

and its denominator is the characteristic polynomial

$$M\left(\bar{s}\right)=\bar{s}\left(\bar{s}^2+\mu\bar{s}+\lambda_1\mu\right). \tag{3.196}$$

Case 4 (*Characteristic polynomial*). The dimensionless Laplace transform of (3.178) under zero initial conditions is obtained as follows

$$\left[\bar{s}^4+\mu\bar{s}^3+\theta\mu\bar{s}^2+\lambda^{-1}\theta\mu\bar{s}+1\right]Y(\bar{s})=K\exp(-\vartheta\bar{s})U(\bar{s}) \tag{3.197}$$

On the left-hand side the characteristic polynomial appears as follows

$$M\left(\bar{s}\right)=\bar{s}^4+\mu\bar{s}^3+\theta\mu\bar{s}^2+\lambda^{-1}\theta\mu\bar{s}+1 \tag{3.198}$$

The fourth-order plant transfer function originates in

$$G(\bar{s})=\frac{Y(\bar{s})}{U(\bar{s})}=\frac{K}{\bar{s}^4+\mu\bar{s}^3+\theta\mu\bar{s}^2+\lambda^{-1}\theta\mu\bar{s}+1}\exp(-\vartheta\bar{s}) \tag{3.199}$$

For the integrating plants (3.185) the transfer function results as

$$G(\bar{s}) = \frac{Y(\bar{s})}{U(\bar{s})} = \frac{K}{\bar{s}^4 + \mu\bar{s}^3 + \theta_I\mu\bar{s}^2 + \lambda_I\theta_I\mu\bar{s}} \exp(-\vartheta\bar{s}) \tag{3.200}$$

and its denominator is the characteristic polynomial as follows

$$M(\bar{s}) = \bar{s}\left(\bar{s}^3 + \mu\bar{s}^2 + \theta_I\mu\bar{s} + \lambda_I\theta_I\mu\right). \tag{3.201}$$

Subsequently the dimensionless PID control loop models with delay are provided for considered plant cases to tune the PID controller by means of the dominant three-pole placement carried out in Chapter 4. Also to test resulting PID settings on disturbance rejection performance corresponding transfer function is computed with the notation in Tab. 1. Add disturbance variable *z* to the control input *u* on the right-hand side of (3.1) and link the PID controller (3.7) to the plant (3.1) with acting disturbance *z* on the plant input in the place of the control variable *u*. Resulting closed loop is described by the following retarded differential equation

$$\begin{aligned} &c_n\frac{d^{n+1}y(t)}{dt^{n+1}} + c_{n-1}\frac{d^n y(t)}{dt^n} + c_{n-2}\frac{d^{n-1}y(t)}{dt^{n-1}} + \ldots \\ &+c_2\frac{d^3y(t)}{dt^3} + Kr_D\frac{d^2y(t-\tau)}{dt^2} + c_1\frac{d^2y(t)}{dt^2} + Kr_P\frac{dy(t-\tau)}{dt} + \frac{dy(t)}{dt} + Kr_I y(t-\tau) = \\ &Kr_I w(t-\tau) + Kr_P\frac{dw(t-\tau)}{dt} + Kr_D\frac{d^2w(t-\tau)}{dt^2} + K\frac{dz(t-\tau)}{dt} \end{aligned} \tag{3.202}$$

Applying the dimensional analysis to (3.202) based on the similarity numbers $\pi_i, i = 1,2,\ldots,n+3,n+4,$ the following differential equation expressing (3.202) in dimensionless parameters is achieved

$$\begin{aligned} &\frac{d^{n+1}y(\bar{t})}{d\bar{t}^{n+1}} + \pi_6\frac{d^n y(\bar{t})}{d\bar{t}^n} + \pi_7\frac{d^{n-1}y(\bar{t})}{d\bar{t}^{n-1}} + \ldots + \pi_{n+3}\frac{d^3y(\bar{t})}{d\bar{t}^3} + \\ &\rho_D\frac{d^2y(\bar{t}-\pi_5)}{d\bar{t}^2} + \pi_{n+4}\frac{d^2y(\bar{t})}{d\bar{t}^2} + \rho_P\frac{dy(\bar{t}-\pi_5)}{dt} + \frac{dy(\bar{t})}{d\bar{t}} + \rho_I y(\bar{t}-\pi_5) = \\ &\rho_I w(\bar{t}-\pi_5) + \rho_P\frac{dw(\bar{t}-\pi_5)}{d\bar{t}} + \rho_D\frac{d^2w(\bar{t}-\pi_5)}{d\bar{t}^2} + K\frac{dz(\bar{t}-\pi_5)}{d\bar{t}} \end{aligned} \tag{3.203}$$

After performing the Laplace transform of (3.203) under zero initial conditions

$$\begin{aligned} &\left[\bar{s}^{n+1} + \pi_6\bar{s}^n + \pi_7\bar{s}^{n-1} + \ldots + \pi_{n+3}\bar{s}^3 + \right. \\ &\left.\left(\pi_{n+4} + \rho_D e^{-\vartheta\bar{s}}\right)\bar{s}^2 + \left(1 + \rho_P e^{-\vartheta\bar{s}}\right)\bar{s} + \rho_I e^{-\vartheta\bar{s}}\right] Y(\bar{s}) = \\ &\left[\rho_I + \rho_P\bar{s} + \rho_D\bar{s}^2\right] e^{-\vartheta\bar{s}} W(\bar{s}) + Ke^{-\vartheta\bar{s}}\bar{s}Z(\bar{s}) \end{aligned} \tag{3.204}$$

both reference and disturbance transfer functions result as follows

$$\frac{Y(\bar{s})}{W(\bar{s})} = \\ = \frac{\left(\rho_I + \rho_P \bar{s} + \rho_D \bar{s}^2\right) e^{-\pi_5 \bar{s}}}{\bar{s}^{n+1} + \pi_6 \bar{s}^n + \pi_7 \bar{s}^{n-1} + ... + \pi_{n+3} \bar{s}^3 + \left(\pi_{n+4} + \rho_D e^{-\pi_5 \bar{s}}\right) \bar{s}^2 + \left(1 + \rho_P e^{-\pi_5 \bar{s}}\right) \bar{s} + \rho_I e^{-\pi_5 \bar{s}}} \tag{3.205}$$

and

$$\frac{Y(\bar{s})}{Z(\bar{s})} = \\ = \frac{K \bar{s} e^{-\pi_5 \bar{s}}}{\bar{s}^{n+1} + \pi_6 \bar{s}^n + \pi_7 \bar{s}^{n-1} + ... + \pi_{n+3} \bar{s}^3 + \left(\pi_{n+4} + \rho_D e^{-\pi_5 \bar{s}}\right) \bar{s}^2 + \left(1 + \rho_P e^{-\pi_5 \bar{s}}\right) \bar{s} + \rho_I e^{-\pi_5 \bar{s}}}. \tag{3.206}$$

In the denominator of both transfer functions there is the characteristic quasi-polynomial of the dimensionless control loop with delay

$$Q(\bar{s}) = \\ = \bar{s}^{n+1} + \pi_6 \bar{s}^n + \pi_7 \bar{s}^{n-1} + ... + \pi_{n+3} \bar{s}^3 + \left(\pi_{n+4} + \rho_D e^{-\pi_5 \bar{s}}\right) \bar{s}^2 + \left(1 + \rho_P e^{-\pi_5 \bar{s}}\right) \bar{s} + \rho_I e^{-\pi_5 \bar{s}} \tag{3.207}$$

that can be modified analogously to (3.85) as follows

$$\left[\bar{s}^{n+1} + \pi_6 \bar{s}^n + \pi_7 \bar{s}^{n-1} + ... + \pi_{n+3} \bar{s}^3 + \pi_{n+4} \bar{s}^2 + \bar{s}\right] e^{\pi_5 \bar{s}} + \\ \rho_D \bar{s}^2 + \rho_P \bar{s} + \rho_I = M(\bar{s}) = 0. \tag{3.208}$$

In case of integrating plants (3.124) the reference and disturbance transfer function differ from (3.205) and (3.206), respectively, in the denominator only, i.e. the characteristic quasi-polynomial. It results as follows

$$Q(\bar{s}) = \\ = \bar{s}^{n+1} + \pi_6 \bar{s}^n + \pi_7 \bar{s}^{n-1} + ... + \pi_{n+3} \bar{s}^3 + \left(\pi_{n+4} + \rho_D e^{-\pi_5 \bar{s}}\right) \bar{s}^2 + \rho_P e^{-\pi_5 \bar{s}} \bar{s} + \rho_I e^{-\pi_5 \bar{s}} \tag{3.209}$$

and the characteristic equation as in (3.88) results

$$\left[\bar{s}^{n+1} + \pi_6 \bar{s}^n + \pi_7 \bar{s}^{n-1} + ... + \pi_{n+3} \bar{s}^3 + \pi_{n+4} \bar{s}^2\right] e^{\pi_5 \bar{s}} + \\ \rho_D \bar{s}^2 + \rho_P \bar{s} + \rho_I = M(\bar{s}) = 0. \tag{3.210}$$

Be aware that $\pi_7, \pi_8, ..., \pi_{n+3}, \pi_{n+4}$ in case of integrating plants differ from those in case of proportional plants, for more details see particular case of time delay plant above.

Case 2 (*Control loop*). The dimensionless PID control loop model with delay has been already developed for the plant (3.114) with the case $n = 2$, [126]. Here the sets of dynamically similar second-order plants either aperiodic or oscillatory are controlled by the PID of which settings correspond to those sets. The PID controller settings are evaluated

versus derived similarity numbers that are achieved in (3.133) and (3.134). As regards the reference and disturbance transfer functions for both proportional and integrating plants they are achieved directly from (3.205) and (3.206) by substituting 2 for *n*

$$\frac{Y(\bar{s})}{W(\bar{s})} = \frac{\left(\rho_I + \rho_P \bar{s} + \rho_D \bar{s}^2\right) e^{-\vartheta \bar{s}}}{\bar{s}^3 + \left(\lambda^{-1} + \rho_D e^{-\vartheta \bar{s}}\right)\bar{s}^2 + \left(1 + \rho_P e^{-\vartheta \bar{s}}\right)\bar{s} + \rho_I e^{-\vartheta \bar{s}}}, \tag{3.211}$$

$$\frac{Y(\bar{s})}{Z(\bar{s})} = \frac{K\bar{s} e^{-\vartheta \bar{s}}}{\bar{s}^3 + \left(\lambda^{-1} + \rho_D e^{-\vartheta \bar{s}}\right)\bar{s}^2 + \left(1 + \rho_P e^{-\vartheta \bar{s}}\right)\bar{s} + \rho_I e^{-\vartheta \bar{s}}} \tag{3.212}$$

and for the second-order integrating plants with delay both transfer functions differ from (3.211) and (3.212) only in the denominator. In the denominator of both (3.211) and (3.212) there is the characteristic quasi-polynomial as follows

$$Q(\bar{s}) = \bar{s}^3 + \left(\lambda^{-1} + \rho_D e^{-\vartheta \bar{s}}\right)\bar{s}^2 + \left(1 + \rho_P e^{-\vartheta \bar{s}}\right)\bar{s} + \rho_I e^{-\vartheta \bar{s}} \tag{3.213}$$

and in the case of second-order integrating plants with delay this quasi-polynomial results

$$Q(\bar{s}) = \bar{s}^3 + \left(\lambda_I^{-1} + \rho_D e^{-\vartheta \bar{s}}\right)\bar{s}^2 + \rho_P e^{-\vartheta \bar{s}}\bar{s} + \rho_I e^{-\vartheta \bar{s}}. \tag{3.214}$$

The modification of both quasi-polynomials according to (3.208) and (3.210) into the characteristic equation results

$$\left[\bar{s}^3 + \lambda^{-1}\bar{s}^2 + \bar{s}\right] e^{\vartheta \bar{s}} + \left[\rho_P \bar{s} + \rho_I + \rho_D \bar{s}^2\right] = M(\bar{s}) = 0 \tag{3.215}$$

and

$$\left[\bar{s}^3 + \lambda_I^{-1}\bar{s}^2\right] e^{\vartheta \bar{s}} + \left[\rho_P \bar{s} + \rho_I + \rho_D \bar{s}^2\right] = M(\bar{s}) = 0 \tag{3.216}$$

respectively. Notice $\vartheta = \pi_5$, $\lambda^{-1} = \pi_6$ and in case of integrating plant $\lambda_I^{-1} = \pi_6$.

Case 3 (*Control loop*). The dimensionless PID control loop model with delay is found for the sets of dynamically similar third-order plants (3.155), aperiodic or oscillatory, characterized by similarity numbers (3.144), (3.146), (3.147), (3.157) and (3.158). Corresponding reference and disturbance transfer functions are attained from (3.205) and (3.206) by substituting 3 for *n*

$$\frac{Y(\bar{s})}{W(\bar{s})} = \frac{\left(\rho_I + \rho_P \bar{s} + \rho_D \bar{s}^2\right) e^{-\vartheta \bar{s}}}{\bar{s}^4 + \mu\bar{s}^3 + \left(\lambda^{-1}\mu + \rho_D e^{-\vartheta \bar{s}}\right)\bar{s}^2 + \left(1 + \rho_P e^{-\vartheta \bar{s}}\right)\bar{s} + \rho_I e^{-\vartheta \bar{s}}}, \tag{3.217}$$

$$\frac{Y(\bar{s})}{Z(\bar{s})} = \frac{K\bar{s} e^{-\vartheta \bar{s}}}{\bar{s}^4 + \mu\bar{s}^3 + \left(\lambda^{-1}\mu + \rho_D e^{-\vartheta \bar{s}}\right)\bar{s}^2 + \left(1 + \rho_P e^{-\vartheta \bar{s}}\right)\bar{s} + \rho_I e^{-\vartheta \bar{s}}} \tag{3.218}$$

and for the third-order integrating plants with delay both transfer functions differ from (3.217) and (3.218) only in the denominator. In the denominator of both (3.217) and (3.218) the characteristic quasi-polynomial takes place as follows

$$Q(\bar{s}) = \bar{s}^4 + \mu\bar{s}^3 + \left(\lambda^{-1}\mu + \rho_D e^{-\vartheta\bar{s}}\right)\bar{s}^2 + \left(1 + \rho_P e^{-\vartheta\bar{s}}\right)\bar{s} + \rho_I e^{-\vartheta\bar{s}} \tag{3.219}$$

and in the case of third-order integrating plants with delay this quasi-polynomial results

$$Q(\bar{s}) = \bar{s}^4 + \mu\bar{s}^3 + \left(\lambda_I\mu + \rho_D e^{-\vartheta\bar{s}}\right)\bar{s}^2 + \rho_P e^{-\vartheta\bar{s}}\bar{s} + \rho_I e^{-\vartheta\bar{s}}. \tag{3.220}$$

The modification of both quasi-polynomials according to (3.208) and (3.210) into the characteristic equation results

$$\left[\bar{s}^4 + \mu\bar{s}^3 + \lambda^{-1}\mu\bar{s}^2 + \bar{s}\right]e^{\vartheta\bar{s}} + \left[\rho_P\bar{s} + \rho_I + \rho_D\bar{s}^2\right] = M(\bar{s}) = 0 \tag{3.221}$$

and

$$\left[\bar{s}^4 + \mu\bar{s}^3 + \lambda_I\mu\bar{s}^2\right]e^{\vartheta\bar{s}} + \left[\rho_P\bar{s} + \rho_I + \rho_D\bar{s}^2\right] = M(\bar{s}) = 0 \tag{3.222}$$

respectively. Notice $\vartheta = \pi_5$, $\mu = \pi_6$, $\lambda^{-1}\mu = \pi_7$ and in case of integrating plant $\lambda_I\mu = \pi_7$.

Case 4 (*Control loop*). The dimensionless PID control loop model with delay is got for the sets of dynamically similar fourth-order plants with delay characterized by similarity number (3.164) through (3.167) and by the numbers (3.180) and (3.181). Corresponding reference and disturbance transfer functions are derived from (3.205) and (3.206) by substituting 4 for *n*

$$\frac{Y(\bar{s})}{W(\bar{s})} = \frac{\left(\rho_I + \rho_P\bar{s} + \rho_D\bar{s}^2\right)e^{-\vartheta\bar{s}}}{\bar{s}^5 + \mu\bar{s}^4 + \theta\mu\bar{s}^3 + \left(\lambda^{-1}\theta\mu + \rho_D e^{-\vartheta\bar{s}}\right)\bar{s}^2 + \left(1 + \rho_P e^{-\vartheta\bar{s}}\right)\bar{s} + \rho_I e^{-\vartheta\bar{s}}}, \tag{3.223}$$

$$\frac{Y(\bar{s})}{Z(\bar{s})} = \frac{K\bar{s}e^{-\vartheta\bar{s}}}{\bar{s}^5 + \mu\bar{s}^4 + \theta\mu\bar{s}^3 + \left(\lambda^{-1}\theta\mu + \rho_D e^{-\vartheta\bar{s}}\right)\bar{s}^2 + \left(1 + \rho_P e^{-\vartheta\bar{s}}\right)\bar{s} + \rho_I e^{-\vartheta\bar{s}}} \tag{3.224}$$

and for the fourth-order integrating plants with delay both transfer functions differ from (3.223) and (3.224) only in the denominator. In the denominator of both (3.223) and (3.224) the characteristic quasi-polynomial appears as follows

$$Q(\bar{s}) = \bar{s}^5 + \mu\bar{s}^4 + \theta\mu\bar{s}^3 + \left(\lambda^{-1}\theta\mu + \rho_D e^{-\vartheta\bar{s}}\right)\bar{s}^2 + \left(1 + \rho_P e^{-\vartheta\bar{s}}\right)\bar{s} + \rho_I e^{-\vartheta\bar{s}} \tag{3.225}$$

and in the case of fourth-order integrating plants with delay this quasi-polynomial results

$$Q(\bar{s}) = \bar{s}^5 + \mu\bar{s}^4 + \theta_I\mu\bar{s}^3 + \left(\lambda_I\theta_I\mu + \rho_D e^{-\vartheta\bar{s}}\right)\bar{s}^2 + \rho_P e^{-\vartheta\bar{s}}\bar{s} + \rho_I e^{-\vartheta\bar{s}}. \tag{3.226}$$

The modification of both quasi-polynomials according to (3.208) and (3.210) into the characteristic equation results

$$\left[\bar{s}^5+\mu\bar{s}^4+\theta\mu\bar{s}^3+\lambda^{-1}\theta\mu\bar{s}^2+\bar{s}\right]e^{\vartheta\bar{s}}+\left[\rho_P\bar{s}+\rho_I+\rho_D\bar{s}^2\right]=M\left(\bar{s}\right)=0 \tag{3.227}$$

and

$$\left[\bar{s}^5+\mu\bar{s}^4+\theta_I\mu\bar{s}^3+\lambda_I\theta_I\mu\bar{s}^2\right]e^{\vartheta\bar{s}}+\left[\rho_P\bar{s}+\rho_I+\rho_D\bar{s}^2\right]=M\left(\bar{s}\right)=0 \tag{3.228}$$

respectively. Notice $\vartheta=\pi_5$, $\mu=\pi_6$, $\theta\mu=\pi_7$, $\lambda^{-1}\theta\mu=\pi_8$ and in case of integrating plants $\theta_I\mu=\pi_7$, $\lambda_I\theta_I\mu=\pi_8$.

To summarize the application of dimensional analysis the dimensionless PID control loop models given by retarded differential equation (3.80) are surpassed in quality by the similar control loops described by (3.203). The control loop quality is measured from dynamic similarity and loop gain tuning points of view. The control loop given by (3.203) respects *retardedness* much more than the loop (3.80) by involving non-fixed dimensionless time delay and in addition due to the plant form (3.114) the loop gains arise straightforwardly from the dimensional analysis as the similarity numbers ρ_P, $\pi_3=\rho_D$, $\pi_4=\rho_I$. Additionally for assumed cases when $n=3,4$ particular selection of the similarity numbers has to be made for achieving the control loop parameter reduction. This reduction is already ensured by plant parameter reduction as shown in the considered plant cases above. In Chapter 4 a generalized dominant three-pole placement is developed for the similar control loops given by (3.203) that are already after particular parameter reduction.

3.3 Plant dynamics investigation using the similarity numbers

Based on the developed similarity numbers the dynamics of the third- and fourth-order plant are investigated with respect to the PID controller tuning made in Chapter 4. Particularly suitable plant parameterization in the framework of the dimensional analysis is found for the purpose of the plant pole spectrum analysis. Moreover only such plants which are safely stable are admissible for control design and considered in the habilitation thesis.

3.3.1 The third-order plant

The third-order plant (3.114) for $n=3$ is analysed in its dynamics. The following three cases of stable plant poles are assumed

1. $s_1=-b_1$, $s_2=-b_2$, $s_3=-b_3$, $b_{1,2,3}>0$ (3.229)
2. $s_{1,2}=\left(-\xi\pm j\eta\right)\omega_n$, $s_3=-b$, $b>0$, $\omega_n>0$, $\eta=\sqrt{1-\xi^2}$, $\xi\le 1$` (3.230)
3. $s_{1,2,3}=-b$, $b>0$ (3.231)

where ω_n is (undamped) natural frequency and ξ is the damping factor of complex conjugates $s_{1,2}$. b is the absolute value of the third real pole s_3 and $-b_{1,2,3}$ are three distinct real poles. The case of double real pole and one single real pole occurs when $\xi=1$. The case of the triple real pole is in analogy to the case of three distinct real poles. In case of complex conjugate pair of poles and one real pole the plant characteristic equation results in

$$\left(s+b\right)\left(s^2+2\xi\omega_n s+\omega_n^2\right)=s^3+\left(b+2\xi\omega_n\right)s^2+\left(\omega_n^2+2\xi\omega_n b\right)s+\omega_n^2 b=0. \tag{3.232}$$

Recall dimensionless variable (3.186) for $n=3$ as follows

$$\overline{s}=s\sqrt[3]{c_3}=s\frac{1}{\sqrt[3]{\omega_n^2 b}} \tag{3.233}$$

and substituting (3.233) into (3.232) the following characteristic equation is obtained

$$\omega_n^2 b\overline{s}^3+\left(b+2\xi\omega_n\right)\sqrt[3]{\left(\omega_n^2 b\right)^2}\,\overline{s}^2+\left(\omega_n^2+2\xi\omega_n b\right)\sqrt[3]{\omega_n^2 b}\,\overline{s}+\omega_n^2 b=0 \tag{3.234}$$

Making $\overline{s}^3$ with unit coefficient as follows

$$\overline{s}^3+\left(b+2\xi\omega_n\right)\frac{1}{\sqrt[3]{\omega_n^2 b}}\overline{s}^2+\left(\omega_n^2+2\xi\omega_n b\right)\frac{1}{\sqrt[3]{\left(\omega_n^2 b\right)^2}}\overline{s}+1=0 \tag{3.235}$$

and applying the equality $\sqrt[3]{c_3}=1\Big/\sqrt[3]{\omega_n^2 b}$

$$\overline{s}^3+\left(b+2\xi\omega_n\right)\sqrt[3]{c_3}\,\overline{s}^2+\left(\omega_n^2+2\xi\omega_n b\right)\sqrt[3]{c_3^2}\,\overline{s}+1=\overline{s}^3+\alpha_2\overline{s}^2+\alpha_1\overline{s}+1=0\,. \tag{3.236}$$

The following dimensionless coefficients result

$$\alpha_1=\left(\omega_n^2+2\xi\omega_n b\right)\sqrt[3]{c_3^2} \tag{3.237}$$

$$\alpha_2=\left(b+2\xi\omega_n\right)\sqrt[3]{c_3}\,. \tag{3.238}$$

In case of three distinct real poles and triple real pole the equation (2.232) is changed to the forms

$$\left(s+b_1\right)\left(s+b_2\right)\left(s+b_3\right)=s^3+\left(b_1+b_2+b_3\right)s^2+\left(b_1b_2+b_1b_3+b_2b_3\right)s+b_1b_2b_3=0 \tag{3.239}$$

and

$$\left(s+b\right)^3=s^3+3bs^2+3b^2s+b^3=0\,, \tag{3.240}$$

respectively. The variable (3.233) is modified in case of three distinct poles as follows

$$\overline{s}=s\sqrt[3]{c_3}=s\frac{1}{\sqrt[3]{b_1b_2b_3}} \tag{3.241}$$

while in case of the triple real pole

$$\overline{s}=s\sqrt[3]{c_3}=s\frac{1}{\sqrt[3]{b^3}}=s\frac{1}{b}\,. \tag{3.242}$$

The characteristic equations (3.239) and (3.240) are transformed to the following forms

$$b_1b_2b_3\bar{s}^3+\left(b_1+b_2+b_3\right)\sqrt[3]{\left(b_1b_2b_3\right)^2}\bar{s}^2+\left(b_1b_2+b_1b_3+b_2b_3\right)\sqrt[3]{b_1b_2b_3}\bar{s}+b_1b_2b_3=0 \tag{3.243}$$

and

$$b^3\bar{s}^3+3bb^2\bar{s}^2+3b^2b\bar{s}+b^3=0, \tag{3.244}$$

respectively. Dimensionless forms of (3.243) and (3.244) are obtained as follows

$$\bar{s}^3+\left(b_1+b_2+b_3\right)\frac{1}{\sqrt[3]{b_1b_2b_3}}\bar{s}^2+\left(b_1b_2+b_1b_3+b_2b_3\right)\frac{1}{\sqrt[3]{\left(b_1b_2b_3\right)^2}}\bar{s}+1=0 \tag{3.245}$$

and

$$\bar{s}^3+3\bar{s}^2+3\bar{s}+1=0, \tag{3.246}$$

respectively. In the former case the equation is expressed in analogous way as (3.236)

$$\bar{s}^3+\left(b_1+b_2+b_3\right)\sqrt[3]{c_3}\bar{s}^2+\left(b_1b_2+b_1b_3+b_2b_3\right)\sqrt[3]{c_3^2}\bar{s}+1=\bar{s}^3+\beta_2\bar{s}^2+\beta_1\bar{s}+1=0 \tag{3.247}$$

where

$$\beta_1=\left(b_1b_2+b_1b_3+b_2b_3\right)\sqrt[3]{c_3^2} \tag{3.248}$$

$$\beta_2=\left(b_1+b_2+b_3\right)\sqrt[3]{c_3}. \tag{3.249}$$

From (3.246) the triple real pole results

$$\bar{s}_{1,2,3}=-1. \tag{3.250}$$

For mapping the similarity numbers λ and μ of the dimensionless model (3.155) the three cases given by (3.229) through (3.231) are considered and original characteristic equations resulted to dimensionless ones (3.236), (3.246) and (3.247). For the case of complex conjugate pair of poles and one real pole the form (3.236) equals the plant (3.155) characteristic equation with the left-hand side (3.193) as follows

$$\bar{s}^3+\mu\bar{s}^2+\lambda^{-1}\mu\bar{s}+1\triangleq\bar{s}^3+\alpha_2\bar{s}^2+\alpha_1\bar{s}+1=0 \tag{3.251}$$

and its roots are poles of the dimensionless model (3.155) of the third-order plant. In case of three distinct real poles the roots of (3.247) are the same as the zeros of (3.193) and the following equality has to be satisfied

$$\bar{s}^3+\mu\bar{s}^2+\lambda^{-1}\mu\bar{s}+1\triangleq\bar{s}^3+\beta_2\bar{s}^2+\beta_1\bar{s}+1=0. \tag{3.252}$$

The triple real pole configuration leads to the following equality

$$\overline{s}^3+\mu\overline{s}^2+\lambda^{-1}\mu\overline{s}+1\triangleq\overline{s}^3+3\overline{s}^2+3\overline{s}+1=0\,. \tag{3.253}$$

from where $\mu=3$ and $\lambda=1$. To distinguish between the case of complex conjugate pair of poles with one real pole and the case of three distinct real poles the following discriminant is evaluated

$$D=18\frac{\mu^2}{\lambda}-4\left(\frac{\mu}{\lambda}\right)^3\left(1+\lambda^3\right)+\frac{\mu^4}{\lambda^2}-27=18\frac{\mu^2}{\lambda}-4\left(\frac{\mu^2}{\lambda}\right)^2\frac{1}{\mu\lambda}\left(1+\lambda^3\right)+\left(\frac{\mu^2}{\lambda}\right)^2-27 \tag{3.254}$$

where μ^2/λ is the ratio satisfying the condition of plant stability

$$\frac{\mu^2}{\lambda}>1\,. \tag{3.255}$$

Using this discriminant and the condition of stability (3.255) the three cases of poles are obtained

1. $D>0$, three distinct poles case (3.229) (3.256)
2. $D\le 0$, case (3.230) (3.257)
3. $D=0$, triple real pole case (3.250) (3.258)

For the case (3.256) λ and μ are expressed by relationships

$$\mu=\beta_2=\left(b_1+b_2+b_3\right)\sqrt[3]{c_3}\,,\ \lambda=\frac{\beta_2}{\beta_1}=\frac{b_1+b_2+b_3}{b_1b_2+b_1b_3+b_2b_3}\frac{1}{\sqrt[3]{c_3}} \tag{3.259}$$

and for the case (3.257)

$$\mu=\alpha_2=\left(b+2\xi\omega_n\right)\sqrt[3]{c_3}\,,\ \lambda=\frac{\alpha_2}{\alpha_1}=\frac{1}{\omega_n}\frac{b+2\xi\omega_n}{\omega_n+2\xi b}\frac{1}{\sqrt[3]{c_3}}\,. \tag{3.260}$$

The case (3.258) is specified already with (3.253). Utilizing the equality $c_3=1/\left(b_1b_2b_3\right)$ and $c_3=1/\omega_n^2b$ the parameters b_1 and b, respectively, are eliminated from (3.259) and (3.260) as follows

$$\mu=\beta_2=\left(\frac{1}{c_3b_2b_3^2}+\frac{b_2}{b_3}+1\right)b_3\sqrt[3]{c_3}\,,\ \lambda=\frac{\beta_2}{\beta_1}=\frac{\dfrac{1}{c_3b_2b_3^2}+\dfrac{b_2}{b_3}+1}{\dfrac{1}{c_3b_3^2b_2}+\dfrac{1}{c_3b_2^2b_3}+1}\frac{1}{b_2\sqrt[3]{c_3}} \tag{3.261}$$

and

$$\mu=\alpha_2=\left(\frac{1}{c_3\omega_n^3}+2\xi\right)\omega_n\sqrt[3]{c_3}\ ,\ \lambda=\frac{\alpha_2}{\alpha_1}=\frac{\dfrac{1}{c_3\omega_n^3}+2\xi}{1+\dfrac{2\xi}{c_3\omega_n^3}}\frac{1}{\omega_n\sqrt[3]{c_3}}\ , \tag{3.262}$$

respectively. Number μ is decisive for the stability of plants (3.155) and also it is important for the achievement of stable control loop dynamics as shown by *Admissibility analysis* in Chapter 4.3. Since λ is the *oscillability* number the opposite margins given by the choice of $\xi=1$ and $\xi=0$ are to be investigated. The former choice finds all the dynamically similar plants (3.155) which are critically damped while the latter leads to all the dynamically similar plants (3.155) that are undamped in oscillation, i.e. unstable. The aperiodic third-order plant with all the three poles as negative real distinct poles is to be investigated by (3.261) where the ratios between real poles b_2/b_3, $c_3b_2^2b_3=b_2/b_1$ and $c_3b_3^2b_2=b_3/b_1$ are far away from zero and simultaneously these ratios are limited. Only such values of λ and μ are considered for the PID controller tuning which correspond to stable and non-stiff plant. Notice the third-order plants with λ values both lower and greater than 1 can result unstable depending on μ according to condition (3.255). Obviously there is equivalence between the condition (3.255) and $\sigma>1$, where σ is given by (3.150). To decide the third-order plant stability by either (3.255) or the relation for σ it is shown in Example 1 below.

Integrating plant. Let relations (3.259) and (3.260) be modified for integrating plants (3.162), i.e. to find mapping for λ_I and μ. The case of three distinct real poles where one of them is the zero pole is obtained from (3.229) by $b_3=0$ and the characteristic equation (3.239) is modified to the form

$$s\left(s+b_1\right)\left(s+b_2\right)=s\left(s^2+\left(b_1+b_2\right)s+b_1b_2\right)=0\,. \tag{3.263}$$

Recall dimensionless variable (3.186) for $n=3$ and (3.263) is changed to the following form

$$\frac{\bar{s}}{\sqrt[3]{c_3}}\left(\frac{\bar{s}^2}{\sqrt[3]{c_3^2}}+\left(b_1+b_2\right)\frac{\bar{s}}{\sqrt[3]{c_3}}+b_1b_2\right)=0\,. \tag{3.264}$$

Multiplying the form (3.264) by $\sqrt[3]{c_3}\sqrt[3]{c_3^2}=c_3$ and comparing the result with the left-hand side (3.196) the following characteristic equation is achieved

$$\bar{s}\left(\bar{s}^2+\mu\bar{s}+\lambda_I\mu\right)\triangleq\bar{s}\left(\bar{s}^2+\left(b_1+b_2\right)\sqrt[3]{c_3}\bar{s}+b_1b_2\sqrt[3]{c_3^2}\right)=0\,. \tag{3.265}$$

The relations in (3.259) are modified as follows

$$\mu=\left(b_1+b_2\right)\sqrt[3]{c_3}\ ,\ \lambda_I=\frac{b_1b_2}{b_1+b_2}\sqrt[3]{c_3} \tag{3.266}$$

where λ_I is instead of λ^{-1}, cf. (3.157). In comparison to (3.247) the equation (3.265) has dimensionless real roots expressed as follows

$$\bar{s}_1 = -\bar{b}_1 = -b_1\sqrt[3]{c_3}\,,\ \bar{s}_2 = -\bar{b}_2 = -b_2\sqrt[3]{c_3}\,,\ \bar{s}_3 = 0 \tag{3.267}$$

and (3.265) can be expressed

$$\bar{s}\left(\bar{s}^2 + \mu\bar{s} + \lambda_I\mu\right) \triangleq \bar{s}\left(\bar{s}^2 + \left(\bar{b}_1 + \bar{b}_2\right)\bar{s} + \bar{b}_1\bar{b}_2\right) = \bar{s}\left(\bar{s} + \bar{b}_1\right)\left(\bar{s} + \bar{b}_2\right) = 0\,. \tag{3.268}$$

The relations (3.266) are simplified as follows

$$\mu = \bar{b}_1 + \bar{b}_2\,,\ \lambda_I = \frac{\bar{b}_1\bar{b}_2}{\bar{b}_1 + \bar{b}_2}\,. \tag{3.269}$$

With respect to similarity numbers (3.269) the integrating plants (3.162) are aperiodic with three distinct real poles $\bar{s}_1 = -\bar{b}_1$, $\bar{s}_2 = -\bar{b}_2$ and $\bar{s}_3 = 0$. The case of complex conjugate pair of poles and one zero pole is obtained from (3.230) by $b = 0$ and the characteristic equation (3.239) is modified to the form

$$s\left(s^2 + 2\xi\omega_n s + \omega_n^2\right) = s^3 + 2\xi\omega_n s^2 + \omega_n^2 s = 0\,. \tag{3.270}$$

Recalling the dimensionless variable (3.186) for $n = 3$ and substituting it into (3.270) one gets

$$\frac{\bar{s}}{\sqrt[3]{c_3}}\left(\frac{\bar{s}^2}{\sqrt[3]{c_3^2}} + 2\xi\omega_n\frac{\bar{s}}{\sqrt[3]{c_3}} + \omega_n^2\right) = \frac{s^3}{c_3} + 2\xi\omega_n\frac{\bar{s}^2}{\sqrt[3]{c_3^2}} + \omega_n^2\frac{\bar{s}}{\sqrt[3]{c_3}} = 0\,. \tag{3.271}$$

Multiplying this by c_3 and comparing the result with the left-hand side (3.196) the following characteristic equation is achieved

$$\bar{s}\left(\bar{s}^2 + \mu\bar{s} + \lambda_I\mu\right) \triangleq \bar{s}\left(\bar{s}^2 + 2\xi\omega_n\sqrt[3]{c_3}\bar{s}^2 + \omega_n^2\sqrt[3]{c_3^2}\right) = 0\,. \tag{3.272}$$

In confrontation with (3.236) the equation (3.272) has dimensionless complex conjugate pair of poles as follows

$$s_{1,2} = \left(-\xi \pm j\eta\right)\nu_n,\quad \nu_n = \omega_n\sqrt[3]{c_3}\,,\ \bar{s}_3 = 0 \tag{3.273}$$

and (3.272) is expressed in the following form

$$\bar{s}\left(\bar{s}^2 + \mu\bar{s} + \lambda_I\mu\right) \triangleq \bar{s}\left(\bar{s}^2 + 2\xi\nu_n\bar{s} + \nu_n^2\right) = 0\,. \tag{3.274}$$

Comparing the coefficients of expressions in brackets of (3.274) the relations for the similarity numbers are obtained

$$\mu = 2\xi\nu_n,\ \lambda_I = \frac{\nu_n}{2\xi}. \tag{3.275}$$

With respect to similarity numbers (3.275) the integrating plants (3.162) are oscillatory with complex conjugate pair of poles $s_{1,2} = (-\xi \pm j\eta)\nu_n$. Beside this pair the integrating plant spectrum is supplemented by real pole $\bar{s}_3 = 0$. In case $\mu = 0$ and $\lambda_I \to \infty$ the integrating plant (3.162) is with undamped oscillation in its impulse response. While $\mu = 2\nu_n$ and $\lambda_I = \nu_n/2$ the integrating plant is without any oscillation in its impulse response, i.e. it is aperiodic integrating plant with a double real pole. The aperiodic integrating plant with three distinct real poles is taken on when

$$\frac{\lambda_I}{\mu} = \frac{c_1 c_3}{c_2^2} \le \frac{1}{4}. \tag{3.276}$$

It results from constraint on the discriminant of quadratic equation in (3.274), $\mu^2 - 4\lambda_I\mu \ge 0$ where $\mu > 0$. Satisfying (3.279) the *stiffness* property introduced with number (3.158) can also appear but only in case λ_I/μ is much less than $1/4$. In fact the integrating plant becomes *stiff* for the case of real pole ratio $\bar{b}_2/\bar{b}_1$ in (3.269) resulting either close to zero or too large. The μ, λ_I mapping distinguishing between integrating plants (3.162) with the oscillatory and aperiodic impulse response is given by functions (3.269) and (3.275). Again only such integrating plants (3.162) that are with the damped impulse responses are considered for the PID control design in Chapter 4.

In the rest of this section the Examples 1 and 2 demonstrate the dimensional analysis on identified third-order plants oscillatory and integrating.

Example 1. Plant (3.114) of the third-order, i.e. $n = 3$, is considered for dynamics investigation using the similarity number relations (3.262) with the following coefficients

$$2\frac{d^3y(t)}{dt^3} + 2\frac{d^2y(t)}{dt^2} + 2.5\frac{dy(t)}{dt} + y(t) = 2u(t - 0.5). \tag{3.277}$$

From the dimensional analysis the scaling factor results in

$$\sqrt[3]{c_3} = \sqrt[3]{2} \tag{3.278}$$

and the dimensionless form of (3.277) results as follows

$$\frac{d^3y(\bar{t})}{d\bar{t}^3} + \sqrt[3]{2}\frac{d^2y(\bar{t})}{d\bar{t}^2} + 1.984\frac{dy(\bar{t})}{d\bar{t}} + y(\bar{t}) = 2u(\bar{t} - 0.397). \tag{3.279}$$

From (3.144) through (3.150) the following values of the similarity numbers result

$$\lambda = \frac{\sqrt[3]{2}}{1.984} = \frac{2}{2.5}\frac{1}{\sqrt[3]{2}} = 0.635,\ \mu = \sqrt[3]{2},\ \sigma = \frac{2 \cdot 2.5}{2} = 2.5,\ \vartheta = \frac{0.5}{\sqrt[3]{2}} = 0.397. \tag{3.280}$$

and according to condition (3.255) as follows

$$\frac{\mu^2}{\lambda}=\frac{\sqrt[3]{4}}{0.635}=2.5=\sigma>1 \tag{3.281}$$

all the dynamically similar plants (3.279) are stable. Before the model (3.279) pole spectrum is evaluated computing the discriminant (3.254), i.e. $D=-15<0$, the plant poles are composed of complex conjugate pair of poles and one real pole. This fact is verified from the characteristic equation of plant (3.277)

$$M(s)=\frac{1}{2}\left(2s^3+2s^2+2.5s+1\right)=(s+0.5)\left(s^2+0.5s+1\right)=0 \tag{3.282}$$

from where $\omega_n=1\,s^{-1}$ and $\xi=0.25$ result. The similarity numbers μ, λ of oscillatory third-order plants are verified substituting ω_n, ξ and c_3 into (3.262)

$$\mu=\left(\frac{1}{c_3\omega_n^3}+2\xi\right)\omega_n\sqrt[3]{c_3}=\left(\frac{1}{2}+2\frac{1}{4}\right)\sqrt[3]{2}=\sqrt[3]{2} \tag{3.283}$$

$$\lambda=\frac{\dfrac{1}{c_3\omega_n^3}+2\xi}{1+\dfrac{2\xi}{c_3\omega_n^3}}\frac{1}{\omega_n\sqrt[3]{c_3}}=\frac{1}{1+\dfrac{1}{4}}\frac{1}{\sqrt[3]{2}}=\frac{4}{5\sqrt[3]{2}}=\frac{2\sqrt[3]{4}}{5}=0.635. \tag{3.284}$$

The dynamically similar plants must have the same all the similarity numbers, namely $\lambda=0.635$, $\vartheta=0.397$, $\mu=\sqrt[3]{2}$, and $\sigma=2.5$, found out from (3.279). For instance another third-order plant (3.114) which is dynamically similar to plant (3.277) is as follows

$$3\frac{d^3y(t)}{dt^3}+2.62\frac{d^2y(t)}{dt^2}+2.8617\frac{dy(t)}{dt}+y(t)=2u(t-0.572). \tag{3.285}$$

The scaling factor is changed to $\sqrt[3]{c_3}=\sqrt[3]{3}$ and substituting it together with $c_1=2.8617\,s$ and $c_2=2.62\,s^2$ into (3.144) through (3.150) the same λ, ϑ, σ and μ are obtained

$$\lambda=\frac{2.62}{3.276}\frac{1}{\sqrt[3]{3}}=0.635,\ \mu=\frac{2.62}{\sqrt[3]{3^2}}=\sqrt[3]{2},\ \sigma=\frac{2.62\cdot 2.8617}{3}=2.5,\ \vartheta=\frac{0.572}{\sqrt[3]{3}}=0.397. \tag{3.286}$$

The differences of (3.285) spectrum from the spectrum of (3.277) are different $\omega_n=0.8735\,s^{-1}$ and $b=0.4368\,s^{-1}$. After substituting ω_n and b together with scaling and damping factors $\sqrt[3]{3}$ and $1/4$ into (3.260) μ and λ result according to (3.286)

$$\mu=\left(b+2\xi\omega_n\right)\sqrt[3]{c_3}=\left(0.4368+\frac{1}{2}0.8735\right)\sqrt[3]{3}=1.2599=\sqrt[3]{2} \tag{3.287}$$

and

$$\lambda = \frac{1}{\omega_n}\frac{b+2\xi\omega_n}{\omega_n+2\xi b}\frac{1}{\sqrt[3]{c_3}} = \frac{1}{0.8735}\frac{0.4368+\frac{1}{2}0.8735}{0.8735+\frac{1}{2}0.4368}\frac{1}{\sqrt[3]{3}} = \frac{1}{1.0919\cdot\sqrt[3]{3}} = 0.635\,, \tag{3.288}$$

respectively. Both dynamically similar plants are compared by their step responses in Fig. 1.

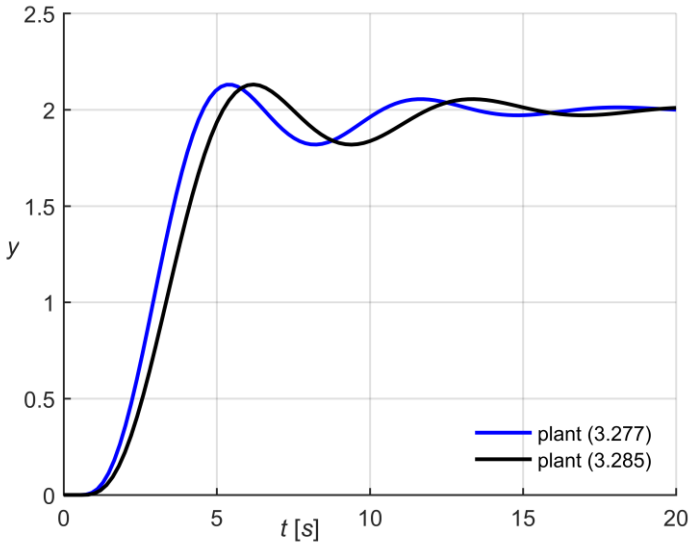

Fig. 1. Step responses of dynamically similar plants belonging to oscillatory plants

In Chapter 4 for all dynamically similar plants characterized by similarity numbers (3.280) the loop gains tuning is performed by means of dominant three-pole placement technique.

Example 2 (*Integrating plant*). The usage of similarity numbers (3.275) describing the sets of dynamically similar integrating plants (3.162) is demonstrated on the following integrating plant (3.117) of the third-order

$$2\frac{d^3y(t)}{dt^3}+2\frac{d^2y(t)}{dt^2}+2.5\frac{dy(t)}{dt} = 2u(t-0.5)\,. \tag{3.289}$$

The similarity numbers result the same as in (3.280) because only missing term $y(t)$ in (3.289) does not take effect on the similarity numbers ϑ and μ computed for plant (3.277). However, the *oscillability* number for integrating plants (3.162) is introduced differently, see (3.157),

$$\lambda_I = \lambda^{-1} = 1.5749 \tag{3.290}$$

and $\pi_7 = \lambda_I\mu$ is given as follows

$$\pi_7 = \frac{c_1}{\sqrt[3]{c_3}} = \frac{2.5}{\sqrt[3]{2}} = 1.9843\,. \tag{3.291}$$

When according to (3.160) and (3.146) $\pi_7 = \lambda_1 \mu = 1.9843$, $\lambda_1^{-1}\pi_7 = \mu = \sqrt[3]{2}$ and $\pi_5 = \vartheta = 0.397$ these numbers are substituted for parameters into (3.162) and the following dimensionless model is obtained

$$\frac{d^3 y(\bar{t})}{d\bar{t}^3} + \sqrt[3]{2}\frac{d^2 y(\bar{t})}{d\bar{t}^2} + 1.984\frac{dy(\bar{t})}{d\bar{t}} = 2u(\bar{t} - 0.397)\,. \tag{3.292}$$

This model would be identical with (3.279) when term $y(t)$ is not missing in (3.292). Of course the spectrum of (3.289) is already changed in comparison with the spectrum of (3.277) as the roots of the following equation

$$M(s) = \frac{1}{2}\left(2s^3 + 2s^2 + 2.5s\right) = s\left(s^2 + s + \frac{5}{4}\right) = 0\,. \tag{3.293}$$

The spectrum of plant (3.289) is parameterized as follows

$$\omega_n = 1.118\, s^{-1},\ \xi = 0.447\,,\ b = 0 \tag{3.294}$$

and applying the scaling factor $\sqrt[3]{2}$ the dimensionless (undamped) natural frequency number results $\nu_n = 1.4086$. This is verified by the spectrum of the characteristic equation of (3.292)

$$\bar{s}^3 + \sqrt[3]{2}\bar{s}^2 + 1.984\bar{s} \triangleq \bar{s}\left(\bar{s}^2 + \sqrt[3]{2}\bar{s} + 1.984\right) = 0 \tag{3.295}$$

where $\nu_n = \sqrt{1.984} = 1.4086$ and $\xi = \dfrac{\sqrt[3]{2}}{2 \cdot 1.4086} = 0.447$. Finally the integrating plants (3.292) are with oscillatory impulse response because with respect to (3.275) the following ratio results

$$\frac{\lambda_I}{\nu_n} = \frac{1}{2\xi} = \frac{1}{2 \cdot 0.447} = 1.118 > 0.5\,. \tag{3.296}$$

Thus this ratio exceeds threshold equal to 1/2. The more this ratio exceeds the threshold the more oscillatory are the integrating plants (3.162) in their impulse response. Analogously to comparing step responses of dynamically similar plants in Fig. 1 the comparison between two similar integrating plants is made, namely (3.289) and the plant derived from (3.285), by omitting the absolute term $y(t)$, as follows

$$3\frac{d^3 y(t)}{dt^3} + 2.62\frac{d^2 y(t)}{dt^2} + 2.8617\frac{dy(t)}{dt} = 2u(t - 0.572)\,. \tag{3.297}$$

This comparison is shown in Fig. 2.

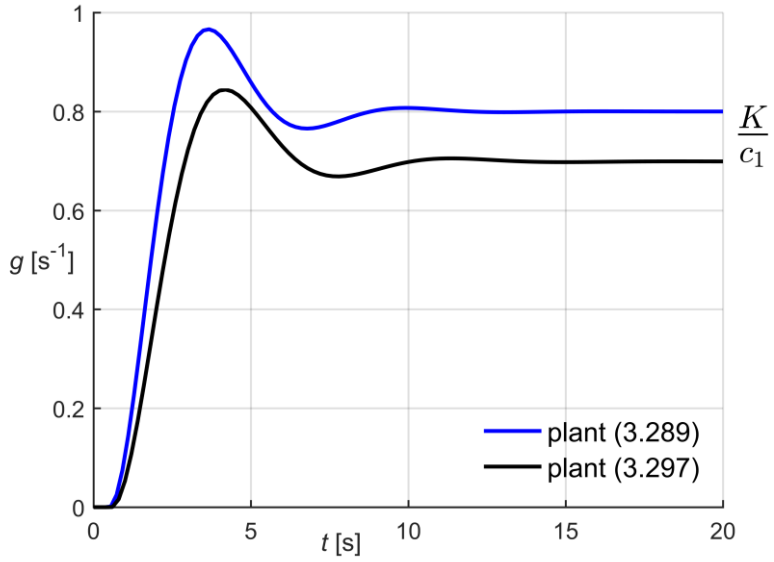

Fig. 2. Oscillatory impulse responses of dynamically similar integrating plants

3.3.2 The fourth-order plant

The fourth-order plant (3.114) for $n=4$ is analysed in its dynamics. The following cases of stable plant poles are investigated

1. $s_1=-b_1,\ s_2=-b_2,\ s_3=-b_3,\ s_4=-b_4,\ b_{1,2,3,4}>0$ (3.298)
2. $s_{1,2}=\left(-\xi\pm j\eta\right)\omega_n,\ s_3=-b_3,\ s_4=-b_4,\ b_{3,4}>0,\ \omega_n>0,\ \eta=\sqrt{1-\xi^2},\ \xi\le 1$ (3.299)
3. $s_{1,2}=\left(-\xi_1\pm j\eta_1\right)\omega_{n1},\ s_{3,4}=\left(-\xi_2\pm j\eta_2\right)\omega_{n2},\ \omega_{n1}>0,\ \omega_{n2}>0,\ \eta_{1,2}=\sqrt{1-\xi_{1,2}^2},\ \xi_{1,2}\le 1$ (3.300)
4. $s_{1,2,3,4}=-b,\ b>0$ (3.301)

where $\omega_{n1,2}$ are (undamped) natural frequencies and $\xi_{1,2}$ are the damping factors corresponding to $\omega_{n1,2}$. b is the absolute value of the real pole and $-b_{1,2,3,4}$ are four distinct real poles. The case of one double real pole and two distinct real poles occurs when $\xi=1$. While $\xi_{1,2}=1$ two double real poles are encountered. When only one of $\xi_{1,2}$ is 1 then one double real pole and a complex conjugate pair of poles take place. The case when $\xi_1=\xi_2<1$ and $\omega_{n1}=\omega_{n2}>0$, i.e. the case of double complex conjugate pair of poles, is not considered. The case of the quadruple real pole is in analogy to the case of four distinct real poles. This case is represented by the following characteristic equation

$$\begin{aligned}&\left(s+b_1\right)\left(s+b_2\right)\left(s+b_3\right)\left(s+b_4\right)=\\&=s^4+\left(b_1+b_2+b_3+b_4\right)s^3+\left(b_1b_2+b_1b_3+b_2b_3+b_1b_4+b_2b_4+b_3b_4\right)s^2+\\&\left(b_1b_2b_3+b_1b_2b_4+b_2b_3b_4+b_1b_3b_4\right)s+b_1b_2b_3b_4=0\end{aligned}\tag{3.302}$$

and in analogy to (3.302) the characteristic equation with quadruple real pole is attained

$$\left(s+b\right)^4=s^4+4bs^3+6b^2s^2+4b^3s+b^4=0.\tag{3.303}$$

Recall dimensionless variable (3.186) for $n=4$ and analogously to (3.241) this variable results

$$\bar{s}=s\sqrt[4]{c_4}=s\frac{1}{\sqrt[4]{b_1b_2b_3b_4}} \tag{3.304}$$

while in case of the quadruple real pole

$$\bar{s}=s\sqrt[4]{c_4}=s\frac{1}{\sqrt[4]{b^4}}=s\frac{1}{b}. \tag{3.305}$$

The characteristic equations (3.302) and (3.303) are transformed to the following forms

$$\begin{aligned}&b_1b_2b_3b_4\bar{s}^4+\left(b_1+b_2+b_3+b_4\right)\sqrt[4]{\left(b_1b_2b_3b_4\right)^3}\bar{s}^3+\\&\left(b_1b_2+b_1b_3+b_2b_3+b_1b_4+b_2b_4+b_3b_4\right)\sqrt{b_1b_2b_3b_4}\bar{s}^2+\\&\left(b_1b_2b_3+b_1b_2b_4+b_2b_3b_4+b_1b_3b_4\right)\sqrt[4]{b_1b_2b_3b_4}\bar{s}+b_1b_2b_3b_4=0\end{aligned} \tag{3.306}$$

and

$$b^4s^4+4bb^3s^3+6b^2b^2s^2+4b^3bs+b^4=0, \tag{3.307}$$

respectively. Dimensionless forms of (3.306) and (3.307) are obtained as follows

$$\begin{aligned}&\bar{s}^4+\left(b_1+b_2+b_3+b_4\right)\frac{1}{\sqrt[4]{b_1b_2b_3b_4}}\bar{s}^3+\left(b_1b_2+b_1b_3+b_2b_3+b_1b_4+b_2b_4+b_3b_4\right)\frac{1}{\sqrt{b_1b_2b_3b_4}}\bar{s}^2+\\&\left(b_1b_2b_3+b_1b_2b_4+b_2b_3b_4+b_1b_3b_4\right)\frac{1}{\sqrt[4]{\left(b_1b_2b_3b_4\right)^3}}\bar{s}+1=0\end{aligned} \tag{3.308}$$

and

$$\bar{s}^4+4\bar{s}^3+6\bar{s}^2+4\bar{s}+1=0, \tag{3.309}$$

respectively. In the former case the equation is expressed with respect to (3.304)

$$\begin{aligned}&\bar{s}^4+\left(b_1+b_2+b_3+b_4\right)\sqrt[4]{c_4}\bar{s}^3+\left(b_1b_2+b_1b_3+b_2b_3+b_1b_4+b_2b_4+b_3b_4\right)\sqrt{c_4}\bar{s}^2+\\&\left(b_1b_2b_3+b_1b_2b_4+b_2b_3b_4+b_1b_3b_4\right)\sqrt[4]{c_4^3}\bar{s}+1=\bar{s}^4+\beta_3\bar{s}^3+\beta_2\bar{s}^2+\beta_1\bar{s}+1=0\end{aligned} \tag{3.310}$$

from where the following dimensionless coefficients result

$$\beta_1=\left(b_1b_2b_3+b_1b_2b_4+b_2b_3b_4+b_1b_3b_4\right)\sqrt[4]{c_4^3} \tag{3.311}$$

$$\beta_2=\left(b_1b_2+b_1b_3+b_2b_3+b_1b_4+b_2b_4+b_3b_4\right)\sqrt{c_4} \tag{3.312}$$

$$\beta_3 = \left(b_1 + b_2 + b_3 + b_4\right)\sqrt[4]{c_4}\,. \tag{3.313}$$

The latter case leads to the quadruple real pole as follows

$$\overline{s}_{1,2,3,4} = -1\,. \tag{3.314}$$

In case of complex conjugate pair of poles and two distinct real poles (3.299) the plant characteristic equation results in

$$\begin{aligned}&\left(s+b_3\right)\left(s+b_4\right)\left(s^2+2\xi\omega_n s+\omega_n^2\right)=\\&=s^4+\left(b_3+b_4+2\xi\omega_n\right)s^3+\left(b_3b_4+\omega_n^2+2\xi\omega_n\left(b_3+b_4\right)\right)s^2+\,.\\&\left(2\xi\omega_n b_3b_4+\omega_n^2\left(b_3+b_4\right)\right)s+\omega_n^2b_3b_4=0\end{aligned} \tag{3.315}$$

The variable (3.304) is modified in this case

$$\overline{s} = s\sqrt[4]{c_4} = s\frac{1}{\sqrt[4]{\omega_n^2 b_3 b_4}} \tag{3.316}$$

and equation (3.315) is transformed using (3.316) as follows

$$\begin{aligned}&\omega_n^2b_3b_4\overline{s}^4+\left(b_3+b_4+2\xi\omega_n\right)\sqrt[4]{\left(\omega_n^2b_3b_4\right)^3}\,\overline{s}^3+\left(b_3b_4+\omega_n^2+2\xi\omega_n\left(b_3+b_4\right)\right)\sqrt{\omega_n^2b_3b_4}\,s^2+\\&\left(2\xi\omega_n b_3b_4+\omega_n^2\left(b_3+b_4\right)\right)\sqrt[4]{\omega_n^2b_3b_4}\,s+\omega_n^2b_3b_4=0\end{aligned}\,. \tag{3.317}$$

Cancelling both the coefficient of $\overline{s}^4$ and the absolute term the equation (3.317) becomes dimensionless as follows

$$\begin{aligned}&\overline{s}^4+\left(b_3+b_4+2\xi\omega_n\right)\frac{1}{\sqrt[4]{\omega_n^2b_3b_4}}\,\overline{s}^3+\left(b_3b_4+\omega_n^2+2\xi\omega_n\left(b_3+b_4\right)\right)\frac{1}{\sqrt{\omega_n^2b_3b_4}}\,\overline{s}^2+\\&\left(2\xi\omega_n b_3b_4+\omega_n^2\left(b_3+b_4\right)\right)\frac{1}{\sqrt[4]{\left(\omega_n^2b_3b_4\right)^3}}\,\overline{s}+1=0\end{aligned}\,. \tag{3.318}$$

Utilizing (3.316) the characteristic equation is expressed

$$\begin{aligned}&\overline{s}^4+\left(b_3+b_4+2\xi\omega_n\right)\sqrt[4]{c_4}\,\overline{s}^3+\left(b_3b_4+\omega_n^2+2\xi\omega_n\left(b_3+b_4\right)\right)\sqrt{c_4}\,\overline{s}^2+\\&\left(2\xi\omega_n b_3b_4+\omega_n^2\left(b_3+b_4\right)\right)\sqrt[4]{c_4^3}\,\overline{s}+1=\overline{s}^4+\alpha_3\overline{s}^3+\alpha_2\overline{s}^2+\alpha_1\overline{s}+1=0\end{aligned}\,. \tag{3.319}$$

and the following dimensionless coefficients result

$$\alpha_1 = \left(2\xi\omega_n b_3b_4+\omega_n^2\left(b_3+b_4\right)\right)\sqrt[4]{c_4^3} \tag{3.320}$$

$$\alpha_2 = \left(b_3 b_4 + \omega_n^2 + 2\xi\omega_n\left(b_3 + b_4\right)\right)\sqrt{c_4} \tag{3.321}$$

$$\alpha_3 = \left(b_3 + b_4 + 2\xi\omega_n\right)\sqrt[4]{c_4}\ . \tag{3.322}$$

The last case considered is the fourth-order plant (3.114) with two complex conjugate pairs of poles, eventually either two double real poles or one double real pole with complex conjugate pair of poles. The characteristic equation is of the following form

$$\begin{aligned}&\left(s^2 + 2\xi_1\omega_{n1}s + \omega_{n1}^2\right)\left(s^2 + 2\xi_2\omega_{n2}s + \omega_{n2}^2\right) = \\ &= s^4 + 2\left(\xi_1\omega_{n1} + \xi_2\omega_{n2}\right)s^3 + \left(4\xi_1\xi_2\omega_{n1}\omega_{n2} + \omega_{n1}^2 + \omega_{n2}^2\right)s^2 + 2\left(\xi_1\omega_{n1}\omega_{n2}^2 + \xi_2\omega_{n2}\omega_{n1}^2\right)s + \omega_{n1}^2\omega_{n2}^2 = 0.\end{aligned} \tag{3.323}$$

The variable (3.316) is modified in this case

$$\overline{s} = s\sqrt[4]{c_4} = s\frac{1}{\sqrt[4]{\omega_{n1}^2\omega_{n2}^2}} \tag{3.324}$$

and equation (3.323) is transformed using (3.324) as follows

$$\begin{aligned}&\omega_{n1}^2\omega_{n2}^2\overline{s}^4 + 2\left(\xi_1\omega_{n1} + \xi_2\omega_{n2}\right)\sqrt[4]{\left(\omega_{n1}^2\omega_{n2}^2\right)^3}\overline{s}^3 + \left(4\xi_1\xi_2\omega_{n1}\omega_{n2} + \omega_{n1}^2 + \omega_{n2}^2\right)\sqrt{\omega_{n1}^2\omega_{n2}^2}\overline{s}^2 + \\ &2\left(\xi_1\omega_{n1}\omega_{n2}^2 + \xi_2\omega_{n2}\omega_{n1}^2\right)\sqrt[4]{\omega_{n1}^2\omega_{n2}^2}\overline{s} + \omega_{n1}^2\omega_{n2}^2 = 0\end{aligned}\ . \tag{3.325}$$

Again cancelling both the coefficient of $\overline{s}^4$ and the absolute term the equation (3.325) becomes dimensionless as follows

$$\begin{aligned}&\overline{s}^4 + 2\left(\xi_1\omega_{n1} + \xi_2\omega_{n2}\right)\frac{1}{\sqrt[4]{\omega_{n1}^2\omega_{n2}^2}}\overline{s}^3 + \left(4\xi_1\xi_2\omega_{n1}\omega_{n2} + \omega_{n1}^2 + \omega_{n2}^2\right)\frac{1}{\sqrt{\omega_{n1}^2\omega_{n2}^2}}\overline{s}^2 + \\ &2\left(\xi_1\omega_{n1}\omega_{n2}^2 + \xi_2\omega_{n2}\omega_{n1}^2\right)\frac{1}{\sqrt[4]{\left(\omega_{n1}^2\omega_{n2}^2\right)^3}}\overline{s} + 1 = 0\end{aligned}\ . \tag{3.326}$$

Applying (3.324) the characteristic equation is changed as follows

$$\begin{aligned}&\overline{s}^4 + 2\left(\xi_1\omega_{n1} + \xi_2\omega_{n2}\right)\sqrt[4]{c_4}\overline{s}^3 + \left(4\xi_1\xi_2\omega_{n1}\omega_{n2} + \omega_{n1}^2 + \omega_{n2}^2\right)\sqrt{c_4}\overline{s}^2 + \\ &2\left(\xi_1\omega_{n1}\omega_{n2}^2 + \xi_2\omega_{n2}\omega_{n1}^2\right)\sqrt[4]{c_4^3}\overline{s} + 1 = \overline{s}^4 + \gamma_3\overline{s}^3 + \gamma_2\overline{s}^2 + \gamma_1\overline{s} + 1 = 0\end{aligned} \tag{3.327}$$

and the following dimensionless coefficients result

$$\gamma_1 = 2\left(\xi_1\omega_{n1}\omega_{n2}^2 + \xi_2\omega_{n2}\omega_{n1}^2\right)\sqrt[4]{c_4^3} \tag{3.328}$$

$$\gamma_2 = \left(4\xi_1\xi_2\omega_{n1}\omega_{n2} + \omega_{n1}^2 + \omega_{n2}^2\right)\sqrt{c_4} \tag{3.329}$$

$$\gamma_3 = 2\left(\xi_1\omega_{n1} + \xi_2\omega_{n2}\right)\sqrt[4]{c_4}\,. \tag{3.330}$$

For mapping the similarity numbers μ, λ and θ of the dimensionless model (3.178) the cases given by (3.298) through (3.301) are considered and original characteristic equations resulted to dimensionless ones (3.309), (3.310), (3.319) and (3.327). Since all these cases belong to the stable fourth-order plants the stability conditions (3.126) has to be satisfied. Based on the plant (3.178) characteristic equation the stability conditions are achieved as follows

$$\theta\mu^2 > \lambda^{-1}\theta\mu\,,\ \mu\left(\lambda^{-1}\theta^2\mu^2 - \mu\right) > \lambda^{-2}\theta^2\mu^2\,. \tag{3.331}$$

Cancelling $\theta\mu$ and μ^2 in (3.331) these conditions are simplified

$$\mu > \lambda^{-1}\,,\ \lambda^{-1}\theta^2\mu - 1 > \lambda^{-2}\theta^2\,. \tag{3.332}$$

For the case of four distinct real poles the form (3.310) equals the plant (3.178) characteristic equation with the left-hand side (3.198) as follows

$$\bar{s}^4 + \mu\bar{s}^3 + \theta\mu\bar{s}^2 + \lambda^{-1}\theta\mu\bar{s} + 1 \triangleq \bar{s}^4 + \beta_3\bar{s}^3 + \beta_2\bar{s}^2 + \beta_1\bar{s} + 1 = 0 \tag{3.333}$$

and its roots are poles of the dimensionless model (3.178) of the fourth-order plant. The quadruple real pole configuration leads to the following equality

$$\bar{s}^4 + \mu\bar{s}^3 + \theta\mu\bar{s}^2 + \lambda^{-1}\theta\mu\bar{s} + 1 \triangleq \bar{s}^4 + 4\bar{s}^3 + 6\bar{s}^2 + 4\bar{s} + 1 = 0 \tag{3.334}$$

from where $\mu = 4$, $\lambda = 1.5$ and $\theta = 1.5$. By inspection of conditions (3.332) the fourth-order plant is stable. The following relationships result for μ, λ and θ with respect to (3.311) through (3.313)

$$\mu = \beta_3 = \left(b_1 + b_2 + b_3 + b_4\right)\sqrt[4]{c_4} \tag{3.335}$$

$$\lambda = \frac{\beta_2}{\beta_1} = \frac{b_1b_2 + b_1b_3 + b_2b_3 + b_1b_4 + b_2b_4 + b_3b_4}{b_1b_2b_3 + b_1b_2b_4 + b_2b_3b_4 + b_1b_3b_4}\,\frac{1}{\sqrt[4]{c_4}} \tag{3.336}$$

$$\theta = \frac{\beta_2}{\beta_3} = \frac{b_1b_2 + b_1b_3 + b_2b_3 + b_1b_4 + b_2b_4 + b_3b_4}{b_1 + b_2 + b_3 + b_4}\,\sqrt[4]{c_4}\,. \tag{3.337}$$

The similarity numbers λ and θ according to (3.336) and (3.337) result greater than 1.5. Keep in mind $\lambda = \theta = 1.5$ when $b_{1,2,3,4} = 1\,s^{-1}$ and c_4 in (3.335) through (3.337) is function of $b_{1,2,3,4}$, see (3.304). In case of complex conjugate pair of poles and two distinct real poles the roots of (3.319) are the same as the zeros of (3.198) and the following equality has to be satisfied

$$\bar{s}^4 + \mu\bar{s}^3 + \theta\mu\bar{s}^2 + \lambda^{-1}\theta\mu\bar{s} + 1 \triangleq \bar{s}^4 + \alpha_3\bar{s}^3 + \alpha_2\bar{s}^2 + \alpha_1\bar{s} + 1 = 0\,. \tag{3.338}$$

For μ, λ and θ with respect to (3.320) through (3.322) the following relationships are obtained from (3.338)

$$\mu = \alpha_3 = \left(b_1 + b_2 + 2\xi\omega_n\right)\sqrt[4]{c_4} \tag{3.339}$$

$$\lambda = \frac{\alpha_2}{\alpha_1} = \frac{b_1 b_2 + \omega_n^2 + 2\xi\omega_n\left(b_1 + b_2\right)}{2\xi\omega_n b_1 b_2 + \omega_n^2\left(b_1 + b_2\right)} \frac{1}{\sqrt[4]{c_4}} \tag{3.340}$$

$$\theta = \frac{\alpha_2}{\alpha_3} = \frac{b_1 b_2 + \omega_n^2 + 2\xi\omega_n\left(b_1 + b_2\right)}{b_1 + b_2 + 2\xi\omega_n} \sqrt[4]{c_4}\,. \tag{3.341}$$

Analogously to (3.336) and (3.337) when $b_{1,2} = 1\,s^{-1}$, $\omega_n = 1\,s^{-1}$ and $\xi = 1$ it results $\lambda = \theta = 1.5$. Numbers λ and θ can result both lower and greater than 1.5, particularly in dependence on $\xi < 1$. Be aware c_4 in (3.339) through (3.341) is function of $b_{1,2}$ and ω_n, see (3.316). When two complex conjugate pairs of poles are the zeros of (3.198) then the plant characteristic equation is described by

$$\bar{s}^4 + \mu\bar{s}^3 + \theta\mu\bar{s}^2 + \lambda^{-1}\theta\mu\bar{s} + 1 \triangleq \bar{s}^4 + \gamma_3\bar{s}^3 + \gamma_2\bar{s}^2 + \gamma_1\bar{s} + 1 = 0\,. \tag{3.342}$$

For μ, λ and θ with respect to (3.328) through (3.330) the following relationships are gained from (3.342)

$$\mu = \gamma_3 = 2\left(\xi_1\omega_{n1} + \xi_2\omega_{n2}\right)\sqrt[4]{c_4} \tag{3.343}$$

$$\lambda = \frac{\gamma_2}{\gamma_1} = \frac{4\xi_1\xi_2\omega_{n1}\omega_{n2} + \omega_{n1}^2 + \omega_{n2}^2}{2\left(\xi_1\omega_{n1}\omega_{n2}^2 + \xi_2\omega_{n2}\omega_{n1}^2\right)} \frac{1}{\sqrt[4]{c_4}} \tag{3.344}$$

$$\theta = \frac{\gamma_2}{\gamma_3} = \frac{4\xi_1\xi_2\omega_{n1}\omega_{n2} + \omega_{n1}^2 + \omega_{n2}^2}{2\left(\xi_1\omega_{n1} + \xi_2\omega_{n2}\right)} \sqrt[4]{c_4}\,. \tag{3.345}$$

Again for $\omega_{n1,2} = 1\,s^{-1}$ and $\xi_{1,2} = 1$ the similarity numbers result $\mu = 4$ and $\lambda = \theta = 1.5$. Once $\xi_{1,2} = 1$ but $\omega_{n1} \neq \omega_{n2}$ two double real poles are in the plant model spectrum. The case when the plant step response oscillates only with one natural frequency $\eta\omega_{n1}$ or $\eta\omega_{n2}$ occurs when the following is considered in (3.343) through (3.345)

$$\xi_1 < 1,\ \xi_2 = 1 \text{ or } \xi_1 = 1,\ \xi_2 < 1\,. \tag{3.346}$$

Thus beside the one complex conjugate pair of poles either $s_{1,2}$ or $s_{3,4}$ there is double real pole either $s_{3,4}$ or $s_{1,2}$. Numbers λ and θ can result both lower and greater than 1.5, particularly in dependence on $\xi_{1,2} < 1$. The undamped oscillation of plant step response takes place for $\xi_1 = 0$ or $\xi_2 = 0$. For $\xi_{1,2} = 0$ the numbers λ and θ result at infinity, i.e. $\lambda \to \infty, \theta \to \infty$. But only fourth-order plants with damped step response are considered, i.e. $\xi_{1,2} > 0$. Again be

aware that the factor c_4 in (3.343) through (3.345) is function of $\omega_{n1,2}$, see (3.324). For modelling the (3.178) plant dynamics it is important to keep a ratio between ω_{n1} and ω_{n2} in proper values as follows

$$0.1 < \frac{\omega_{n1}}{\omega_{n2}} < 10 \tag{3.347}$$

guaranteeing that both pairs in (3.300) are of comparable significance for the plant dynamics. Also the ratios between particular $b_i, i = 1,2,3,4$, are to be considered far away from zero and limited in order to prevent the fourth-order plant from stiff dynamics. As regards μ this number has to result at least $\mu > \lambda^{-1}$ for admissible loop gains tuning as investigated in *Admissibility analysis* in Chapter 4.4. The plant itself can be investigated on the stability by means of conditions (3.332) or $\sigma > 1$, where σ is due to (3.169), as shown in Example 3 below.

Integrating plant. Consider a modification of similarity numbers μ, λ_I and θ_I for *integrating* plants (3.185), i.e. to find mapping for λ_I and θ_I. The case of four distinct real poles where one of them is the zero pole is obtained from (3.298) by $b_4 = 0$ and the characteristic equation (3.302) is modified to the form

$$s(s+b_1)(s+b_2)(s+b_3) = s^4 + (b_1+b_2+b_3)s^3 + (b_1b_2 + b_1b_3 + b_2b_3)s^2 + b_1b_2b_3 s = 0 \tag{3.348}$$

Recall dimensionless variable (3.186) for $n = 4$ and (3.348) is changed to the following form

$$\frac{\bar{s}}{\sqrt[4]{c_4}}\left(\frac{\bar{s}^3}{\sqrt[4]{c_4^3}} + (b_1+b_2+b_3)\frac{\bar{s}^2}{\sqrt{c_4}} + (b_1b_2 + b_1b_3 + b_2b_3)\frac{\bar{s}}{\sqrt[4]{c_4}} + b_1b_2b_3\right) = 0\,. \tag{3.349}$$

Multiplying the form (3.349) by $\sqrt[4]{c_4}\sqrt[4]{c_4^3} = c_4$ and comparing the result with the left-hand side (3.201) the following characteristic equation is achieved

$$\begin{aligned} &\bar{s}\left(\bar{s}^3 + \mu\bar{s}^2 + \theta_I\mu\bar{s} + \lambda_I\theta_I\mu\right) \triangleq \\ &\triangleq \bar{s}\left(\bar{s}^3 + (b_1+b_2+b_3)\sqrt[4]{c_4}\bar{s}^2 + (b_1b_2 + b_1b_3 + b_2b_3)\sqrt{c_4}\bar{s} + b_1b_2b_3\sqrt[4]{c_4^3}\right) = 0 \end{aligned}\,. \tag{3.350}$$

The relations for the similarity numbers (3.335) through (3.337) are modified as follows

$$\mu = (b_1+b_2+b_3)\sqrt[4]{c_4} \tag{3.351}$$

$$\lambda_I = \frac{b_1b_2b_3}{b_1b_2 + b_1b_3 + b_2b_3}\sqrt[4]{c_4} \tag{3.352}$$

$$\theta_I = \frac{b_1b_2 + b_1b_3 + b_2b_3}{b_1 + b_2 + b_3}\sqrt[4]{c_4} \tag{3.353}$$

where λ_I and θ_I are instead of λ^{-1} and θ, respectively, cf. (3.180) and (3.181). In comparison to (3.310) the equation (3.350) has dimensionless real roots expressed as follows

$$\bar{s}_1 = -\bar{b}_1 = -b_1\sqrt[4]{c_4}\,,\ \bar{s}_2 = -\bar{b}_2 = -b_2\sqrt[4]{c_4}\,,\ \bar{s}_3 = -\bar{b}_3 = -b_3\sqrt[4]{c_4}\,,\ \bar{s}_4 = 0 \tag{3.354}$$

and (3.350) can be expressed

$$\bar{s}\left(\bar{s}^3 + \mu\bar{s}^2 + \theta_I\mu\bar{s} + \lambda_I\theta_I\mu\right) \triangleq \bar{s}\left(\bar{s}^3 + \left(\bar{b}_1 + \bar{b}_2 + \bar{b}_3\right)\bar{s}^2 + \left(\bar{b}_1\bar{b}_2 + \bar{b}_1\bar{b}_3 + \bar{b}_2\bar{b}_3\right)\bar{s} + \bar{b}_1\bar{b}_2\bar{b}_3\right) = 0\,. \tag{3.355}$$

The relation (3.351) through (3.353) are simplified as follows

$$\mu = \bar{b}_1 + \bar{b}_2 + \bar{b}_3\,,\ \lambda_I = \frac{\bar{b}_1\bar{b}_2\bar{b}_3}{\bar{b}_1 + \bar{b}_2 + \bar{b}_3}\,,\ \theta_I = \frac{\bar{b}_1\bar{b}_2 + \bar{b}_1\bar{b}_3 + \bar{b}_2\bar{b}_3}{\bar{b}_1 + \bar{b}_2 + \bar{b}_3}\,. \tag{3.356}$$

With respect to similarity numbers (3.356) the integrating plants (3.185) are aperiodic with four distinct real poles $\bar{s}_1 = -\bar{b}_1$, $\bar{s}_2 = -\bar{b}_2$, $\bar{s}_3 = -\bar{b}_3$ and $\bar{s}_4 = 0$. The case of complex conjugate pair of poles and two distinct real poles where one of them is the zero pole is obtained from (3.299) by $b_4 = 0$ and the characteristic equation (3.315) is modified to the form

$$s\left(s + b_3\right)\left(s^2 + 2\xi\omega_n s + \omega_n^2\right) = s^4 + \left(b_3 + 2\xi\omega_n\right)s^3 + \left(\omega_n^2 + 2\xi\omega_n b_3\right)s^2 + \omega_n^2 b_3 s = 0\,. \tag{3.357}$$

Using dimensionless variable (3.186) for $n = 4$ (3.357) is changed to the following form

$$\frac{\bar{s}}{\sqrt[4]{c_4}}\left(\frac{\bar{s}^3}{\sqrt[4]{c_4^3}} + \left(b_3 + 2\xi\omega_n\right)\frac{\bar{s}^2}{\sqrt{c_4}} + \left(\omega_n^2 + 2\xi\omega_n b_3\right)\frac{\bar{s}}{\sqrt[4]{c_4}} + \omega_n^2 b_3\right) = 0\,. \tag{3.358}$$

Multiplying the form (3.358) by $\sqrt[4]{c_4}\sqrt[4]{c_4^3} = c_4$ and comparing the result with the left-hand side (3.201) the following characteristic equation is achieved

$$\begin{aligned}&\bar{s}\left(\bar{s}^3 + \mu\bar{s}^2 + \theta_I\mu\bar{s} + \lambda_I\theta_I\mu\right) \triangleq \\ &\triangleq \bar{s}\left(\bar{s}^3 + \left(b_3 + 2\xi\omega_n\right)\sqrt[4]{c_4}\,\bar{s}^2 + \left(\omega_n^2 + 2\xi\omega_n b_3\right)\sqrt{c_4}\,\bar{s} + \omega_n^2 b_3\sqrt[4]{c_4^3}\right) = 0\end{aligned}\,. \tag{3.359}$$

The relations for the similarity numbers (3.339) through (3.341) are modified as follows

$$\mu = \left(b_3 + 2\xi\omega_n\right)\sqrt[4]{c_4} \tag{3.360}$$

$$\lambda_I = \frac{\omega_n^2 b_3}{\omega_n^2 + 2\xi\omega_n b_3}\sqrt[4]{c_4} \tag{3.361}$$

$$\theta_I = \frac{\omega_n^2 + 2\xi\omega_n b_3}{b_3 + 2\xi\omega_n}\sqrt[4]{c_4}\,. \tag{3.362}$$

In comparison to (3.319) the equation (3.359) has dimensionless roots expressed as follows

$$s_{1,2} = \left(-\xi \pm j\eta\right)\nu_n, \quad \nu_n = \omega_n \sqrt[4]{c_4}\,,\ \bar{s}_3 = -\bar{b}_3 = -b_3 \sqrt[4]{c_4}\,,\ \bar{s}_4 = 0\,. \tag{3.363}$$

Denoting $\bar{b}_3 = \beta$ the equation (3.359) is expressed in the following form

$$\bar{s}\left(\bar{s}^3 + \mu\bar{s}^2 + \theta_I\mu\bar{s} + \lambda_I\theta_I\mu\right) \triangleq \bar{s}\left(\bar{s}^3 + \left(\beta + 2\xi\nu_n\right)\bar{s}^2 + \left(\nu_n^2 + 2\xi\nu_n\beta\right)\bar{s} + \nu_n^2\beta\right) = 0\,. \tag{3.364}$$

The relation (3.360) through (3.362) are simplified as follows

$$\mu = \left(\beta + 2\xi\nu_n\right),\ \lambda_I = \frac{\nu_n\beta}{\nu_n + 2\xi\beta},\ \theta_I = \lambda_I^{-1}\mu^{-1}\beta\nu_n^2 = \frac{\nu_n^2 + 2\xi\nu_n\beta}{\beta + 2\xi\nu_n}\,. \tag{3.365}$$

With respect to similarity numbers (3.365) the integrating plants (3.185) are oscillatory with complex conjugate pair of poles $s_{1,2} = \left(-\xi \pm j\eta\right)\nu_n$. The integrating plant spectrum also contains two distinct real poles $\bar{s}_3 = -\beta$ and $\bar{s}_4 = 0$. For mapping purposes it is worth to make the following manipulations with λ_I and θ_I in (3.365)

$$\frac{\lambda_I}{\beta} = \frac{\dfrac{\nu_n}{\beta}}{\dfrac{\nu_n}{\beta} + 2\xi},\ 0 < \frac{\nu_n}{\beta} < \infty,\ \xi > 0 \tag{3.366}$$

and

$$\frac{\theta_I}{\beta} = \frac{\left(\dfrac{\nu_n}{\beta}\right)^2 + 2\xi\dfrac{\nu_n}{\beta}}{1 + 2\xi\dfrac{\nu_n}{\beta}},\ 0 < \frac{\nu_n}{\beta} < \infty,\ \xi > 0 \tag{3.367}$$

respectively. By the choice of $\xi = 1$ and $\xi = 0$ the region of integrating plants (3.185) with oscillatory impulse response is found out. This region including the region where the dynamically similar plants (3.185) are with aperiodic impulse response is drawn in Fig. 3. Let be remarked the plant (3.185) is integrating thus already on the stability margin. When $\xi = 0$ it means the plant impulse response becomes undamped. In Fig. 3 the undamped cases ($\xi = 0$) of ratios λ_I/β and θ_I/β are removed in order to tune the PID controller for integrating plants with damped impulse responses only. Notice the integrating plants (3.185) with more oscillatory impulse response give the greater value of λ_I/β. The undamped oscillation of plant (3.185) impulse response arises when $\lambda_I/\beta = 1$ while the damped oscillatory plants appear when $\lambda_I/\beta < 1$, for more details see Fig. 3. The integrating plant is with damped impulse response when

$$\theta_I\mu^2 > 1. \tag{3.368}$$

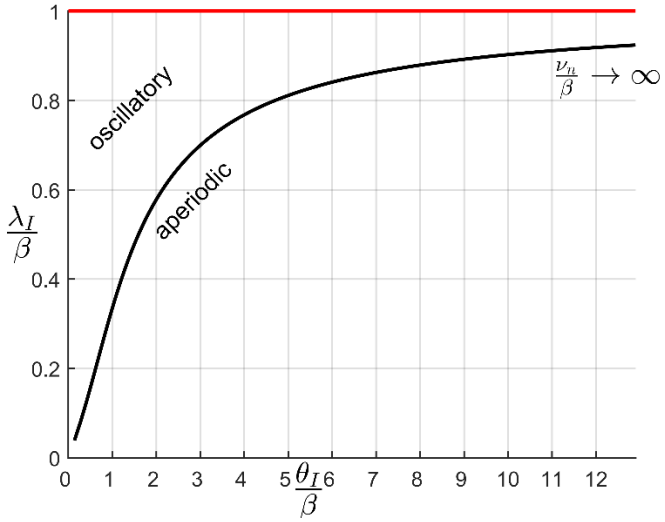

Fig. 3. Similarity numbers mapping to distinguish between oscillatory and aperiodic cases of (3.185)

It results from the stability condition (3.125). As regards integrating plant *stiffness* evaluation the following ratio is introduced

$$\sigma_I = \xi \frac{\nu_n}{\beta},\ 0 < \xi \le 1. \tag{3.369}$$

This ratio can be also understood as dimensionless spectral abscissa, thus very analogous to number (3.169), the *dampeningness* number. Only σ_I is used instead of σ. Then relation (3.367) is altered as follows

$$\frac{\theta_I}{\beta} = \frac{\left(\frac{\sigma_I}{\xi}\right)^2 + 2\sigma_I}{1 + 2\sigma_I},\ 0 < \xi \le 1. \tag{3.370}$$

Taking into account the discussion below (3.158) and expressing from (3.369)

$$\frac{\sigma_I}{\xi} = \frac{\nu_n}{\beta} \tag{3.371}$$

(3.371) is changed into the following form

$$\frac{\xi}{\nu_n}\theta_I = \frac{\sigma_I + 2\xi^2}{1 + 2\sigma_I} \le \frac{\sigma_I + 2}{1 + 2\sigma_I},\ 0 < \xi \le 1,\ \nu_n > 0. \tag{3.372}$$

Let the opposite behaviour be modelled, i.e. the integrating plants (3.185) are *non-stiff*. This case happens for $\sigma_I = 1$ and upper bound of (3.372) is expressed as the following ratio

$$\frac{\sigma_I + 2}{1 + 2\sigma_I} = 1. \tag{3.373}$$

In contrast to (3.373) all ratios $(\sigma_I+2)/(1+2\sigma_I)$ resulting either lower or greater than 1 belong to *stiff* integrating plants (3.185) when either the lower bound or upper bound of this ratio is approaching. The lower bound of this ratio results in $(\sigma_I+2)/(1+2\sigma_I)=1/2$ when $\sigma_I\to\infty$ and the upper bound results in $(\sigma_I+2)/(1+2\sigma_I)=2$ when $\sigma_I\to 0$. Application of (3.372) assumes the integrating plant impulse response is damped hence undamped case is not considered for stiffness evaluation.

Plant (3.114) of the fourth-order, i.e. $n=4$, is considered for its dynamics investigation using the similarity numbers in examples. Most common cases of such plants in practice are the fourth-order aperiodic plants when all its poles are real poles or the plants with only one pair of complex conjugate poles. The case of the fourth-order oscillatory plants with two pairs of complex conjugate poles are not so much frequently identified in practice. But this case is from the point of view of the PID controller capability the worst case of the stable non-stiff fourth-order plants considered. In the rest of this section the Examples 3, 4, 5 and 6 demonstrate the dimensional analysis on identified fourth-order plants aperiodic, oscillatory and integrating.

Example 3. The fourth-order aperiodic plant when all its poles are distinct real poles is identified as follows

$$0.47\frac{d^4y(t)}{dt^4}+2.682\frac{d^3y(t)}{dt^3}+5.2\frac{d^2y(t)}{dt^2}+3.988\frac{dy(t)}{dt}+y(t)=u(t-0.25) \tag{3.374}$$

from where the scaling factor originates in

$$\sqrt[4]{c_4}=\sqrt[4]{0.47}\,. \tag{3.375}$$

Using (3.375) and similarity number (3.164) through (3.168) as follows

$$\lambda=\frac{5.2}{3.988}\frac{1}{\sqrt[4]{0.47}}=1.574,\qquad \theta=\frac{5.2}{2.682}\sqrt[4]{0.47}=1.605,\qquad \theta\mu=\pi_7=\frac{5.2}{\sqrt{0.47}}=7.58,$$
$$\mu=\frac{2.682}{\sqrt[4]{0.47^3}}=4.721,\ \vartheta=\frac{0.25}{\sqrt[4]{0.47}}=0.302,\ \lambda^{-1}\theta\mu=\pi_8=\frac{3.988}{\sqrt[4]{0.47}}=4.815 \tag{3.376}$$

the dimensionless form of (3.374) is obtained applying model (3.178)

$$\frac{d^4y(\bar{t})}{d\bar{t}^4}+4.721\frac{d^3y(\bar{t})}{d\bar{t}^3}+7.58\frac{d^2y(\bar{t})}{d\bar{t}^2}+4.815\frac{dy(\bar{t})}{d\bar{t}}+y(\bar{t})=u(\bar{t}-0.302)\,. \tag{3.377}$$

One can see both λ and θ result greater than 1.5 as expected. On the right-hand side of (3.377) there is $K=1$. For the stability assessment the number σ is evaluated

$$\sigma=\frac{c_1c_2}{\sqrt[4]{c_4^{\,3}}}=\frac{4.815\cdot 7.58}{\sqrt[4]{0.47^3}}=64.3>1 \tag{3.378}$$

which expresses in value that the plants (3.377) satisfy the necessary condition of stability due to condition (3.175). The plant stability is confirmed by the conditions (3.332)

$$\mu = 4.721 > \lambda^{-1} = 0.635,\ \lambda^{-1}\theta^2\mu - 1 = 6.726 > \lambda^{-2}\theta^2 = 1.04. \tag{3.379}$$

From the characteristic equation of plant (3.374)

$$\begin{aligned} M(s) &= \frac{1}{0.47}\left(0.47s^4 + 2.682s^3 + 5.2s^2 + 3.988s + 1\right) = \\ &= (s+0.5)(s+1)(s+1.7)(s+2.5) = 0 \end{aligned} \tag{3.380}$$

$b_1 = 0.5\,s^{-1}$, $b_2 = 1\,s^{-1}$, $b_3 = 1.7\,s^{-1}$ and $b_4 = 2.5\,s^{-1}$. In the plant (3.374) spectrum the four distinct real poles are as follows

$$s_1 = -b_1 = -0.5\,s^{-1},\ s_2 = -b_2 = -1\,s^{-1},\ s_3 = -b_3 = -1.7\,s^{-1},\ s_4 = -b_4 = -2.5\,s^{-1}. \tag{3.381}$$

Using relation (3.335) through (3.337) the similarity numbers μ, λ and θ are verified

$$\mu = (0.5+1+1.7+2.5)\sqrt[4]{0.47} = 4.721 \tag{3.382}$$

$$\lambda = \frac{0.5\cdot 1 + 0.5\cdot 1.7 + 1\cdot 1.7 + 0.5\cdot 2.5 + 1\cdot 2.5 + 1.7\cdot 2.5}{0.5\cdot 1\cdot 1.7 + 0.5\cdot 1\cdot 2.5 + 1\cdot 1.7\cdot 2.5 + 0.5\cdot 1.7\cdot 2.5}\,\frac{1}{\sqrt[4]{0.47}} = 1.574 \tag{3.383}$$

$$\theta = \frac{0.5\cdot 1 + 0.5\cdot 1.7 + 1\cdot 1.7 + 0.5\cdot 2.5 + 1\cdot 2.5 + 1.7\cdot 2.5}{0.5+1+1.7+2.5}\sqrt[4]{0.47} = 1.605. \tag{3.384}$$

Model (3.377) describes all the dynamically similar plants with similarity numbers (3.376). For instance the following fourth-order plant

$$1.5\frac{d^4y(t)}{dt^4} + 6.4\frac{d^3y(t)}{dt^3} + 9.28\frac{d^2y(t)}{dt^2} + 5.3275\frac{dy(t)}{dt} + y(t) = u(t-0.334) \tag{3.385}$$

is dynamically similar to the plant (3.374) because the similarity numbers result the same with (3.376). To verify it the following evaluations are made

$$\begin{aligned} &\lambda = \frac{9.28}{5.3275}\frac{1}{\sqrt[4]{1.5}} = 1.574,\ \theta = \frac{9.28}{6.4}\sqrt[4]{1.5} = 1.605,\ \theta\mu = \pi_7 = \frac{9.28}{\sqrt{1.5}} = 7.58,\ \mu = \frac{6.4}{\sqrt[4]{1.5^3}} = 4.721, \\ &\vartheta = \frac{0.334}{\sqrt[4]{1.5}} = 0.302,\ \lambda^{-1}\theta\mu = \pi_8 = \frac{5.3275}{\sqrt[4]{1.5}} = 4.815. \end{aligned} \tag{3.386}$$

In comparison to (3.374) the (3.385) pole spectrum is already changed as follows

$$s_1 = -b_1 = -0.374\,s^{-1},\ s_2 = -b_2 = -0.753\,s^{-1},\ s_3 = -b_3 = -1.256\,s^{-1},\ s_4 = -b_4 = -1.882\,s^{-1}. \tag{3.387}$$

In Fig. 4 step responses of dynamically similar plants (3.374) and (3.385) are compared.

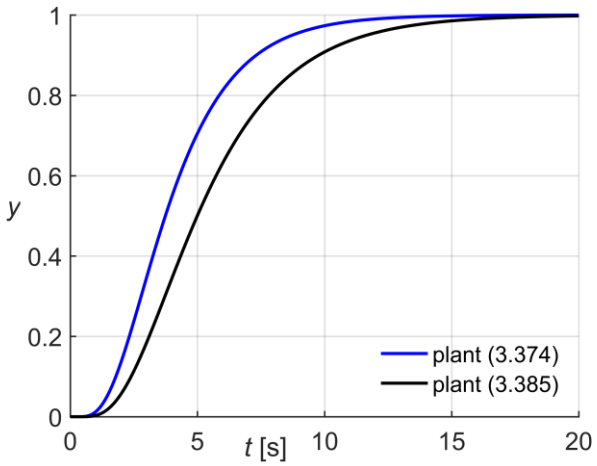

Fig. 4. Step responses of dynamically similar plants belonging to aperiodic plants

Example 4. As announced before Example 3 next sample of the fourth-order plant is the oscillatory plant such that the plant pole spectrum is composed of one pair of complex conjugate poles and two distinct real poles. Such a plant is identified as follows

$$0.2667\frac{d^4y(t)}{dt^4}+1.653\frac{d^3y(t)}{dt^3}+2.093\frac{d^2y(t)}{dt^2}+2.667\frac{dy(t)}{dt}+y(t)=u(t-0.2) \tag{3.388}$$

from where the scaling factor is as follows

$$\sqrt[4]{c_4}=\sqrt[4]{0.2667}=0.7186\,. \tag{3.389}$$

Based on (3.389) and similarity number (3.164) through (3.168) as follows

$$\lambda=\frac{2.093}{2.667\cdot\sqrt[4]{0.2667}}=1.0922\,,\ \theta=\frac{2.093}{1.653}\sqrt[4]{0.2667}=0.9098\,,\ \theta\mu=\pi_7=\frac{2.093}{\sqrt{0.2667}}=4.0531\,,$$
$$\mu=\frac{4.0531}{0.9098}=4.4546\,,\ \vartheta=\frac{0.2}{\sqrt[4]{0.2667}}=0.2783\,,\ \lambda^{-1}\theta\mu=\pi_8=\frac{2.667}{\sqrt[4]{0.2667}}=3.711 \tag{3.390}$$

where $\sqrt{0.2667}=\sqrt[4]{(0.2667)^2}$ and the dimensionless form of (3.388) is obtained due to model (3.178)

$$\frac{d^4y(\bar{t})}{d\bar{t}^4}+4.4546\frac{d^3y(\bar{t})}{d\bar{t}^3}+4.0531\frac{d^2y(\bar{t})}{d\bar{t}^2}+3.711\frac{dy(\bar{t})}{d\bar{t}}+y(\bar{t})=u(\bar{t}-0.2783)\,. \tag{3.391}$$

The right-hand side of (3.327) is with $K=1$. To make the list of the similarity numbers in (3.390) complete the number (3.169) is evaluated

$$\sigma=c_1c_2\Big/\sqrt[4]{c_4^{\,3}}=\frac{2.667\cdot2.093}{\sqrt[4]{0.2667^3}}=15.04\gg1. \tag{3.392}$$

This number considerably exceeds the threshold and it means as in case of (3.378) the plant satisfies supplementary necessary condition of the stability. The plant stability is confirmed by the conditions (3.332)

$$\mu = 4.4546 > \lambda^{-1} = 0.915,\ \lambda^{-1}\theta^2\mu - 1 = 2.376 > \lambda^{-2}\theta^2 = 0.694. \tag{3.393}$$

Specifying the characteristic equation of plant (3.388)

$$M(s) = \frac{1}{0.2667} \times \\ \left(0.2667s^4 + 1.653s^3 + 2.093s^2 + 2.667s + 1\right) = \left(s + 0.5\right)\left(s + 5\right)\left(s^2 + 0.7s + 1.5\right) = 0 \tag{3.394}$$

one undamped natural frequency exist, $\omega_n = 1.2247\ s^{-1}$, together with damping factor $\xi = 0.2857$ and two real poles result as $s_3 = -0.5\ s^{-1}$ and $s_4 = -5\ s^{-1}$. Using relation (3.339) through (3.341) the similarity numbers μ, λ and θ are verified

$$\mu = \left(0.5 + 5 + 2 \cdot 0.2857 \cdot 1.2247\right)\sqrt[4]{0.2667} = 4.454 \tag{3.395}$$

$$\lambda = \frac{0.5 \cdot 5 + 1.2247^2 + 2 \cdot 0.2857 \cdot 1.2247\left(0.5 + 5\right)}{2 \cdot 0.2857 \cdot 1.2247 \cdot 0.5 \cdot 5 + 1.2247^2\left(0.5 + 5\right)} \frac{1}{\sqrt[4]{0.2667}} = 1.092 \tag{3.396}$$

$$\theta = \frac{0.5 \cdot 5 + 1.2247^2 + 2 \cdot 0.2857 \cdot 1.2247\left(0.5 + 5\right)}{0.5 + 5 + 2 \cdot 0.2857 \cdot 1.2247}\sqrt[4]{0.2667} = 0.909. \tag{3.397}$$

Model (3.391) describes all the dynamically similar plants with similarity numbers (3.390).

Example 5. The fourth-order oscillatory plant of which poles are two pairs of complex conjugates is identified as follows

$$0.5\frac{d^4y(t)}{dt^4} + 0.375\frac{d^3y(t)}{dt^3} + 1.5625\frac{d^2y(t)}{dt^2} + 0.625\frac{dy(t)}{dt} + y(t) = u(t - 0.25) \tag{3.398}$$

from where the scaling factor originates in

$$\sqrt[4]{c_4} = \frac{1}{\sqrt[4]{2}}. \tag{3.399}$$

Utilizing (3.399) and similarity number (3.164) through (3.168) as follows

$$\lambda = \frac{1.5625}{0.625}\sqrt[4]{2} = 2.973, \qquad \theta = \frac{1.5625}{0.375}\frac{1}{\sqrt[4]{2}} = 3.5037, \qquad \theta\mu = \pi_7 = 1.5625 \cdot \sqrt[4]{4} = 2.2097, \\ \mu = 0.375 \cdot \sqrt[4]{8} = 0.6307,\ \vartheta = 0.25 \cdot \sqrt[4]{2} = 0.297,\ \lambda^{-1}\theta\mu = \pi_8 = 0.625 \cdot \sqrt[4]{2} = 0.7432 \tag{3.400}$$

the dimensionless form of (3.398) is obtained with respect to model (3.178)

$$\frac{d^4y(\bar{t})}{d\bar{t}^4}+0.6307\frac{d^3y(\bar{t})}{d\bar{t}^3}+2.2097\frac{d^2y(\bar{t})}{d\bar{t}^2}+0.7432\frac{dy(\bar{t})}{d\bar{t}}+y(\bar{t})=u(\bar{t}-0.297). \tag{3.401}$$

On the right-hand side of (3.401) there is $K=1$. For the stability assessment the number σ is evaluated

$$\sigma=\frac{c_1c_2}{\sqrt[4]{c_4{}^3}}=\frac{0.625\cdot 1.5625}{\sqrt[4]{0.5^3}}=1.642>1 \tag{3.402}$$

which expresses in value that the plants (3.401) satisfy the necessary condition of stability due to condition (3.175). The plant stability is proved by the conditions (3.332)

$$\mu=0.6307>\lambda^{-1}=0.336,\ \lambda^{-1}\theta^2\mu-1=1.604>\lambda^{-2}\theta^2=1.388. \tag{3.403}$$

From the characteristic equation of plant (3.398)

$$M(s)=2\left(0.5s^4+0.375s^3+1.5625s^2+0.625s+1\right)=\left(s^2+0.25s+2\right)\left(s^2+0.5s+1\right)=0 \tag{3.404}$$

two undamped natural frequencies ω_{n1} and ω_{n2} result as $\omega_{n1}=1.4142\,s^{-1}$ and $\omega_{n2}=1\,s^{-1}$. Corresponding damping factors are $\xi_1=0.088$ and $\xi_2=0.25$. Using relation (3.343) through (3.345) the similarity numbers μ, λ and θ are verified

$$\mu=2\left(0.088\cdot 1.4142+0.25\cdot 1\right)\frac{1}{\sqrt[4]{2}}=0.63 \tag{3.405}$$

$$\lambda=\frac{4\cdot 0.088\cdot 0.25\cdot 1.4142\cdot 1+1.4142^2+1^2}{2\left(0.088\cdot 1.4142\cdot 1^2+0.25\cdot 1\cdot 1.4142^2\right)}\sqrt[4]{2}=2.97 \tag{3.406}$$

$$\theta=\frac{4\cdot 0.088\cdot 0.25\cdot 1.4142\cdot 1+1.4142^2+1^2}{2\left(0.088\cdot 1.4142+0.25\cdot 1\right)}\frac{1}{\sqrt[4]{2}}=3.5. \tag{3.407}$$

Analogously to model (3.391) all dynamically similar plants to (3.398) have to be characterized with the same similarity numbers (3.400). For all these similar plants the loop gains setting is determined by dominant three-pole placement technique in Chapter 4.4.

Example 6 (*Integrating plant*). The example of dynamically similar integrating plants (3.185) of the fourth-order is demonstrated on the identified integrating plant (3.117) for $n=4$

$$0.2667\frac{d^4y(t)}{dt^4}+1.52\frac{d^3y(t)}{dt^3}+1.333\frac{d^2y(t)}{dt^2}+2\frac{dy(t)}{dt}=u(t-0.2). \tag{3.408}$$

Based on the scaling factor common with (3.388) and similarity numbers given by (3.166), (3.167) and (3.180), (3.181) as follows

$$\lambda_I = \frac{2}{1.333}\sqrt[4]{0.2667} = 1.0779, \qquad \theta_I = \frac{1.333}{1.52}\sqrt[4]{0.2667} = 0.63036, \tag{3.409}$$
$$\lambda_I\theta_I\mu = \pi_8 = \frac{2}{\sqrt[4]{0.2667}} = 2.782,\ \mu = \frac{2.782}{1.0779\cdot 0.63036} = 4.0961,\ \vartheta = 0.2/\sqrt[4]{0.2667} = 0.2782.$$

the dynamically similar integrating plants (3.185) where (3.408) is one of them result in

$$\frac{d^4y(\bar{t})}{d\bar{t}^4} + 4.0961\frac{d^3y(\bar{t})}{d\bar{t}^3} + 2.582\frac{d^2y(\bar{t})}{d\bar{t}^2} + 2.782\frac{dy(\bar{t})}{d\bar{t}} = u(\bar{t} - 0.2782). \tag{3.410}$$

Utilizing the condition (3.368) the damped impulse responses of (3.410) are guaranteed because

$$\theta_I\mu^2 = 10.57 > 1. \tag{3.411}$$

The dimensional analysis based on similarity numbers λ_I, θ_I, μ and ϑ gives rise to the pole spectrum of (3.410) as the roots of the following equation

$$\bar{s}^4 + 4.096\bar{s}^3 + 2.582\bar{s}^2 + 2.782\bar{s} \triangleq \bar{s}\left(\bar{s} + 3.593\right)\left(\bar{s}^2 + 0.5029\bar{s} + 0.7744\right) = 0. \tag{3.412}$$

These roots can be also computed from the roots of the characteristic equation (3.364) of model (3.408)

$$M(s) = \frac{1}{0.2667}\left(0.2667s^4 + 1.52s^3 + 1.333s^2 + 2s\right) = s\left(s+5\right)\left(s^2 + 0.7s + 1.5\right) = 0 \tag{3.413}$$

as follows

$$\bar{s}_{1,2} = s_{1,2}\sqrt[4]{c_4} = -0.35\cdot\sqrt[4]{0.2667} \pm j1.1737\cdot\sqrt[4]{0.2667} = -0.25151 \pm j0.84341,$$
$$\bar{s}_3 = s_3\sqrt[4]{c_4} = -5\cdot\sqrt[4]{0.2667} = -3.593,\ \bar{s}_4 = s_4\sqrt[4]{c_4} = 0\cdot\sqrt[4]{0.2667} = 0. \tag{3.414}$$

Due to (3.363) it results from (3.414)

$$\nu_n = \omega_n\sqrt[4]{c_4} = 1.2247\cdot\sqrt[4]{0.2667} = 0.88,\ \beta = 3.593 \tag{3.415}$$

and the damping factor of the integrating plant impulse response is $\xi = 0.2857$. The relations for the similarity numbers μ, λ_I and θ_I given by (3.360) through (3.362) are applied to verify (3.409) as follows

$$\mu = \left(5 + 2\cdot 0.2857\cdot 1.2247\right)\sqrt[4]{0.2667} = 4.096 \tag{3.416}$$

$$\lambda_I = \frac{1.2247^2\cdot 5}{1.2247^2 + 2\cdot 0.2857\cdot 1.2247\cdot 5}\sqrt[4]{0.2667} = 1.077 \tag{3.417}$$

$$\theta_I = \frac{1.2247^2 + 2 \cdot 0.2857 \cdot 1.2247 \cdot 5}{5 + 2 \cdot 0.2857 \cdot 1.2247} \sqrt[4]{0.2667} = 0.63 . \tag{3.418}$$

In Fig. 3 the similarity numbers (3.409) correspond to point $\theta_I / \beta = 0.175$ and $\lambda_I / \beta = 0.3$ which confirms the integrating plants (3.410) with oscillatory impulse response shown in Fig. 5. As regards the integrating plant stiffness evaluating (3.369)

$$\sigma_I = \xi \frac{\nu_n}{\beta} = 0.2857 \frac{0.88}{3.593} = 0.0699 \tag{3.419}$$

and substituting it into the upper bound of (3.372) as follows

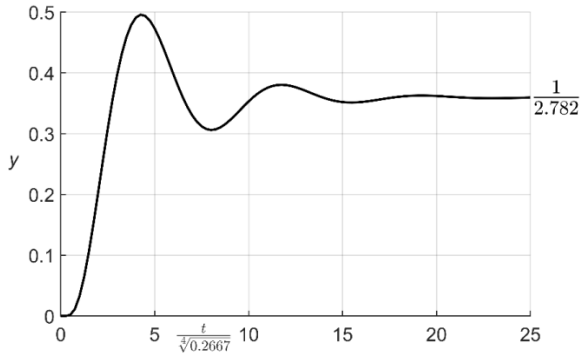

Fig. 5. Oscillatory impulse response of integrating plants (3.410)

$$\frac{\sigma_I + 2}{1 + 2\sigma_I} = \frac{0.0699 + 2}{1 + 2 \cdot 0.0699} = 1.816 , \; 0 < \frac{\xi}{\nu_n} = 0.3246 \ll \infty . \tag{3.420}$$

One can conclude that the integrating plants (3.410) are *stiff* because $(\sigma_I + 2)/(1 + 2\sigma_I) > 1$ and (3.420) approaches its upper limit given by 2. In Chapter 4.4 the loop gains tuning is provided for the integrating plants (3.410) by dominant three-pole placement method.

3.4 Conclusions

The application of dimensional analysis is presented to describe the higher-order plants by means of the dimensionless models providing deep analysis of the plants dynamics. In addition the dimensionless models provide reducing the number of original plants parameters and at the same time introduce the similarity numbers making possible to distinguish among the plants dynamics features. Namely plants *oscillability, retardedness (laggardness), dampeningness (dimensionless spectral abscissa)* and *stiffness* belong to these features. In summary two options of the dimensional analysis application are presented. The first option oversimplifies the resulting dimensionless model of the plant due to fixing the dimensionless delay to one. The second option removes this delay fixing and consequently introduces another similarity number much better accounting for the delay phenomenon. This number is called *retardedness*. Next based on corresponding similarity numbers the third- and fourth-order plants are investigated in order to map the plant spectral properties. Mapping these properties the admissible ranges of the similarity numbers are found out within which the PID controller is capable to cope with the higher-order dynamics and the delay of plant. Not only the stability but also safe distance from the stability margin is assessed. This mapping concerns also the third- and fourth-order integrating plants. For the plants of the third- and

fourth-order selected in parameters admissible for the PID controller design the dimensionless control loop models with delay are developed which are subsequently in Chapter 4 optimized combining the generalized dominant three-pole placement with the IAE criterion. In other words the controller design for retarded systems benefits from the introduced similarity numbers because of allowing only for dynamically reasonable constraints (limited damping and speed of control response, limited level of controller gain magnitude etc.) in control synthesis. These constraints applied to the delayed control loop design simultaneously with the generalized dominant three-pole placement give off controller parameters enumeration that is acceptable in practice and leads to the pole dominance guarantee or at least safe distance from the stability margin (i.e. spectral abscissa exceeding 0.2) as presented in Chapter 4.

4. Generalized dominant three-pole placement

4.1 Introduction

The ultimate gain and the ultimate frequency are well-known quantities utilized in the PID controller tuning [3]. While the ultimate gain is dimensionless due to the ratio of variables *u* and *y*, the ultimate frequency becomes ultimate angle (or ultimate frequency number) [123], [125, 126], in dimensionless description of the control loop.

As it results from the dimensional analysis in Chapter 3 the key parameter for the dimensionless control loop description is the natural frequency ω and for PID controller tuning the most significant parameter is the ultimate frequency. Hence the following idea resulted that the natural frequency should be very close to or the same as the ultimate frequency when assigning the delayed control loop poles composed of pair of complex conjugates and one real pole [123], [126]. Beside the natural frequency optimization also the control loop damping is optimized by searching for a trade-off between the absolute error integral (IAE) optimum and the dominance degree of placed poles in delayed PID control loop [121], [124, 125]. This dominance can be evaluated by rightmost roots computation, e.g. [97], or argument increment rule application [95], [124].

In this chapter the dominant three-pole placement for the second-order plant, [126], is extended to the third- and fourth-order plants. A trio of poles is assigned in the fourth- or fifth-order PID control loop with delay to obtain proportional, integration and derivative loop gains. Simultaneously the assigned trio of poles has to become *dominant* in infinite spectrum of control loop poles. In other words the three poles have to be the rightmost poles in the system spectrum which are separated from the rest of the infinite spectrum. Truly there is the technical note, [100], on a mapping all the stabilizing PID settings for the third-order aperiodic plants with delay. In this note the spectral abscissa is guaranteed predominantly not greater than 0.1. Hence one of the goals of this chapter is to achieve greater spectral abscissa in the fourth- or fifth-order control loops with delay. In fact in view of the exhaustive study on computing all the stabilizing PID controller settings for general retarded systems in [46] only a small portion, if any at all, of entire tuning set is applicable due to the requirement from industry on minimum spectral abscissa. Thus next aim of this chapter is to specify to which higher-order plants with delay and their parameter constraints the developed PID settings are applicable. In other words the PID tuning rules applicable to all dynamically similar plants of the third- and fourth-order are developed rather than all the stabilizing PID controller settings. Let be pointed out that in [103] the degradation-free PID tuning is made possible for higher-order plants with delay by considering these plants models of maximum relative order equal to three. With respect to the pole dominance guarantee in the higher-order control loops the complex conjugate pair of poles is regularly assigned within the root locus technique as in [105]. However to guarantee this dominance the natural frequency is prescribed in examples of [105] three to ten times lower than the ultimate frequency. In [119] a universal map of three dominant pole assignment for PID controller tuning is achieved applying the dimensional analysis. Hence another goal of this chapter is to assign the natural frequency number as close as possible to the ultimate frequency number and simultaneously to guarantee this frequency number resulting as dominant. Obviously crucial for the PID controller tuning is to assess the ultimate frequency number. In Chapter 4.2 the case of $n = 2$ is summed up.

The following classification of the PID control is expectable:

1. **3PP admissibility**: If the dominant three-pole placement (3PP) method is admissible then this method is capable to tune up the PID controller and vice versa. In case of the inadmissible 3PP method this method fails in the PID controller tuning but the PID controller tuned by another approach is applicable.
2. **PID admissibility**: If the PID controller is admissible then it is applicable to controlling the delayed plant and vice versa. In case of the inadmissible PID this controller is not applicable and other than PID control has to be used.

Both classes of the PID control are presented for $n=3$ and $n=4$ in Chapter 4.3 and 4.4, respectively. The examples are included. The first class of the PID control is shown in Examples 7 and 8 at the end of Chapter 4.3. Next two examples (Examples 11 and 12) are added to the end of Chapter 4.4. The case of the inadmissible 3PP method appears in Counterexamples 9 and 10, presented at the end of Chapter 4.3. The second class is shown in Counterexamples 13 and 14 at the end of Chapter 4.4. Surprisingly the 3PP method is unable to tune the PID controller while the other method, the Ziegler-Nichols (Z-N) method, is able to tune the PID as shown in Counterexamples 9 and 10. Notice the classification of the PID control for $n=2$ is not considered because the second-order dynamics of the plant is well tackled by the PID controller.

4.2 Dominant three-pole placement for $n=2$

The results of the dominant three-pole placement in the third-order PID control loop with delay described by model (3.203) for $n=2$ are presented as appeared in [123, 124] and [126]. Some discussions to these results are added to point out the merit of the dominant three-pole placement. Once a trio of poles is assigned in the third-order PID control loop with delay the proportional, integration and derivative loop gains are adjusted. Assume the following trio of poles, [123], [126],

$$\overline{p}_{1,2}=\left(-\delta\pm j\right)\nu,\ \overline{p}_3=-\kappa\delta\nu,\ \delta>0,\ \nu>0,\ \kappa>0 \tag{4.1}$$

is assigned where δ is the relative damping and ν is the natural frequency number already defined by π_1 for $n=2$, see Chapter 3. κ is the root ratio given as follows

$$\kappa=\frac{\overline{p}_3}{\mathrm{Re}\left(\overline{p}_{1,2}\right)}>0. \tag{4.2}$$

In (4.1) the dimensionless natural frequency ν is used instead of undamped frequency ν_n in (3.273) (Chapter 3.3). As regards the ultimate frequency assessment for the case $n=2$, [126], the ultimate frequency number, ν_K, results in simple relations for proportional and integrating plants given by (3.141) and (3.142), respectively, as follows

$$\cot\left(\vartheta\nu_K\right)=\frac{\lambda\left(\nu_K^2-1\right)}{\nu_K} \tag{4.3}$$

and

$$\cot\left(\vartheta\nu_K\right)=\lambda_I\nu_K \tag{4.4}$$

respectively, where λ, λ_I and ϑ are the *swingability*, *inertiality* and *laggardness* numbers, for more details on them see Chapter 3 (*Case 2*). The solution to (4.3) is obtained with MATLAB in Chapter 4.5. In both [123] and [126] the natural frequency number is identified with the ultimate frequency number for the purpose of dominant three-pole placement. The ultimate frequency number ν_K in dependence on λ and ϑ is recorded in Fig. 6. From Fig. 6 it is apparent that with growing swingability number decreases the ultimate frequency number. The same takes place with growing laggardness number. Admissibility ranges of both λ and ϑ are $\lambda\in\langle 0.25,2\rangle$ and $\vartheta\in\langle 0.25,1.5\rangle$ for which the values of ultimate frequency number ν_K fall within $\nu_K\in\langle 1,3.6\rangle$. The second-order oscillatory plants appear for $\lambda>0.5$. In case $\vartheta<0.2$ the delay effect of second-order plant becomes negligible. For $\lambda>2$ and $\vartheta>1.5$ the PID controller settings drop in gain values below 0.5.

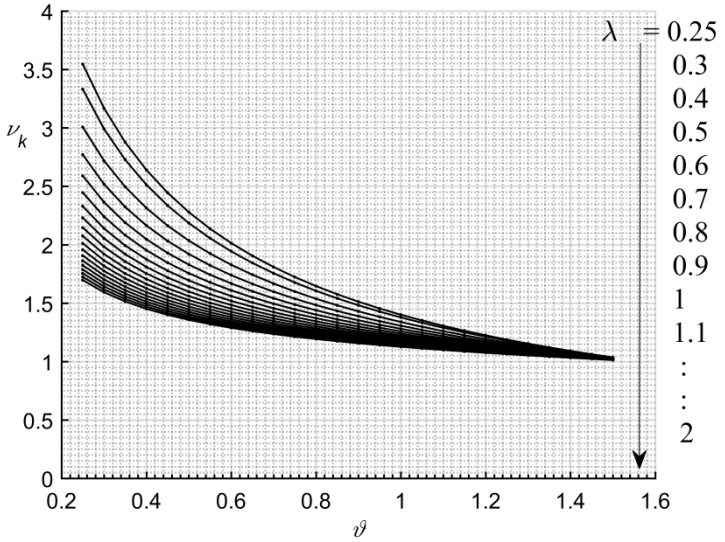

Fig. 6. ν_K dependence on numbers λ and ϑ, [126]

To assign (4.1) the three poles have to be the roots of (3.215) and in case of integrating plants the trio of poles (4.1) have to be roots of (3.216), see *Case 2* in Chapter 3. Substituting each pole from (4.1) into (3.215) and starting with $\overline{s}=\overline{p}_1=\left(-\delta+j\right)\nu$ one gets

$$\begin{aligned}&\rho_P(-\delta+j)\nu+\rho_D(\delta^2-1-j2\delta)\nu^2+\rho_I=\exp(-\delta\vartheta\nu)[\cos(\vartheta\nu)+\\&+j\sin(\vartheta\nu)]\left[(\delta-j)\nu+\frac{1}{\lambda}(1-\delta^2+j2\delta)\nu^2-(3\delta-\delta^3-j(1-3\delta^2))\nu^3\right]=\widetilde{B}\end{aligned} \tag{4.5}$$

After substituting $\overline{p}_3=-\kappa\delta\nu$ for $\overline{s}$ in (3.215) the following equation is obtained

$$-\rho_P\kappa\delta\nu+\rho_D(\kappa\delta\nu)^2+\rho_I=\exp(-\kappa\delta\vartheta\nu)\left[\kappa\delta\nu-\frac{1}{\lambda}(\kappa\delta\nu)^2+(\kappa\delta\nu)^3\right]. \tag{4.6}$$

To express the right-hand side of (4.5), $\widetilde{B}$, the following supplementary expressions are found out

$$b_R = \delta + \frac{1}{\lambda}(1-\delta^2)\nu - (3\delta - \delta^3)\nu^2, \tag{4.7}$$

$$b_I = -1 + \frac{1}{\lambda}2\delta\nu + (1-3\delta^2)\nu^2. \tag{4.8}$$

Then real and imaginary part of $\tilde{B}$ result in

$$\mathrm{Re}\left(\tilde{B}\right) = B_R\nu = \exp\left(-\delta\vartheta\nu\right)\left[b_R\cos\left(\vartheta\nu\right) - b_I\sin\left(\vartheta\nu\right)\right]\nu, \tag{4.9}$$

$$\mathrm{Im}\left(\tilde{B}\right) = B_I\nu = \exp\left(-\delta\vartheta\nu\right)\left[b_I\cos\left(\vartheta\nu\right) + b_R\sin\left(\vartheta\nu\right)\right]\nu, \tag{4.10}$$

and from the right-hand side of (4.6) it stems

$$B_3\nu = \exp\left(-\kappa\delta\vartheta\nu\right)\kappa\delta\left[1 - \frac{1}{\lambda}\kappa\delta\nu + \kappa^2\delta^2\nu^2\right]\nu. \tag{4.11}$$

The right-hand sides, namely (4.9) through (4.11), can be inserted into the following vector

$$\mathbf{B} = \left[B_R \;\; B_I \;\; B_3\right]^T \nu \tag{4.12}$$

and the left-hand sides of (4.5) and (4.6) constitute the following matrix

$$\mathbf{A} = \begin{bmatrix} -\delta\nu, & \nu^2\left(\delta^2 - 1\right), & 1 \\ \nu, & -2\delta\nu^2, & 0 \\ -\kappa\delta\nu, & \kappa^2\delta^2\nu^2, & 1 \end{bmatrix} \tag{4.13}$$

with respect to the vector composed of searched control loop gains as follows

$$\mathbf{P} = \left[\rho_P \;\; \rho_D \;\; \rho_I\right]^T. \tag{4.14}$$

Equations (4.5) and (4.6) can be rewritten into the matrix form using (4.12) through (4.14)

$$\mathbf{AP} = \mathbf{B} \tag{4.15}$$

To solve (4.15) for $\mathbf{P}$ the matrix $\mathbf{A}$ has to be inverted thus $\det\left(\mathbf{A}\right) \neq 0$. Since $\det\left(\mathbf{A}\right) = \nu^3\left(1 + \delta^2\left(\kappa - 1\right)^2\right) \neq 0$ for $\nu > 0$ Cramer's rule is utilized for solution to (4.15). Thus

$$\mathbf{P}\left(i\right) = \frac{\det\left(\mathbf{A}_i\right)}{\det\left(\mathbf{A}\right)}, \; i = 1, 2, 3 \tag{4.16}$$

where

$$\mathbf{A}_1=\begin{bmatrix} B_R, & \nu^2\left(\delta^2-1\right), & 1 \\ B_I, & -2\delta\nu^2, & 0 \\ B_3, & \kappa^2\delta^2\nu^2, & 1 \end{bmatrix},\ \mathbf{A}_2=\begin{bmatrix} -\delta\nu, & B_R, & 1 \\ \nu, & B_I, & 0 \\ -\kappa\delta\nu, & B_3, & 1 \end{bmatrix},\ \mathbf{A}_3=\begin{bmatrix} -\delta\nu, & \nu^2\left(\delta^2-1\right), & B_R \\ \nu, & -2\delta\nu^2, & B_I \\ -\kappa\delta\nu, & \kappa^2\delta^2\nu^2, & B_3 \end{bmatrix}. \tag{4.17}$$

Particular control loop gains are found out as follows

$$\mathbf{P}(1)=\rho_P,\ \mathbf{P}(2)=\rho_D,\ \mathbf{P}(3)=\rho_I. \tag{4.18}$$

Due to inner cancellation of powers of ν this rule leads to the following solutions for ρ_P,ρ_D,ρ_I. Namely in ratio for ρ_P and ρ_I there is the cancellation of ν^3, and in ratio for ρ_D it is cancelled ν^2. Hence (4.18) are rewritten into separate relations equivalent with (4.16) as follows

$$\rho_P=\frac{1}{\delta^2\left(\kappa-1\right)^2+1}\det\begin{bmatrix} B_R, & \delta^2-1, & 1 \\ B_I, & -2\delta, & 0 \\ B_3, & \kappa^2\delta^2, & 1 \end{bmatrix}, \tag{4.19}$$

$$\rho_D=\frac{1}{\nu\left(\delta^2\left(\kappa-1\right)^2+1\right)}\det\begin{bmatrix} -\delta, & B_R, & 1 \\ 1, & B_I, & 0 \\ -\kappa\delta, & B_3, & 1 \end{bmatrix}, \tag{4.20}$$

$$\rho_I=\frac{\nu}{\delta^2\left(\kappa-1\right)^2+1}\det\begin{bmatrix} -\delta, & \delta^2-1, & B_R \\ 1, & -2\delta, & B_I \\ -\kappa\delta, & \kappa^2\delta^2, & B_3 \end{bmatrix} \tag{4.21}$$

where (4.9) through (4.11) are applied without factorized ν. The proof of (4.19) through (4.21) is presented in [126]. Let be remarked the formulae (4.19), (4.20) and (4.21) are applicable to integrating plants (3.142), too. Only entries of **B** appearing in these formulae have to be changed to

$$b_R=\frac{1}{\lambda}\left(1-\delta^2\right)\nu-\left(3\delta-\delta^3\right)\nu^2 \tag{4.22}$$

$$b_I=\frac{1}{\lambda}2\delta\nu+\left(1-3\delta^2\right)\nu^2 \tag{4.23}$$

$$B_3=\exp\left(-\kappa\delta\vartheta\nu\right)\kappa\delta\left[-\frac{1}{\lambda}\kappa\delta\nu+\kappa^2\delta^2\nu^2\right] \tag{4.24}$$

where in comparison to (4.7), (4.8) and (4.11) δ, -1 and +1, respectively, disappear.

The question what is proper selection of the pole coordinates, namely ν, δ and κ, is answered by the IAE optimization combined with the trio (4.1) dominance test. This test reveals whether any other pole than the placed trio of poles exists in the position more to the right from (4.1) in the complex plane of system poles or not. A sample of the IAE

optimization results within the pole placement procedure in case of dynamically similar plants characterized by $\lambda = 0.6$ and $\vartheta = 0.4$ is shown in Fig. 7. For the purpose of the IAE evaluation the control loop gains are computed by (4.19) through (4.21). In Fig. 7 local IAE minima in the pole coordinate space are displayed where particular surfaces are for selected κ values. The higher κ the lower results the IAE. However for $\kappa > 1.5$ the trio (4.1) dominance is not already achieved and $\nu > \nu_{\text{opt}}$ where ν_{opt} is the optimum natural frequency. This optimum frequency number results as a trade-off between the IAE optimization and the three-pole dominance. In other words at the optimum, $[\nu \quad \delta \quad \kappa] = [2.77 \quad 0.22 \quad 1.5]$, resulting from Fig. 7 the lowest possible IAE is achieved when the three-pole dominance is not lost yet. Naturally this optimum is variable with respect to λ and ϑ. Nevertheless the optimum κ does not exceed 1.5 and the optimum relative damping is close to 0.25 or higher for all admissible λ and ϑ. Only the natural frequency number ν is in its optimum, ν_{opt}, relatively variable with respect to variable ν_K. This variability is shown as ratio ν_{opt}/ν_K for

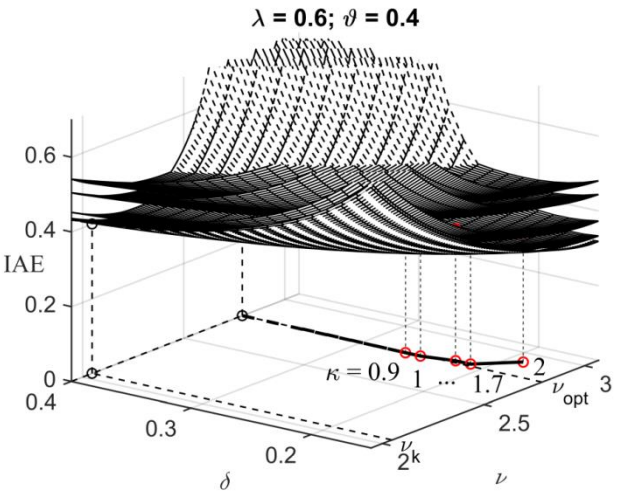

Fig. 7. 3D plot of IAE criterion dependence on the pole coordinates, [126]

all admissible λ and ϑ in Fig. 8. For $\nu = \nu_{\text{opt}}$ from Fig. 8 the proportional loop gain given by (4.19) is recorded in Fig. 9 when $\delta = 0.35$ and $\kappa = 1$. This pole coordinate option guarantees the (4.1) dominance and results, $\rho_P < 0.5$, are omitted in Fig. 9.

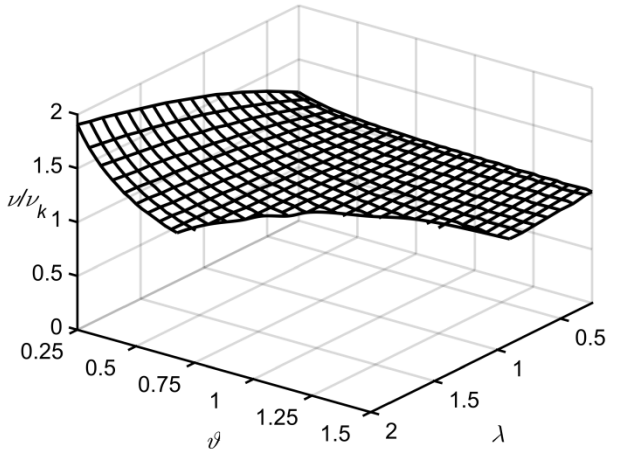

Fig. 8. Natural frequency ratio ν/ν_K versus the plant (3.141) similarity numbers, [126]

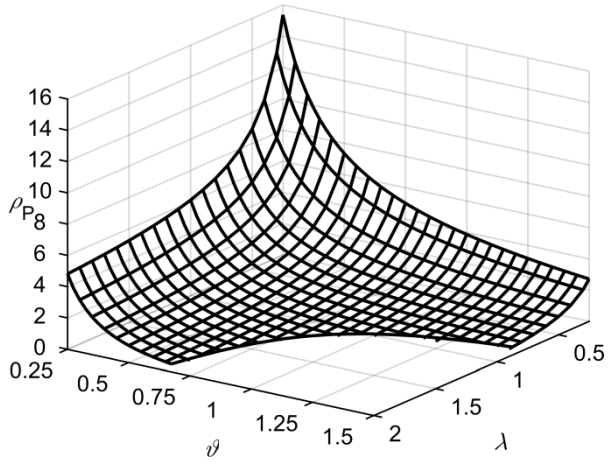

Fig. 9. Proportional gain ρ_P dependence on plant (3.141) similarity numbers, [126]

Generally assigning the natural frequency ν greater than the ultimate frequency ν_K, particularly $\nu = \nu_{\text{opt}}$, there is no guarantee the trio (4.1) becomes the dominant trio of poles. The other two pole placement coordinates, δ and κ, have to be appropriately selected. In [123] the option, $\nu = \nu_K$, has been proved as acceptable from the three-pole dominance point of view if both λ and ϑ are within their admissible ranges. Once ν exceeds ν_K the pole dominance test is necessary, as a rule. Recall the argument increment test, [124], where the dominance check for the following trio of poles

$$p_{1,2} = -\alpha \pm j\Omega = (-\delta \pm j)\Omega, \qquad p_3 = -\beta = -\kappa\delta\Omega \tag{4.25}$$

is performed. Trio (4.25) is specified by frequency Ω and dimensionless parameters (ratios)

$$\delta = \frac{\alpha}{\Omega}, \qquad \kappa = \frac{\beta}{\alpha} \tag{4.26}$$

that are common with dimensionless trio of poles (4.1). Only between Ω and ν with respect to $\pi_1 = \nu$ there is the following relation

$$\Omega = \frac{\nu}{\sqrt{c_2}} \tag{4.27}$$

where $\sqrt{c_2}$ is the scaling factor resulting from the dimensional analysis carried out for $n = 2$ in Chapter 3 (*Case 2*). As already presented in [120, 121] $\Omega = \omega_K$ and instead of (4.27) it is obtained

$$\omega_K = \frac{\nu_K}{\sqrt{c_2}} \tag{4.28}$$

where ω_K is the ultimate frequency. Between (4.1) and (4.25) the following relation exist

$$\bar{p}_{1,2} = p_{1,2}\sqrt{c_2} = (-\delta \pm j)\Omega\sqrt{c_2} = (-\delta \pm j)\nu, \qquad \bar{p}_3 = p_3\sqrt{c_2} = -\kappa\,\delta\,\Omega\sqrt{c_2} = -\kappa\,\delta\nu\,. \tag{4.29}$$

Once the dominance of $p_{1,2,3}$ is proved automatically the same is proved in case of $\bar{p}_{1,2,3}$ ($\sqrt{c_2}$ only shifts whole pole spectrum) and vice versa. To perform the dominance check for (4.1) and in fact also for (4.25) the characteristic quasi-polynomial of the investigated PID control loop with delay is considered in the retarded form (if $n \geq 2$)

$$M(\bar{s}) = \bar{s}^{n+1} + \sum_{i=0}^{n}\left[m_i + d_i \exp(-\bar{s}\,\vartheta)\right]\bar{s}^i, \quad n \geq 2 \tag{4.30}$$

where $d_0 = Kr_I\sqrt{c_2} = \rho_I$, $d_1 = Kr_P = \rho_P$ and $d_2 = Kr_D/\sqrt{c_2} = \rho_D$. $m_i, i = 0,1,...,n,$ are coefficients originating from π_i in dimensionless plant model (3.123). The dominance of $\bar{p}_{1,2,3}$ means that none of the poles is lying to the right from $\bar{p}_{1,2,3}$. According to the general argument increment rule along the Jordan curve shown in Fig. 10 it is therefore necessary and sufficient for $\bar{p}_{1,2,3}$ dominance that the argument increment of (4.30) satisfies the following condition

$$\lim_{\nu\to\infty} \arg M(\bar{s})\Big|_{\bar{s}=-\beta_m+j\nu} - \arg M(-\beta_m) = (n-5)\frac{\pi}{2} \tag{4.31}$$

with

$$\beta_m > 0\,. \tag{4.32}$$

The proof of (4.31) with (4.32) is presented in [124]. Let be remarked, practically, the dominance of $\bar{p}_{1,2,3}$ is checked with the parameter β_m set as $\beta_m \geq 1.05\beta$ where $\beta = \kappa\delta\nu$ or $\beta = \delta\nu$ for $\kappa < 1$ and the argument increment of $M(-\beta_m + j\nu)$ is evaluated for ν growing from zero to an upper boundary frequency

$$\nu = \nu_M, \nu_M >> \nu_K\,. \tag{4.33}$$

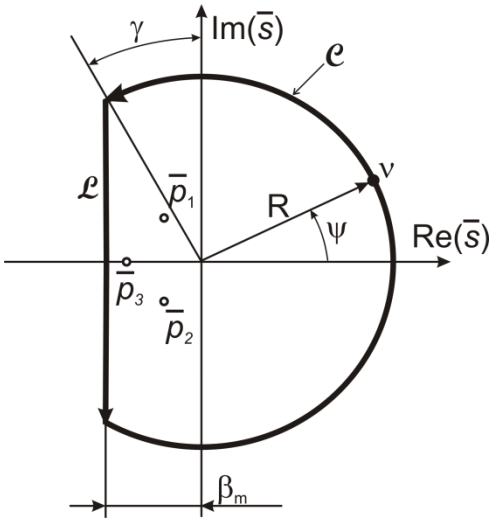

Fig. 10. The Jordan curve for the argument increment test, [126]

Additionally, for ν growing from zero to infinity and for $\beta_m > \kappa\delta\nu > \delta\nu$ the following relation for the spectral abscissa results

$$\max_{\bar{s}\in C}(\mathrm{Re}(M(\bar{s}+\kappa\delta\nu))) = \delta\nu(\kappa-1). \tag{4.34}$$

When relation (4.34) is nullified the spectral abscissa of the delayed PID control loop is equal to $\delta\nu$, i.e. $\kappa = 1$. Then the disturbance rejection is free of negative overshoots and the equality between the integrals of idealized (delay cancelled) and real disturbance responses holds, for more details see [121], [124]. Since (4.31) together with (4.32) is a modification of Mikhaylov criterion the $M(\bar{s})$ function is evaluated with respect to its argument increment limit. However to facilitate the argument increment evaluation instead of $M(\bar{s})$ its Poincaré-like mapping is used in (4.31). This mapping is a dimensionless extension of $M(s)$ mapping from [98] as follows

$$\tilde{M}(\bar{s}) = \frac{M(\bar{s})}{1+\left|M(\bar{s})\right|^{\chi}},\ \chi > 1. \tag{4.35}$$

For the three-pole dominance test the relation (4.30) through (4.33) are implemented in MATLAB in Chapter 4.5 by their extension to the dimensionless PID control loops with delay (3.203). In order to measure the degree of the three-pole dominance the so-called *dominance index* has been introduced by the author in [123]. This index is formulated, [123], either as

$$\eta = \frac{\mathrm{Re}(\bar{p}_4)}{\bar{p}_3} > 1,\ \textit{when}\ \kappa \geq 1 \tag{4.36}$$

or

$$\eta = \frac{\mathrm{Re}(\bar{p}_4)}{\mathrm{Re}(\bar{p}_{1,2})} > 1,\ \textit{when}\ \kappa < 1 \tag{4.37}$$

where $\bar{p}_4$ is the fourth pole from the control loop spectrum lying more to the left from $\bar{p}_{1,2,3}$. The fourth pole and some further poles are computed by quasi-polynomial root finder, [97]. Analogously to (4.27) and (4.28) between the classical and dimensionless control loop response there is a relation concerning the IAE value as follows

$$Q_{AE} = \frac{I_{AE}}{\sqrt{c_2}} \tag{4.38}$$

where

$$I_{AE} = \int_0^{\infty} \left| e(t) \right| dt \tag{4.39}$$

and

$$Q_{AE} = \int_0^{\infty} |e(\bar{t})| d\bar{t} \ . \tag{4.40}$$

Relation (4.38) is the consequence of the dimensional analysis performed in [126] and in subsequent subchapters (4.38) is extended to the fourth- and fifth-order control loops with delay.

Conclusions. From both IAE optimum and pole dominance points of view for the second-order plant admissible ranges

$$\lambda \in \langle 0.25, 2 \rangle, \ \vartheta \in \langle 0.25, 1.5 \rangle \tag{4.41}$$

the pole coordinates ν, δ and κ are constrained to the following intervals

$$\nu \in \langle \nu_K, \nu_{\text{opt}} \rangle, \ \delta \in \langle 0.22, 0.35 \rangle, \ \kappa \in \langle 0.9, 1.3 \rangle \tag{4.42}$$

where $\nu_{\text{opt}} > \nu_K$, [126]. Dominance degree η resulted for admissible ranges (4.41) predominantly close to 2. In PID control loop optimization by magnitude optimum method, [32], the natural frequency $\nu = \nu_{\text{opt}}$ resulted less than ν_K and the relative damping resulted greater than 0.35, i.e. $\delta = 0.4$. Reversely, in case of the IAE optimization, [30], the resulting $\nu = \nu_{\text{opt}}$ exceeds ν_K by more than 25% for all dynamically similar plants considered but optimum damping results extremely low, i.e. $\delta \approx 0.17$. The constraints on pole placement coordinates (4.42) represent the trade-off between the more sluggish but sufficiently damped control response and the faster but poorly damped control response. The admissible gain ρ_P is displayed in Fig. 9 for admissible similarity numbers λ, ϑ. For other two gains, ρ_D, ρ_I, the admissible values are recorded in [126].

4.3 Dominant three-pole placement for $n = 3$

The difference between this case and the case of $n = 2$ is that the PID controller gains do not reach all the coefficient terms of $\bar{s}^0, \bar{s}, \bar{s}^2$ and $\bar{s}^3$ in the characteristic equation (3.221) introduced in Chapter 3 (*Case 3*). The first three terms are influenced by the controller gains and the fourth term, at $\bar{s}^3$, is not modifiable at all. In fact no one of the first three terms is corrected exactly by the PID due to the plant retardedness ϑ. Therefore the admissible ranges of both the similarity numbers and the pole placement coordinates are tighter than the ranges resulting in case of $n = 2$. Even the PID controller is not tuneable by means of the dominant three-pole placement method for inadmissible stable third-order plants because the controller gains result in poor values, i.e. zeros in fact. The examples of unacceptable PID controller tuning by means of the dominant three-pole placement method is shown in Counterexamples 9 and 10 at the end of Chapter 4.3. These counterexamples show that the goal of the dominant three-pole placement to change the stable third-order plant dynamics into desirable dynamics are not achieved for an area of plant similarity numbers.

To find a proper trio of poles (4.1) analogously to case $n = 2$ the ultimate frequency number is evaluated. Recall the third-order plant (3.114) (for $n = 3$) linked with the PID controller. The resulting dimensionless control loop is described by the characteristic equation (3.221)

$$M(\overline{s}) = \left[\overline{s}^4 + \mu\overline{s}^3 + \lambda^{-1}\mu\overline{s}^2 + \overline{s}\right]e^{\vartheta\overline{s}} + \rho_D\overline{s}^2 + \rho_P\overline{s} + \rho_I = 0. \tag{4.43}$$

Setting $\rho_D = \rho_I = 0$ in (4.33) and the result is next cancelled by $\overline{s}$ after multiplying this result by $e^{-\vartheta\overline{s}}$ and substituting $\overline{s} = j\nu$ one has

$$e^{-j\vartheta\nu}\rho_{P,K} = -\left[(j\nu)^3 + \mu(j\nu)^2 + \lambda^{-1}\mu j\nu + 1\right]. \tag{4.44}$$

Dividing by $\rho_{P,K}$ for real and imaginary parts of (4.34) the following equalities are obtained

$$\begin{aligned} \rho_{P,K}\cos(\vartheta\nu) &= \mu\nu^2 - 1 \\ \rho_{P,K}\sin(\vartheta\nu) &= -\nu^3 + \lambda^{-1}\mu\nu. \end{aligned} \tag{4.45}$$

From their ratio it follows

$$\cot(\vartheta\nu) = \frac{1}{\nu}\cdot\frac{\mu\nu^2 - 1}{\lambda^{-1}\mu - \nu^2} \tag{4.46}$$

and the ultimate gain $\rho_{P,K}$ is cancelled. In (4.36) $\nu = \nu_K$ and ν_K is the dimensionless ultimate frequency (or ultimate frequency number). Then $\vartheta\nu = \vartheta\nu_K = \phi_K$ and ϕ_K is the ultimate angle. From physical point of view only the smallest positive solution of (4.46) with respect to ν can really mean ν_K. Of course obeying the rule for $\pi_1 = \nu = \omega\sqrt[n]{c_n}$ and $\phi_K = \vartheta\nu_K = \tau\omega_K$ the dimensionless ultimate frequency is also defined as follows

$$\nu_K = \omega_K\sqrt[3]{c_3} \tag{4.47}$$

where ω_K is the ultimate frequency in case of plant (3.114) for $n = 3$. In Fig. 9 ν_K is drawn versus λ, ϑ for fixed value of μ. The map in Fig. 9 is computed applying MATLAB solution to the ultimate frequency number evaluation from Chapter 4.5.

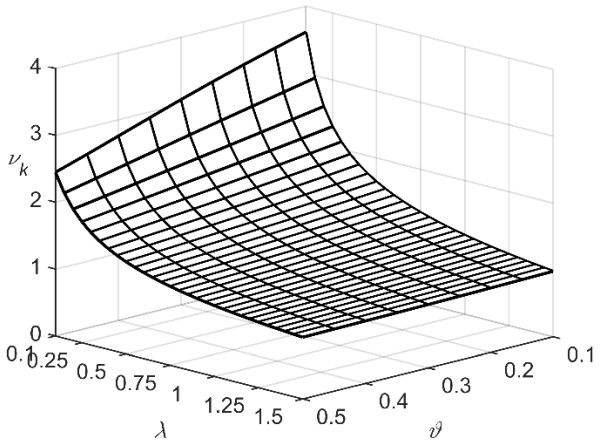

Fig. 11. 3D plot of ν_K dependence on similarity numbers λ, ϑ with fixed $\mu = 1.5$

In fact λ, ϑ cannot be arbitrary and the admissible combinations are in Fig. 11 where ν_K is limited to interval $\langle 1,4)$. Whether the third-order dynamically similar plants (3.155) are oscillatory or not it depends on the combination of λ and μ values, see *Case 3* in Chapter 3.3. The admissible ranges of μ and λ are found with respect to ϑ by the following admissibility analysis.

3PP admissibility analysis. Analogously to stability conditions (3.126) the fourth-order control loop with characteristic equation (4.43) is to be investigated on the admissibility of the similarity numbers μ and λ. Assume $\rho_P > 0, \rho_D > 0, \rho_I > 0$ and the following conditions

$$\mu\left[\rho_D + \lambda^{-1}\mu\right] > 1 + \rho_P \tag{4.48}$$

$$\mu\left[(1+\rho_P)\left(\rho_D + \lambda^{-1}\mu\right) - \rho_I\mu\right] > (1+\rho_P)^2 \tag{4.49}$$

are to be satisfied. Numbers μ and λ which satisfy these conditions are the admissible similarity numbers. The admissible *retardedness* number ϑ is shown in Fig. 11. This number is reflected in conditions (4.48) and (4.49) by high enough ρ_D setting in (4.48) and (4.49). The greater ρ_D the greater can be the number ϑ which is limited to 0.5, as shown in Fig. 11. In case $\vartheta > 0.3$ the fourth-order control loop is considerably delayed for the PID controller tuning if the third-order dynamics of plant (3.155), see Chapter 3.2 (*Case 3*), is poorly damped or too lagged. The Counterexamples 9 and 10 demonstrate this plant property impact on the PID tuning by means of the inadmissible dominant three-pole placement. As regards λ its admissible values are in the neighbourhood of $\lambda = 1$ as shown in Fig. 11. This fact results from the analysis of third-order plant dynamics in Chapter 3.3 (*Case 3*). For μ admissibility analysis with respect to λ the relation (4.48) is expressed as follows

$$\mu\rho_D + \lambda^{-1}\mu^2 - 1 > \rho_P \tag{4.50}$$

where with respect to the worst case considered, i.e. $\rho_D \to 0$, it results

$$0.5\rho_{P,K} < \rho_P . \tag{4.51}$$

In (4.51) the gain ρ_P is free of any upper bound because for $\lambda \to 0$ the upper bound is at infinity as apparent from (4.50). If

$$\lambda^{-1}\mu^2 = \sigma > 1 \tag{4.52}$$

and this product does not result high enough the numbers μ and λ cannot be considered as admissible ones. Thus the admissibility conditions (4.48) and (4.49) can be scarcely satisfied for tuned gains ρ_P, ρ_D, ρ_I in the way the left hand side of both (4.48) and (4.49) are greater than the corresponding right hand sides to an extent as shown below. The numbers μ, λ result in the admissible ones in case of the plant with non-stiff dynamics characterized by the triple real pole (3.250), specified by $\mu = 3$ and $\lambda = 1$. Then the product in (4.52) results in

$$\lambda^{-1}\mu^2 = \sigma = 9 > 1 \tag{4.53}$$

that exceeds the condition for the admissibility of both μ and λ nine times. The inequality (4.52) is the plant stability condition (3.255) in Chapter 3 (*Case 3*) where the number σ is greater than one, see (3.151). If the product in (4.52) is close to one then the gain ρ_P results in negligible value because of small $\rho_{P,K}$. For lower and upper bounds $\lambda = 0.25$ and $\lambda = 1.5$, respectively, in Fig. 11 the inequalities for μ result from the admissibility condition (4.52) as follows

$$\mu > \frac{1}{2} \tag{4.54}$$

and

$$\mu > \frac{\sqrt{3}}{\sqrt{2}} \tag{4.55}$$

respectively. Again considering the best non-stiff dynamics of the plant, i.e. the plant with triple real pole (3.250) characterized by $\mu = 3$ and $\lambda = 1$, the specific range is derived from the admissibility condition (4.52) and (4.54) as follows

$$\mu \in \left\langle \frac{1}{2}, 3 \right\rangle. \tag{4.56}$$

The inequality (4.55) confirms (4.56) and for $\lambda > 1$ the number μ is greater than one. Again utilizing $\rho_D \to 0$ and with respect to (4.51), (4.56) from the condition (4.49) the following inequalities originate

$$\left(1+\rho_P\right)\lambda^{-1} - \rho_I > \lambda^{-1} - \rho_I > 0. \tag{4.57}$$

From inequality (4.57) the lower and upper bound for setting ρ_I are specified. Substituting the lower and upper bounds of λ into

$$\rho_I < \lambda^{-1} \tag{4.58}$$

the admissible ρ_I setting is constrained to

$$\frac{2}{3} < \rho_I < 4. \tag{4.59}$$

Analogously to the lower bound only in (4.51) also in (4.59) the lower bound only is considered as follows

$$\frac{2}{3} < \rho_I \tag{4.60}$$

because for $\lambda \to 0$ the upper bound is at infinity. Analogously to ρ_P if the product in (4.52) is close to one then the gain ρ_I results in negligible value. The admissible range of ρ_I is stricter than the admissible range of ρ_P. The derivative loop gain ρ_D is in the role of free parameter by which setting the faster control loop response is achieved. With growing delay effect by means of ϑ the settings for ρ_P and ρ_I approach the lower bounds of (4.51) and (4.60), respectively. For $\vartheta > 0.3$ all three loop gains ρ_P, ρ_D, ρ_I can result in negligible values, i.e. zeros in fact, depending on other two numbers μ, λ. In this case the dominant three-pole placement method is behind its applicability to the PID controller tuning for poorly damped or too lagged third-order plants. The Counterexample 9 demonstrates this case at the end of Chapter 4.3. With respect to (4.52) the specific ranges of μ, λ

$$\mu \in \langle 0.5, 3 \rangle, \ \lambda \in \langle 0.25, 1.5 \rangle \tag{4.61}$$

can be next analysed. Combinations $\mu < 1$ and $\lambda > 1$ cannot meet the condition (4.52) because it results less than 1. In case of combinations $\mu < 1$ and $\lambda < 1$, the product in (4.52) results less than 4 within the ranges (4.61). But this is less than half of the product in (4.53). Only the case of $\mu > 1$ and $\lambda < 1$ gives the products of high values that are greater than the products originating from the combinations $\mu > 1$ and $\lambda > 1$. The ranges (4.61) then result in true admissible ranges as follows

$$\mu \in \langle 1, 3 \rangle, \ \lambda \in \langle 0.25, 1 \rangle \tag{4.62}$$

at which the product in (4.52) resulting in high value as in (4.53) corresponds to the admissible numbers μ and λ. As a rule, in case $\rho_P < 0.5\rho_{P,K}$ or $\rho_I < 2/3$, eventually $\sigma \le 1$ the trio of poles (4.1) cannot become dominant or even some of other loop poles lie in the right-hand part (RHP), i.e. the delayed control loop is unstable. In other words the delayed control loop is close to the stability margin or even unstable. Beside the reasonable constraints on ϑ depicted in Fig. 11 the constraints on μ and λ are due to (4.62). The numbers λ, μ are admissible if the condition (4.52) is satisfied. Notice these numbers in their admissible ranges characterize the third-order plant dynamics that is not *stiff* in order to prevent from the model order reduction. The result of the loop gains tuning by means of the dominant three-pole placement has to be checked on the control loop stability even if all the similarity numbers fall within admissible ranges and the trio of poles (4.1) is properly selected. In fact the conditions (4.48) and (4.49) are the admissibility conditions for the dominant three-pole placement. To find the proper trio of poles (4.1) applying the inequality (4.51) a region of proper trio of poles (4.1) is found out by gain ρ_P mapping versus prescribed ν, δ and κ in the dominant three-pole placement. In forthcoming examples this mapping is shown.

PID admissibility analysis. Assume the third-order plant is stable thus the condition (4.52) is satisfied. From the characteristic equation (4.43) the term of $\overline{s}^3$ is not modifiable at all and this corresponds to the similarity number μ. Simultaneously the number μ together with the

number λ has to satisfy the condition (4.52). From the analysis leading to the admissible ranges (4.62) the PID admissibility is lost when

$$\mu<1,\ \lambda>1. \tag{4.63}$$

But the combinations (4.63) correspond to the unstable third-order plants. Since the PID control design is limited to the stable plants only the potential loss of the PID admissibility can occur when

$$\mu<1,\ \lambda<1. \tag{4.64}$$

From the original specific ranges in (4.61) the maximum of the product in (4.52) results with respect to combination (4.64) in 4. But the true loss of the PID admissibility is expectable when the product in (4.52) is close to one. This is obtained by the combination of lower bounds in (4.61) satisfying the inequalities (4.64) as follows

$$\mu\le 0.5,\ \lambda\le 0.25. \tag{4.65}$$

The inequalities in (4.65) are rewritten into the following ranges

$$\mu\in\langle 0.3,0.5\rangle,\ \lambda\in\langle 0.09,0.25\rangle \tag{4.66}$$

from which only such combinations of μ and λ are selected that satisfy the condition (4.52) and do not appear in the original ranges (4.61). Appearing μ and λ in the ranges (4.66) an inadmissible application of the PID controller becomes particularly with respect to the retardedness number ϑ. The case of $\mu\to 0$ is avoided due to the plant stability loss and the case of $\lambda\to 0$ is also avoided due to the limited value of the product in (4.52). Be aware that beyond the admissible ranges (4.62) satisfying the condition (4.52) some of the loop gains ρ_P,ρ_D,ρ_I can result negative. Nevertheless the delayed control loop is stabilized but the PID control is not already admissible. As a contradiction to ranges (4.66) the ranges of the PID admissibility are defined by (4.61). In fact the 3PP admissibility is a subset of the PID admissibility.

Integrating plant. In case of integrating plants (3.162) the ultimate frequency is determined from the characteristic equation (3.222) in Chapter 3 (*Case 3*)

$$M\left(\overline{s}\right)=\left[\overline{s}^4+\mu\overline{s}^3+\lambda_I\mu\overline{s}^2\right]e^{\vartheta\overline{s}}+\rho_D\overline{s}^2+\rho_P\overline{s}+\rho_I=0. \tag{4.67}$$

Suppose again, that $\rho_D=\rho_I=0$ and then multiply (4.67) by $e^{-\vartheta\overline{s}}$ and cancel the result by $\overline{s}$. Utilizing $\overline{s}=j\nu$ (4.63) is rewritten as follows

$$e^{-j\vartheta\nu_K}\rho_{P,K}=-\left[\left(j\nu_K\right)^3+\mu\left(j\nu_K\right)^2+\lambda_I\mu j\nu_K\right]. \tag{4.68}$$

Separating (4.68) into real and imaginary parts and subsequently dividing them by each other the ultimate gain, $\rho_{P,K}$, is cancelled as follows

$$\cot\left(\vartheta\nu_K\right)=\frac{\mu\nu_K}{\lambda_I\mu-\nu_K^2}\,. \tag{4.69}$$

Only the smallest positive solution of (4.69) is ν_K in fact again. This solution is obtained with MATLAB in Chapter 4.5. Analogously the ultimate frequency number can be determined by (4.47). Notice λ^{-1} is replaced with λ_I in both conditions (4.48) and (4.49) for the integrating plants (3.162) and additionally in case of the condition (4.49) the unit, 1, disappears.

Remark 4. The ultimate frequency numbers for the case of $n=2$, given by solution of (4.3) and (4.4), result in simpler relations than both (4.46) and (4.69). With rising order *n* the complexity of control loop design is increasing but the approaches to this design are kept the same, particularly the dominant three-pole placement.

Admissible dominant pole placement. The goal of this section is to achieve the dominant three-pole placement in the fourth-order PID control loop with delay where loop gains ρ_P,ρ_D,ρ_I result in admissible values. First the trio of poles to be assigned for determining the proportional, integration and derivative loop gains requires its proper selection. After finding a region of admissible ρ_P setting by means of ρ_P mapping versus prescribed ν, δ and κ the admissible settings of ν, δ and κ are obtained. In case the trio of poles is selected within the admissible ranges of ν, δ and κ then assigning $\nu=\nu_K$ the three-pole dominance in infinite spectrum of the control loop poles is obtained as a rule. This dominance is proved by argument increment (4.31) evaluation for $n=3$ or alternatively the quasi-polynomial root finder from [97] is applied. The argument increment is evaluated with MATLAB in Chapter 4.5. Strictly speaking the dominance of (4.1) needs not be achieved by assigning the natural frequency number greater than the ultimate frequency number. But the fourth pole, $\overline{p}_4$, resulting close to $\overline{p}_{1,2,3}$ does not make the transient dynamics more sluggish. The fourth pole is still spontaneously placed more to the left from the trio (4.1). In case the pole dominance index results at least 2, [123], the fourth pole is far away in the left from the trio of placed poles $\overline{p}_{1,2,3}$ and this trio is dominant. To assign (4.1) the three poles have to be the roots of (4.43) and in case of integrating plants the trio of poles (4.1) have to be roots of (4.67). Hence substituting each pole from (4.1) into (4.43) and starting with $\overline{s}=\overline{p}_1=\left(-\delta+j\right)\nu$ one gets

$$\begin{aligned}&M\left(\overline{s}\right)=\\&\left[\begin{matrix}\nu^4\left(\delta^4-6\delta^2+1+4\delta\left(1-\delta^2\right)j\right)+\mu\nu^3\left(3\delta-\delta^3+\left(3\delta^2-1\right)j\right)+\lambda^{-1}\mu\nu^2\left(\delta^2-1-2\delta j\right)+\\ \nu\left(-\delta+j\right)\end{matrix}\right]e^{\vartheta\nu\left(-\delta+j\right)}\\&+\rho_D\nu^2\left(\delta^2-1-2\delta j\right)+\rho_P\nu\left(-\delta+j\right)+\rho_I=0.\end{aligned} \tag{4.70}$$

After substituting $\overline{p}_3=-\kappa\delta\nu$ for $\overline{s}$ in (4.43) the following equation is obtained

$$M\left(\overline{s}\right)=\left[\left(\kappa\delta\nu\right)^4-\mu\left(\kappa\delta\nu\right)^3+\lambda^{-1}\mu\kappa^2\delta^2\nu^2-\kappa\delta\nu\right]e^{-\kappa\delta\nu\vartheta}+\rho_D\kappa^2\delta^2\nu^2-\rho_P\kappa\delta\nu+\rho_I=0\,. \tag{4.71}$$

After rearranging both real and imaginary parts of (4.70) and (4.71) in such a way to be expressions free of searched ρ_P,ρ_D,ρ_I on the right-hand side of the following equations

$$\rho_D \nu^2\left(\delta^2-1-2\delta j\right)+\rho_P \nu\left(-\delta+j\right)+\rho_I=-e^{-\delta\vartheta\nu}\left[\cos\left(\vartheta\nu\right)+j\sin\left(\vartheta\nu\right)\right]\times$$
$$\left[\begin{array}{l}\nu^4\left(\delta^4-6\delta^2+1+4\delta\left(1-\delta^2\right)j\right)+\mu\nu^3\left(3\delta-\delta^3+\left(3\delta^2-1\right)j\right)+\\ \lambda^{-1}\mu\nu^2\left(\delta^2-1-2\delta j\right)+\nu\left(-\delta+j\right)\end{array}\right] \tag{4.72}$$
$$\rho_D\kappa^2\delta^2\nu^2-\rho_P\kappa\delta\nu+\rho_I=-e^{-\kappa\delta\nu\vartheta}\left[\left(\kappa\delta\nu\right)^4-\mu\left(\kappa\delta\nu\right)^3+\lambda^{-1}\mu\kappa^2\delta^2\nu^2-\kappa\delta\nu\right] \tag{4.73}$$

these equations can be rewritten in matrix form (4.15). The solution to (4.15) is the same with (4.19) through (4.21) for the gains ρ_P, ρ_D and ρ_I, respectively. Only the elements of **B** are then given as follows

$$B_R\nu=e^{-\delta\vartheta\nu}\left[b_R\cos\left(\vartheta\nu\right)-b_I\sin\left(\vartheta\nu\right)\right], \tag{4.74}$$
$$B_I\nu=e^{-\delta\vartheta\nu}\left[b_I\cos\left(\vartheta\nu\right)+b_R\sin\left(\vartheta\nu\right)\right], \tag{4.75}$$
$$B_3\nu=e^{-\kappa\delta\nu\vartheta}\kappa\delta\nu\left[-\left(\kappa\delta\nu\right)^3+\mu\left(\kappa\delta\nu\right)^2-\lambda^{-1}\mu\kappa\delta\nu+1\right], \tag{4.76}$$

where

$$b_R=\nu\left[\nu^3\left(-\delta^4+6\delta^2-1\right)+\mu\nu^2\left(\delta^3-3\delta\right)+\lambda^{-1}\mu\nu\left(1-\delta^2\right)+\delta\right], \tag{4.77}$$
$$b_I=\nu\left[\nu^3 4\delta\left(\delta^2-1\right)+\mu\nu^2\left(1-3\delta^2\right)+\lambda^{-1}\mu 2\delta\nu-1\right]. \tag{4.78}$$

In the same way as in (4.12) the factorized ν is cancelled applying the Cramer's rule (4.16) and relation (4.74) through (4.76) are changed to B_R, B_I and B_3, respectively. Thus the right-hand side of (4.76) through (4.78) is without the factorized ν as follows

$$B_3=e^{-\kappa\delta\nu\vartheta}\kappa\delta\left[-\left(\kappa\delta\nu\right)^3+\mu\left(\kappa\delta\nu\right)^2-\lambda^{-1}\mu\kappa\delta\nu+1\right], \tag{4.79}$$
$$b_R=\nu^3\left(-\delta^4+6\delta^2-1\right)+\mu\nu^2\left(\delta^3-3\delta\right)+\lambda^{-1}\mu\nu\left(1-\delta^2\right)+\delta, \tag{4.80}$$
$$b_I=\nu^3 4\delta\left(\delta^2-1\right)+\mu\nu^2\left(1-3\delta^2\right)+\lambda^{-1}\mu 2\delta\nu-1. \tag{4.81}$$

In case of integrating plants (3.162) from Chapter 3 (*Case 3*) relation (4.79) through (4.81) are changed as follows

$$B_3=e^{-\kappa\delta\nu\vartheta}\nu\left(\kappa\delta\right)^2\left[-\left(\kappa\delta\nu\right)^2+\mu\kappa\delta\nu-\lambda_I\mu\right], \tag{4.82}$$
$$b_R=\nu\left[\nu^2\left(-\delta^4+6\delta^2-1\right)+\mu\nu\left(\delta^3-3\delta\right)+\lambda_I\mu\left(1-\delta^2\right)\right], \tag{4.83}$$
$$b_I=\nu\left[\nu^2 4\delta\left(\delta^2-1\right)+\mu\nu\left(1-3\delta^2\right)+\lambda_I\mu 2\delta\right] \tag{4.84}$$

because in (4.79) and (4.81) +1 and -1, respectively, disappear and in (4.80) the stand-alone δ disappears, too. In addition $\lambda_I\mu$ takes over the role of $\lambda^{-1}\mu$.

Example 7. Consider the following third-order plant of type (3.114)

$$2\frac{d^3y(t)}{dt^3}+3.8\frac{d^2y(t)}{dt^2}+3.4\frac{dy(t)}{dt}+y(t)=u(t-0.25)\,. \tag{4.85}$$

with $\omega_n=1\,s^{-1}$, $\xi=0.7$ and $b=0.5\,s^{-1}$, see (3.260) in Chapter 3.3. Utilizing the numbers (3.144) through (3.147) and (3.149) for the *Case 3* in Chapter 3 the following similarity numbers result

$$\mu=2.3938\,,\ \lambda=0.887\,,\ \vartheta=0.1984\,,\ \sigma=6.46 \tag{4.86}$$

where the scaling factor $\sqrt[3]{2}$ is applied. Since the numbers (4.86) describe non-stiff dynamics and the condition (4.52) is satisfied with respect to (4.53) as $\sigma=6.46>1$ the similarity numbers are admissible. Based on these numbers overdamped oscillatory plants (3.155) are obtained as follows

$$\frac{d^3y(\bar{t})}{d\bar{t}^3}+2.3938\frac{d^2y(\bar{t})}{d\bar{t}^2}+2.6986\frac{dy(\bar{t})}{d\bar{t}}+y(\bar{t})=u(\bar{t}-0.1984) \tag{4.87}$$

where $K=1$. Before the dominant three-pole placement can be carried out the proper selection of the trio of poles (4.1) has to be made for the dimensionless PID control loop with overdamped oscillatory plants (4.87) characterized by the similarity numbers (4.86). This selection is based on mapping ρ_P versus ν and δ under constant κ, $\kappa=1$, in Fig. 12. The resulting map is compared with zero and $\rho_{P,K}$ level of ρ_P according to (4.51). This map shows that assignable ν is within $\nu\in(1,2.5)$ to get $\rho_P>0.5\rho_{P,K}$ where $\rho_{P,K}=3.8161$. The frequency number ν_K results in 1.3968 from (4.46) applying the MATLAB solution in Chapter 4.5. Since the map is nearly the same for $0.8<\kappa<1.3$ the only parameter for optimization remains δ, which should result less than 0.35 with respect to the experience from [123], [126]. From Fig. 12 one can find out that $\delta<0.3$ because ρ_P higher than 1.9 is desired. For the dimensionless control loop with oscillatory plants (4.87) the loop gains ρ_P,ρ_D,ρ_I are computed by the formula (4.19) through (4.21) when the following trio of poles is assigned

$$\bar{p}_{1,2}=-0.405\pm j2.025\,,\ \bar{p}_3=-0.405\,. \tag{4.88}$$

Then $\nu=2.025$, $\delta=0.2$ and $\kappa=1$. These values appear in the region of their assignability, see Fig. 12. Natural frequency number ν is identified with $1.45\cdot\nu_K$. The ultimate frequency number can be equivalently obtained from ultimate frequency of dynamically similar plant (4.85) using (4.47) as follows

$$\nu_K=\omega_K\sqrt[3]{c_3}=1.1086\cdot\sqrt[3]{2}=1.3968 \tag{4.89}$$

The ultimate angle, $\phi_K=\nu_K\vartheta$, results as follows

$$\phi_K=\omega_K\tau=1.1086\cdot0.25=1.3968\cdot0.1984=0.277\,. \tag{4.90}$$

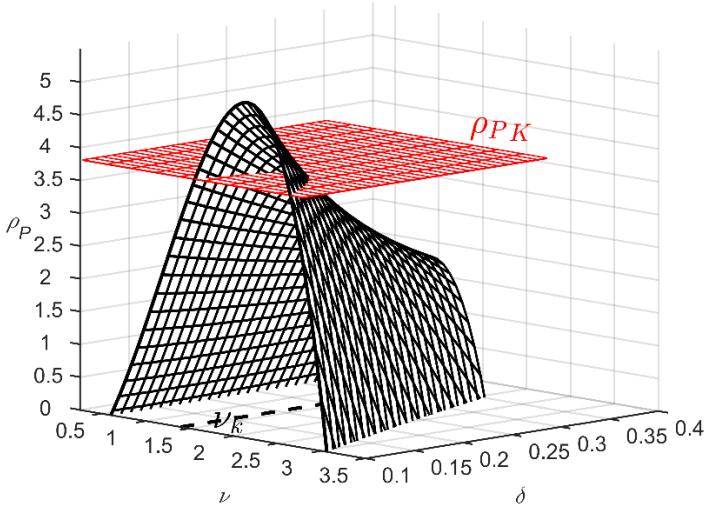

Fig. 12. Map of ρ_P for proper selection of the trio of poles (4.1) in case of plants (4.87)

From Fig. 12 the proportional gain falls within the interval (4.51) with lower bound given by $\rho_P > 1.9$. Correspondingly $\rho_D > 1.9$ to compensate the retardedness number $\vartheta = 0.1984$. The loop gains result from (4.19) through (4.21) where (4.79) through (4.81) are used. Thus

$$\rho_P = 3.3,\ \rho_D = 3.442,\ \rho_I = 0.859. \tag{4.91}$$

As suggested the gain ρ_P results in greater value than the half of $\rho_{P,K}$, i.e. 1.9. To check the dominance of (4.88) the argument increment (4.31) is evaluated with MATLAB (see Chapter 4.5). The resulting Poincaré-like mapping (4.35) is shown in Fig. 13 and its zooming at $\nu = 0$ in Fig. 14. How the three poles as the rightmost poles in the complex plane are separated from the rest of the infinite spectrum presents Fig. 15 and in Fig. 16 the detail of

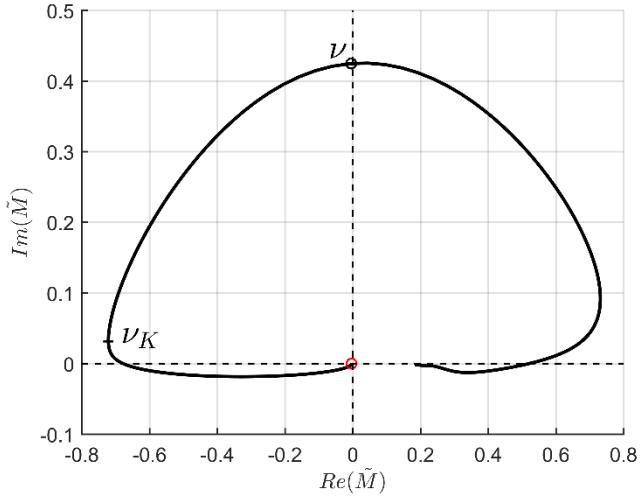

Fig. 13. Argument increment test on trio of poles dominance resulting from (4.31) in $-\pi$

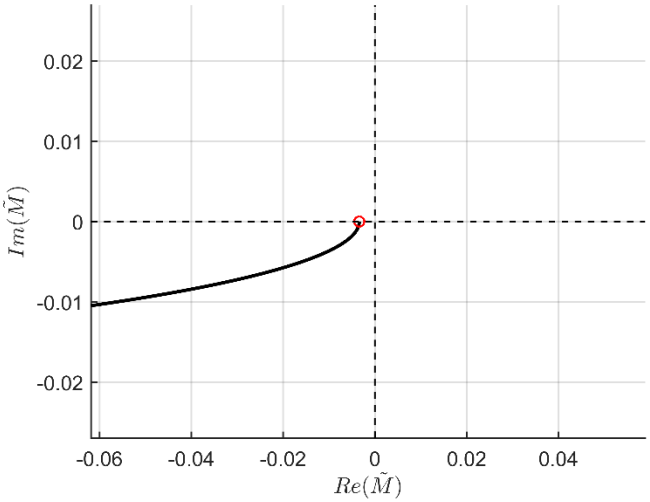

Fig. 14. Detail of Fig. 13 at $\nu = 0$

Fig. 15 shows the four rightmost poles for determining the dominance index by (4.36). According to (4.31) with (4.32) given as $\beta_m = 1.1 \times 0.405 = 0.4455$ the argument increment results $-\pi$ as verified in Figs. 13 and 14. As shown in Fig. 15 the poles $\bar{p}_{1,2,3,4}$ are separated enough from the rest of the infinite spectrum and the dominance index is determined as $\eta = 1.162 > 1$. Since this index does not result at least 2, [123], the trio of placed poles $\bar{p}_{1,2,3}$ cannot be considered as the dominant poles. Strictly speaking the dominance of (4.88) is lost but the fourth pole, $\bar{p}_4 = 0.465$, is near to $\bar{p}_{1,2,3}$ and does not change significantly the transient dynamics. In addition the spectral abscissa results in 0.4, i.e. four times greater than that in [100]. The rightmost spectrum is computed by the quasi-polynomial root finder from [97]. The disturbance rejection with setting (4.91) is recorded in Fig.17. For comparison purposes the disturbance rejection with the PID controller tuned by the Z-N method is added to Fig. 17. This tuning is given for $\nu_K = 1.3968$ and $\rho_{P,K} = 3.8161$ as follows

$$\rho_P = 2.289,\ \rho_D = 1.287,\ \rho_I = 1.018. \tag{4.92}$$

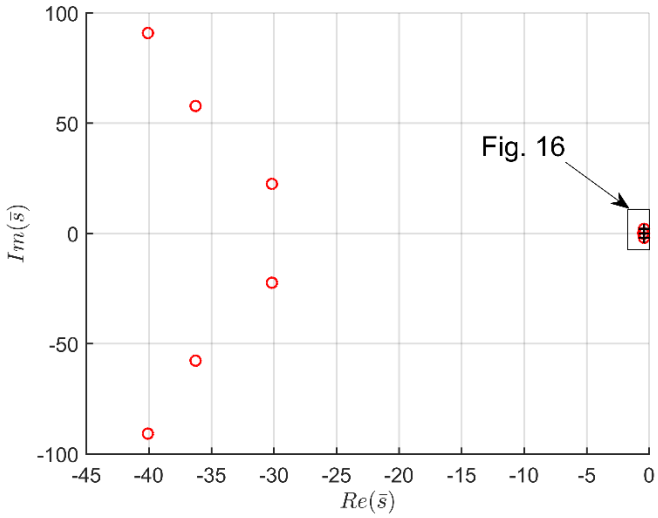

Fig. 15. Rightmost poles of the fourth-order PID control loop with delay

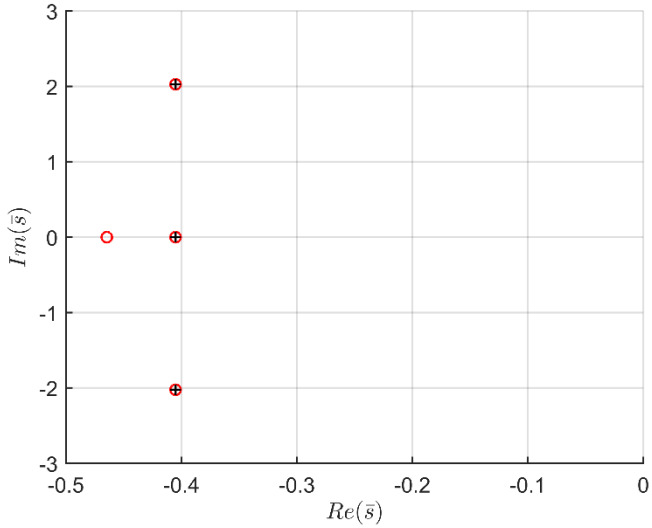

Fig. 16. Four rightmost poles composed of assigned trio $\bar{p}_{1,2,3}$ and the fourth $\bar{p}_4 = -0.465$

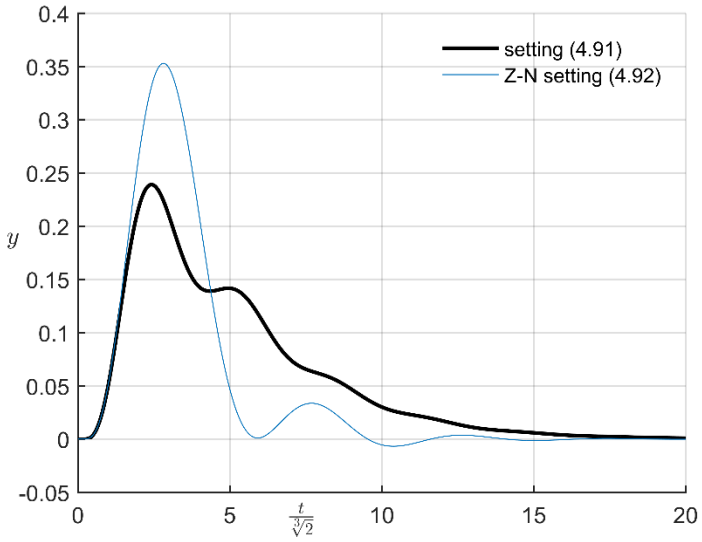

Fig. 17. Disturbance rejection in case of overdamped oscillatory plants (4.87)

Comparing the setting (4.91) with the setting (4.92) in the IAE the Z-N method gives moderately lower value applying (4.40) as follows

$$Q_{AE} = 1.005 \tag{4.93}$$

than the dominant three-pole placement method that results with the IAE as follows

$$Q_{AE} = 1.164\,. \tag{4.94}$$

On the other hand the dominant three-pole placement method results with 32% lower overshoot than the Z-N method as apparent from Fig. 17. In case of the dominant three-pole placement method the PID controller setting results from (4.87) with respect to similarity numbers π_3, π_4 introduced in Chapter 3 as follows

$$r_P = 3.3,\ r_D = \sqrt[3]{2}\cdot\rho_D = 4.336\ [s],\ r_I = \frac{\rho_I}{\sqrt[3]{2}} = 0.682\ \left[s^{-1}\right] \tag{4.95}$$

while in case of the Z-N method the PID controller setting is obtained

$$r_P = 2.289,\ r_D = \sqrt[3]{2}\cdot\rho_D = 1.621\ [s],\ r_I = \frac{\rho_I}{\sqrt[3]{2}} = 0.808\ \left[s^{-1}\right]. \tag{4.96}$$

The IAE values corresponding to the settings (4.95) and (4.96) are obtained due to (4.38) as follows

$$I_{AE} = \sqrt[3]{2}\cdot Q_{AE} = 1.266\,[s]. \tag{4.97}$$

and

$$I_{AE} = \sqrt[3]{2}\cdot Q_{AE} = 1.466\,[s] \tag{4.98}$$

respectively.

Example 8 (*Integrating plant*). Consider the following third-order integrating plant of type (3.117)

$$2\frac{d^3y(t)}{dt^3} + 3.8\frac{d^2y(t)}{dt^2} + 3.4\frac{dy(t)}{dt} = u(t-0.25). \tag{4.99}$$

with $\omega_n = 1.303\,s^{-1}$ and $\xi = 0.728$, see (3.273) in Chapter 3.3. Utilizing the numbers (3.146), (3.147), (3.157) and (3.158) for the *Case 3* in Chapter 3 the following similarity numbers result

$$\mu = 2.3938,\ \lambda_I = \theta_I = 1.1273,\ \vartheta = 0.1984 \tag{4.100}$$

where the scaling factor $\sqrt[3]{2}$ is applied. Since the condition (4.52) is satisfied with respect to (4.53) as $\lambda_I\mu^2 = 6.46 > 1$ the similarity numbers are admissible. Be aware that λ_I corresponds to λ^{-1} in (4.52), see (3.157) for *Case 3* in Chapter 3. Based on these numbers the integrating plants (3.162) with overdamped impulse response ($\xi = 0.728$) are obtained as follows

$$\frac{d^3y(\bar{t})}{d\bar{t}^3} + 2.3938\frac{d^2y(\bar{t})}{d\bar{t}^2} + 2.6986\frac{dy(\bar{t})}{d\bar{t}} = u(\bar{t} - 0.1984) \tag{4.101}$$

where $K = 1$. For the dimensionless PID control loop with integrating plants (4.101) the following trio of poles is assigned

$$\bar{p}_{1,2} = -0.421 \pm j1.684,\ \bar{p}_3 = -0.505 \tag{4.102}$$

and then $\nu = 1.684$, $\delta = 0.25$ and $\kappa = 1.2$. Natural frequency number ν is identified with $1.25 \cdot \nu_K$ where ν_K is evaluated from (4.69). This evaluation is obtained with MATLAB in Chapter 4.5. The ultimate frequency number can be equivalently obtained from the ultimate frequency of dynamically similar plant (4.99) using (4.47) as follows

$$\nu_K = \omega_K \sqrt[3]{c_3} = 1.069 \cdot \sqrt[3]{2} = 1.347 . \tag{4.103}$$

The ultimate angle, $\phi_K = \nu_K \vartheta$, results as follows

$$\phi_K = \omega_K \tau = 1.069 \cdot 0.25 = 0.267 . \tag{4.104}$$

The loop gains ρ_P, ρ_D, ρ_I are computed by the formula (4.19) through (4.21) where (4.82) through (4.84) are utilized. Then the loop gains result as follows

$$\rho_P = 3.791, \ \rho_D = 2.4214, \ \rho_I = 0.894 . \tag{4.105}$$

As suggested the gain ρ_P results in greater value than the half of $\rho_{P,K}$, i.e. 2.25. Again the trio of placed poles $\bar{p}_{1,2,3}$ cannot be considered as the dominant poles because the fourth pole, $\bar{p}_4 = -0.56$, is near to $\bar{p}_{1,2,3}$ as apparent from Fig. 19. Nevertheless the fourth pole does not change significantly the transient dynamics. From Fig. 18 it is apparent the considerable separation of $\bar{p}_{1,2,3,4}$ from the rest of the infinite spectrum. Additionally, the spectral abscissa results greater than 0.4, i.e. it is at least four times greater than that in [100]. The rightmost spectrum is computed by the quasi-polynomial root finder from [97]. In Fig. 20 the disturbance rejection with setting (4.105) is recorded together with the disturbance rejection obtained by the Z-N setting as follows

$$\rho_P = 2.703, \ \rho_D = 1.576, \ \rho_I = 1.159 . \tag{4.106}$$

This setting is due to $\nu_K = 1.347$ and $\rho_{P,K} = 4.505$. For the plants (4.101) the dominant three-pole placement method gives moderately lower value of the IAE applying (4.40) as follows

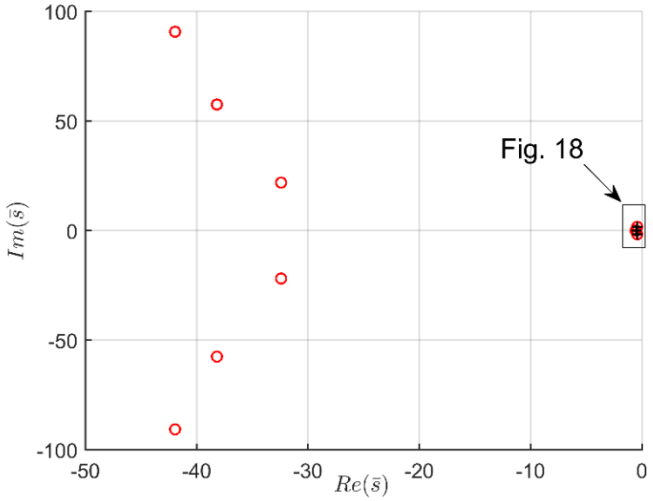

Fig. 18. Rightmost poles of the fourth-order PID control loop with delay

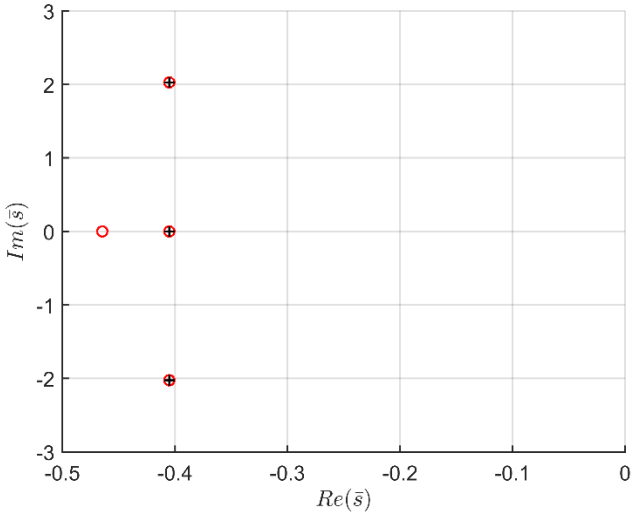

Fig. 19. Four rightmost poles composed of assigned trio $\bar{p}_{1,2,3}$ and the fourth $\bar{p}_4 = -0.56$

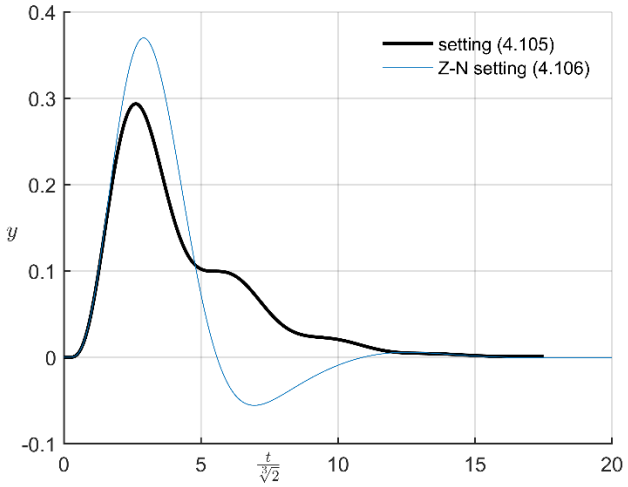

Fig. 20. Disturbance rejection in case of integrating plants (4.101) with overdamped impulse response

$$Q_{AE} = 1.1181 \tag{4.107}$$

than the Z-N method that results with the IAE as follows

$$Q_{AE} = 1.1873. \tag{4.108}$$

In addition the dominant three-pole placement method results with 25% lower overshoot than the Z-N method as apparent from Fig. 20. In case of the dominant three-pole placement method the PID controller setting results from (4.105) with respect to similarity numbers π_3, π_4 introduced in Chapter 3 as follows

$$r_P = 3.791,\ r_D = \sqrt[3]{2} \cdot \rho_D = 3.05\ [s],\ r_I = \frac{\rho_I}{\sqrt[3]{2}} = 0.709\ [s^{-1}] \tag{4.109}$$

while in case of the Z-N method the PID controller setting is obtained

$$r_P = 2.703,\ r_D = \sqrt[3]{2}\cdot\rho_D = 1.985\ [s],\ r_I = \frac{\rho_I}{\sqrt[3]{2}} = 0.92\ \left[s^{-1}\right]. \tag{4.110}$$

The IAE values corresponding to the settings (4.109) and (4.110) are obtained due to (4.38) as follows

$$I_{AE} = \sqrt[3]{2}\cdot Q_{AE} = 1.266[s] \tag{4.111}$$

and

$$I_{AE} = \sqrt[3]{2}\cdot Q_{AE} = 1.466[s] \tag{4.112}$$

respectively.

Counterexample 9. Before the dominant three-pole placement method can be applied the proper selection of the trio of poles (4.1) has to be made for the dimensionless control loop with oscillatory plants (3.279) characterized by the similarity numbers $\mu = \sqrt[3]{2}$, $\lambda = 0.635$, $\vartheta = 0.397$ and $\sigma = 2.5$, for more details see Example 1 in Chapter 3.3. The plants (3.279) are poorly damped with $\xi = 0.25$ and the retardedness number, ϑ, is greater than 0.3. Applying the condition (4.52) together with (4.53) $\lambda^{-1}\mu^2 = \sigma = 2.5 > 1$ but it does not satisfy the assumption that the product in (4.52) is high enough as in (4.53). Thus these similarity numbers are not admissible and the oscillatory plants (3.279) are inadmissible plants. The trio (4.1) selection is based on mapping ρ_P versus ν and δ under constant κ, $\kappa = 1$, in Fig. 21. The resulting map is compared with zero and $\rho_{P,K}$ level of ρ_P according to (4.51). This map shows that assignable ν is very close to $\nu_K = 1.25$ to get $\rho_P > 0.5\rho_{P,K}$ where $\rho_{P,K} = 1.1035$. The frequency number ν_K results in 1.25 from (4.46) applying the MATLAB solution in Chapter 4.5 and it is in the middle of ν interval. Since the map is nearly the same for $0.8 < \kappa < 1.3$ the only parameter for optimization remains δ, which should result less than 0.35 with respect to the experience from [123], [126]. From Fig. 21 one can find out that $\delta < 0.3$. For the dimensionless control loop with oscillatory plants (3.279) the loop gains are computed by the formula (4.19) through (4.21) when the following trio of poles is assigned

$$\overline{p}_{1,2} = -0.291 \pm j1.165,\ \overline{p}_3 = -0.291. \tag{4.113}$$

Then $\nu = 1.165$, $\delta = 0.25$ and $\kappa = 1$. These values appear in the region of their assignability, see Fig. 21. Natural frequency number ν is identified with $0.93\cdot\nu_K$ where $\nu_K = 1.25$. The ultimate frequency number is obtained from the solution to (4.46) with MATLAB in Chapter 4.5. The loop gains result from (4.19) through (4.21) as follows

$$\rho_P = 0.1185,\ \rho_D = 3.64\times10^{-3},\ \rho_I = 0.165. \tag{4.114}$$

Again strictly speaking the dominance of (4.113) is lost but the fourth pole, resulting in

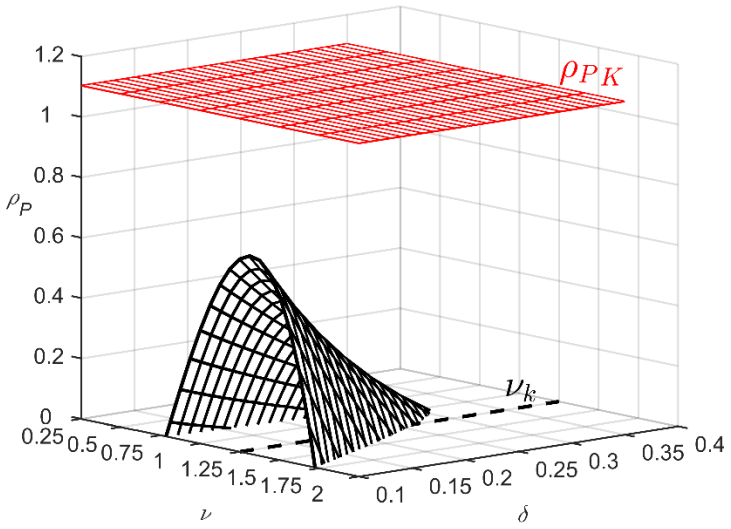

Fig. 21. Map of ρ_P for proper selection of the trio of poles (4.1) in case of plant (3.279)

$\bar{p}_4 = -0.393$, is near to $\bar{p}_{1,2,3}$ and does not alter significantly the transient dynamics. As expected in case of the inadmissible plants with $\vartheta = 0.397 > 0.3$ and $\xi = 0.25 < 0.3$ the gain ρ_P results in lower value than the half of $\rho_{P,K}$, i.e. 0.55, and the other loop gains in setting (4.114) originate in poor values, too. This setting is not acceptable in practice. The dominant three-pole placement method lacks in case of the plants (3.279). On contrary using $\nu_K = 1.25$ and $\rho_{P,K} = 1.1035$ the Z-N method still gives fair PID setting in comparison to (4.114) as follows

$$\rho_P = 0.662,\ \rho_D = 0.416,\ \rho_I = 0.263. \tag{4.115}$$

This setting overcomes the setting (4.114) and in ρ_P this gain is increased nearly six times. If the natural frequency number, ν, is prescribed equal to the ultimate frequency number, ν_K, the dominance of three poles (4.113) is not achieved at all and the fourth pole $\bar{p}_4$ results close to the imaginary axis. Additionally any attempt of increasing the relative damping over $1/4$ results in the control loop instability.

Counterexample 10 (*Integrating plant*). Consider the integrating plants (3.292), see *Case 3* in Chapter 3.3, with poorly damped impulse responses, characterized by the similarity numbers $\mu = \sqrt[3]{2}$, $\lambda_I = 1.5749$, $\vartheta = 0.397$ and $\sigma = 2.5$, for more details see Example 2 in Chapter 3.3. The plants (3.292) are with damped impulse response ($\xi = 0.447$) and the retardedness number, ϑ, is greater than 0.3. Applying the condition (4.52) for the integrating plants (3.292) $\lambda_I \mu^2 = 2.5 > 1$ but it does not satisfy the product in (4.52) to be high enough with respect to (4.53). Then these similarity numbers are not admissible and the integrating plants (3.292) are inadmissible plants. Again the number λ_I corresponds to λ^{-1} in (4.52), see (3.157) for *Case 3* in Chapter 3. For the dimensionless control loop with integrating plants (3.292) the following trio of poles is assigned

$$\bar{p}_{1,2} = -0.284 \pm j1.136,\ \bar{p}_3 = -0.284 \tag{4.116}$$

and then $\nu = 1.136$, $\delta = 0.25$ and $\kappa = 1$. Natural frequency number ν is identified with ν_K that is evaluated from (4.69). This evaluation is obtained with MATLAB in Chapter 4.5. The loop gains ρ_P, ρ_D, ρ_I are computed by the formula (4.19) through (4.21) where (4.82) through (4.84) are utilized. Then the loop gains result as follows

$$\rho_P = 1.02,\ \rho_D = 0.275,\ \rho_I = 0.144. \tag{4.117}$$

Again strictly speaking the dominance of (4.116) is not achieved but the fourth pole, resulting in $\bar{p}_4 = -0.364$, is near to $\bar{p}_{1,2,3}$ and does not alter significantly the transient dynamics. As expected in case of the inadmissible integrating plants with $\vartheta = 0.397 > 0.3$ the loop gains (4.117) originate in poor values that are not acceptable in practice. The dominant three-pole placement method lacks in case of the integrating plants (3.292). On contrary using $\nu_K = 1.136$ and $\rho_{P,K} = 1.807$ the Z-N method still gives satisfactory PID setting as follows

$$\rho_P = 1.084,\ \rho_D = 0.749,\ \rho_I = 0.392. \tag{4.118}$$

This setting overcomes the setting (4.117) and in ρ_D, ρ_I these gains are increased more than twice. In case the natural frequency number, ν, is prescribed greater than the ultimate frequency number, $\nu_K = 1.136$, the fourth pole results more to the right from $\bar{p}_{1,2,3}$. The relative damping greater than $1/4$ brings about too sluggish control loop responses due to moving $\bar{p}_4$ close to the imaginary axis and if the relative damping is $\delta = 0.35$ then the control loop stability is already broken.

Conclusions. The 3PP admissibility analysis provides the following results. From both the dominant three-pole placements and the IAE optimization points of view for the third-order plant it results the specific ranges

$$\mu \in \langle 1, 3 \rangle,\ \lambda \in \langle 0.25, 1 \rangle,\ \vartheta \in \langle 0.1, 0.3 \rangle. \tag{4.119}$$

The similarity numbers λ, μ from (4.119) are admissible due to satisfying the condition (4.52) with respect to (4.53). The pole coordinates ν, δ and κ are constrained to the following intervals

$$\nu \in \langle \nu_K, \nu_{\text{opt}} \rangle,\ \delta \in \langle 0.2, 0.3 \rangle,\ \kappa \in \langle 0.9, 1.3 \rangle. \tag{4.120}$$

Notice the specific ranges (4.119) define non-stiff third-order plants to prevent from the model order reduction. If $\nu = \nu_{\text{opt}} > \nu_K$, then the plant retardedness ϑ is to be less than 0.3 or the plant damping factor ξ is greater than 0.3. It results from Examples 7 and 8 confronted with Counterexamples 9 and 10, respectively. The frequency number ν_{opt} can exceed ν_K by 50% in maximum and the spectral abscissa results at least 0.4 as shown in examples. The dominant three-pole placement method fails in prescribing greater natural frequency number than the ultimate one if the third-order plants are characterized with both $\vartheta > 0.3$ and $\xi < 0.3$.

Then the loop gains ρ_P, ρ_D, ρ_I originate in poor values that are not acceptable in practice. Let be pointed out that in this case the PID control does not lack but only the PID tuning method fails. The admissible ranges of ρ_P, ρ_I results in (4.51) and (4.60) corresponding to specific ranges of the similarity numbers (4.61). As regards the derivative loop gain ρ_D this gain increases the admissible retardedness number ϑ with respect to conditions (4.48) and (4.49). The longer ϑ is the greater can be considered ρ_D. In case of the PID admissibility the specific ranges (4.119) are enlarged to (4.61) as follows

$$\mu \in \langle 0.5, 3 \rangle,\ \lambda \in \langle 0.25, 1.5 \rangle,\ \vartheta \in \langle 0.1, 0.5 \rangle \tag{4.121}$$

within which the PID controller is still applicable. Beyond these intervals identified by (4.66) as follows

$$\mu \in \langle 0.3, 0.5 \rangle,\ \lambda \in \langle 0.1, 0.25 \rangle \tag{4.122}$$

the PID controller is not already admissible for controlling the stable third-order plants. This admissibility loss takes place already for short retardedness number ϑ, $\vartheta < 0.15$. In (4.122) the cases, $\mu \to 0$ and $\lambda \to 0$, are missing due to the plant stability guarantee and due to the prevention from the plant stiff dynamics.

4.4 Dominant three-pole placement for $n = 4$

As in the case $n = 3$ the PID controller is limited again in its potential to change the fourth-order plant dynamics. The PID controller gains do not reach all the coefficient terms of $\bar{s}^0, \bar{s}, \bar{s}^2, \bar{s}^3$ and $\bar{s}^4$ in the characteristic equation (3.227) introduced in Chapter 3 (*Case 4*). Only the first three terms are modified by the controller gains and the terms of $\bar{s}^3$ and $\bar{s}^4$ are not influenced at all. Therefore the admissible ranges of both the similarity numbers and the pole placement coordinates are tighter than the ranges resulting in cases of $n = 2$ and $n = 3$. As in the case $n = 3$ the PID controller is not tuneable by means of the dominant three-pole placement method for inadmissible stable fourth-order plants because the controller gains result in zeros in fact. The examples of unacceptable PID controller tuning by means of the dominant three-pole placement method is shown in Counterexamples 13 and 14 at the end of Chapter 4.4. These counterexamples show that the goal of the dominant three-pole placement to change the stable fourth-order plant dynamics into desirable dynamics needs not be achieved. In fact Counterexamples 13 and 14 demonstrate the loss of the PID admissibility to controlling the delayed and poorly damped fourth-order plant.

To find a proper trio of poles (4.1) analogously to case $n = 3$ the ultimate frequency number is evaluated. Recall the fourth-order plant (3.114) (when $n = 4$) linked with the PID controller. The resulting characteristic equation (3.227) for the dimensionless control loop is

$$M(\bar{s}) = \left[\bar{s}^5 + \mu \bar{s}^4 + \theta\mu \bar{s}^3 + \lambda^{-1}\theta\mu \bar{s}^2 + \bar{s} \right] e^{\vartheta \bar{s}} + \rho_D \bar{s}^2 + \rho_P \bar{s} + \rho_I = 0 . \tag{4.123}$$

Analogously to deriving (4.46) $\rho_D = \rho_I = 0$ in (4.123) and the result is cancelled by $\bar{s}$. After multiplying this result by $e^{-\vartheta \bar{s}}$ and substituting $j\nu$ for $\bar{s}$ the characteristic equation (4.123) is changed to

$$e^{-j\vartheta\nu}\rho_{P,K} = -\left[(j\nu)^4 + \mu(j\nu)^3 + \theta\mu(j\nu)^2 + \lambda^{-1}\theta\mu j\nu + 1\right]. \tag{4.124}$$

Isolating real and imaginary parts from (4.124) as follows

$$\begin{aligned}\rho_{P,K}\cos(\vartheta\nu) &= -\nu^4 + \theta\mu\nu^2 - 1\\ \rho_{P,K}\sin(\vartheta\nu) &= -\mu\nu^3 + \lambda^{-1}\theta\mu\nu\end{aligned} \tag{4.125}$$

and dividing them each other the ultimate gain, $\rho_{P,K}$, is cancelled as follows

$$\cot(\vartheta\nu_K) = \frac{1}{\mu\nu_K}\frac{-\nu_K^4 + \theta\mu\nu_K^2 - 1}{\lambda^{-1}\theta - \nu_K^2}. \tag{4.126}$$

Again only the smallest positive solution of (4.126) is ν_K in fact. Equivalently the ultimate frequency number can be determined with respect to $\pi_1 = \nu = \omega\sqrt[n]{c_n}$ and $\vartheta\nu_K = \tau\,\omega_K = \phi_K$ by

$$\nu_K = \omega_K\sqrt[4]{c_4}. \tag{4.127}$$

3PP admissibility analysis. As regards the reasonable constraints to numbers λ, θ, μ and ϑ these constraints result differently from those in Chapter 3.2 where θ is in the reciprocal relationship to λ given by (3.145). On contrary, in case of the fourth-order plants the numbers λ and θ are in such a relation that ratio $\lambda^{-1}\theta$ can be different from one. Analogously to the admissibility conditions (4.48) and (4.49) the admissibility condition for $n = 4$ is found. Again assuming $\rho_P > 0, \rho_D > 0, \rho_I > 0$ the following condition

$$\theta\mu\left(\mu - \lambda^{-1}\right) > \rho_D \tag{4.128}$$

is to be satisfied. Since ρ_D in (4.128) is unknown the greater all the numbers λ, θ, μ the more admissible are these numbers. Numbers λ, θ, μ are the admissible similarity numbers if the condition (4.128) is satisfied. The longer *retardedness* number ϑ the greater can be gain ρ_D if the following two conditions

$$\mu\lambda > 1 \tag{4.129}$$

and

$$\theta\mu > 1 \tag{4.130}$$

are satisfied together with the condition (4.128). Both conditions (4.129) and (4.130) are derived from (4.128) and the condition (4.129) is one of the stability conditions of the fourth-order plants, see (3.332) in Chapter 3.3 (*Case 4*). Counterexamples 13 and 14 show the limit to admissible number ϑ where this number is greater than 0.25. Again the admissible range of ϑ depends on other three similarity numbers λ, θ, μ. For poorly damped or too lagged fourth-order plants the PID tuning via the dominant three-pole placement fails because loop

gains ρ_P, ρ_D, ρ_I result in practically zero values. Particularly this is the case of retarded PID control loop with significant number ϑ. Looking for the best non-stiff fourth-order plant this plant is with quadruple real pole (3.314) from Chapter 3.3 (*Case 4*). The similarity numbers corresponding to this multiple pole are as follows

$$\mu = 4,\ \lambda = 1.5 \text{ and } \theta = 1.5. \tag{4.131}$$

For these numbers the conditions (4.129) and (4.130) result in

$$\mu\lambda = 6 > 1,\ \theta\mu = 6 > 1. \tag{4.132}$$

Both products are six times greater than one. If the similarity numbers λ, θ, μ do not satisfy the condition (4.128) through (4.130) then these numbers cannot be considered as the admissible plant numbers. In Examples 11 and 12 the admissible fourth-order plants are controlled satisfying the condition (4.128) through (4.130) while in Counterexamples 13 and 14 the inadmissible fourth-order plants are controlled. Be aware that the condition (4.128) through (4.130) have to be satisfied to an extent analogous to (4.132) for covering the impact of *retardedness* (ϑ) on specific ranges of λ, θ, μ. The numbers λ, θ, μ in their admissible ranges characterize the fourth-order plant dynamics that is not *stiff* in order to avoid the model order reduction. Analogously to rule (4.51) for $n = 3$ the gain ρ_P is mapped versus prescribed ν, δ and κ to obtain a region of proper trio of poles (4.1). In Example 11 and Counterexample 13 this mapping is shown. Again the resulting ρ_P map is compared to $\rho_{P,K}$. The result of the loop gains tuning by means of the dominant three-pole placement has to be checked on the control loop stability even if the condition (4.128) through (4.130) are satisfied by all the similarity numbers and the trio of poles (4.1) is properly selected.

PID admissibility analysis. Assume the fourth-order plant is stable thus the conditions (3.332) in Chapter 3.3 (*Case 4*) are satisfied. From the characteristic equation (4.123) the term of $\bar{s}^4$ is not modifiable at all and this term corresponds to the similarity number μ. The same concerns the term of $\bar{s}^3$, that is not influenced by the PID at all. Thus the number μ together with the number λ and θ has to satisfy the condition (4.128) through (4.130). If these conditions are not satisfied in the manner as in (4.132) the PID admissibility is lost and vice versa. Once the dominant three-pole placement method fails in tuning the PID controller it becomes true for any tuning method. This means that the PID control fails. The immediate loss of the PID admissibility after the 3PP method fails is shown in Counterexamples 13 and 14.

Integrating plant. In case of integrating plant (3.185) the ultimate frequency number is determined from the characteristic equation (3.228) in Chapter 3 (*Case 4*)

$$M(\bar{s}) = \left[\bar{s}^5 + \mu\bar{s}^4 + \theta_I\mu\bar{s}^3 + \lambda_I\theta_I\mu\bar{s}^2\right]e^{\vartheta\bar{s}} + \rho_D\bar{s}^2 + \rho_P\bar{s} + \rho_I = 0. \tag{4.133}$$

Analogously to (4.61) when $\rho_D = \rho_I = 0$ in (4.133) and the result is cancelled by $\bar{s}$ after multiplying this result by $e^{-\vartheta\bar{s}}$ and substituting $\bar{s} = j\nu$ the characteristic equation (4.133) is modified into

$$e^{-j\vartheta\nu}\rho_{P,K}=-\left[(j\nu)^4+\mu(j\nu)^3+\theta_I\mu(j\nu)^2+\lambda_I\theta_I\mu j\nu\right]. \tag{4.134}$$

After real and imaginary parts from (4.134) are isolated and subsequently divided each other the ultimate gain, $\rho_{P,K}$, is cancelled as follows

$$\cot(\vartheta\nu_K)=\frac{\nu_K}{\mu}\frac{\theta_I\mu-\nu_K^2}{\lambda_I\theta_I-\nu_K^2}. \tag{4.135}$$

Only the smallest positive solution to (4.135) is ν_K in fact. The solution to (4.135) is computed with MATLAB in Chapter 4.5. Analogously the ultimate frequency number is given by (4.127). Be aware that λ^{-1} is replaced with λ_I and θ is replaced with θ_I in the condition (4.128) for the integrating plants (3.185).

Admissible dominant pole placement. The aim of this section is the dominant three-pole placement such that the trio of poles given by (4.1) is assigned in the fifth-order PID control loop with delay in case of aperiodic, oscillatory and integrating plants characterized by the similarity numbers $\lambda,\lambda_I,\theta,\theta_I,\mu,\vartheta$ constrained to their admissible ranges. As a result of this placement are the loop gain settings admissible for the PID control. Again after finding a region of admissible ρ_P setting by means of ρ_P mapping versus prescribed ν, δ and κ the admissible settings of ν, δ and κ are obtained. In case the trio of poles is selected within the admissible ranges of ν, δ and κ then assigning $\nu=\nu_K$ the three-pole dominance in infinite spectrum of the control loop poles is obtained as a rule. This dominance is proved again by argument increment (4.31) evaluation for $n=4$ or alternatively the quasi-polynomial root finder from [97] is applied. The argument increment is evaluated with MATLAB in Chapter 4.5. Even though the dominance of (4.1) is not achieved by assigning the natural frequency number greater than the ultimate frequency number in rigorous manner the fourth pole, $\overline{p}_4$, resulting in close position to $\overline{p}_{1,2,3}$ does not make the transient dynamics more sluggish. In fact the fourth pole is spontaneously placed more to the left from the trio (4.1). In case the pole dominance index results at least 2, [123], the fourth pole is far away in the left from the trio of placed poles $\overline{p}_{1,2,3}$ and this trio is dominant. To assign (4.1) the three poles has to be the roots of (4.123) or (4.133). Hence substituting each pole from (4.1) into (4.116) and starting with $\overline{s}=\overline{p}_1=(-\delta+j)\nu$ one attains

$$\begin{aligned}M(\overline{s})=&\left[\nu^5\left(-\delta^5+6\delta^3-\delta-4\delta(1-\delta^2)+\left(\delta^4-6\delta^2+1-4\delta^2(1-\delta^2)\right)j\right)+\right.\\&\mu\nu^4\left(\delta^4-6\delta^2+1+4\delta(1-\delta^2)j\right)+\theta\mu\nu^3\left(3\delta-\delta^3+(3\delta^2-1)j\right)+\lambda^{-1}\theta\mu\nu^2\left(\delta^2-1-2\delta j\right)+\\&\left.\nu(-\delta+j)\right]e^{\vartheta\nu(-\delta+j)}+\rho_D\nu^2\left(\delta^2-1-2\delta j\right)+\rho_P\nu(-\delta+j)+\rho_I=0.\end{aligned} \tag{4.136}$$

After substituting $\overline{p}_3=-\kappa\delta\nu$ for $\overline{s}$ in (4.123) the following equation is got

$$\begin{aligned}M(\overline{s})=&\left[(\kappa\delta\nu)^5+\mu(\kappa\delta\nu)^4-\theta\mu(\kappa\delta\nu)^3+\lambda^{-1}\theta\mu\kappa^2\delta^2\nu^2-\kappa\delta\nu\right]e^{-\kappa\delta\nu\vartheta}+\\&\rho_D\kappa^2\delta^2\nu^2-\rho_P\kappa\delta\nu+\rho_I=0.\end{aligned} \tag{4.137}$$

After rearranging both real and imaginary parts of (4.136) and (4.137) in such a way to be expressions free of searched ρ_P, ρ_D, ρ_I on the right-hand side of the following equations

$$\rho_D \nu^2\left(\delta^2-1-2\delta j\right)+\rho_P\nu\left(-\delta+j\right)+\rho_I=-e^{-\delta\vartheta\nu}\left[\cos\left(\vartheta\nu\right)+j\sin\left(\vartheta\nu\right)\right]\times \tag{4.138}$$
$$\left[\begin{array}{l}\nu^5\left(-\delta^5+6\delta^3-\delta-4\delta\left(1-\delta^2\right)+\left(\delta^4-6\delta^2+1-4\delta^2\left(1-\delta^2\right)\right)j\right)+\\ \mu\nu^4\left(\delta^4-6\delta^2+1+4\delta\left(1-\delta^2\right)j\right)+\theta\mu\nu^3\left(3\delta-\delta^3+\left(3\delta^2-1\right)j\right)+\lambda^{-1}\theta\mu\nu^2\left(\delta^2-1-2\delta j\right)+\\ \nu\left(-\delta+j\right)\end{array}\right]$$
$$\rho_D\kappa^2\delta^2\nu^2-\rho_P\kappa\delta\nu+\rho_I=-e^{-\kappa\delta\nu\vartheta}\left[-\left(\kappa\delta\nu\right)^5+\mu\left(\kappa\delta\nu\right)^4-\theta\mu\left(\kappa\delta\nu\right)^3+\lambda^{-1}\theta\mu\kappa^2\delta^2\nu^2-\kappa\delta\nu\right] \tag{4.139}$$

these equations can be gained in the matrix form (4.15) where only the elements of matrix **B** undergo changes. Thus the matrix, **A**, is without any change. From the elements of **B** only particular changes apply, i.e. (4.9) through (4.11) are extended to the fifth-order PID control loop with delay as follows

$$B_3=e^{-\kappa\delta\nu\vartheta}\kappa\delta\nu\left[\left(\kappa\delta\nu\right)^4-\mu\left(\kappa\delta\nu\right)^3+\theta\mu\left(\kappa\delta\nu\right)^2-\lambda^{-1}\theta\mu\kappa\delta\nu+1\right], \tag{4.140}$$
$$\begin{aligned}b_R=\nu\Big[&\nu^4\left(\delta^5-6\delta^3+\delta+4\delta\left(1-\delta^2\right)\right)+\\ &\mu\nu^3\left(-\delta^4+6\delta^2-1\right)+\theta\mu\nu^2\left(\delta^3-3\delta\right)+\lambda^{-1}\theta\mu\nu\left(1-\delta^2\right)+\delta\Big],\end{aligned} \tag{4.141}$$
$$\begin{aligned}b_I=\nu\Big[&\nu^4\left(-\delta^4+6\delta^2-1+4\delta^2\left(1-\delta^2\right)\right)+\\ &\mu\nu^3 4\delta\left(\delta^2-1\right)+\theta\mu\nu^2\left(1-3\delta^2\right)+\lambda^{-1}\theta\mu 2\delta\nu-1\Big].\end{aligned} \tag{4.142}$$

Again due to the cancellation of ν^3 in formulae for ρ_P, ρ_I, and ν^2 in the formula for ρ_D these formulae, given by (4.19) through (4.21), are applied to loop gains evaluation. Then the entries (4.140) through (4.142) are simplified in those formulae as follows

$$B_3=e^{-\kappa\delta\nu\vartheta}\kappa\delta\left[\left(\kappa\delta\nu\right)^4-\mu\left(\kappa\delta\nu\right)^3+\theta\mu\left(\kappa\delta\nu\right)^2-\lambda^{-1}\theta\mu\kappa\delta\nu+1\right], \tag{4.143}$$
$$\begin{aligned}b_R=&\nu^4\left(\delta^5-6\delta^3+\delta+4\delta\left(1-\delta^2\right)\right)+\\ &\mu\nu^3\left(-\delta^4+6\delta^2-1\right)+\theta\mu\nu^2\left(\delta^3-3\delta\right)+\lambda^{-1}\theta\mu\nu\left(1-\delta^2\right)+\delta\end{aligned}, \tag{4.144}$$
$$\begin{aligned}b_I=&\nu^4\left(-\delta^4+6\delta^2-1+4\delta^2\left(1-\delta^2\right)\right)+\\ &\mu\nu^3 4\delta\left(\delta^2-1\right)+\theta\mu\nu^2\left(1-3\delta^2\right)+\lambda^{-1}\theta\mu 2\delta\nu-1.\end{aligned} \tag{4.145}$$

In case of integrating plants (3.185) relations (4.143) through (4.145) are changed analogously into relation (4.82) through (4.84) as follows

$$B_3=e^{-\kappa\delta\nu\vartheta}\nu\left(\kappa\delta\right)^2\left[\left(\kappa\delta\nu\right)^3-\mu\left(\kappa\delta\nu\right)^2+\theta_I\mu\kappa\delta\nu-\lambda_I\theta_I\mu\right], \tag{4.146}$$
$$\begin{aligned}b_R=\nu\Big[&\nu^3\left(\delta^5-6\delta^3+\delta+4\delta\left(1-\delta^2\right)\right)+\\ &\mu\nu^2\left(-\delta^4+6\delta^2-1\right)+\theta_I\mu\nu\left(\delta^3-3\delta\right)+\lambda_I\theta_I\mu\left(1-\delta^2\right)\Big],\end{aligned} \tag{4.147}$$
$$b_I=\nu\left[\nu^3\left(-\delta^4+6\delta^2-1+4\delta^2\left(1-\delta^2\right)\right)+\mu\nu^2 4\delta\left(\delta^2-1\right)+\theta_I\mu\nu\left(1-3\delta^2\right)+\lambda_I\theta_I\mu 2\delta\right]. \tag{4.148}$$

Thus +1 and -1 disappear from (4.143) and (4.145), respectively, and stand-alone δ disappears from (4.144), too. At the same time $\theta_I\mu$ is instead of $\theta\mu$ and $\lambda_I\theta_I\mu$ takes over the role of $\lambda^{-1}\theta\mu$.

Example 11. Before the dominant three-pole placement method can be applied to the PID controller tuning the proper selection of the trio of poles (4.1) has to be made for the dimensionless PID control loop with aperiodic plants (3.377) characterized by the similarity numbers $\mu = 4.721$, $\lambda = 1.574$, $\theta = 1.605$, $\vartheta = 0.302$ and $\sigma = 64.3$, for more details see Example 3 in Chapter 3.3. The plants (3.377) are aperiodic with the spectrum of four distinct real poles where the ratio between the leftmost and rightmost pole is five and the retardedness number, ϑ, is greater than 0.25. These similarity numbers characterize non-stiff plant dynamics. In view of (4.132) the numbers μ, λ and θ are admissible because

$$\mu\lambda = 7.44 > 1,\ \theta\mu = 7.58 > 1. \tag{4.149}$$

Both products in (4.149) are more than seven times greater than one. The proper selection of the trio of poles (4.1) is based on mapping ρ_P versus ν and δ under constant κ, $\kappa = 1$, in Fig. 22. The resulting map is compared with zero and $\rho_{P,K}$ level of ρ_P. This map shows that assignable ν is within $\nu \in (0.5, 1.25)$ to get $\rho_P > 0.5\rho_{P,K}$ where $\rho_{P,K} = 4.269$. The frequency number ν_K results in 0.8658 from (4.126) applying the MATLAB solution in Chapter 4.5. Since the map is nearly the same for $0.8 < \kappa < 1.3$ the only parameter for optimization remains δ, which should result less than 0.35 with respect to the experience from [123], [126]. From Fig. 22 one

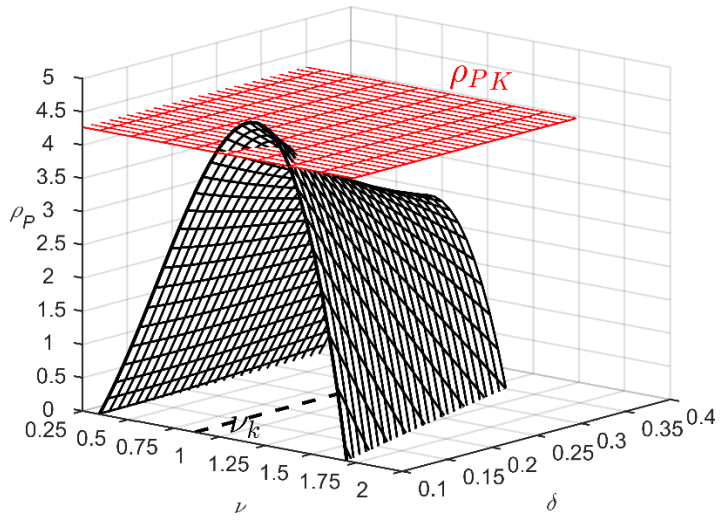

Fig. 22. Map of ρ_P for proper selection of the trio of poles (4.1) in case of plants (3.377)

can find out that $0.15 < \delta \le 0.35$ because the gain ρ_P is still high enough and simultaneously lower than $\rho_{P,K}$. For the dimensionless PID control loop with aperiodic plants (3.377) the loop gains ρ_P, ρ_D, ρ_I are computed by the formula (4.19) through (4.21) when the following trio of poles is assigned

$$\bar{p}_{1,2} = -0.216 \pm j1.082\,,\ \bar{p}_3 = -0.26\,. \tag{4.150}$$

Then $\nu = 1.082$, $\delta = 0.2$ and $\kappa = 1.2$. These values appear in the region of their assignability, see Fig. 22. Natural frequency number ν is identified with $1.25 \cdot \nu_K$. The ultimate frequency number can be equivalently obtained from ultimate frequencies of dynamically similar plants (3.374) and (3.385) using (4.127) as follows

$$\nu_K = \omega_K \sqrt[4]{c_4} = 1.0457 \cdot \sqrt[4]{0.47} = 0.8658 \tag{4.151}$$

and

$$\nu_K = \omega_K \sqrt[4]{c_4} = 0.7825 \cdot \sqrt[4]{1.5} = 0.8658\,. \tag{4.152}$$

The ultimate angle, $\phi_K = \nu_K \vartheta$, results as follows

$$\phi_K = \omega_K \tau = 1.0457 \cdot 0.25 = 0.7825 \cdot 0.334 = 0.8658 \cdot 0.302 = 0.261\,. \tag{4.153}$$

From Fig. 22 the proportional gain falls within the interval $\rho_P \in (0, 4.25)$ in the space of $\nu \in \langle 0.375, 1.3 \rangle$, $\delta \in (0.15, 0.35\rangle$ and $\kappa \in \langle 0.9, 1.3 \rangle$. The gain ρ_P margin specified by $\rho_{P,K} = 4.269$ allows for the retardedness number $\vartheta = 0.302$. The loop gains result from (4.19) through (4.21) where (4.143) through (4.145) are used. Thus

$$\rho_P = 3.723,\ \rho_D = 3.821,\ \rho_I = 0.753\,. \tag{4.154}$$

As suggested the gain ρ_P results in greater value than the half of $\rho_{P,K} = 4.269$ and also the condition (4.128) on the 3PP admissibility is verified as $\theta\mu\left(\mu - \lambda^{-1}\right) = 1.605 \cdot 4.721\left(4.721 - 1.574^{-1}\right) = 31 > \rho_D = 3.821$. Thus the left hand side of (4.128) exceeds the right hand side more than eight times. To check the dominance of (4.150) the argument increment (4.31) is evaluated with MATLAB (see Chapter 4.5). The resulting Poincaré-like mapping (4.35) is shown in Fig. 23.

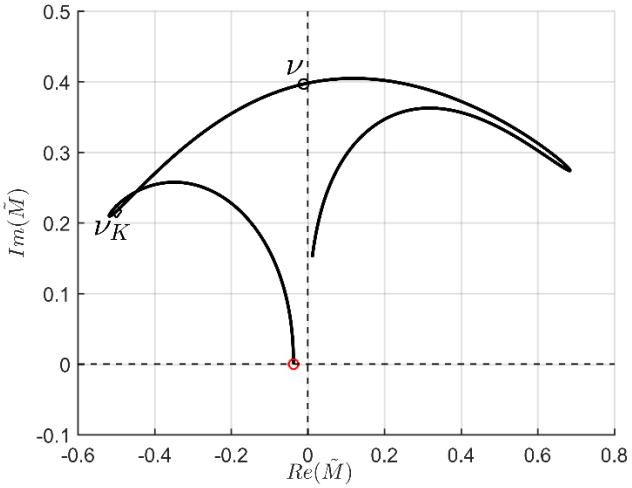

Fig. 23. Argument increment test on trio of poles dominance resulting from (4.31) in $-\pi/2$

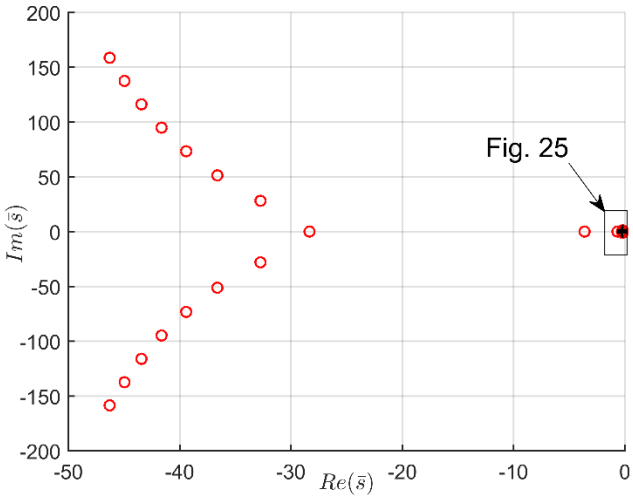

Fig. 24. Rightmost poles of the fifth-order PID control loop with delay

According to (4.31) with (4.32) given as $\beta_m = 1.1 \times 0.26 = 0.286$ the argument increment results $-\pi/2$ as verified in Fig. 23. How the three poles as the rightmost poles in the complex plane are separated from the rest of the infinite spectrum presents Fig. 24 and in Fig. 25 the four rightmost poles are shown for determining the dominance index by (4.36). The rightmost spectrum is computed by the quasi-polynomial root finder from [97]. As shown in Fig. 24 the poles $\bar{p}_{1,2,3,4}$ are separated enough from the rest of the infinite spectrum and the dominance index is determined as $\eta = 2.5 > 1$. This index results at least 2, [123], hence the trio of placed poles $\bar{p}_{1,2,3}$ are the dominant poles. The spectral abscissa results in 0.2 only but it is still twice greater than that in [100] where the third-order plant is considered. The disturbance rejection with setting (4.154) is recorded in Fig. 26. For comparison purposes the disturbance rejection with the PID controller tuned by the Z-N method is added to Fig. 26. This tuning is given for $\nu_K = 0.8658$ and $\rho_{P,K} = 4.269$ as follows

$$\rho_P = 2.561,\ \rho_D = 2.323,\ \rho_I = 0.706\,. \tag{4.155}$$

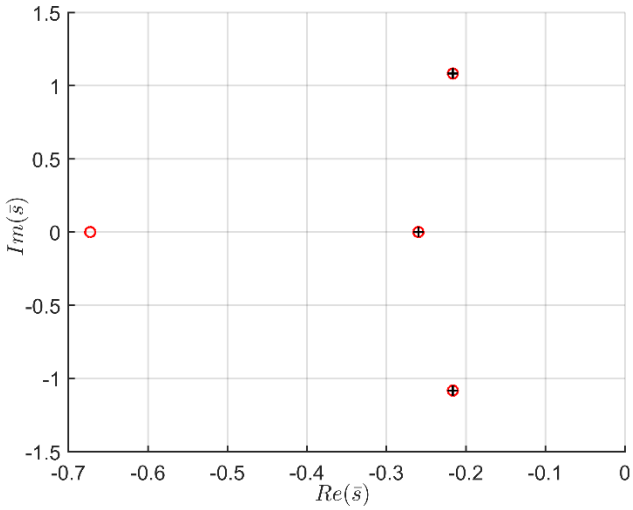

Fig. 25. Four rightmost poles composed of assigned trio $\bar{p}_{1,2,3}$ and the fourth $\bar{p}_4 = -0.672$

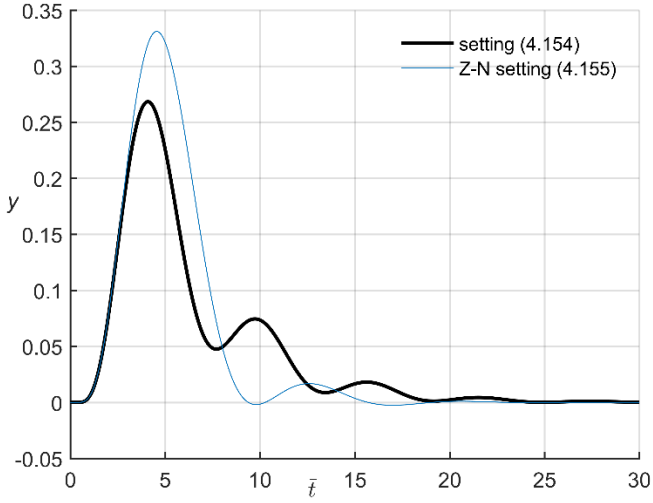

Fig. 26. Disturbance rejection in case of aperiodic plants (3.377)

Comparing the setting (4.154) to the setting (4.155) in the IAE the dominant three-pole placement method gives moderately lower value applying (4.40) as follows

$$Q_{AE} = 1.328 \tag{4.156}$$

than the Z-N method that results with the IAE as follows

$$Q_{AE} = 1.43\,. \tag{4.157}$$

Moreover the dominant three-pole placement method results with 18% lower overshoot than the Z-N method as shown in Fig. 26. In case of the dominant three-pole placement method the PID controller setting for the dynamically similar plants (3.374) and (3.385) results from (4.154) with respect to similarity numbers π_3, π_4 introduced in Chapter 3 as follows

$$r_P = 3.723,\ r_D = \sqrt[4]{0.47}\cdot\rho_D = 3.164\ [s],\ r_I = \frac{\rho_I}{\sqrt[4]{0.47}} = 0.909\ \left[s^{-1}\right] \tag{4.158}$$

and

$$r_P = 3.723,\ r_D = \sqrt[4]{1.5}\cdot\rho_D = 4.228\ [s],\ r_I = \frac{\rho_I}{\sqrt[4]{0.47}} = 0.68\ \left[s^{-1}\right], \tag{4.159}$$

respectively. While in case of the Z-N method the PID controller setting is obtained for plant (3.374)

$$r_P = 2.561,\ r_D = \sqrt[4]{0.47}\cdot\rho_D = 1.923\ [s],\ r_I = \frac{\rho_I}{\sqrt[4]{0.47}} = 0.853\ \left[s^{-1}\right] \tag{4.160}$$

and for plant (3.385) it is as follows

$$r_P = 2.561,\ r_D = \sqrt[4]{1.5}\cdot\rho_D = 2.57\ [s],\ r_I = \frac{\rho_I}{\sqrt[4]{1.5}} = 0.638\ [s^{-1}]. \tag{4.161}$$

The IAE values corresponding to the settings (4.158), (4.159) and (4.160), (4.161) are obtained due to (4.38) as follows

$$I_{AE} = \sqrt[4]{0.47}\cdot Q_{AE} = 1.1[s],\ I_{AE} = \sqrt[4]{1.5}\cdot Q_{AE} = 1.47[s] \tag{4.162}$$

and

$$I_{AE} = \sqrt[4]{0.47}\cdot Q_{AE} = 1.184[s],\ I_{AE} = \sqrt[4]{1.5}\cdot Q_{AE} = 1.58[s] \tag{4.163}$$

respectively.

Example 12 (*Integrating plant*)**.** Consider the integrating fourth-order plant of type (3.117) as follows

$$0.5\frac{d^4y(t)}{dt^4} + 2.6\frac{d^3y(t)}{dt^3} + 4.225\frac{d^2y(t)}{dt^2} + 2.125\frac{dy(t)}{dt} = u(t-0.25). \tag{4.164}$$

with $b_1 = 1\,s^{-1}$, $b_2 = 1.7\,s^{-1}$, $b_3 = 2.5\,s^{-1}$ and $b_4 = 0$, see (3.348) in Chapter 3.3 (*Case 4*). Utilizing the numbers (3.164) through (3.167) and (3.169) for the *Case 4* in Chapter 3 the following similarity numbers result

$$\mu = 4.3727,\ \lambda_I = 0.423,\ \theta_I = 1.3665,\ \vartheta = 0.2973 \tag{4.165}$$

where the scaling factor $\sqrt[4]{0.5}$ is applied. Due to (4.132) modified to the integrating plants (3.185) the numbers μ, λ_I and θ_I are admissible because

$$\mu\lambda_I^{-1} = 10.33 > 1,\ \theta_I\mu = 5.975 > 1. \tag{4.166}$$

Both products in (4.166) are nearly six times greater than one. Based on these numbers the integrating plants (3.185) with aperiodic impulse response are obtained as follows

$$\frac{d^4y(\bar{t})}{d\bar{t}^4} + 4.3727\frac{d^3y(\bar{t})}{d\bar{t}^3} + 5.975\frac{d^2y(\bar{t})}{d\bar{t}^2} + 2.527\frac{dy(\bar{t})}{d\bar{t}} = u(\bar{t} - 0.2973) \tag{4.167}$$

where $K = 1$. For the dimensionless PID control loop with integrating plants (4.167) the following trio of poles is assigned

$$\bar{p}_{1,2} = -0.1487 \pm j0.7435,\ \bar{p}_3 = -0.1784 \tag{4.168}$$

and then $\nu = 0.7435$, $\delta = 0.2$ and $\kappa = 1.2$. Natural frequency number ν is identified with $1.15\cdot\nu_K$ where ν_K is evaluated from (4.135). This evaluation is obtained with MATLAB in Chapter 4.5. The ultimate frequency number can be equivalently obtained from the ultimate frequency of dynamically similar plant (4.164) using (4.127) as follows

$$\nu_K = \omega_K \sqrt[3]{c_3} = 0.7688 \cdot \sqrt[4]{0.5} = 0.6465. \tag{4.169}$$

The ultimate angle, $\phi_K = \nu_K \vartheta$, results as follows

$$\phi_K = \omega_K \tau = 0.7688 \cdot 0.25 = 0.1922. \tag{4.170}$$

The loop gains ρ_P, ρ_D, ρ_I are computed by the formula (4.19) through (4.21) where (4.146) through (4.148) are utilized. Then the loop gains result as follows

$$\rho_P = 2.3315,\ \rho_D = 2.1467,\ \rho_I = 0.2995. \tag{4.171}$$

As suggested the gain ρ_P is greater than the half of $\rho_{P,K} = 2.366$ and also the condition (4.128) on the 3PP admissibility is verified as $\theta_I \mu (\mu - \lambda_I) = 1.366 \cdot 4.372 (4.372 - 0.423) = 23.5 > \rho_D = 2.146$. Thus the left hand side of (4.128) exceeds the right hand side more than ten times. The separation of $\bar{p}_{1,2,3}$ from the rest of the infinite spectrum is apparent from Fig. 27 where the rightmost poles are recorded. In Fig. 28 the trio of placed poles $\bar{p}_{1,2,3}$ is with respect to the fourth pole $\bar{p}_4 = -0.963$ dominant because the dominance index according to (4.36) results in $\eta = 5.4 > 2$. In addition the fifth pole $\bar{p}_5 = -3.07$ is remoted thrice more to the left from the fourth pole $\bar{p}_4 = -0.963$ as readable from Fig. 28. For the considerable $\bar{p}_{1,2,3}$ dominance it is paid by poor spectral abscissa, 0.15. The rightmost spectrum is computed by the quasi-polynomial root finder from [97].

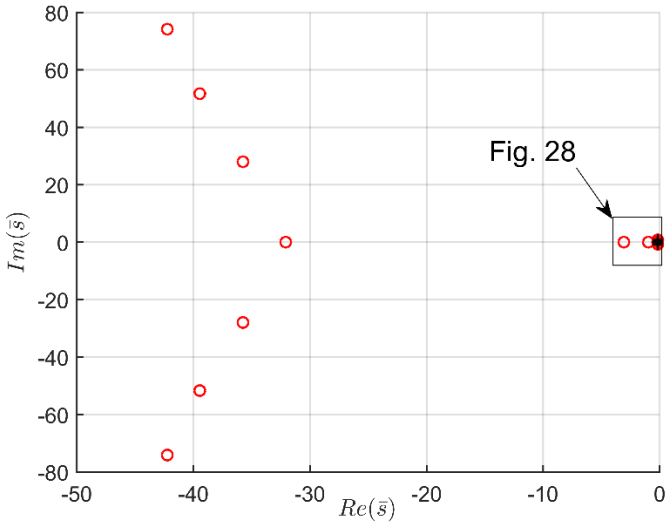

Fig. 27. Rightmost poles of the fifth-order PID control loop with delay

In Fig. 29 the disturbance rejection with setting (4.171) is recorded together with the disturbance rejection obtained by the Z-N setting as follows

$$\rho_P = 1.42,\ \rho_D = 1.725,\ \rho_I = 0.292. \tag{4.172}$$

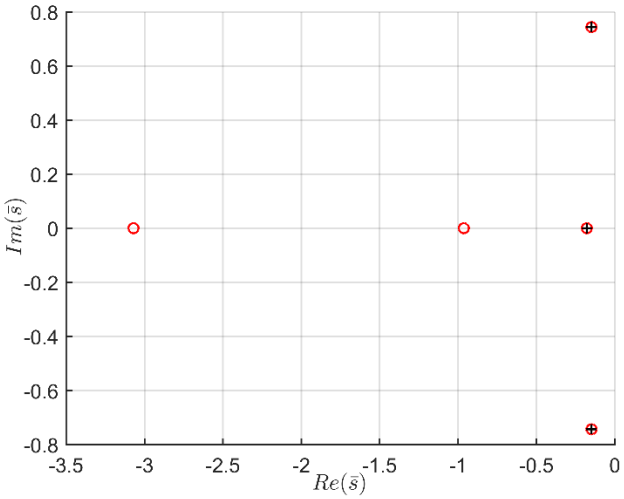

Fig. 28. Five rightmost poles composed of assigned trio $\bar{p}_{1,2,3}$, the fourth $\bar{p}_4 = -0.963$ and the fifth $\bar{p}_5 = -3.07$

This setting is due to $\nu_K = 0.6465$ and $\rho_{P,K} = 2.366$. For the plants (4.167) the dominant three-pole placement method gives considerably lower value of the IAE applying (4.40) as follows

$$Q_{AE} = 3.368 \tag{4.173}$$

than the Z-N setting that results with the IAE as follows

$$Q_{AE} = 4.92. \tag{4.174}$$

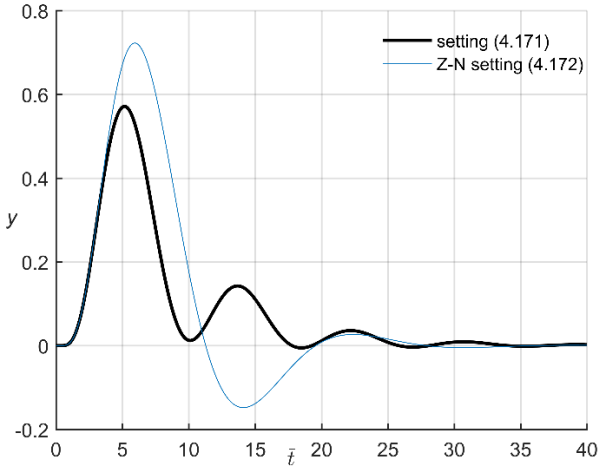

Fig. 29. Disturbance rejection in case of integrating plants (4.167)

The dominant three-pole placement method results with 20% lower overshoot than the Z-N method as apparent from Fig. 29. In addition the Z-N setting leads to the disturbance rejection that oscillates with the natural frequency number $\nu = 0.377$. This number is over 40% less than the ultimate frequency number $\nu_K = 0.6465$. In case of the dominant three-pole

placement method the PID controller setting results from (4.171) with respect to similarity numbers π_3, π_4 introduced in Chapter 3 as follows

$$r_P = 2.3315,\ r_D = \sqrt[4]{0.5}\cdot\rho_D = 1.805\ [s],\ r_I = \frac{\rho_I}{\sqrt[4]{0.5}} = 0.356\ \left[s^{-1}\right] \tag{4.175}$$

while in case of the Z-N method the PID controller setting is obtained

$$r_P = 1.42,\ r_D = \sqrt[4]{0.5}\cdot\rho_D = 1.45\ [s],\ r_I = \frac{\rho_I}{\sqrt[4]{0.5}} = 0.347\ \left[s^{-1}\right]. \tag{4.176}$$

The IAE values corresponding to the settings (4.175) and (4.176) are obtained due to (4.38) as follows

$$I_{AE} = \sqrt[4]{0.5}\cdot Q_{AE} = 2.832\,[s]. \tag{4.177}$$

and

$$I_{AE} = \sqrt[4]{0.5}\cdot Q_{AE} = 4.137\,[s] \tag{4.178}$$

respectively.

Counterexample 13. First the proper selection of the trio of poles (4.1) has to be made for the dimensionless PID control loop with double oscillatory plants (3.401). The plants (3.401) are characterized with similarity numbers $\mu = 0.6307$, $\lambda = 2.973$, $\theta = 3.5037$ and $\vartheta = 0.297$, for more details see Example 5 in Chapter 3.3. The plants (3.401) are double oscillatory and poorly damped with $\xi_1 = 0.088$ and $\xi_2 = 0.25$. The retardedness number, ϑ, is greater than 0.25. In view of (4.132) the numbers μ, λ and θ are not admissible because

$$\mu\lambda = 1.875 > 1,\ \theta\mu = 2.21 > 1. \tag{4.179}$$

Both products in (4.179) are not satisfied in the manner as in (4.132). Then these similarity numbers are not admissible and the oscillatory plants (3.401) are inadmissible plants. The trio of poles selection is based on mapping ρ_P versus ν and δ under constant κ, $\kappa = 1$, in Fig. 30. The resulting map is compared with zero and $\rho_{P,K}$ level of ρ_P. This map shows that assignable ν is within $\nu \in \langle 0.9, 1.1\rangle$ to get $\rho_P > 0.5\rho_{P,K}$ where $\rho_{P,K} = 0.23$. The number ν_K results in 1.035 from (4.126) applying the MATLAB solution in Chapter 4.5. This number is in the middle of ν interval. For the dimensionless PID control loop with double oscillatory plants (3.401) the loop gains ρ_P, ρ_D, ρ_I are computed by the formula (4.19) through (4.21) when the following trio of poles is assigned. Thus

$$\bar{p}_{1,2} = -0.126 \pm j0.788,\ \bar{p}_3 = -0.1136 \tag{4.180}$$

and then $\nu = 0.788$, $\delta = 0.16$ and $\kappa = 0.9$. Natural frequency number ν is identified as $0.76\cdot\nu_K$. The loop gains result in the following setting

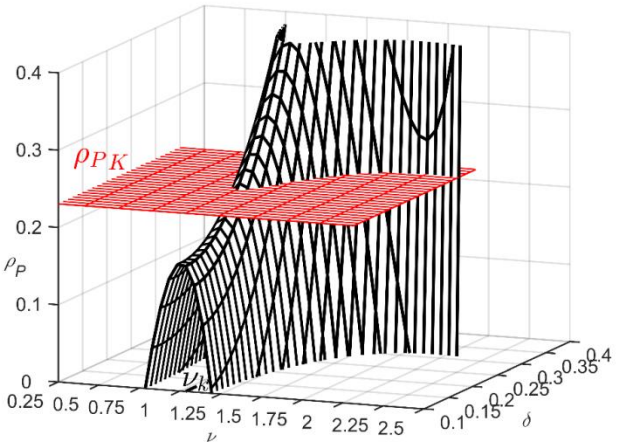

Fig. 30. Map of ρ_P for proper selection of the trio of poles (4.1) where $\rho_{P,K}=0.23$

$$\rho_P=8.2\times10^{-3},\ \rho_D=3.02\times10^{-2},\ \rho_I=0.104. \tag{4.181}$$

Again strictly speaking the dominance of (4.180) is lost but the fourth- and fifth pole, resulting in complex conjugate pair $\overline{p}_{4,5}=-0.133\pm j1.191$, is near to $\overline{p}_{1,2,3}$ and does not alter significantly the transient dynamics. As expected in case of the inadmissible plants with $\vartheta=0.297>0.25$ and $\xi_1=0.088<0.3$, $\xi_2=0.25<0.3$ the gain ρ_P results in much lower value than the half of $\rho_{P,K}=0.23$ and the remaining loop gains in (4.181) originate in poor values, too. The setting of these gains is not acceptable in practice. The dominant three-pole placement method lacks in case of the plants (3.401). Moreover not only this method but also the Z-N method fails in tuning the PID controller. The Z-N setting is obtained for $\nu_K=1.035$ and $\rho_{P,K}=0.23$ as follows

$$\rho_P=0.138,\ \rho_D=0.105,\ \rho_I=4.55\cdot10^{-2}. \tag{4.182}$$

Again the setting (4.182) is unacceptable adjustment of the PID leading to very poorly damped control response close to the stability margin. The tuning given by (4.181) leads to the natural frequency number as 76% of the ultimate one but the IAE optimum damping results in $1/6$ only. Prescribing higher natural frequency number brings about approaching the stability margin and other from rightmost poles than the prescribed poles lie more to the right from the prescribed ones. The poor damping does not result randomly but it has been already revealed as a lower bound of the relative damping of the IAE optimum third-order PID control loop with delay, [30]. Notice an upper bound of the relative damping originated in 0.4 for the magnitude optimum third-order PID control loop with delay, [32], where the natural frequency number fallen down below 80% of the ultimate frequency number. One can see the upper bound is not achievable at all in higher-order plants with delay. If $\delta=1/3$ is assigned the fifth-order PID control loop with delay becomes already unstable. The poor damping is balanced by positioning the third real pole more to the right from $\overline{p}_{1,2}$ by $\kappa=0.9$. The lower value of κ the higher is value of the IAE. Also the spectral abscissa becomes very low, not far away from 0.1 that corresponds to stabilizing PID controller tuning obtained in [100] but for the third-order plants with delay. This example of the fifth-order PID control loop with delay shows that one is already behind the capability of the PID controller to cope with

higher-order dynamics because the control loop response takes overlong and achieves extreme overshoot and also the relative damping significantly drops below 0.2.

Counterexample 14 (*Integrating plant*). For the dimensionless PID control loop with fourth-order integrating plants of form (3.185) the loop gains ρ_P, ρ_D, ρ_I are computed by means of the dominant three-pole placement. As the integrating plants of form (3.185) the plants (3.410) are considered, for more details see Example 6 in Chapter 3.3. These plants are characterized by the similarity numbers $\mu = 4.0961$, $\lambda_I = 1.0779$, $\theta_I = 0.63036$ and $\vartheta = 0.2782$. The plants (3.410) are with underdamped impulse response ($\xi = 0.2857$) and the retardedness number, ϑ, is greater than 0.25. These similarity numbers characterize *stiff* plant dynamics because the position of real pole is shifted fifteen times more to the left from the complex conjugate pair of poles, see Example 6 in Chapter 3.3. Due to (4.132) modified to the integrating plants (3.185) the numbers μ, λ_I and θ_I are not admissible because

$$\mu\lambda_I^{-1} = 3.8 > 1,\ \theta_I\mu = 2.58 > 1. \tag{4.183}$$

Both products in (4.183) are not satisfied in the manner as in (4.132). Then these similarity numbers are not admissible and the integrating plants (3.410) are inadmissible plants. The following trio of poles is selected

$$\bar{p}_{1,2} = -0.124 \pm j0.773,\ \bar{p}_3 = -0.111 \tag{4.184}$$

and then $\nu = 0.773$, $\delta = 0.16$ and $\kappa = 0.9$. Natural frequency number ν is identified with ν_K where ν_K is evaluated from (4.135) applying MATLAB solution in Chapter 4.5. The loop gains are computed by the formula (4.19) through (4.21) where element (4.146) through (4.148) are utilized

$$\rho_P = 0.63,\ \rho_D = 0.17,\ \rho_I = 3.763\times10^{-2}. \tag{4.185}$$

Trio $\bar{p}_{1,2,3}$ results in the rightmost position of the complex plane but another real pole $\bar{p}_4$ spontaneously assumed a position close to $\bar{p}_{1,2,3}$. Thus the dominance of (4.184) is lost but the fourth pole does not change significantly the transient dynamics. As expected in case of the inadmissible plants with $\vartheta = 0.2782 > 0.25$ and $\xi = 0.2857 < 0.3$ the loop gains (4.185) originate in poor values that are not acceptable in practice. The dominant three-pole placement method lacks in case of the plants (3.410) and also the Z-N method fails in tuning the PID controller in this case of plants. This tuning is obtained for $\nu_K = 0.773$ and $\rho_{P,K} = 1.214$ as follows

$$\rho_P = 0.728,\ \rho_D = 0.74,\ \rho_I = 0.179. \tag{4.186}$$

The setting (4.186) cannot be considered as satisfactory in industrial applications. Prescribing the natural frequency number greater than ν_K the control loop response becomes strikingly sluggish because the assigned trio of poles loses its dominance and the rightmost pole originates spontaneously in the close position to the imaginary axis. Again to obtain as low as possible value of the IAE the relative damping is selected close to $1/6$ and to compensate

poorer loop damping the third real pole is placed more to the right from the pair $\overline{p}_{1,2}$, i.e. $\kappa = 0.9$. Hence very poor spectral abscissa is achieved near to 0.1 that also results from the stabilizing PID tuning in [100] but for the third-order plants with delay. The decision on the PID controller applicability to integrating plants (3.410) is to reject this control.

Conclusions. It turned out both the 3PP admissibility and the PID admissibility analyses provide the same results on the admissible fourth-order plants. In fact the PID control also fails if the 3PP method fails in the PID controller tuning. From both the IAE optimization and the pole dominance points of view the following plant retardedness range turned out to be admissible

$$\vartheta \in \langle 0.1, 0.3 \rangle . \tag{4.187}$$

If the following relations hold among the similarity numbers μ, λ and θ

$$\mu\lambda > 5, \ \theta\mu > 5 \tag{4.188}$$

then these similarity numbers are admissible. The pole coordinates ν, δ and κ are then constrained to the following intervals

$$\nu \in \langle \nu_K, \nu_{\text{opt}} \rangle, \ \delta \in \langle 0.2, 0.3 \rangle, \ \kappa \in \langle 0.9, 1.3 \rangle \tag{4.189}$$

where particularly the relative damping results in the tight interval. The number ν_{opt} surpasses ν_K by 30% in maximum. If $\nu = \nu_{\text{opt}} > \nu_K$, then the plant retardedness ϑ is to be less than 0.25 or the plant damping factor ξ is greater than 0.3. It results from Examples 11 and 12 confronted with Counterexamples 13 and 14, respectively. The dominant three-pole placement method fails in prescribing the natural frequency number greater than the ultimate one if the fourth-order plants are characterized with both $\vartheta > 0.25$ and $\xi_1 < 0.3$ (eventually $\xi_2 < 0.3$). Then the loop gains ρ_P, ρ_D, ρ_I originate in poor values that are not acceptable in practice. Beside the dominant three-pole placement method also the Z-N method fails in the PID tuning for the fourth-order plants with these characteristics. In fact in this case of plants, called *stringent* plants in control engineering, the PID fails in controlling the inadmissible plants and other controller or control scheme need be used.

4.5 Solving dominant pole placement problem with MATLAB

All the MATLAB® solutions to the dominant three-pole placement problem in the third-, fourth- and fifth-order PID control loops with delay are provided, namely ultimate frequency assessment, loop gains tuning and three-pole dominance test. As mentioned in Introduction to Chapter 4 the crucial knowledge for the PID control loop design and optimization is the ultimate frequency. To provide the ultimate frequency number assessment, the relation (4.3) is extended by

$$\left(\frac{\vartheta}{\phi_K} \right)^2 \tag{4.190}$$

in both the numerator and denominator where $\phi_K = \vartheta\nu_K$ and ϕ_K is referred to as the ultimate angle (cf. Tab. 2 in Chapter 3). Then the relation (4.3) is equivalently expressed as follows

$$\cot\left(\phi_K\right) = \frac{\phi_K}{\vartheta}\lambda\left(1-\left(\frac{\vartheta}{\phi_K}\right)^2\right) \tag{4.191}$$

of which solution is ϕ_K only when this solution is the smallest positive root of the following equation

$$\cot\left(\phi_K\right) + \frac{\vartheta}{\phi_K}\lambda\left(1-\left(\frac{\phi_K}{\vartheta}\right)^2\right) = 0\,. \tag{4.192}$$

Relation (4.192) is achieved when the right-hand side of (4.191) is backwardly multiplied both in the numerator and denominator as follows

$$\frac{\lambda\left(1-\left(\frac{\vartheta}{\phi_K}\right)^2\right)}{\frac{\vartheta}{\phi_K}} \cdot \frac{\left(\frac{\phi_K}{\vartheta}\right)^2}{\left(\frac{\phi_K}{\vartheta}\right)^2} = \frac{\vartheta}{\phi_K}\lambda\left(\left(\frac{\phi_K}{\vartheta}\right)^2 - 1\right) \triangleq \cot\left(\phi_K\right) \tag{4.193}$$

and subsequently (4.193) takes on negative sign due to (4.192). After that the ultimate frequency number is calculated as follows

$$\nu_K = \frac{\phi_K}{\vartheta} \tag{4.194}$$

and the (dimensional) ultimate frequency is obtained by (4.28). Be aware that the scaling factor is fixed in (4.28) while the laggardness number ϑ in (4.194) is variable. For the purpose of ultimate frequency number evaluation in case of $n = 3$ the relation (4.46) is modified using (4.190) and (4.194) as follows

$$\cot\left(\phi\right) = \frac{\vartheta}{\phi}\frac{\mu\left(\frac{\phi}{\vartheta}\right)^2 - 1}{\lambda^{-1}\mu - \left(\frac{\phi}{\vartheta}\right)^2} \tag{4.195}$$

where $\phi = \vartheta\nu$. Since $\nu = \nu_K$ $\vartheta\nu_K = \phi_K$ and $\nu_K = \phi_K/\vartheta$. Thus ϕ_K, the ultimate angle, is the smallest positive solution of (4.195) and ν_K given by ratio ϕ_K/ϑ is the same as the smallest positive solution of (4.46). The ultimate frequency number for the third-order integrating plants (3.162) is computed by the function (4.69) altered using (4.190) and (4.194) as follows

$$\cot\left(\phi_K\right)=\frac{\phi_K}{\vartheta}\frac{\mu}{\lambda_I\mu-\left(\frac{\phi_K}{\vartheta}\right)^2} \tag{4.196}$$

where ϕ_K as the smallest positive solution of (4.196) determines ν_K as ratio ϕ_K/ϑ. To facilitate the solution of (4.126) for the case of $n=4$ this is made by the multiplication of both the numerator and denominator with $\left(\vartheta/\phi_K\right)^4$ as follows

$$\cot\left(\phi_K\right)=\frac{\phi_K}{\mu\vartheta}\frac{-\left(\frac{\vartheta}{\phi_K}\right)^4+\theta\mu\left(\frac{\vartheta}{\phi_K}\right)^2-1}{\lambda^{-1}\theta\left(\frac{\vartheta}{\phi_K}\right)^2-1} \tag{4.197}$$

and subsequently backwardly the relation (4.197) multiplied by $\left(\phi_K/\vartheta\right)^4$ in both the numerator and denominator results in

$$\cot\left(\phi_K\right)=\frac{\vartheta}{\mu\phi_K}\frac{-1+\theta\mu\left(\frac{\phi_K}{\vartheta}\right)^2-\left(\frac{\phi_K}{\vartheta}\right)^4}{\lambda^{-1}\theta-\left(\frac{\phi_K}{\vartheta}\right)^2}. \tag{4.198}$$

In (4.197) and (4.198) the angle ϕ_K as the smallest positive solution determines ν_K as ratio ϕ_K/ϑ. The ultimate frequency number in case of integrating plants (3.185) in Chapter 3 (*Case 4*) is evaluated by modifying (4.135) as follows

$$\cot\left(\phi_K\right)=\frac{\phi_K}{\mu\vartheta}\frac{\theta_I\mu\left(\frac{\vartheta}{\phi_K}\right)^2-1}{\lambda_I\theta_I\left(\frac{\vartheta}{\phi_K}\right)^2-1} \tag{4.199}$$

and subsequently as to (4.197)

$$\cot\left(\phi_K\right)=\frac{\phi_K}{\mu\vartheta}\frac{\theta_I\mu-\left(\frac{\phi_K}{\vartheta}\right)^2}{\lambda_I\theta_I-\left(\frac{\phi_K}{\vartheta}\right)^2}. \tag{4.200}$$

Again from all the solutions to (4.200) only the smallest positive solution is found out and determines ν_K as ratio ϕ_K/ϑ. Making use of the MATLAB® environment the root computation of (4.192) together with (4.194) is implemented as follows

```
% U(k) theta
% V(i) lambda
init_value_fi
tol = 1e-8;
options = optimset('Algorithm','Levenberg-Marquardt','MaxFunEvals',1000,
'TolFun',tol,'TolX',tol);
fi = fsolve(@(fi) tan(fi) + (1/U(k))*fi/(1-(1/(U(k)^2))*fi^2)/V(i),fi0,
options);
nu(k) = fi/U(k)    % Ultimate frequency number
```

In the analogous way the other relations for the ultimate frequency number computation are implemented using `fsolve` in MATLAB®. MATLAB® solution also concerns proportional, derivative and integration loop gain setting according to (4.19) through (4.21) which makes the placement of trio of poles (4.1). Formally (4.19) through (4.21) are applicable to arbitrary plant order *n* but the relations for B_R, B_I and B_3 have to be appropriately modified to orders $n=2$, $n=3$ and $n=4$. For $n=2$ these relations are given in Chapter 4.2 and their modifications for $n=3$ and $n=4$ are achieved in Chapters 4.3 and 4.4, respectively. For $n=2$ the formula (4.19) through (4.21) are implemented in MATLAB® environment as follows

```
% d delta
% kapa kappa
% rP roP, rD roD, rI roI
b_R = d + (1/V(i))*(1-d^2)*nu(k) - (3*d-d^3)*nu(k)^2;
b_I = -1 + (1/V(i))*2*d*nu(k) + (1-3*d^2)*nu(k)^2;
B_1 = exp(-d*U(k)*nu(k))*(b_R*cos(U(k)*nu(k))-b_I*sin(U(k)*nu(k)));
B_2 = exp(-d*U(k)*nu(k))*(b_R*sin(U(k)*nu(k))+b_I*cos(U(k)*nu(k)));
B_3 = exp(-kapa*d*U(k)*nu(k))*(nu(k)^2*(kapa*d)^3-nu(k)*(1/V(i))*
(kapa*d)^2+kapa*d);
cramer_P = [B_1 -(1 - d^2) 1; B_2 -2*d 0; B_3 kapa^2*d^2 1];
cramer_I = [-d -(1 - d^2) B_1; 1 -2*d B_2; -kapa*d kapa^2*d^2 B_3];
cramer_D = [-d B_1 1; 1 B_2 0; -kapa*d B_3 1];
rP = (1/(1 + d^2*(kapa-1)^2))*det(cramer_P);
rI = (nu(k)/(1 + d^2*(kapa-1)^2))*det(cramer_I);
rD = (1/(nu(k)*(1 + d^2*(kapa-1)^2)))*det(cramer_D);
```

The loop gains, ρ_P, ρ_D, ρ_I, place the trio of poles that the three poles are in the spectrum of delayed control loop but placing these poles themselves there is no guarantee of their dominance, i.e. these poles do not necessarily lie in the rightmost position in the system spectrum. Hence the so-called three-pole dominance test based on argument increment rule according to (4.31) and (4.32) is made. This increment rule together with Poincaré-like mapping (4.35) is implemented in MATLAB® environment for dimensionless control loops with delay (3.203). The implementation is described for order $n=2$ step by step as follows

- Declaration of the (4.31) parameters β, β_m, β_m/β, ν_K, ν_M and display parameters

```
% DIMENSIONLESS CONTROL LOOP for n = 2
% Checking for three-pole dominance
nasob = 1.1;            % multiple of beta satisfying beta_m/beta = nasob >
                        1.05
rozsah = 0.32;          % axis range for M-function
krok_w = 0.025;         % frequency step for drawing hodograph
Wmax = 15*nu(k);        % upper boundary frequency
W_M = 0:krok_w:Wmax;
n = max(size(W_M));
```

```
alfa = d*nu(k);          % alpha
if kapa < 1
    beta = alfa;         % real part of complex conjugate pair in (4.1)
else
    beta = kapa*alfa;    % third real pole in (4.1)
end
beta_m = nasob*beta;     %
```

- Computation of *M*-curve and its Poincaré-like mapping due to (4.35) where $\chi = 1.1$

```
ReM = [];
ImM = [];
for l = 1:n
    s = - beta_m + sqrt(-1)*W_M(l);
    Mp = s^2 + (1/V(i))*s + 1;
    M = s*Mp + exp(-U(k)*s)*(rD*s^2 + r0*s + rI);      % M-function (4.30)
    M = M/(1+(abs(M))^1.1);
    ReM = [ReM real(M)];
    ImM = [ImM imag(M)];
End
```

- Calculation of significant points on *M*-curve

```
s = - beta_m + sqrt(-1)*nu(k);
Mp = s^2 + (1/V(i))*s + 1;
HM1 = s*Mp + exp(-U(k)*s)*(rD*s^2 + r0*s + rI);
HM1 = HM1/(1+(abs(HM1))^1.1);
s = - beta_m;          % beginning of M-curve
Mp = s^2 + (1/V(i))*s + 1;
HM0 = s*Mp + exp(-U(k)*s)*(rD*s^2 + r0*s + rI);
HM0 = HM0/(1+(abs(HM0))^1.1);
```

- Drawing the hodograph of *M*-function modified by Poincaré-like mapping

```
figure(1)
title('Argument increment test on trio poles dominance');
hold on
plot(ReM(1,:),ImM(1,:),'k','linewidth',2);
hold on
plot(real(HM0),imag(HM0),'ko','linewidth',2);
hold on
plot(real(HM1),imag(HM1),'k+','linewidth',2);
hold on
plot([0 0]',rozsah*[-3 3]','k--','linewidth',1);
hold on
plot(rozsah*[-3 3]',[0 0]','k--','linewidth',1);
```

In case of higher-order plants, namely the third- or fourth-order plants, $n > 2$, this program is appropriately modified in `Mp` which is of higher degree than 2. The above described program gives off the logical output whether the trio of poles is dominant in the control loop spectrum or not. In order to measure the degree of this dominance the following MATLAB® function evaluates the dominance index, `d_index`, according to either (4.36) or (4.37).

```
[roots_true, d_index] =
spektrum_rightmost_index(a0,a1,b0,tau,fi,kor,beta_lambert,r0,rD,rI);
```

where

```
v = V(i);          % swingability number, lambda
u = U(k);          % laggardness number, theta
w = nu(k);         % ultimate frequency number
a0 = 1;
a1 = 1/v;          % a1 = 1/lambda
b0 = a0;           %
kor = 3;           % correction parameter
beta_lambert = kor*kapa*d*w;    % w > w_k
```

Parameter `beta_lambert` delimits the region for searching the rightmost poles in the system spectrum. This parameter is next used in the MATLAB® function `spektrum_rightmost_index` for the computation of the rightmost poles applying spectral method by [107]. This function implements both (4.36) and (4.37) as follows

```
function [roots_true, d_index] = spektrum_rightmost_index(a0,a1,b0,tau,fi,
kor,beta_lambert,r0,rD,rI)
global v A Ad
A = [0 0 0; 1 0 -a0; 0 1 -a1];          % coefficient matrix of the system
Ad = [0 0 -b0*rI; 0 0 -b0*r0; 0 0 -b0*rD;]; % coefficient matrix of the
% system
h = [0 u];
% Recalling spectral method by WU Z. & MICHIELS W.
% principal branch k = 0 - rightmost pole(s)
tds = tds_create({A Ad},h);
options = tdsrootsoptions;
options.minimal_real_part = - kor*beta_lambert;
[eigenvalues, N, size_eigenvalue_problem] = tds_charateristic_roots(tds,
options);
if v > 1/2
    eigenplot1(eigenvalues);
else
    eigenplot(eigenvalues);
end
roots_true = eigenvalues.l1;
if isempty(roots_true) == 1
    display('V hledane oblasti zadne koreny nenalezeny')
    kor = kor + 0.05;
    return
else
    alfa = real(roots_true(1));
    w_1 = abs(imag(roots_true(1)));
    d = - alfa/w_1;         % determination of relative damping
    podil_w = w_1/w;        % ratio other than 1 if nu(k) is not prescribed
end
if max(size(roots_true)) < 4
    beta = abs(alfa);
    w_2 = 0.4*w_1;
    kapa_ = - beta/alfa;    % third pole position characterized by multiple
    kor = kor + 0.05;
    d_index = kapa_;        % dominance index is not determined yet, i.e.
                            % d_index = 1
    display('Je treba prodlouzit minimal_real_part')
    return
else
    beta = abs(real(roots_true(4)));    % beta = - real(roots_true(4));
    w_2 = abs(imag(roots_true(4)));
    % Computation of fourth pole position
    if kapa < 1
       d_index = - beta/alfa;           % relation (4.37)
    else
```

```
        d_index = beta/(kapa*d*w_1);     % relation (4.36)
    end
    kor = 1.05;
end
display(roots_true)
end
```

In case of higher-order plants, namely the third- or fourth-order plants, $n > 2$, this function is appropriately modified in system matrices, `A` and `Ad`, which are in compatible dimensions 3×3 or 4×4. Alternatively the quasi-polynomial root finder in [97] can be applied instead of the spectral method by [107]. From essential optimization techniques, mostly used for the PID controller tuning, the IAE is applied. For fast computation of the IAE in MATLAB® environment function `sae` is used.

All the programs presented are applicable to the design and optimization of the higher-order PID control loops with delay. The design of these loops is developed in case of controlling the third- and fourth-order plants both aperiodic and oscillatory, including the integrating plants of appropriate order.

4.6 Conclusions

The dominant three-pole placement method is generalized for the fourth- and fifth-order PID control loops with delay. In case the admissible third-order plants are controlled the natural frequency number is assigned greater than the ultimate frequency number and the disturbance rejection response results in the overshoot by about 30% lower than the overshoot achieved in the control loop tuned by the Z-N method. Simultaneously with respect to achieving the three-pole dominance the relative damping needs be prescribed less than 0.3. Although this pole dominance is not achieved in the rigorous manner, thus one or pair of other rightmost poles assumes close position to the placed trio of poles, the other pole or pair of poles does not significantly alter the transient dynamics. On the other hand the spectral abscissa results at least 0.4. In case of the inadmissible third-order plants it is not possible to assign the natural frequency number the same with the ultimate frequency number because arising control loop gains spontaneously place the rightmost poles of the control loop in critical positions, i.e. close to imaginary axis or in RHP. Thus the three placed poles do not result as dominant ones at all and even the spontaneously placed poles can result as unstable. In fact the natural frequency number has to be prescribed lower than the ultimate one to achieve the three-pole dominance. As a consequence the PID setting results in poor gain values that are zeros in fact. In other words the dominant three-pole placement method fails in the PID tuning while on contrary the Z-N method for some of the inadmissible third-order plants is still able to provide a fair PID tuning. Even though the inadmissible third-order *integrating* plants allow assigning the natural frequency number identical with the ultimate one the resulting PID controller setting is not acceptable.

Once the admissible fourth-order plants are to be controlled the natural frequency number is assigned greater than the ultimate frequency number and the disturbance rejection response results in the overshoot by about 20% lower than the overshoot achieved in the control loop tuned by the Z-N method. Simultaneously the PID tuning by means of the dominant three-pole placement method surpasses the Z-N tuning in the value of the IAE and considerable three-pole dominance is achieved measured by the dominance degree greater than 2. The IAE dropping is achieved by the relative damping prescribed as 0.2 and for the high pole dominance degree it is paid by poor spectral abscissa about 0.2. In case of the inadmissible fourth-order plants the three placed poles do not result as dominant ones and even the

spontaneously placed poles can result as unstable. Then the natural frequency number has to be assigned lower than the ultimate one. Nevertheless the inadmissible fourth-order *integrating* plants allow assigning the natural frequency number identical with the ultimate one but the PID controller setting results in zero values in fact. Not only the dominant three-pole placement method but also the Z-N method fails in the PID tuning for the inadmissible fourth-order plants, including the fourth-order integrating plants. It turned out the PID controller is not applicable to the inadmissible fourth-order plants with delay and other controller or control scheme is to be applied instead.

All the results achieved are enabled by the dimensional analysis applied to obtaining the universal control loop model with delay. The similarity numbers are mapped in their reasonable constraints not only from the plant dynamics but also control design points of view. As a result the admissible third- and fourth-order plants are found out together with acceptable PID controller settings originating from the pole assignability regions mapped for both the fourth- and fifth-order PID control loops with delay. Thus not only the similarity numbers but also the pole assignment coordinates are constrained to tight intervals. On contrary the PID controller tuning lacks in case of inadmissible third- and fourth-order plants. For the third-order plants it becomes due to the deficiency of the dominant three-pole placement method while for the fourth-order plants this is the case because the PID controller fails as a whole.

5. Conclusions to the habilitation thesis

In the habilitation thesis author's research results are presented in the area of process control design for time delay systems and in the similarity theory application in this design. The presented design method is the generalized dominant three-pole placement and is aimed at the universal PID controller setting common for a set of dynamically similar plants with delay. Moreover this thesis is the study on applicability of the dominant three-pole placement method to the PID controller tuning for higher-order plants with delay, namely the third- and fourth-order plants. This study reveals that the dominant three-pole placement method is still able to tune the PID controller for the admissible third- and fourth-order plants. In case of the inadmissible third- and fourth-order plants this method fails in tuning the PID controller. Thus the control loop gains result nearly zero, i.e. the PID controller is somewhat degraded. The admissible third- and fourth-order plants are mapped by means of the admissibility analysis resulting in the admissible similarity numbers. The disturbance rejection response is achieved in admissible dimensionless control loops with significantly lower overshoot than the overshoot obtained in those control loops tuned by ideal-relay feedback test. In case of the inadmissible fourth-order plants the PID controller is not tunable at all. Thus the PID control fails in case of any tuning method. To point out the significance of the dimensional analysis this analysis is performed because without the dimensionless control loop description the admissibility analyses and the PID control classification are barely possible.

Author's list of publications

Only works cited in the habilitation thesis are included.
Also the number of citations in WoS/MathSci/Scopus is specified.

Fišer, J., Červený, J., and Zítek, P. (2010). Oscillators for Modelling Circadian Rhythms in Cyanobacteria Growth. *In*: Modelling, Simulation, and Optimization - Focus on Applications, Ed. Sh. Cakaj, Wien: In-Tech, 2010, chap. 7, 105–119.

Fišer, J., and Zítek, P. (2001). Double Controller Anisochronic Structure with Disturbance Compensation. *In*: Proc. of the Conf. on Information Engineering and Process Control IEPC'2001, September 4, Masaryk Academy of Work, Prague, Czech Republic, 67–68.

Fišer, J., Zítek, P., and Kučera, V. (2014). IAE optimization of delayed PID control loops using dimensional analysis approach. In: Proceedings of the 6th International Symposium on Communications, Control and Signal Processing. Patras: University of Patras, 262–265.

Fišer, J., Zítek, P., Skopec, P., Knobloch, J., and Vyhlídal, T. (2017). Dominant root locus in state estimator design for material flow processes: A case study of hot strip rolling. *ISA Transactions*, 68 (2017), 381–401.

Fišer, J., Zítek, P., and Vyhlídal, T. (2015). Magnitude Optimum Design of PID Control Loop with Delay. In: Proceedings of the 12th IFAC Workshop on Time Delay Systems, TDS 2015, 446–451 (*IFAC-PapersOnLine*, 48(12), 2015).
WoS: 3

Fišer, J., Zítek, P., and Vyhlídal, T. (2018). Neutral PID Control Loop Investigated in Terms of Similarity Theory. *IFAC-PapersOnLine*, 51(14), 212–217.

Fišer, J., Zítek, P., and Vyhlídal, T. (2018). Robust PID Controller Design for Plants with Delay Using Similarity Theory. *IFAC-PapersOnLine*, 51(14), 236–241.

Zítek, P., and Fišer, J. (2006). Predictor Based Control Design for Time Delay Systems. *In*: International Conference on Computational Intelligence for Modelling, Control and Automation (CIMCA06), Los Alamitos: IEEE Computer Society, 2006, vol. 2, 517–522.

Zítek, P., and Fišer, J. (2018). A Universal Map of Three Dominant Pole Assignment for PID Controller Tuning, *International Journal of Control*. 2018, 1–8. doi: 10.1080/00207179.2018.1554267 (in press)

Zítek, P., Fišer, J., and Vyhlídal, T. (2010). Ultimate-Frequency based Dominant Pole Placement. *In*: Proceedings of 9th IFAC Workshop on Time Delay Systems, TDS 2010, June 7-9, 2010, Prague, Czech Republic, Vol. 9, 87–92. (*IFAC-PapersOnLine*, 43(2), 2010).
WoS: 3

Zítek, P., Fišer, J., and Vyhlídal, T. (2012). Ultimate-frequency Based Three-pole Dominant Placement in Delayed PID Control Loop. *In*: Proceedings of the 10th IFAC Workshop on Time Delay Systems, Boston, MA, June 22-24, Vol. 10, Part 1, 2012, 150–155 (*IFAC-PapersOnLine*, 45(14), 2012).
WoS: 5

Zítek P., Fišer J., and Vyhlídal T. (2013). Dominant three pole placement in PID control loop with delay. *In*: 9th Asian Control Conference (ASCC), Istanbul, Turkey, New York: IEEE, 1–6.
WoS: 3

Zítek, P., Fišer, J., and Vyhlídal, T. (2013). Dimensional analysis approach to dominant three-pole placement in delayed PID control loops. *Journal of Process Control*, 23(8), 1063–1074.
WoS: 22

Zítek, P., Fišer, J., and Vyhlídal, T. (2014). Dominant Trio of Poles Assignment in Delayed PID Control Loop. *In*: Delay Systems: From Theory to Numerics and Applications vol. 1, Eds. T. Vyhlídal, J-F. Lafay, and R. Sipahi, New York: Springer, 2014, 57–70.
WoS/MathSci: 3/3

Zítek, P., Fišer, J., and Vyhlídal, T. (2016). IAE Optimization of PID Control Loop with Delay in Pole Assignment Space. *In*: Proceedings of the 13th IFAC Workshop on Time Delay Systems, Istanbul, Turkey, IFAC-PapersOnLine, 49(10), 177–181.
WoS: 3

Zítek, P., Fišer, J., and Vyhlídal, T. (2017). Dynamic similarity approach to control system design: delayed PID control loop. *International Journal of Control*, 2017, 1–10. doi: 10.1080/00207179.2017.1354398 (in press)
Scopus: 2

References

[1] Alevisakis, G., and Seborg, D. E. (1974). Control of Multivariable Systems Containing Time Delays Using a Multivariable Smith Predictor. *Chemical Engineering Science*, 29(2), 373 – 380.

[2] Alferov, V. G., and Fuk, H. K. (1993). Root-hodograph evaluation of the dynamic properties and the pair of dominant roots. *Soviet electrical engineering*, 64(6), 35–40.

[3] Åström, K. J., and Hägglund, T. (1995). *PID Controllers Theory Design and Tuning*. 2nd ed., Instrument Society of America, Research Triangle Park, North Carolina.

[4] Åström, K. J., Hang, C. C., and Lim, B.C. (1994). A new Smith predictor for controlling a process with an integrator and long time delay. *IEEE Transactions on Automatic Control*, 39(3), 343–345.

[5] Åström, K. J., and Wittenmark, B. (1980). Self-tuning controllers based on pole-zero placement. *IEE Proceedings D - Control Theory and Applications*, 127 (3), 120–130.

[6] Balaguer, P. (2013). *Application of Dimensional Analysis in Systems Modeling and Control Design*. London: IET.

[7] Balaguer, P., Ibeas, A., Pedret, C., and Alcántara, S. (2009). Controller Parameter Dependence on Model Information Through Dimensional Analysis, *In*: Proc. of IEEE Conf. on Decision and Control, Shanghai, 1914 – 1919.

[8] Baron, J. S. (1992). Dimensional analysis and process control of body-in-white processes, Ph.D. Thesis, University of Michigan, pg. 170.

[9] Benaroya, H., Nagurka, M., and Han, S. (2017). Mechanical vibration: analysis, uncertainties, and control. Boca Raton, CRC Press.

[10] Bennett, S. (1996). A brief history of automatic control. *IEEE Control Systems Magazine*, 16(3), 17–25.

[11] Bolster, D., Hershberger, R. E., and Donnelly, R. J. (2011). Dynamic similarity, the dimensionless science. *Physics Today*, 64(9), 42–47.

[12] Bošek, B. (1989). Absolutely autonomous and invariant control for systems with transport delay. *Automatizace*, 32(11), 287-290. (in Czech)

[13] Breda, D., Maset, S., and Vermiglio, R. (2009). TRACE-DDE: a Tool for Robust Analysis and Characteristic Equations for Delay Differential Equations. *In*: Topics in Time Delay Systems, J. J. Loiseau, W. Michiels, S. Niculescu and R. Sipahi, eds., Lecture Notes in Control and Information Sciences, Springer, Berlin, 145–155.

[14] Brennan, S. N. (2002). On size and control: the use of dimensional analysis in controller design. PhD Thesis, University of Illinois at Urbana-Champaign.

[15] Brethé, D., and Loiseau, J. J. (1998). An effective algorithm for finite spectrum assignment of single-input systems with delays. *Mathematics and Computers in Simulation*, 45(3-4), 339–348.

[16] Bridgman, P. W. (1920). *Dimensional Analysis*. New Haven: Yale University Press.

[17] Buchberger, B. (1985). Gröbner Bases: An Algorithmic Method in Polynomial Ideal Theory. In: Bose, N. K. Ed., Multidimensional Systems Theory - Progress, Directions

and Open Problems in Multidimensional Systems (pp. 184–232), Reidel Publishing Company.

[18] Buckingham, E. (1914). On physically similar systems: illustrations of the use of dimensional equations. *Physical Review*, 4(4), 345–376.

[19] Callender, A., Hartree, D. R., and Porter, A. (1936). Time-lag in a control system. *Phil. Trans. R. Soc. Lond. A*, 235(756), 415–444.

[20] Castaños, F., Estrada, E., Mondié, S., and Ramírez, A. (2017). Passivity-based PI control of first-order systems with I/O communication delays: a frequency domain analysis. *International Journal of Control*, 1-14.

[21] Cheng, Y. T., and Cheng, C. M. (2004). Scaling, dimensional analysis, and indentation measurements, *Materials Science and Engineering: R: Reports*, 44(4), 91–149.

[22] Cohen, G. H., and Coon, G. A. (1953). Theoretical consideration of retarded control. *Trans. ASME*, 75, 827–834.

[23] Cvejn, J. (2013). The design of PID controller for non-oscillating time-delayed plants with guaranteed stability margin based on the modulus optimum criterion. *Journal of Process Control*, 23(4), 570–584.

[24] Das, S., Halder, K. and Gupta, A. (2018). Performance analysis of robust stable PID controllers using dominant pole placement for SOPTD process models. *Knowledge-Based Systems*, 146, 12–43.

[25] De la Sen, M. (1993). On the stabilizability, controllability and observability of linear hereditary systems with distributed commensurate delays. *International journal of systems science*, 24(1), 33–52.

[26] De Paor, M. A., and Egan, R. P. K. (1989). Extension and Partial Optimization of Modified Smith Predictor and Controller for Unstable Processes with Time Delay. *International Journal of Control*, 50(4), 1315 – 1326.

[27] Eller, D., Aggarwal, J., and Banks, H. (1969). Optimal control of linear time-delay systems. *IEEE Transactions on Automatic Control*, 14(6), 678–687.

[28] Fišer, J., Červený, J., and Zítek, P. (2010). Oscillators for Modelling Circadian Rhythms in Cyanobacteria Growth. *In*: Modelling, Simulation, and Optimization - Focus on Applications, Ed. Sh. Cakaj, Wien: In-Tech, 2010, chap. 7, 105-119.

[29] Fišer, J., and Zítek, P. (2001). Double Controller Anisochronic Structure with Disturbance Compensation. *In*: Proc. of the Conf. on Information Engineering and Process Control IEPC'2001, September 4, Masaryk Academy of Work, Prague, Czech Republic, 67–68.

[30] Fišer, J., Zítek, P., and Kučera, V. (2014). IAE optimization of delayed PID control loops using dimensional analysis approach. In: Proceedings of the 6th International Symposium on Communications, Control and Signal Processing. Patras: University of Patras, 262–265.

[31] Fišer, J., Zítek, P., Skopec, P., Knobloch, J., and Vyhlídal T. (2017). Dominant root locus in state estimator design for material flow processes: A case study of hot strip rolling. *ISA Transactions*, 68 (2017), 381–401.

[32] Fišer, J., Zítek, P., and Vyhlídal, T. (2015). Magnitude Optimum Design of PID Control Loop with Delay. *In*: Proceedings of the 12th IFAC Workshop on Time Delay Systems. New York: IFAC, 446–451.

[33] Fišer, J., Zítek, P., and Vyhlídal, T. (2018). Neutral PID Control Loop Investigated in Terms of Similarity Theory. *IFAC-PapersOnLine*, 51(14), 212-217.

[34] Fišer, J., Zítek, P., and Vyhlídal, T. (2018). Robust PID Controller Design for Plants with Delay Using Similarity Theory. *IFAC-PapersOnLine*, 51(14), 236-241.

[35] Fliess, M., Marquez, R., and Mounier, H. (2002). An extension of predictive control, PID regulators and Smith predictors to some linear delay systems. *International Journal of Control*, 75(10), 728–743.

[36] Furukawa, T., and Shimemura, E. (1983). Predictive control for systems with time delay. *International Journal of Control*, 37(2), 399–412.

[37] Gao, Q., and Olgac, N. (2015). Optimal sign inverting control for time-delayed systems, a concept study with experiments. *International Journal of Control*, 88(1), 113–122.

[38] García, P., and Albertos, P. (2008). A new dead-time compensator to control stable and integrating processes with long dead-time. *Automatica*, 44(4), 1062–1071.

[39] Goodwin, G. C., Graebe, S. F., and Salgado, M. E. (2000). *Control System Design*. Prentice Hall, New Jersey.

[40] Górecki, H., Fuksa, S., Grabowski, P., and Korytowski, A. (1989). *Analysis and Synthesis of Time Delay Systems*. Polish. Scient. Publ., Warszawa.

[41] Gumussoy, S., and Michiels, W. (2012). Root locus for SISO dead-time systems: A continuation based approach. *Automatica*, 48(3), 480–489.

[42] Haftay, H., and Brennan, S. N. (2005). Use of Dimensional Analysis to Reduce the Parametric Space for Gain-Scheduling, In: Proc. ACC'05, Portland, 598 – 602.

[43] Hale, J. K., and Lunel, S. M. V. (1993). Introduction to Functional Differential Equations. Springer-Verlag, New York.

[44] Hanuš, B., and Le, Q. T. (1992). Controller with flexible feedback. Automatizace, 35(9), 279–283. (in Czech)

[45] Hirschfelder, J. O. (1963). Applied mathematics as used in theoretical chemistry. In: Proc. Symposia in Applied Mathematics: Experimental Arithmetic, High Speed Computing and Mathematics (Vol. 15, pp. 367–376).

[46] Hohenbichler, N. (2009). All stabilizing PID controllers for time delay systems. *Automatica*, 45(11), 2678–2684.

[47] Huang, S., Tan, K. K., and Lee, T. H. (2002). Applied Predictive Control. Advances in industrial control, Springer-Verlag, London.

[48] Huang, Y. J., and Yeung, K. S. (1994). A control scheme robust against all parameter variations and disturbances. *International Journal of Systems Science*, 25(10), 1621–1629.

[49] Huang, H. P., and You, H. S. (1994). State analytical predictor for systems with multiple time delays. *International journal of systems science*, 25(6), 991–1014.

[50] Hutter, K., and Jöhnk, K. (2013). Continuum Methods of Physical Modeling: Continuum Mechanics, Dimensional Analysis, Turbulence, Berlin: Springer.

[51] Hwang, S. H. (1993). Adaptive Dominant Pole Design of PID Controllers Based on a Single Closed-Loop Test, *Chemical Eng. Comm.*, 124 (1993), 131 – 152.

[52] Hwang, S.-H., and Chang, H.-C. (1987). A Theoretical Examination of Closed-Loop Properties and Tuning Methods of Single Loop PI Controllers. *Chemical Engineering Science*, 42, 2395 – 2415.

[53] Hwang, S.-H., and Fang, S.-M. (1995). Closed Loop Tuning Method Based on Dominant Pole Placement, *Chemical Eng. Comm.*, 136 (1995), 45 – 66.

[54] Ichikawa, K. (1985). Frequency-domain pole assignment and exact model-matching for delay systems. *Int. J. Control*, 41 (1985), 1015–1024.

[55] Keel, L. H., and Bhattacharyya, S. P. (2008). Controller synthesis free of analytical models: Three term controllers. *IEEE Transactions on Automatic Control*, 53(6), 1353–1369.

[56] Kožešník, J. (1965). Základy teorie přístrojů, Praha: SNTL.

[57] Kučera, V., Pilbauer, D., Vyhlídal, T., and Olgac, N. (2017). Extended delayed resonators – Design and experimental verification. *Mechatronics*, 41, 29–44.

[58] Liu, J., Wang, H., and Zhang, Y. (2015). New result on PID controller design of LTI systems via dominant eigenvalue assignment. *Automatica*, 62, 93–97.

[59] Manitius, A., and Olbrot, A. (1979). Finite spectrum assignment problem for systems with delays. *IEEE Transactions on Automatic Control*, 24(4), 541–552.

[60] Matušů, R., and Prokop, R. (2011). Single-parameter tuning of PI controllers: Theory and application. *Journal of the Franklin Institute*, 348(8), 2059–2071.

[61] Medvedev, A. (1997). Disturbance Attenuation in Finite - Spectrum - Assignment. *Automatica*, 33(6), 1163–1168.

[62] Merrit, H. E. (1965). Theory of self excited-tool chatter: Research 1. ASME Journal of Eng. for Industry, 87, 447–454.

[63] Michiels, W., Engelborghs, K., Vansevenant, P., and Roose, D. (2002). Continuous pole placement for delay equations. *Automatica*, 38(5), 747–761.

[64] Michiels, W., and Vyhlídal, T. (2005). An Eigenvalue Based Approach for the Stabilization of Linear Time-Delay Systems of Neutral Type. *Automatica*, 41(6), 991–998.

[65] Michiels, W., Vyhlídal, T., and Zítek, P. (2010). Control Design for Time-delay Systems Based on Quasi-direct Pole Placement. *Journal of Process Control*, 20(3), 337–343.

[66] Modrlák, O., and Zajcev, A. V. (1992). Störungskompensation in Smithregler. *In*: Regelungstechnisches Kolloquium, Zittau, Germany.

[67] Moelja, A. A., and Meinsma, G. (2003). Parametrization of Stabilizing Controllers for Systems with Multiple I/O Delays. *In*: 4th IFAC Workshop on Time-Delay Systems (TDS'03), September 8-10, INRIA, Rocquencourt, France.

[68] Morari, M., and Zafiriou, E. (1989). Robust Process Control. Prentice Hall, Englewood Cliffs New Jersey.

[69] Niculescu, S. I. (2002). On delay robustness analysis of a simple control algorithm in high-speed networks. *Automatica*, 38(5), 885–889.

[70] Normey-Rico, J. E., and Camacho, E. F. (2000). Multivariable Generalised Predictive Controller Based on the Smith Predictor. *IEE Proceedings - Control Theory and Applications*, 147(5), 538–546.

[71] O'Dwyer, A. (2012). An Overview of Tuning Rules for the PI and PID Continuous-Time Control of Time-Delayed Single-Input, Single-Output (SISO) Processes. *In*: Vilanova R., Visioli A. (eds) PID Control in the Third Millennium. Advances in Industrial Control. Springer, London.

[72] Olbrot, A. W. (1978). Stabilizability, Detectability and Spectrum Assignment for Linear Autonomous Systems with General Time Delays. *IEEE Transactions on Automatic Control*, AC-23(5), 887–890.

[73] Oliveira, de M. C., and Geromel, J. C. (2004). Synthesis of non-rational controllers for linear delay systems. *Automatica*, 40(2), 171–188.

[74] Palmor, Z. J. (1996). Time delay compensation-smith predictor and its modifications. In: W. S. Levine (Ed.), Control handbook (pp. 224–237). CRC Press.

[75] Persson, P., and Åström, K. J. (1993). Dominant Pole Design – a Unified View of PID Controller Tuning (In: L. Dugard, M'Saad, I.D. Landau (Eds.), Adaptive Systems in Control and Signal Processing, Pergamon Press Oxford, 377–382.

[76] Prokop, R., and Corriou, J. P. (1997). Design and analysis of simple robust controllers. *International Journal of Control*, 66(6), 905–921.

[77] Rayleigh, L. (1915). The principle of similitude, *Nature*, 95(2368), 66–68.

[78] Saha S., Das, S., Das, S., and Gupta, A. (2012). A conformal mapping based fractional order approach for sub-optimal tuning of PID controllers with guaranteed dominant pole placement. *Communications in Nonlinear Science and Numerical Simulation*, 17(9), 3628–3642.

[79] Šebek, M. (1993). n-D Polynomial Equations. In: Polynomial Methods in Optimal Control and Filtering (K. J. Hunt, ed.), ch. 7, 184–209, London: Peter Peregrinus, Ltd.

[80] Seborg, D. E., Edgar, T. F., Mellichamp, D. A., and Doyle, F. J. (2016). Process dynamics and control, John Wiley and Sons, 4th ed.

[81] Smith, O. J. (1957). Closer control of loops with dead time. *Chemistry Engineering Progress*, 53(5), 217–219.

[82] Silva, G. J., Datta, A., and Bhattacharyya, S. P. (2005). PID Controllers for Time-Delay Systems. Birkhäuser, Basel.

[83] Srivastava, S., Misra, A., Thakur, S. K., and Pandit, V. S. (2016). An optimal PID controller via LQR for standard second order plus time delay systems. *ISA Transactions*, 60, 244 – 253.

[84] Stépán, G. (1998). Delay-differential equation models for machine tool chatter. *In*: Dynamics and chaos in manufacturing processes, F. C. Moon (ed). Wiley, New York, 165–192.

[85] Strejc, V. (1965). Syntéza regulačních obvodů s číslicovým počítačem. Academia, Praha.

[86] Strutt, J. W. (1871). XV. On the light from the sky, its polarization and colour, *Philosophical Magazine Series 4*, 41(271), 107–120.

[87] Szirtes, T. (2007). Applied Dimensional Analysis and Modeling, 2nd Edition, Butterworth-Heinemann.

[88] Tang, W., Wang, Q-G., Ye, Z., and Zhang, Z. (2007). PID Tuning for Dominant Poles and Phase Margin. *Asian Journal of Control*, 9(4), 466–469.

[89] Tavakoli, S., and Fleming, P. (2003). Optimal tuning of PI controllers for first order plus dead time/long dead time models using dimensional analysis. In: European Control Conference (ECC), 2003, Cambridge: IEEE, 2196–2200.

[90] Tian, Y. -C., and Gao, F. (1998). Double - Controller Scheme for Control of Processes with Dominant Delay. *IEE Proceedings - Control Theory and Applications*, 145(5), 479–484.

[91] Tse, E., and Athans, M. (1973). Observer theory for continuous-time linear systems. *Information and Control*, 22(5), 405–434.

[92] Turkoglu, K., and Olgac, N. (2009). Robust Control for Multiple Time Delay MIMO Systems with Delay-Decouplability Concept. *In*: Topics in Time Delay Systems (pp. 37–47). Springer, Berlin, Heidelberg.

[93] Uchida, K., Shimemura, E., Kubo, T., and Abe, N. (1988). The linear-quadratic optimal control approach to feedback control design for systems with delay. *Automatica*, 24(6), 773–780.

[94] Vettori, P., and Zampieri, S. (2000). Controllability of Systems Described by Convolutional or Delay-Differential Equations. *SIAM Journal on Control and Optimization*, 39(3), 728–756.

[95] Vítečková, M., and Víteček, A. (2015). Stability and pole dominance of control systems. In: Proc. 16th International Carpathian Control Conference (ICCC), 580–585, IEEE, Budapest.

[96] Vyhlídal, T., and Hromčík, M. (2015). Parameterization of input shapers with delays of various distribution. *Automatica*, 59, 256–263.

[97] Vyhlídal, T., and Zítek, P. (2009). Mapping Based Algorithm for Large-Scale Computation of Quasi-Polynomial Zeros. *IEEE Transactions on Automatic Control*, 54(1), 171–177.

[98] Vyhlídal, T., and Zítek, P. (2009). Modification of Mikhaylov criterion for neutral time-delay systems. *IEEE Transactions on Automatic Control*, 54(10), 2430–2435.

[99] Wang, D. J. (2007). Further results on the synthesis of PID controllers. *IEEE Transactions on Automatic Control*, 52(6), 1127–1132.

[100] Wang, D. J. (2009). Synthesis of PID controllers for high-order plants with time-delay. *Journal of Process Control*, 19(10), 1763–1768.

[101] Wang, Q-G., Lee, T. H., and Tan, K. K. (1999). Finite-Spectrum Assignment for Time-Delay Systems. Lecture notes in control and information sciences, 239, Springer-Verlag, London.

[102] Wang, H., Liu, J., Yang, F., and Zhang, Y. (2015). Controller design for delay systems via eigenvalue assignment–on a new result in the distribution of quasi-polynomial roots. *International Journal of Control*, 88(12), 2457–2476.

[103] Wang, H., Liu, J., and Zhang, Y. (2017). New Results on Eigenvalue Distribution and Controller Design for Time Delay Systems. *IEEE Transactions on Automatic Control*, 62(6), 2886–2901.

[104] Wang, Q. G., Ye, Z., and Chieh Hang, C. (2006). Tuning of phase-lead compensators for exact gain and phase margins. *Automatica*, 42(2), 349–352.

[105] Wang, Q. G., Zhang, Z., Åström, K. J., and Chek, L. S. (2009). Guaranteed Dominant Pole Placement with PID Controllers. *Journal of Process Control*, 19, 349 – 352.

[106] Weiss, G., and Xu, C. Z. (2005). Spectral properties of infinite-dimensional closed-loop systems. *Mathematics of Control, Signals and Systems*, 17(3), 153–172.

[107] Wu, Z., and Michiels, W. (2012). Reliably computing all characteristic roots of delay differential equations in a given right half plane using a spectral method. *Journal of Computational and Applied Mathematics*, 236(9), 2499–2514.

[108] Yamanaka, K., and Shimemura, E. (1993). Use of multiple time-delays as controllers in IMC schemes. *International Journal of Control*, 57(6), 1443–1451.

[109] Yi, S., Ulsoy, A. G., and Nelson, P. W. (2010). Design of observer-based feedback control for time-delay systems with application to automotive powertrain control. *Journal of the Franklin Institute*, 347(1), 358–376.

[110] Zhang, W., Sun, Y., and Xu, X. (1998). Two degree-of-freedom Smith predictor for processes with time delay. *Automatica*, 34(10), 1279–1282.

[111] Zhang, Y., Wang, Q-G., and Åström, K. J. (2002). Dominant pole placement for multi-loop control systems. *Automatica*, 38(7), 1213–1220.

[112] Zhong, Q.-C. (2003). Unified Smith Predictor for Dead-time Systems. In: 4th IFAC Workshop on Time-Delay Systems (TDS'03), September 8-10, INRIA, Rocquencourt, France.

[113] Zítek, P. (1986). Anisochronic modelling and stability criterion of hereditary systems. *Prob. Control Info. Theory*, 15(6), 413–424.

[114] Zítek, P. (1997). Frequency-domain synthesis of hereditary control systems via anisochronic state space. *International Journal of Control*, 66(4), 539–556.

[115] Zítek, P. (1998). Anisochronic State Observers for Hereditary Systems. *International Journal of Control*, 71(4), 581–599.

[116] Zítek, P. (1998). Time Delay Control System Design Using Functional State Models, *In*: CTU Reports. Prague: CTU, 1998, p. 7–92.

[117] Zítek, P., Bušek, J., and Vyhlídal, T. (2014). Anti-Windup Conditioning for Actuator Saturation in Internal Model Control with Delays. In: *Low-Complexity Controllers for Time-Delay Systems* (pp. 31–45). Springer, Cham.

[118] Zítek, P., and Fišer, J. (2006). Predictor Based Control Design for Time Delay Systems. In: International Conference on Computational Intelligence for Modelling, Control and Automation (CIMCA06), Los Alamitos: IEEE Computer Society, 2006, vol. 2, 517–522.

[119] Zítek, P., and Fišer, J. (2018). A Universal Map of Three Dominant Pole Assignment for PID Controller Tuning. *International Journal of Control*, 2018, 1–8. doi: 10.1080/00207179.2018.1554267 (in press)

[120] Zítek, P., Fišer, J., and Vyhlídal, T. (2010). Ultimate-Frequency based Dominant Pole Placement. *In*: Proceedings of 9th IFAC Workshop on Time Delay Systems, Praha: IFAC, 2010, vol. 1, 87–92.

[121] Zítek, P., Fišer, J., and Vyhlídal, T. (2012). Ultimate-frequency Based Three-pole Dominant Placement in Delayed PID Control Loop. *In*: Proceedings of the 10th IFAC Workshop on Time Delay Systems, New York: IFAC, 2012, vol. 1, 150–155.

[122] Zítek, P., Fišer, J., and Vyhlídal, T. (2013). Dominant three pole placement in PID control loop with delay. *In*: 9th Asian Control Conference (ASCC), Istanbul, Turkey, New York: IEEE, 1–6.

[123] Zítek, P., Fišer, J., and Vyhlídal, T. (2013). Dimensional analysis approach to dominant three-pole placement in delayed PID control loops. *Journal of Process Control*, 23(8), 1063–1074.

[124] Zítek, P., Fišer, J., and Vyhlídal, T. (2014). Dominant Trio of Poles Assignment in Delayed PID Control Loop. *In*: Delay Systems: From Theory to Numerics and Applications vol. 1, Eds. T. Vyhlídal, J-F. Lafay, and R. Sipahi, New York: Springer, 2014, 57–70.

[125] Zítek, P., Fišer, J., and Vyhlídal, T. (2016). IAE Optimization of PID Control Loop with Delay in Pole Assignment Space. *In*: Proceedings of the 13th IFAC Workshop on Time Delay Systems, Istanbul, Turkey, IFAC-PapersOnLine, 49(10), 177–181.

[126] Zítek, P., Fišer, J., and Vyhlídal, T. (2017). Dynamic similarity approach to control system design: delayed PID control loop. *International Journal of Control*, 2017, 1–10. doi: 10.1080/00207179.2017.1354398 (in press)

[127] Zítek, P., and Hlava, J. (2001). Anisochronic Internal Model Control of Time Delay Systems. *Control Engineering Practice*, 9(5), 501–516.

[128] Zítek, P., and Kučera, V. (2003). Algebraic design of anisochronic controllers for time delay systems. *International Journal of Control*, 76(16), 1654–1665.

[129] Zítek, P., Kučera, V., and Vyhlídal, T. (2008). Meromorphic observer-based pole assignment in time delay systems. *Kybernetika*, 44(5), 633–648.

[130] Zítek, P., and Víteček, A. (1999). Control design for subsystems with time delays and nonlinearities. Prague: CTU. (in Czech)

[131] Zítek, P., and Vyhlídal, T. (2003). Quasi-polynomial based design of time delay control systems. *IFAC Proceedings Volumes*, 36(19), 233–238.

[132] Zlokarnik, M. (1991). *Dimensional Analysis and Scale-up in Chemical Engineering*, Berlin: Springer-Verlag.

[133] Zohuri, B. (2015). *Dimensional Analysis and Self-Similarity Methods for Engineers and Scientists*, Springer.